THE ASTROPHYSICAL JOURNAL

AN INTERNATIONAL REVIEW OF SPECTROSCOPY AND ASTRONOMICAL PHYSICS

VOLUME 99 MARCH 1944 NUMBER 2

ANALYSIS OF THE MILKY WAY IN CASSIOPEIA

ROBERT H. BAKER AND ELAINE NANTKES

University of Illinois Observatory

Received December 23, 1943

ABSTRACT

The analysis of this region of the Milky Way is based on star counts to magnitude 15, color excesses of stars determined here and elsewhere, and published counts of extragalactic nebulae. The obscuration is ascribed to two cloud systems: the first, at the distance of 500 parsecs, is chiefly responsible for the variety in the appearance of this part of the Milky Way; the second, at 800 parsecs, is nearly uniform in density throughout the low latitudes. However, an equally good representation of the counts and colors is obtained by employing constant coefficients of absorption. In all divisions of the region the star-density functions decrease with increasing distance from the sun; the gradient in the plane of the galactic equator is somewhat less steep than in the previously studied region of Auriga.

An earlier study of this region of the Milky Way by one of us[1] was based on plates taken with the 4-inch Ross-Lundin camera of Harvard Observatory. To facilitate the analysis it was assumed that the southern part of the region is mostly free from dust clouds to within 6° of the galactic equator. Magnitude measures of stars then available in this area showed little or no color excess, though there was no assurance of the absence of dust beyond those stars. The star-density gradients for the apparently unobscured zones were then extended arbitrarily to the equator. It was pointed out that the absorption introduced in the analysis is, therefore, a minimum throughout and is subject to upward revision when further data become available.

The present study is confined generally to the southern galactic latitudes. The material supplied by the Harvard plates on 17 centers is supplemented by plates on 20 centers, which extend the original region to higher latitudes and somewhat to the east. The region now under discussion lies generally between galactic latitudes $+1°$ and $-34°$, and longitudes 75° and 105°. The supplementary plates were taken at the University of Illinois Observatory with the 4-inch Ross-Fecker camera, which is similar to the Harvard Observatory camera. The scale of the plates is 290″ per millimeter.

THE STAR COUNTS

The method of counting is the same as that described in the earlier paper. Magnitude standards for calibrating the reference scale are available on plates containing Selected Areas 8, 9, 19, 20, 21, 22, 42, and 43 and are carried by overlapping plates to the re-

[1] *Harvard Circ.*, No. 424, 1939.

mainder of the region. Standards are taken from *Bergedorfer Spektral-Durchmusterung* for the brighter stars and from the *Mount Wilson Catalogue*[2] for the fainter ones. No corrections are made to our counts for distance from center of the plate or for any other reason.

In preparation for the analysis of the counts, the region is divided into areas arbitrarily lettered, in each of which the surface distribution of the stars seems fairly uniform and

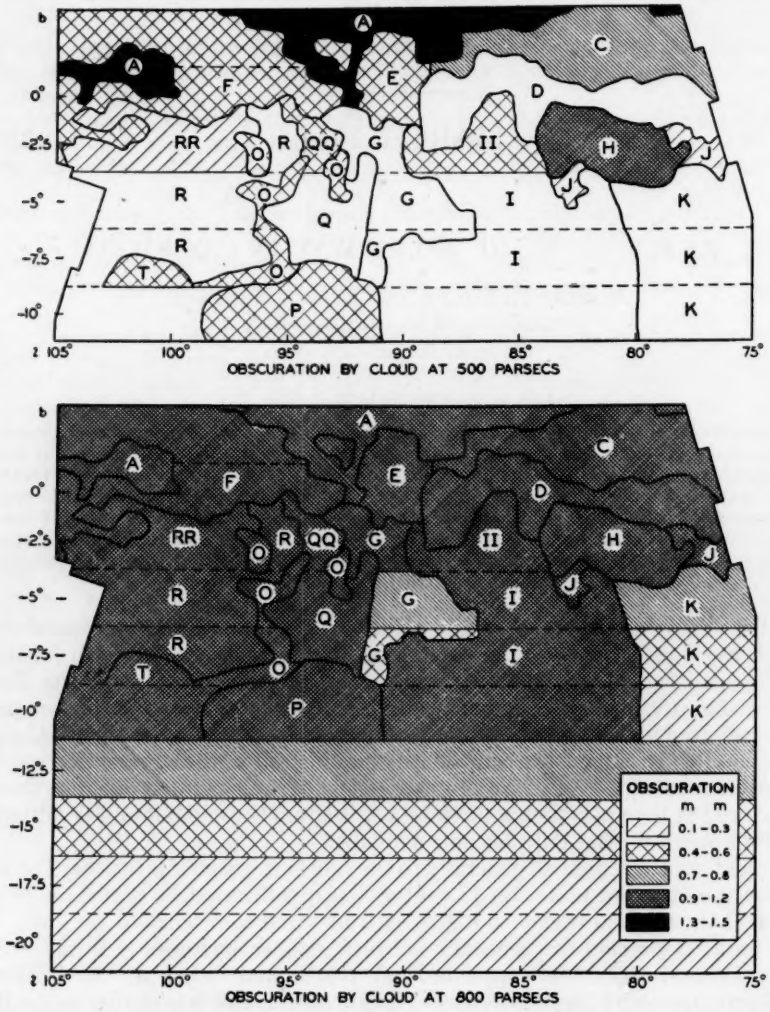

FIG. 1.—Divisions of Cassiopeia region, showing obscuration at 500 and 800 parsecs. The −22.5° to −32.5° zones, which are unobscured, are not shown.

different from that in the neighboring areas. The region is further divided by parallels of galactic latitude into zones 2.5° wide, in accordance with the usual practice. The arrangement of the divisions is shown in Figure 1, in which the zones of higher latitude are omitted to save space. The following changes in the designations of divisions for the present study may be noticed by comparing Figure 1 with the corresponding one in the earlier

[2] *Mt. W. Contr., Carnegie Inst. Washington*, No. 402, 1930.

paper. Area T is added. Area K is extended to the $-10°$ zone, and areas G and R are extended to the $-7.5°$ zone. The original areas I, Q, and R in the $-2.5°$ zone prove to be considerably different from the similarly lettered areas in the higher latitudes and are now distinguished from them by the double letters II, QQ, and RR. We have also omitted in the new diagram small patches in the $-7.5°$ and $-10°$ zones which are darker than

TABLE 1

MEAN LOG $N(m)$ FOR THE DIFFERENT DIVISIONS

AREA	ZONE	LONGITUDE OF CENTER*	LIMITING MAGNITUDE							OBSCURATION AT 500 PARSECS	ADDITIONAL AT 800 PARSECS	CONST. COEFF. PER 1000 PARSECS
			9.0	10.0	11.0	12.0	13.0	14.0	15.0			
C.....	+ 2.5°	82	0.52	0.99	1.37	1.73	2.07	2.38	2.57	$0^m.8$	$1^m.0$	$1^m.5$
A.....	0	97	.41	0.81	1.23	1.59	1.88	2.18	2.44	1.5	1.1	2.6
D.....	0	83	.69	1.16	1.56	1.96	2.36	2.67	2.88	0.0	1.0	0.7
E.....	0	90	.55	1.00	1.41	1.78	2.10	2.41	2.66	0.5	1.2	1.7
F.....	0	99	.55	0.98	1.41	1.76	2.07	2.38	2.65	0.5	1.2	1.7
G.....	− 2.5	91	.72	1.19	1.55	1.91	2.27	2.58	2.90	0.0	1.0	0.7
H.....	− 2.5	81	.52	0.90	1.30	1.66	2.03	2.34	2.60	1.0	0.9	1.5
II.....	− 2.5	87	.39	0.94	1.36	1.76	2.14	2.45	2.70	0.5	1.0	1.2
QQ.....	− 2.5	94	.46	0.99	1.44	1.78	2.11	2.41	2.73	0.5	1.1	1.3
R.....	− 2.5	95	.70	1.04	1.51	1.93	2.28	2.56	2.87	0.0	1.0	0.7
RR....	− 2.5	100	.68	1.08	1.48	1.85	2.20	2.50	2.78	0.2	1.0	1.0
G.....	− 5	90	.78	1.18	1.51	1.90	2.28	2.62	2.89	0.0	0.8	0.5
I.....	− 5	84	.69	1.12	1.50	1.87	2.22	2.56	2.82	0.0	1.0	0.7
J.....	− 5	80	.60	0.98	1.42	1.78	2.19	2.46	2.75	0.3	1.0	1.0
K.....	− 5	78	.55	1.02	1.53	1.90	2.32	2.62	2.91	0.0	0.8	0.5
O.....	− 5	95	.50	0.90	1.35	1.72	2.06	2.36	2.62	0.5	1.1	1.3
Q.....	− 5	94	.54	1.00	1.48	1.84	2.19	2.51	2.79	0.0	1.0	0.7
R.....	− 5	100	.62	1.09	1.56	1.90	2.26	2.54	2.85	0.0	1.0	0.7
G.....	− 7.5	91	.82	1.15	1.53	1.90	2.31	2.62	2.90	0.0	0.5	0.3
I.....	− 7.5	85	.74	1.10	1.48	1.87	2.24	2.55	2.85	0.0	0.9	0.6
K.....	− 7.5	77	.62	1.12	1.54	1.92	2.35	2.66	2.94	0.0	0.5	0.3
O.....	− 7.5	96	.36	0.90	1.36	1.67	1.98	2.33	2.63	0.5	1.2	1.3
R.....	− 7.5	100	.65	1.03	1.46	1.83	2.21	2.53	2.85	0.0	0.9	0.6
T.....	− 7.5	101	.53	0.87	1.38	1.72	2.04	2.36	2.72	0.5	1.0	1.2
K.....	−10	76	.72	1.17	1.50	1.89	2.29	2.62	2.90	0.0	0.3	0.2
P.....	−10	95	.49	0.88	1.28	1.62	1.98	2.32	2.61	0.4	1.0	1.1
.....	−10	97	.71	1.05	1.40	1.76	2.12	2.48	2.77	0.0	1.0	0.6
.....	−12.5	93	.56	0.97	1.35	1.71	2.07	2.42	2.68	0.0	0.8	0.5
.....	−15	93	.53	0.92	1.32	1.66	2.01	2.35	2.62	0.0	0.5	0.3
.....	−17.5	92	.48	0.87	1.27	1.62	1.95	2.30	2.57	0.0	0.3	0.2
.....	−20	90	.37	0.76	1.19	1.57	1.90	2.25	2.51	0.0	0.2	0.1
.....	−22.5	90	.23	0.61	1.01	1.45	1.81	2.18	2.45	0.0	0.0	0.0
.....	−25	89	.17	0.60	1.01	1.44	1.80	2.16	2.42	0.0	0.0	0.0
.....	−27.5	89	.20	0.63	0.98	1.39	1.72	2.05	2.34	0.0	0.0	0.0
.....	−30	94	.18	0.60	0.96	1.36	1.67	1.99	2.29	0.0	0.0	0.0
.....	−32.5	95	0.10	0.56	0.90	1.30	1.64	1.94	2.24	0.0	0.0	0.0

* All galactic co-ordinates in this paper are referred to the conventional pole at right ascension 12^h40^m, declination $+28°$.

their surroundings and are probably wisps detached from the main body of the nearer dust cloud to the north. Owing to their small areas, these patches are omitted from the analysis as before.

The values of the mean log $N(m)$ representing the counts in the different divisions appear in Table 1, where $N(m)$ is the number of stars per square degree brighter than apparent photographic magnitude m. Before the analysis of the counts is made, these are

converted to log $A(m)$ at magnitude intervals of from $m = 9.5$ to $m = 14.5$, where $A(m)$ is the number of stars per square degree between $m - \frac{1}{2}$ and $m + \frac{1}{2}$.

ANALYSIS OF THE STAR COUNTS

The analysis is made with the (m, log π) tables whose construction and use have been described by Bok.[3] The amount of absorption introduced in the analysis is determined for the higher latitudes chiefly by the nebula counts and for the lower latitudes by the star colors that are available; these independent data will be discussed later. The absorption over the entire region can be ascribed to two layers of dust clouds at the distances of 500 and 800 parsecs, whose effectiveness in the various divisions is shown in Table 1 and also by the different degrees of shading in Figure 1. No considerable amount of obscuration is indicated south of the $-20°$ zone. In that zone the 800-parsec cloud makes its appearance and increases in density until its maximum absorption of around 1.0 mag. is attained in the $-10°$ zone. From there to the equator this cloud remains practically uniform in density except in areas G and K, where it is appreciably thinner. On the other hand, the 500-parsec cloud is irregular in density and is therefore chiefly responsible for the variety in the appearance of the Milky Way in Cassiopeia. Fragments of the nearer dust cloud appear as far south as the $-10°$ zone, in area P and probably in a few other places which are too small to analyze. Area H, a conspicuous dark spot in the photographs, is the densest patch of the 500-parsec cloud south of the galactic equator. Immediately north of the equator the dark area A marks the beginning of the well-known "Cepheus flare" of heavy obscuration.

The earlier study of the Milky Way in Cassiopeia was considered as provisional because it introduced minimum absorption and did not arrive at a physical picture of the absorption. While satisfactory agreement between observed and computed log $A(m)$ in the different divisions of the region was obtained by employing constant coefficients of absorption and superposing an absorbing cloud at 800 parsecs, both coefficient and absorption in the cloud were required to increase in the more heavily obscured divisions. Fairly satisfactory agreement was obtained by introducing two clouds at 200 and 800 parsecs, respectively; but here again the increase of the obscuration in the darker areas had to be divided proportionately between the two clouds.

The present analysis is well served by two dust clouds which operate independently. It will be noticed in Figure 1 that each bright or dark area is an irregularity in one or the other of the two cloud layers and never in the two together. However, we find that the hypothesis of constant coefficients of absorption can produce an equally good agreement between the observed and the computed log $A(m)$. When the values of the unobscured log $A(m)$ are kept about the same as in the two-cloud analysis, the appropriate coefficients per kiloparsec of distance from the sun are shown in the last column of Table 1. Moreover, we have not found any evidence from the available data independent of the star counts that seems to favor one construction over the other.

COMPARISONS WITH RELATED DATA

Color excesses of stars of spectral classes B8–A7 and chiefly between red magnitudes 9.0 and 12.0 have been determined in Selected Areas 8, 19, and 43 by Dr. Lois Kiefer and Dr. J. C. Bell. The red magnitudes were measured on Eastman 103E plates, taken with the Ross-Fecker camera, the plates given 60 minutes' exposure behind a ciné-red filter. Three or four such plates were employed for each Area. Magnitude standards were obtained by pairing each plate with a similarly exposed and developed plate centered at the north pole.[4] The blue magnitudes and spectral classes of these stars were taken from the Bergedorf catalogue. The color excess for each star is the amount by which the observed

[3] *Distribution of the Stars in Space,* University of Chicago Press, 1937.

[4] *Harvard Ann.*, **89**, No. 5, 1935.

color index (blue *minus* red magnitude) exceeds the normal color index to be expected for a star of the particular spectral class.

In Table 2 the color excesses for the individual stars are assembled into means with respect to the spectral classes and red magnitudes of these stars. When the mean color

TABLE 2

COLOR EXCESSES

Spectral Class	No. of Stars	Mean Red Mag.	Color Excess (Mag.)	Distance (Parsecs)
	Area C at +2.5°			
A0.....	10	11.5	+0.24	1150
	17	11.0	+ .30	830
	11	10.5	+ .33	630
	10	9.5	+ .12	520
A1–A2...	7	11.5	+ .37	600
	7	11.0	+ .33	500
A3–A7...	12	11.5	+ .20	480
	14	10.7	+0.14	360
	Areas E and F at 0°			
B8–B9...	9	11.0	+0.32	1260
A0–A1...	10	11.6	+ .24	1200
	7	11.1	+ .11	1150
	5	10.6	+ .09	910
A2.....	4	11.9	+ .10	1600
	8	11.4	+ .23	690
A3–A7...	6	12.0	− .02	960
	12	11.1	+0.06	480
	Area H at −2.5°			
A0.....	19	11.5	+0.57	720
	20	11.0	+ .53	600
	14	10.5	+ .61	440
	9	10.0	+ .61	350
A1–A2...	10	11.5	+ .60	440
	8	11.0	+ .48	420
	6	10.5	+ .52	320
A3–A7...	9	11.5	+ .46	330
	11	11.0	+ .60	220
	7	10.5	+0.49	200

Spectral Class	No. of Stars	Mean Red Mag.	Color Excess (Mag.)	Distance (Parsecs)
	Area D at 0°			
A0.....	34	11.5	+0.37	960
	27	11.0	+ .25	870
	19	10.5	+ .28	690
	16	10.0	+ .28	550
	7	9.5	+ .13	520
	6	9.0	+ .10	440
A1–A2...	28	11.5	+ .28	690
	30	11.0	+ .22	580
	10	10.5	+ .24	460
	8	9.1	+ .11	290
A3–A7...	20	11.5	+ .20	480
	10	11.0	+ .17	400
	11	10.5	+0.13	330
	Area G at −2.5°			
B8–B9...	7	11.6	+0.30	1700
	9	11.0	+ .43	1100
	7	10.5	+ .30	660
	6	10.0	+ .25	550
A0–A1...	13	12.0	+ .17	1600
	11	11.5	+ .27	1100
	12	11.0	+ .27	870
	4	10.4	− .02	960
A2.....	6	11.8	+ .07	1600
	11	11.3	+ .20	690
A3–A7...	12	12.0	− .14	960
	11	11.5	.00	790
	7	11.0	+0.21	500

excess is multiplied by the factor 3, the result is supposed to represent on the International Scale the photographic absorption, K, by the intervening dust. The corresponding mean distance of each group of stars is computed in the usual way by comparing the apparent red magnitude with the absolute magnitude adopted for the particular spectral class and correcting for absorption.

When the values of the photographic absorption derived from Table 2 are plotted for

each division against the distances, it is noticed that the scatter of the points is in some cases greater than in most of the previous color determinations made here. The only departure from former procedure is that the blue magnitudes are taken from the Bergedorf catalogue instead of being measured on our plates. Whatever the cause may be, the scatter is so pronounced for areas *E*, *F*, and *G* that the absorption in these areas cannot be regarded as very reliably determined. The results in areas *D* and *H* are satisfactorily consistent. In the latter area, however, the full amount of the absorption which we expect behind the 800-parsec cloud makes its appearance at 200 parsecs from the sun and remains constant as far out as the points go, an effect that is equally difficult to reconcile with the constant-coefficient hypothesis.

The values of the absorption at 800 parsecs, which we adopt from the evidence of the Illinois colors, are included in Table 3 for comparison with the absorptions employed in the analysis of the star counts. The agreement would be considered quite good if we could assume that the stars whose colors were determined in areas *C*, *E*, and *F* are mostly in front of the 800-parsec dust cloud and that those in areas *D*, *G*, and *H* are mostly behind that cloud. The stars observed for color in Selected Area 43 are somewhat too few to provide a definitive value of the absorption in the $-17.5°$ zone; yet they suggest absorption of the order of 0.5 mag., as compared with the value 0.3 mag., which we have adopted in the analysis.

Many photoelectric color excesses of class-B stars by Stebbins, Huffer, and Whitford[5] are available in this region. We have converted them to photographic absorptions on the scale we employ here by multiplying by the factor 7, and we list the means for the various divisions in Table 3. The corresponding mean distances are calculated from the distance moduli given by these investigators. The comparison of these results with the absorptions introduced in our analysis is conveniently made under three heads.

1. In six divisions within 5° of the galactic equator these B stars have a mean distance slightly exceeding 800 parsecs. We therefore compare their mean absorptions with those in our analysis at 800 parsecs. The differences (SHW *minus* Illinois analysis) are quite small, with the exception of area *F;* the average difference is $+0^m.1$.

2. In four divisions from the $-7.5°$ to the $-15°$ zone the B stars considered have a mean distance somewhat less than 500 parsecs, and the majority are in front of the 800-parsec cloud. Thus it is not surprising that the average absorption for all these stars is $0^m.5$ less than is employed in our analysis at 800 parsecs.

3. There are six of these B stars scattered in the $-22.5°$ to $-30°$ zones. Since their average distance is only 300 parsecs, the agreement of their absorption with that employed in the analysis is fortuitous.

Table 3 also contains the values of the obscurations derived from Hubble's[6] nebula counts, where we take his $\log N(m) = 1.90$ as representing no obscuration. In the higher latitudes, where no considerable amount of dust is likely to lie beyond the range of the star counts, these values are employed to guide the amounts of absorption introduced in the analysis. No such agreement is expected, of course, near the galactic equator.

As an example of the agreement between the absorptions by dust clouds introduced in our analysis and the values derived independently, we consider area *D*. This bright area along the galactic equator is an opening in the nearer dust-cloud system. No obscuration enters until the 800-parsec cloud is encountered; here $K = 1^m.0$. The Illinois color excesses of 226 stars between 300 and 900 parsecs suggest the value of $K = 0^m.8$ produced by a cloud at the distance of 600–800 parsecs; or they may be represented by a coefficient of $1^m.2$ per kiloparsec. The photoelectric color excesses of 15 stars mostly between 400 and 1600 parsecs give the average $K = 0^m.9$. W. Becker,[7] from color excesses of stars in the northern part of Selected Area 19, finds no reddening of the stars as far as 1000 parsecs

[5] *Ap. J.*, **91**, 20, 1940; *Mt. W. Contr.*, No. 621, 1940.

[6] *Ap. J.*, **79**, 8, 1934; *Mt. W. Contr.*, No. 485, 1934.

[7] *Zs. f. Ap.*, **17**, 285, 1939.

from the sun, where absorption sets in and increases to $K = 1^m.0$ at 2000 parsecs. Bok's[8] color excesses of 81 stars show no absorption as far as 800 parsecs and, from there on, absorption whose rate of increase is represented by the coefficient $1^m.2$/kpc. Zug[9] has

TABLE 3

OBSCURATIONS FROM STAR COLORS AND NEBULA COUNTS COMPARED WITH ADOPTED OBSCURATIONS

Area	Zone	From Illinois Colors (At 800 Parsecs)	From SHW Color Excesses			From Hubble's Nebula Counts (Total Obscuration)	Adopted in Analysis	
			No. of Stars	Mean Obscuration	Mean Distance (Parsecs)		At 500 Parsecs	Additional (At 800 Parsecs)
C	+ 2.5°	0.9	18	1.9	600	.....	0.8	1.0
A	0.0	.....	.....	.....	.....	.....	1.5	1.1
D	0.0	0.8	15	0.9	800	.....	0.0	1.0
E	0.0	0.5:	7	1.9	630	>3.0	0.5	1.2
F	0.0	0.5:	27	2.3	730	.....	0.5	1.2
G	− 2.5	0.8:	.....	.....	.....	.....	0.0	1.0
H	− 2.5	1.7	.....	.....	.....	.....	1.0	0.9
II	− 2.5	.....	.....	.....	.....	.....	0.5	1.0
QQ	− 2.5	.....	.....	.....	.....	.....	0.5	1.1
R	− 2.5	.....	.....	.....	.....	.....	0.0	1.0
RR	− 2.5	.....	34	1.2	1400	.....	0.2	1.0
G	− 5.0	.....	.....	.....	.....	>3.0	0.0	0.8
I	− 5.0	.....	4	0.7	850	.....	0.0	1.0
J	− 5.0	.....	.....	.....	.....	.....	0.3	1.0
K	− 5.0	.....	.....	.....	.....	>3.0	0.0	0.8
O	− 5.0	.....	.....	.....	.....	.....	0.5	1.1
Q	− 5.0	.....	.....	.....	.....	.....	0.0	1.0
R	− 5.0	.....	.....	.....	.....	2.2	0.0	1.0
G	− 7.5	.....	.....	.....	.....	.....	0.0	0.5
I	− 7.5	.....	4	0.4	400	.....	0.0	0.9
K	− 7.5	.....	.....	.....	.....	.....	0.0	0.5
O	− 7.5	.....	.....	.....	.....	.....	0.5	1.2
R	− 7.5	.....	.....	.....	.....	.....	0.0	0.9
T	− 7.5	.....	.....	.....	.....	.....	0.5	1.0
K	−10.0	.....	.....	.....	.....	0.4	0.0	0.3
P	−10.0	.....	.....	.....	.....	.....	0.4	1.0
.....	−10.0	.....	4	0.4	500	0.9	0.0	1.0
.....	−12.5	.....	5	0.2	400	0.7	0.0	0.8
.....	−15.0	.....	9	0.2	480	0.4	0.0	0.5
.....	−17.5	0.5:	.....	.....	.....	.....	0.0	0.3
.....	−20.0	.....	.....	.....	.....	0.2	0.0	0.2
.....	−22.5	.....	6	0.0	300	0.0	0.0	0.0
.....	−25.0	.....				0.1	0.0	0.0
.....	−27.5	.....				.....	0.0	0.0
.....	−30.0	.....				0.0	0.0	0.0
.....	−32.5	.....	.....	.....	.....	.....	0.0	0.0

measured the color excess of one open cluster, NGC 7654, in area *D* within the range of our counts; the distance is 1400 parsecs. Multiplying his value by 1.9, we obtain $K = 1^m.0$. With allowance for possible distance errors, we find reasonable agreement betweeen all these results and the value $K = 1^m.0$ at 800 parsecs, which we have employed in the analysis.

[8] *Ap. J.*, **90**, 249, 1939.

[9] *Lick Obs. Bull.*, No. 454, 1933.

THE GRADIENTS OF STAR DENSITY

Table 4 shows the actual values of log $A(m)$ for the different zones, provided that the correct amounts of absorption by the intervening dust have been adopted in the analysis. The same provision applies to the density factors of Table 5. These factors are fractions

TABLE 4

ADOPTED VALUES OF UNOBSCURED LOG $A(m)$

ZONE	MAGNITUDE					
	9.5	10.5	11.5	12.5	13.5	14.5
0.0°	1.16	1.59	2.00	2.35	2.62	2.86
− 2.5	1.06	1.53	1.94	2.30	2.58	2.80
5.0	1.00	1.48	1.89	2.25	2.55	2.78
7.5	0.97	1.44	1.86	2.22	2.52	2.77
10.0	0.88	1.34	1.77	2.14	2.39	2.73
12.5	0.82	1.26	1.75	2.02	2.32	2.58
15.0	0.71	1.14	1.48	1.87	2.12	2.39
17.5	0.65	1.06	1.45	1.76	2.06	2.35
20.0	0.59	1.00	1.38	1.72	2.00	2.25
22.5	0.41	0.79	1.20	1.57	1.89	2.17
25.0	0.42	0.81	1.18	1.54	1.89	2.12
27.5	0.41	0.76	1.08	1.45	1.77	2.00
30.0	0.38	0.75	1.11	1.41	1.72	1.95
−32.5	0.32	0.68	1.08	1.36	1.67	1.91

TABLE 5

DENSITY FACTORS, $D(r)$, FOR NO OBSCURATION

ZONE	DISTANCE IN PARSECS							
	125	200	300	500	800	1250	2000	3000
0.0°	1.00	1.00	0.90	0.90	0.75	0.45	0.20	0.03
− 2.5	1.00	1.00	.90	.90	.75	.45	.20	.03
5.0	1.00	1.00	.90	.85	.75	.45	.20	.03
7.5	1.00	1.00	.90	.85	.75	.45	.20	.03
10.0	1.00	0.90	.85	.70	.60	.40	.20	.03
12.5	1.00	0.90	.80	.65	.50	.30	.10	.03
15.0	1.00	0.80	.70	.45	.30	.20	.10	.02
17.5	1.00	0.80	.65	.40	.30	.15	.06	0.02
20.0	1.00	0.60	.30	.18	.12	.15	.06	.....
22.5	1.00	0.60	.30	.20	.15	.16	.07	.....
25.0	1.00	0.60	.30	.20	.11	.12	.06	.....
27.5	1.00	0.60	.30	.20	.10	.06	.06	.....
30.0	1.00	0.60	.30	.20	.10	.06	.04	.....
−32.5	1.00	0.50	0.25	0.15	0.10	0.05	0.04	.....

of the star density in the immediate neighborhood of the sun, which is taken as unity. The factors at 3000 parsecs are not considered very reliable; they are included because they were used in the analysis. The negative gradients with increasing distance from the sun show that the sun is situated in a region of high star density with respect to the direction of Cassiopeia.

Since its inauguration by Bok[10] the analysis of the Milky Way based on extensive star counts over the various regions has proceeded far enough to suggest certain features of the galactic system within a radius of some 2000 parsecs around the sun. We mention a few of these which can be noticed in the results of analyses at this observatory.

1. The gradients of star density are generally negative with increasing distance from the sun. Thus the sun seems to be situated amid a high congestion of stars as compared with its less immediate surroundings.

TABLE 6

COMPARISON OF DENSITY FACTORS IN 0° ZONE

Region	Galactic Longitude	Distance in Parsecs							
		125	200	300	500	800	1250	2000	3000
Auriga	130°	1.00	1.00	0.90	0.90	0.60	0.30	0.15	0.05
Cassiopeia	90	1.00	1.00	0.90	.90	.75	.45	.20	.03
Ophiuchus	340	1.00	1.00	1.00	0.90	0.70	0.50	0.50	0.40

2. The gradients appear to be steeper in the direction of the galactic anticenter. At least this is true for the regions of Auriga,[11] Cassiopeia, and Ophiuchus,[12] whose density factors in the galactic plane are shown in Table 6.

3. Exceptions to the rule of 1 are found in the Scutum cloud and the little Sagittarius cloud, where the density factors exceed the unit value assigned to the sun's vicinity. Other probable exceptions are found in Aquila[13] and in Selected Area 9, in Perseus.

4. Features often associated with the galactic system as a whole, including the dust clouds as well as the star clouds, are prominent in the "local system" within 2000 parsecs of the sun.

[10] *Harvard Circ.*, No. 371, 1931.

[11] *Ap. J.*, **94**, 482, 1941.

[12] *Ap. J.*, **96**, 224, 1942.

[13] *Ap. J.*, **94**, 493, 1941.

THE SYSTEM OF β CORONAE BOREALIS*

F. J. NEUBAUER
Lick Observatory
Received December 27, 1943

ABSTRACT

From 341 radial-velocity observations of the spectroscopic binary β Coronae Borealis made in the interval 1931–1942 with the three-prism Mills spectrograph, the writer has derived the orbital elements of the system, whose period is 10.496 years. Some evidence is found for the presence also of a shorter period of 320 days.

The star β Coronae Borealis (1900 $\alpha = 15^h23^m7$, $\delta = +29°27'$, ptm 3.72, class F0p) was announced as a spectroscopic binary by Dr. J. H. Moore[1] in 1907. In 1912 Mr. J. B. Cannon[2] published orbital elements for the star, basing his investigation upon 153 spectrograms taken with one-prism dispersion at the Dominion Observatory in Ottawa in the interval 1910–1912. On account of the large accidental errors to which his velocity determinations were subject, he had considerable difficulty in finding a period for the velocity oscillation, but by combining a period of 40.9 days with a secondary one of 490.8 days he was able to represent the observations fairly well by an approximate set of elements.

In 1931 a request came to the Lick Observatory from the parallax observers at the Allegheny Observatory to check, if possible, Mr. Cannon's two periods; and Dr. Moore turned over to me the investigation of this star. Observations were begun in May, 1931, and continued until October of that year, when the star could no longer be observed, the interval covered being almost five times the period of 40.9 days. The 58 velocities obtained that season hovered fairly constantly around the value of -16 km/sec and could not be represented by Cannon's orbital elements. One striking fact, however, was revealed, namely, that there was a progressive run in the individual residuals from the season's mean velocity, the range being about 2.5 km/sec, indicating the presence of a true variation with a period greater than six months.

Since observations throughout a single night showed no variation in velocity, a very short period could be left out of consideration. In February, 1932, another set of observations was begun and was continued until October of that year, 55 additional plates being obtained in the interval. Again the same characteristics as in the previous year were evident, the range of the residuals derived from the annual mean velocity being of the same magnitude and exhibiting the same progressive tendency as did those of the year before. Neither series of observations could be represented by either of Cannon's periods, and it was at once evident that the period would have to be of the order of ten or eleven years in order to represent the velocities of the present series, together with those obtained here in the years 1900–1902 with the original Mills spectrograph and those since 1905 with the new Mills spectrograph. Observations were therefore continued through the following ten years, thus affording a continuous series extending over one cycle, and these form the basis of the present investigation.

In the interval from May, 1931, to September, 1942, 341 spectrograms were taken by

* *Contributions from the Lick Observatory*, Ser. II, No. 8.

[1] *Lick Obs. Bull.*, **4**, 162, 1907.

[2] *Pub. Dom. Obs.*, Ottawa, **1**, 375, 1912.

the writer with occasional help from Dr. Moore and Dr. G. F. Paddock. They were made with the three-prism Mills spectrograph, which has a linear dispersion of about 10 A/mm at λ 4500. Prior to the spring of 1941, Eastman 40 plates were employed, for which the normal exposure time for this star was 56 minutes. At that time the prisms were coated with a film of lithium fluoride, and the collimator and camera lenses with one of magnesium fluoride, which effected a 60 per cent decrease in the required exposure time, thus permitting the use of Eastman 33 with an exposure time of only 30 minutes. The slit-width throughout the program was 0.025 mm.

The spectrum of β Coronae Borealis contains numerous excellent lines suitable for radial-velocity measurement and is classified by Harvard as F0p. It is peculiar in "the relative intensities of the lines and resembles the spectrum of α Persei, except that the lines appear to be less narrow." Mount Wilson assigns the spectrum to an earlier class, A7s. No secondary spectrum is visible, nor has any evidence of change in width of the lines been found. The measurable region of the spectrograms lies between λλ 4390 and 4620, the line λ 4500 being central. In this region the spectrum of β Coronae Borealis has about 200 measurable lines, all of which may readily be identified by means of the data given in Dunham's description of the spectrum of α Persei.[3] Of these, 60 lines that were free from blends were selected for the measurement on a plate of this star which was taken for use as a standard on the Hartmann spectrocomparator. This spectrogram, obtained on April 7, 1934, was measured by me several times on a Toepfer measuring engine, yielding the adopted velocity of −22.10 km/sec, corresponding to the displacement of the stellar lines with reference to those of the comparison spectrum. The other 340 plates were measured against this standard, and data for these are given in Table 1.

A velocity-curve was obtained by plotting the data for the series of observations 1931–1942, given in Table 1, and has a double amplitude of 18 km/sec with a period of approximately 10.5 years. Upon this there appears to be superimposed a variation having a double amplitude of nearly 3 km/sec with a period of a little less than a year.

Preliminary elements for the long-period system were first derived from the velocity-curve drawn through normal points formed by taking the annual means of the velocities, the eight early observations of 1900–1907 being utilized in determining the period. The period being regarded as known, differential corrections to the other five elements were computed by the method of least squares, which yielded the following values:

PRELIMINARY ELEMENTS

P =	10.504		years
T =	2428964.3	± 49.5	JD
K =	9.09	± 0.42	km/sec
e =	0.51	± 0.03	
ω =	176.4°	± 5.5°	
γ =	−19.11		km/sec

The 341 observations were then regrouped into 57 normal places, consisting of monthly means of the velocities. On the basis of the preliminary elements derived above from annual means, the residuals given for the 57 normal places were formed, and a second set of elements was derived by a least-squares solution, in which the period was included. These elements, which resulted in a 50 per cent decrease in the sums of the

[3] *Contr. Princeton Obs.*, No. 9, 1929.

TABLE 1

RADIAL-VELOCITY OBSERVATIONS OF β CORONAE BOREALIS, 1931–1942

Date	JD	Vel. (Km/Sec)	Date	JD	Vel. (Km/Sec)
	2420000+			2420000+	
1931 May 5.....	6466.724	−16.30	1931 Oct. 2.....	6616.617	−14.16
	.884	17.32	5.....	19.632	14.92
	.923	16.43	12.....	26.622	13.86
6.....	67.729	16.90	15.....	29.606	13.47
	.886	16.68	19.....	33.606	13.97
7.....	68.746	16.66			
10.....	71.823	16.24	1932 Feb. 19.....	6756.972	15.21
16.....	77.742	16.74			
	.788	16.99	Mar. 28.....	94.923	16.17
	.850	17.46			
27.....	88.822	17.10	Apr. 8.....	6805.826	15.50
	.862	17.76		.871	15.90
	.900	17.25	9.....	6.843	15.93
				.908	16.48
June 2.....	94.854	16.56	11.....	8.848	16.68
	.883	17.56		.912	15.55
3.....	95.850	16.29			
	.878	16.26	May 10.....	37.882	16.74
4.....	96.872	14.96		.923	16.32
11.....	6503.871	15.20	11.....	38.919	16.31
12.....	4.805	16.06		.960	16.08
	.849	15.93	12.....	39.741	16.39
17.....	9.712	16.68		.797	16.10
	.766	15.48		.858	15.73
22.....	14.758	15.16		.906	16.16
	.803	15.24		.956	16.04
			13.....	40.931	16.27
July 1.....	23.888	15.78	16.....	43.853	16.18
2.....	24.815	16.67	17.....	44.738	16.16
12.....	34.713	16.16		.787	15.40
15.....	37.742	15.53		.856	15.65
	.790	15.60	19.....	46.785	15.84
23.....	45.682	15.29	26.....	53.837	15.52
27.....	49.686	14.97	27.....	54.748	15.18
	.721	14.90			
			June 4.....	62.816	16.28
Aug. 1.....	54.717	15.39		.868	15.55
	.757	15.59	8.....	66.782	15.60
7.....	60.671	15.29		.832	15.48
13.....	66.683	15.29	9.....	67.785	15.74
19.....	72.691	14.98		.834	16.10
28.....	81.650	14.55	10.....	68.705	16.15
				.746	16.33
Sept. 7.....	91.693	15.07	17.....	75.784	15.61
10.....	94.669	14.71		.834	15.22
14.....	98.654	15.26	20.....	78.805	15.34
16.....	6600.641	15.16		.854	15.85
17.....	1.634	16.00	24.....	82.739	15.93
18.....	2.646	15.39		.790	15.66
21.....	5.639	14.97	26.....	84.799	15.44
22.....	6.654	14.60		.841	15.40
23.....	7.643	14.71	29.....	87.790	15.25
24.....	8.610	15.08		.840	14.71
25.....	9.628	14.06			
26.....	10.625	14.64	July 3.....	91.840	14.26
28.....	12.629	−14.87		.895	−14.31

TABLE 1—*Continued*

Date	JD	Vel. (Km/Sec)	Date	JD	Vel. (Km/Sec)
	2420000+			2420000+	
1932 July 7	6895.705	−15.17	1934 Apr. 7	7534.897	−15.20
	.751	15.35		.974	15.46
15	6903.690	14.97	13	40.846	15.53
	.736	14.91		.888	15.20
	.782	15.06	26	53.852	16.15
				.913	15.54
Aug. 15	34.627	14.57			
	.677	13.35	May 18	75.852	15.69
31	50.654	14.69		.904	14.26
	.699	14.30			
			Aug. 6	7655.709	13.44
1933 Feb. 27	7130.940	15.25		.772	15.44
	.990	15.17			
			1935 Mar. 11	7872.871	15.70
Mar. 9	40.914	14.77		.922	15.31
	.967	15.43	14	75.883	16.62
19	50.885	14.69	31	93.024	16.46
	.948	15.19			
			May 3	7925.913	16.66
Apr. 2	64.875	15.77		.962	16.85
	.923	15.43	8	30.884	16.75
	.971	15.59		.927	16.75
13	75.886	16.04	14	36.904	16.11
	.950	15.22	28	50.816	16.43
May 19	7211.748	15.56	June 5	58.866	16.73
	.798	15.32	15	68.857	16.36
24	16.730	15.38		.914	16.98
	.773	15.80	22	75.756	16.97
June 21	44.756	15.69	July 10	93.798	17.27
	.801	15.89		.843	16.96
July 3	56.752	14.64	Sept. 11	8056.655	19.08
	.795	14.49	20	65.656	17.67
	.828	15.00			
5	58.715	15.71	1936 Feb. 4	8202.929	18.58
	.758	14.66		.974	18.88
7	60.757	14.12	27	25.947	19.26
	.799	15.13		.989	19.23
12	65.806	14.69			
14	67.805	15.16	Mar. 5	32.923	20.92
15	68.796	13.68		33.007	20.41
31	84.714	14.84	14	42.912	19.44
				.955	19.03
Aug. 29	7313.661	13.84	20	48.945	20.00
30	14.654	14.80			
			Apr. 14	72.820	20.34
Sept. 7	22.960	13.69		.863	19.79
28	43.612	13.83	25	83.751	19.74
Oct. 18	63.600	14.45	June 9	8328.852	19.96
			17	36.826	19.52
1934 Jan. 31	7469.006	16.59	24	43.828	19.25
	.055	17.19			
			1937 Apr. 16	8639.938	25.84
Mar. 2	98.938	16.56		.982	25.51
	.987	−15.84	25	49.949	−26.08

TABLE 1—*Continued*

Date	JD	Vel. (Km/Sec)	Date	JD	Vel. (Km/Sec)
	2420000+			2420000+	
1937 May 5	8658.938	−26.76	1939 May 2	9385.890	−24.50
	.992	26.11		.929	24.75
17	70.697	25.54		.973	25.83
	.757	26.24			
	.801	26.36	Aug. 24	9499.697	22.37
	.850	26.70		.740	23.05
	.892	26.31	31	9506.666	22.98
	.935	26.51			
	.977	26.75	Sept. 7	13.648	22.19
July 26	8740.727	30.28	1940 Feb. 9	9669.052	19.53
	.770	31.70			
			Mar. 3	91.925	18.87
Sept. 10	86.654	32.84	8	96.989	19.43
	.697	32.22		97.048	19.63
			13	9701.958	19.00
1938 Feb. 20	8950.023	30.58		2.023	19.27
24	53.939	32.16	23	12.958	18.27
Apr. 1	90.015	32.74	Apr. 13	32.971	19.00
17	9006.019	33.04		33.017	19.27
			21	40.972	19.49
May 8	26.956	34.62			
	.998	34.19	May 21	70.847	17.90
15	33.918	34.82		.890	17.95
18	36.938	33.47			
24	42.827	33.22	June 13	93.784	17.37
31	49.833	34.43			
			July 16	9826.755	17.47
June 9	58.836	33.03		.795	17.04
			17	27.735	17.89
1939 Mar. 14	9336.906	25.33		.778	17.03
	.956	25.69	19	29.785	17.15
16	38.910	25.10			
	.955	25.30	Aug. 22	63.670	16.59
29	51.848	25.81			
31	53.885	26.11	Sept. 10	82.651	16.80
	.928	25.47			
	.979	26.30		2430000+	
			1941 Apr. 13	0097.989	16.41
Apr. 1	54.896	25.60	14	98.932	16.26
4	57.793	25.29	20	104.973	16.47
	.863	25.58		5.013	15.94
	.906	25.00			
7	60.921	26.27	May 7	21.912	16.09
	.971	25.40			
8	61.780	25.85	June 9	54.828	16.09
	.826	25.67	13	58.815	15.97
14	67.966	25.85		.848	15.21
18	71.768	25.82			
28	81.901	24.95	July 10	85.732	15.28
29	82.892	25.80			
	.935	25.65	1942 Mar. 1	0420.020	14.80
			3	21.954	14.85
May 2	85.725	25.29	5	23.954	14.74
	.769	25.11		.978	15.15
	.810	25.31	8	26.979	15.52
	.847	−24.17	17	35.902	15.41
				.921	−14.65

TABLE 1—*Continued*

Date	JD	Vel. (Km/Sec)	Date	JD	Vel. (Km/Sec)
	2430000+			2430000+	
1942 Apr. 15.....	0464.861	−15.07	1942 June 19.....	0529.705	−13.42
	.885	14.23	21.....	31.715	13.35
25.....	74.936	14.53		.750	13.89
26.....	75.803	13.99	30.....	40.679	14.06
	.839	14.47		.717	13.67
May 3.....	82.779	13.59	July 5.....	45.780	13.73
	.815	14.25		.809	14.02
6.....	85.776	14.27	7.....	47.698	13.75
	.809	14.26		.725	13.34
	.840	14.16	9.....	49.693	13.58
	.882	14.13		.723	13.99
	.915	13.73	14.....	54.716	13.40
17.....	96.813	14.33		.742	13.78
	.851	13.51	19.....	59.670	13.87
19.....	98.698	13.57		.692	13.30
	.738	13.95	26.....	66.734	14.02
	.772	13.71		.757	13.73
	.802	13.07			
	.833	13.48	Aug. 2.....	73.685	13.95
	.861	12.88		.711	14.39
	.891	12.86	4.....	75.663	14.49
				.685	14.15
June 3.....	0513.726	13.93	25.....	96.673	15.17
	.759	13.75		.699	14.52
	.798	13.03			
	.835	13.03	Sept. 10.....	0612.640	14.40
13.....	23.687	14.00		.664	−14.65
	.721	−13.87			

squares of the residuals, are adopted as the final ones for the long-period system and are as follows:

FINAL ELEMENTS

$$
\begin{aligned}
P &= 10.496 \pm 0.001 \text{ years} \\
T &= 2428971.3 \pm 18.09 \text{ JD} \\
K &= 9.19 \pm 0.23 \text{ km/sec} \\
e &= 0.406 \pm 0.025 \\
\omega &= 185.4^\circ \pm 2.2^\circ \\
\gamma &= -18.03 \text{ km/sec} \\
a \sin i &= 442{,}000{,}000 \text{ km} \\
f(m) &= 0.24 \odot
\end{aligned}
$$

The probable error of a normal place of unit weight is ±0.67 km/sec. Data for the 57 normal places are entered in Table 2, the first two columns of which contain, respectively, the mean date of the observation in Julian Days and the corresponding mean radial velocity. In the third column are given the residuals O − C for the normal places computed on the basis of the final elements, the number of observations combined to form the normal place or its assigned weight being listed in the final column. The fourth column will be explained later.

TABLE 2

NORMAL PLACES

JD	Vel. (Km/Sec)	Orbit (O−C)	Corrected for Secondary (O′−C′)	Weight
2420000+				
6475.129	−16.91	−2.00	−0.60	13
6503.408	15.95	−1.12	+0.18	12
38.005	15.61	−0.85	+0.33	8
67.558	15.15	−0.49	+0.36	7
6603.951	14.96	−0.37	+0.15	13
25.217	14.08	+0.48	+0.66	5
6756.972	15.21	−0.83	−1.22	1
94.923	16.17	−1.72	−0.32	1
6807.173	16.01	−1.69	−0.29	6
43.461	16.00	−1.68	−0.48	18
75.136	15.65	−1.34	−0.34	18
98.057	14.86	−0.56	+0.26	7
6942.664	14.28	+0.07	+0.29	4
7140.941	15.08	−0.66	+0.50	6
69.321	15.61	−1.17	+0.13	5
7214.262	15.52	−1.00	−0.10	4
44.778	15.79	−1.23	−0.75	2
63.320	14.74	−0.15	−0.03	11
7317.002	14.11	+0.58	−0.30	3
53.606	14.14	+0.64	−0.64	2
7483.965	16.54	−1.43	−0.14	4
7543.238	15.45	−0.14	+0.65	6
75.878	14.98	+0.45	+0.74	2
7655.740	14.44	+1.31	+0.19	2
7878.675	16.02	+0.92	+1.47	4
7933.568	16.59	+0.72	+0.40	6
68.098	16.76	+0.81	−0.19	4
93.820	17.12	+0.64	−0.68	2
8061.156	18.38	−0.07	+0.73	2
8214.460	18.99	+0.79	+1.09	4
40.148	19.96	+0.27	+0.17	5
76.478	19.95	+0.75	+0.15	3
8336.502	19.55	+1.97	+0.69	3
8642.956	25.81	+1.67	+0.27	3
68.204	26.45	+1.72	+0.94	9
8740.748	30.99	−1.20	+0.16	2
86.676	31.90	−1.76	−0.65	2
8951.981	32.43	+0.35	−0.93	2
98.017	32.89	−0.42	−0.82	2
9036.245	34.12	−2.11	−0.71	6
58.836	33.03	−1.32	+0.06	1
9345.671	25.63	−0.88	+0.22	8
73.118	25.46	−1.32	+0.08	20
9503.950	−22.65	−1.16	−0.90	4

TABLE 2—*Continued*

JD	Vel. (Km/Sec)	Orbit (O−C)	Corrected for Secondary (O′−C′)	Weight
2420000+				
9669.052.....	−19.53	−0.45	+0.73	1
9710.048.....	19.08	− .38	+0.93	6
35.653.....	19.25	− .93	+0.33	3
78.507.....	17.74	+ .17	+1.01	3
9828.098.....	17.34	+ .10	+0.22	6
73.166.....	16.70	+ .37	−0.33	2
2430000+				
0105.764.....	16.24	− .59	+0.07	5
164.556.....	15.64	− .22	−0.36	4
0426.958.....	15.83	− .40	+0.26	7
487.448.....	13.91	+ .60	+0.44	21
525.190.....	14.46	+ .05	−0.87	11
554.062.....	13.71	+ .70	−0.68	12
589.675.....	−14.46	−0.08	−0.86	8

The velocity-curve of the long-period system of β Coronae Borealis in the interval 1931–1942 is given in Figure 1. It was computed from the final elements; and upon the diagram the 57 normal points representing the 341 observations have been indicated by small circles. The small secondary variation in velocity, to which reference has already been made, is apparent on the diagram, as well as in the run of the residuals in the third column of Table 2, especially for the first four years of observation, 1931–1934. Since the amplitude of the variation is small, considerable difficulty was encountered in deriving a curve which would represent the residual velocities from the long-period velocity-curve. After numerous trials the best representation was obtained by the curve for the secondary variation reproduced in Figure 2, in which the 57 normal places are represented by circles and the 9 normal points into which they were combined by dots. From this curve the following approximate elements were derived:

$$P' = 320.13 \text{ days} \qquad \omega' = 102°$$
$$T' = 2426475 \text{ JD} \qquad a' \sin i' = 4{,}400{,}000 \text{ km}$$
$$K' = 1.4 \text{ km/sec} \qquad f'(m) = 0.000034\ \odot$$
$$e' = 0.7$$

When the 57 normal places were corrected for the effect of the secondary variation having the elements derived above, the residuals O′ − C′ with reference to the long-period velocity-curve, given in the fourth column of Table 3, were obtained. By this procedure the probable error of a normal place of unit weight was reduced to ±0.4 km/sec, while the sum of the squares of the residuals was reduced from (O − C) 336.89 to (O′ − C′) 97.35. Although the 70 per cent reduction in residuals thus effected would seem to offer evidence of considerable weight in favor of the reality of the short-period variation, it cannot be considered conclusive, for the secondary curve was obviously so derived as to effect a reduction in the original residuals of the normal places. After the removal of the secondary variation, the 57 normal places were again plotted on the long-period velocity-curve, and the diagram thus obtained is reproduced in Figure 3. While the representation of the observations has obviously been somewhat improved over that shown in Figure 1, especially in the portion of the curve for the years 1931–1934, it must

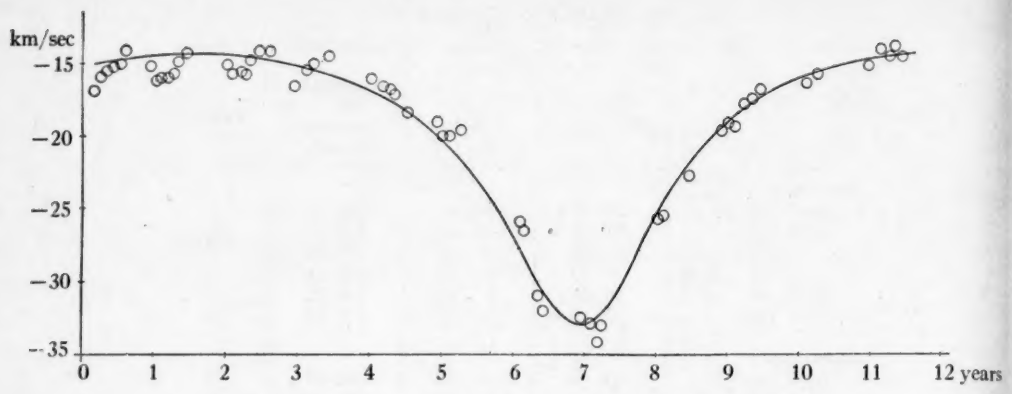

FIG. 1.—Velocity-curve of β Coronae Borealis, 1931–1942

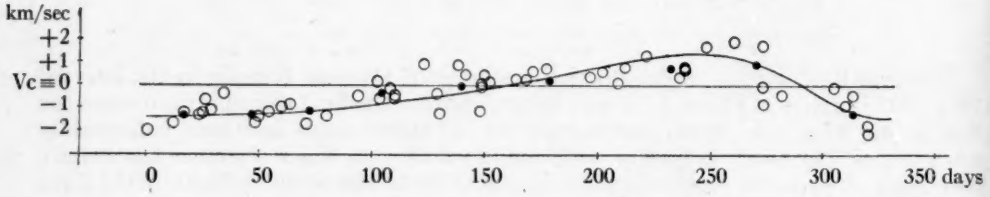

FIG. 2.—Velocity-curve of secondary variation

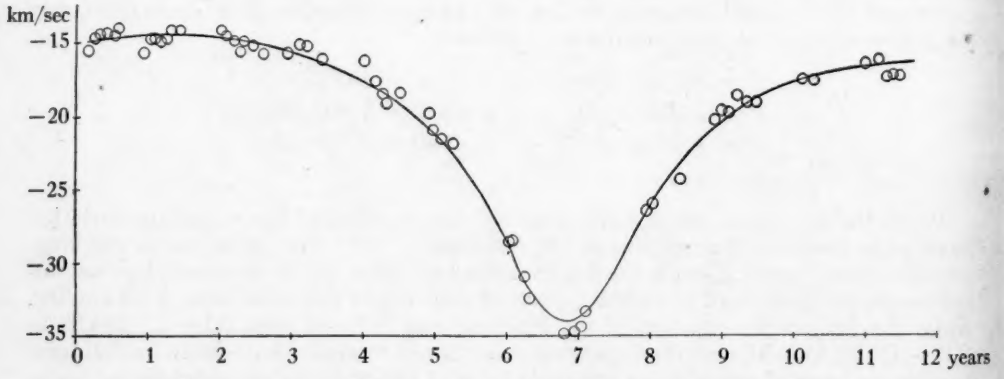

FIG. 3.—Velocity-curve of β Coronae Borealis, 1931–1942. Observations corrected for short-period variation.

be admitted that little or no improvement appears to have been effected in the representation of the observations for other parts of the curve obtained in later years.

Since the period of secondary variation indicated is nearly a year, consideration has been given to the question of its possible origin in instrumental or other errors of a seasonal nature. Thus it is known[4] that small errors in the velocity determinations made with the Mills spectrograph are produced by changes in collimation due to flexure in the tube of the 36-inch refractor. Such errors depend upon the declination and hour angle of the star and are of opposite signs for spectrograms obtained with the telescope on opposite sides of the pier, positions of the instrument required in observing the same star at different seasons of the year. The effects of such errors, however, have been carefully determined for all positions of the telescope, and corrections for them are applied to all observations made with this spectrograph, including those of the present investigation. Constants used in computing the "reduction to sun," errors which would introduce seasonal effects in the velocity, also have been checked. Furthermore, an examination of the radial-velocity measures of other stars made with this instrument in the interval 1931–1942 shows no evidence of the presence of variations of the character here considered. The evidence, therefore, appears to be quite definite that secondary variations of several kilometers per second do occur in the radial velocity of β Coronae Borealis, although the available data are not sufficient to determine satisfactorily whether these are strictly periodic. In order to throw further light upon the nature of these small variations, further observations will be required, and to this end it is planned to obtain several series of spectrograms within the next few years.

TABLE 3

RADIAL-VELOCITY OBSERVATIONS OF β CORONAE BOREALIS
PRIOR TO 1931 AND IN 1943

Date	JD	Vel. (Km/Sec)	(O−C)	(O′−C′)	Remarks
1900 Apr. 18....	2415128.89	−17.8	−3.0	.....	*Pub. Lick Obs.* Vol. **16**, 1928
May 13....	53.79	18.1	−3.6	.....	
01 May 6....	5511.83	18.1	−3.8	.....	
02 Feb. 13....	5794.06	15.1	−0.5	.....	
05 Apr. 11....	6947.03	23.2	+0.4	.....	
07 Mar. 29....	7664.06	29.4	0.0	.....	
Apr. 8....	74.96	31.0	−1.9	.....	
July 17....	7774.71	26.8	−0.2	.....	
13 Feb. 13....	9798.64	15.7	−0.6	.....	Cape*
Mar. 19....	9826.57	22.3	−7.1	.....	Cape
16 June 16....	2421031.30	26.3	+2.6	.....	Cape
30 Feb. 16....	6023.975	17.68	−0.37	−0.37	Lick
Mar. 11....	46.924	17.27	−0.22	+ .89	
43 July 17....	2430922.708	13.93	+0.43	+ .25	
Sept. 4....	971.649	15.86	+1.45	+ .07	
	.674	15.53	+1.08	− .30	
14....	981.641	−15.98	+1.55	+0.23	

* Observations made at the Cape of Good Hope, *Cape Ann.*, **10**, Part VIII, 1928.

[4] *Pub. Lick Obs.*, **16**, xxv, 1916.

Observations made with the three-prism dispersion prior to and later than those listed in Table 1, which were used in the above discussion only for a determination of the period of the long-period system are given in Table 3. Data for the first four, taken with the original three-prism Mills spectrograph, are published in *Publications of the Lick Observatory*, Volume 16. The radial velocities entered for the Lick observations 1905–1930 are my measures of these spectrograms made on the Hartmann spectrocomparator against the same standard plate that was used in the measurement of the plates listed in Table 1. After completion of the present investigation, four spectrograms were obtained in 1943, and these are included in Table 3. The residuals (O − C) with reference to the long-period curve, and the (O′ − C′) after correction for the secondary variation are entered in the fourth and fifth columns. On account of the uncertainty in the short-period O′ − C′ residuals have not been given for observations earlier than 1930.

Mr. Cannon's 153 one-prism observations of this star were made in the interval February 23, 1910—July 23, 1912, during which time the velocity computed on the basis of the elements here derived for the long-period system varies from −15.2 to −14.3 km/sec. His observations for this interval range from −25.2 to −18.9 km/sec and, when compared with the computed values, yield a mean residual of (O − C) = −7.03 km/sec.

The trigonometric parallax of this star given in Schlesinger's *General Catalogue of Stellar Parallaxes* (1935) is 0″.033, which yields a value for $a \sin i$ of 0″.09. There is thus a possibility that the two components could be separated near apastron with a large telescope, the favorable time for such observations being in 1944–1946. In this connection it should be noted that the Allegheny observers have found from their parallax plates evidence of the orbital motion of the brighter star in a period which is of the order of that obtained for the long-period system in the present investigation.

RADIAL VELOCITIES OF 283 STARS OF SPECTRAL CLASSES R AND N*

ROSCOE F. SANFORD
Mount Wilson Observatory
Received December 2, 1943

ABSTRACT

Radial velocities of 283 stars of spectral classes R and N are given in Table 1. By intercomparison with velocities obtained from spectrograms of high dispersion, these are found to be free from systematic errors. Thirty-four class-N stars (28 known to be light-variables) with *emission lines of hydrogen* have a mean difference of -20.4 ± 0.9 km/sec between the velocity from the emission lines (mostly $H\alpha$ alone) and that from the absorption lines.

Galactic concentration is marked for class-N stars, slight for class-R.

Mean absolute magnitudes of -2.3 ± 0.2 for class-N stars and of -0.4 ± 0.4 for class-R stars have been derived from differential galactic rotation.

Interstellar sodium lines.—The radial velocities of 2 class-N stars and 4 class-R stars are sufficiently large to separate the stellar from the interstellar sodium lines. Velocities and approximate values of the equivalent widths have been derived from the interstellar lines. The distances and absolute magnitudes have been obtained from the equivalent widths. The mean magnitude for the 2 class-N stars is -1.8 and for the 4 class-R stars, 0.0.

Stars of high velocity.—Table 4 contains 1 class-N star and 7 class-R stars, whose velocities, when freed from solar motion, are numerically larger than 100 km/sec. All 7 class-R stars have spectra with strong g-bands, but with few atomic lines.

A catalogue of radial velocities, mostly of stars of spectral classes N and R, was published by the writer eight years ago in *Mount Wilson Contributions*, No. 525.[1] This catalogue contains 191 stars, of which 187 were observed at Mount Wilson and 4 at Santiago, Chile, by the D. O. Mills Expedition. The distribution in type is: class N, 147 stars; class R, 40; class S, 3; peculiar, 1.

Some of these velocities were measured with the Hartmann spectrocomparator, but most of them with a micrometer measuring engine. The velocities for the standards used on the Hartmann spectrocomparator were based upon velocities obtained by J. H. Moore[2] for class-N stars and upon those obtained by W. C. Rufus[3] for class-R stars. For the micrometer, lines were chosen and their wave lengths determined on the basis of Moore's velocities for class N and Rufus' velocities for class R.

In *Mt. W. Contr.* No. 525 it was concluded that Moore's velocities for class-N stars and those derived both by the Hartmann comparator and by micrometric measurement at Mount Wilson needed a systematic correction of -7 km/sec, and this correction was applied. The velocities of class-R stars appear as measured originally.

Observations of class-N and class-R stars were resumed at Mount Wilson in 1935 and have been continued when conditions permitted during the next eight years. Improved photographic plates, especially the Eastman 103 F-emulsion for the yellow-red region, have greatly facilitated observing the fainter stars and have made it possible to observe many of the brighter stars with high dispersion.

Spectrograms of the faint stars of class N having a dispersion of 65 A/mm were obtained in the yellow-red region with the Cassegrain plane-grating spectrograph.[4] For

* *Contributions from the Mount Wilson Observatory, Carnegie Institution of Washington*, No. 689.

[1] *Ap. J.*, **82**, 202, 1935.

[2] *Lick Obs. Bull.*, **10**, 79, 1923.

[3] *Pub. Astr. Obs. U. Michigan*, **2**, 45, 1916.

[4] *Mt. W. Contr.*, No. 432; *Ap. J.*, **74**, 188, 1931.

class R, spectrograms with a dispersion of about 70 A/mm at $H\gamma$ for the brighter stars and 100 A/mm for the fainter ones were obtained in the blue-violet region with one-prism spectrographs. Spectrograms (dispersion either 20, 10, or 5.9 A/mm) of 30 bright class-N and 10 bright class-R stars have been obtained with the coudé plane-grating spectrograph.

Additional velocities are now available for 106 of the stars in *Mt. W. Contr.* No. 525 and for 45 class-N and 48 class-R stars not previously measured. These 93 stars, observed for the first time, were largely selected from the *Henry Draper Catalogue* and from the lists of discoveries made by objective prism at Mount Wilson[5] and at the Dearborn Observatory.[6] The improved values for velocities in *Contribution* No. 525, together with the velocities for the 93 other stars, make it desirable to issue a completely new catalogue.

The catalogue.—All stars of classes N and R with measured radial velocities are listed in Table 1. Of the 283 stars included, all have been observed at Mount Wilson except 4 class-N stars observed at Santiago, Chile. The designation MSB indicates the Mount Wilson lists of stars discovered on objective-prism plates;[5] Lee indicates stars similarly discovered at the Dearborn Observatory.[6]

The magnitudes have been taken from various sources. Visual magnitudes for non-variable stars are from the *Henry Draper* and *Bonner Durchmusterung* catalogues, from the *Dearborn Observatory Annals*, and, lastly, if no value is available, from estimates by the writer at the finder or at the guiding telescope. These estimates are in parentheses. The magnitudes for the maxima and minima of variable stars are, for the most part, from Schneller's "Catalogue and Ephemeris of Variable Stars."[7] Photographic magnitudes are underscored.

All the stars are placed in one or the other of the Harvard spectral classes N or R. Those in class N have not, however, been subdivided with the letters a, b, and c, as in the Harvard classification, or with the numbers 1–9, as in C. D. Shane's[8] classification. Only the broad classification N has been used, with e appended when the spectrum has bright lines and p when the spectrum is peculiar.

Keenan and Morgan[9] have published a new system of classification for stars with carbon bands. Two of the data which they use as criteria are given in Table 1; the eleventh column contains estimates of the strength of the D lines on an arbitrary scale of 1–9, and the twelfth column, estimates of the strength of the Swan band-head at λ 6192 on a scale of 1–5. By means of these two columns at least a rough conversion of class-N stars to the classification of Keenan and Morgan can be made, if desired.

The subdivisions of class R in the tenth column of Table 1 resemble closely those of the *Henry Draper Catalogue*, except that the progression in the strength of the isotope bands of $C^{12}C^{13}$ has here relatively more influence. These class-R stars may be put into Keenan and Morgan's classification by using the nearly linear relation which it bears to the *Henry Draper* classification.[10]

Although their classification may provide a better temperature sequence than the Harvard classification, it is still unsatisfactory in some respects; it seems not to be consistent with the observed relatively low intensity of the D lines in the spectrum of some extremely red class-N stars, like VX Andromedae, for example. The contents of the tenth, eleventh, and twelfth columns may therefore serve as a compromise classification until such difficulties are removed.

The mean absorption-line velocities in Table 1 have been formed with appropriate

[5] *Pub. A.S.P.*, **45**, 306, 1933; **54**, 107, 1942.

[6] *Dearborn Obs. Annals*, **4**, Part 16, 1940.

[7] *Kleinere Veröff. Sternwarte Berlin-Babelsberg*, No. 21, 1939.

[8] *Lick Obs. Bull.*, **13**, 123, 1928.

[9] *Ap. J.*, **94**, 501, 1941.

[10] *Ibid.*, Fig. 1.

weight for the velocities of class-R stars by Rufus and of class-N stars by Moore. A systematic correction of −7 km/sec was first applied to Moore's values.

The letters accompanying the velocities express the writer's judgment of the probable accuracy. The uncertainties are about as follows: a, 1 km/sec; b, 2–3 km/sec; c, 4–5 km/sec; d, 6–8 km/sec. Velocities with the letter e usually depend upon a single low-dispersion spectrogram taken primarily to check the spectral classification. It was not practicable to obtain more spectrograms. The underscored velocities depend largely or wholly upon those obtained from coudé spectrograms. The emission-line velocities in the last column of Table 1 are derived for the most part from *Hα*.

The radial velocities from absorption lines.—The velocities of class-N and class-R stars in Table 1 are on the same basis as those in *Mt. W. Contr.* No. 525. Before using these velocities it had to be ascertained whether they were free from systematic errors, which was done by comparing the velocities obtained with the coudé spectrograph with those for the same stars with the smaller dispersions.

The velocities from coudé spectrograms could be so used because experience has shown that this spectrograph is practically free from instrumental errors and because the following considerations assured accurate wave lengths for the absorption lines used for velocity measurement. Many atomic lines with well-known wave lengths are well isolated for measurement in the blue-violet region of classes N and R and in the yellow-red region of early class R. Lines of comparable quality in the yellow-red region of the spectrum of late class-R and class-N stars belong to the band spectrum of cyanogen. Wave lengths for these lines were obtained by referring them to the lines in the neon comparison spectrum on a coudé spectrogram of the carbon arc. Comparison showed that the weighted mean difference, coudé *minus* low dispersion, for 26 suitably observed class-N stars is −0.4 ± 0.6 km/sec and for 7 class-R stars +0.0 ± 0.8 km/sec. There appears, therefore, no reason to apply systematic corrections to the velocities of class-R or class-N stars obtained with lower dispersion.

Velocities from bright hydrogen lines.—Thirty-four stars of class N with hydrogen emission lines appear in Table 1. All are known variable stars with the exception of six of the Mount Wilson objective-prism discoveries and one of Lee's stars. These also may turn out to be variable when adequately observed. At any rate, the evidence is strong that emission lines of hydrogen are favored by variability. Sufficient spectroscopic observations have been made at all phases of a number of these variables to show that the emission lines are at their maximum strength near maximum light and practically vanish for a considerable interval before and after light-minimum.

For the most part, the emission-line velocity has been derived from *Hα* alone. This velocity is invariably smaller algebraically than the absorption-line velocity. The weighted mean difference (emission *minus* absorption) for these 34 stars is −20.4 ± 0.9 km/sec. The correlation of this difference with the length of the period of light-variation is weak, there being, perhaps, a slight tendency to larger negative values for the longer periods.

Galactic distribution.—Stars of class N are plotted by galactic co-ordinates in Figure 1, which shows marked galactic concentration; only about 10 per cent of the stars are more than 30° from the galactic plane, and these are predominantly bright stars whose real distances from the plane cannot be great. In contrast, stars of magnitude 9.0 or fainter lie for the most part within 10° of the galactic plane. The galactic concentration of stars of class R (Fig. 2) is not marked.

The mean absolute magnitudes.—Studies of the motions of distant celestial objects have amply demonstrated the differential effects of galactic rotation. This rotation produces a double sine-curve of velocity variation for the 360° of galactic longitude. Previous values of the semi-amplitude of this curve for a distance of 1000 parsecs range from 15 to about 20 km/sec. A recent discussion by R. E. Wilson[11] of the best available data gives 17.7 km/sec/kiloparsec.

[11] *Mt. W. Contr.*, No. 631; *Ap. J.*, **92**, 170, 1939.

TABLE 1

RADIAL VELOCITIES OF STARS OF CLASSES R AND N

Star	HD or MSB	1900 R.A.	1900 Decl.	Galactic l	Galactic b	Magnitude Max.	Magnitude Min.	Period (Days)	Spect.	Intensity Na	Intensity C_2	Vel.(Km/sec) Abs.	Vel.(Km/sec) Em.
UX Cas	MSB 43	$0^h\ 8^m.0$	+62°54'	86°	+ 1°	12.0	13.8	...	R2	.	.	-11 d	...
ST Cas	1306	12.2	+49 44	85	-12	7.5	9.0	...	N	5	4	-43 c	...
VX And	1546	14.6	+44 9	85	-18	8.1	9.5	367?	N	5	4	+ 9 a	...
MSB 44	.....	17.2	+58 34	87	- 4	(9.8)	....	...	N	6	3	-46 c	...
.....	1994	19.1	+53 44	87	- 8	9.7	....	...	R6	.	.	-36 c	...
AQ And	2342	22.2	+35 2	86	-27	7.8	8.0	332	N	5	4	-14 a	...
.....	5223	48.9	+23 32	91	-32	8.8	....	...	R3	.	.	-232 a	...
MSB 45	.....	1 5.0	+53 11	94	- 9	(10.5)	....	...	Ne	4	3	-19 c	-44
Z Psc	7561	10.6	+25 14	98	-36	7.4	8.1	...	N	7	3	+18 a	...
R Scl	8879	22.4	-33 4	211	-80	6.2	8.8	376	Np	6	4	- 8 c	...
WW Cas	MSB 1	27.1	+57 14	96	- 4	9.1	11.7	...	N	6	4	-59 b	...
.....	10636	38.7	+53 28	99	- 8	9.9	....	...	R6	.	.	-30 c	...
X Cas	.....	49.8	+58 46	99	- 1	8.4	13.1	425	Ne	5	4	-55 a	-80
V Ari	13826	2 9.6	+11 47	122	-44	8.3	9.0	...	R0	0	3	-176 a	...
MSB 2	.....	20.1	+51 37	105	- 8	(9.5)	....	...	N	6	3	-45 b	...
R For	.....	24.8	-26 33	181	-66	8.1	13.3	393	Ne	4	2	+30 b	+ 2
.....	16115	30.2	- 9 53	150	-58	8.3	....	...	R4	.	.	+16 a	...
VZ Per	MSB 46	31.6	+55 20	106	- 4	13.3	13.6	...	R4	.	.	-16 c	...
UY And	16326	32.1	+38 44	113	-18	11.0	14.0	149	N	6	4	-63 b	...
.....	19557	3 3.7	+57 31	108	0	8.1	....	...	R6	.	.	- 8 a	...
.....	19881	6.7	+47 27	114	- 8	9.2	....	...	Np	7	3	+ 8 b	...
.....	20234	10.0	-57 41	240	-50	5.7	....	...	N	.	.	+14 a	...
Y Per	21280	20.9	+43 50	118	- 9	8.3	11.0	254	R4e	2	2	- 9 a	-14
U Cam	22611	33.2	+62 19	109	+ 7	6.9	9.0	419	N	5	4	- 3 c	...
+51°762	MSB 3	33.9	+51 11	115	- 2	8.9	....	...	N	6	4	+ 6 c	...
AC Per	MSB 4	38.1	+44 28	120	- 7	10.2	12.3	...	N	6	4	-32 d	...
.....	25408	57.2	+61 32	111	+ 8	7.9	....	...	R8	.	.	- 8 a	...
+50°920	MSB 47	4 4.0	+51 4	119	+ 1	9.5	....	...	R3	.	.	-11 b	...
SY Per	MSB 6	8.9	+50 23	120	+ 1	9.5	12.5	476	Ne	4	4	- 1 d	-39
.....	27108	11.8	+26 6	138	-16	(10.2)	....	...	R4	.	.	-81 b	...
MSB 7	.....	13.0	+40 53	128	- 5	(9.0)	....	...	N	5	3	- 2 e	...
MSB 8	.....	22.9	+39 38	129	- 5	(9.0)	....	...	N	7	4	+ 9 c	...
AV Per	MSB 9	32.6	+41 26	130	- 2	13.5	15.0	...	N	5	5	+51 c	...
ST Cam	30243	40.8	+67 59	110	+16	7.0	8.3	...	N	6	4	-12 a	...
.....	30443	42.7	+34 49	136	- 5	9.0	....	...	R4	.	.	+70 a	...

T Cae	30593	4^h43^m8	-36°23'	205°	-39°	8.7	10.3	...	N	6	4	- 7 e	...
.....	30710	44.9	+15 37	151	-16	10.1	....	...	N	6	2	+38 c	...
TT Tau	30755	45.2	+28 21	142	- 9	8.1	8.8	166	N	6	3	+16 a	...
+38°955	MSB 10	45.7	+38 20	133	- 2	8.8	....	...	N	8	2	+32 b	...
AU Aur	MSB 11	46.8	+49 46	125	+ 5	13.5	[15	...	Ne	7	2	- 3 b	-23
Lee 8	.....	47.6	+22 35	147	-12	9.4	....	...	N	6	3	+48 d	...
R Lep	31996	55.0	-14 57	182	-31	6.1	9.7	440	Ne	6	5	+34 a	+21
.....	32088	55.6	+50 29	125	+ 7	9.0	....	...	N	4	3	-12 e	...
W Ori	32736	5 0.2	+ 1 2	167	-21	5.9	7.7	200	N	5	4	+16 a	...
TX Aur	33016	2.2	+38 52	135	+ 1	8.5	9.2	330	N	4	4	- 6 c	...
SY Eri	33404	4.9	- 5 38	173	-24	8.0	9.6	...	N	7	3	+ 8 d	...
+11°755	Lee 16	10.4	+11 52	158	-14	9.4	....	...	N	5	3	-11 c	...
.....	34467	12.5	+35 41	139	+ 1	9.1	....	...	N	7	3	+15 d	...
UV Aur	34842	15.3	+32 24	142	- 1	7.9	10.1	350	Ne	8	1	-10 a	-15
Lee 18	.....	15.8	+ 7 16	163	-15	10.4	....	...	N	5	3	-17 e	...
S Aur	35556	20.5	+34 4	141	+ 1	8.3	[12	591	N	6	4	+ 3 d	...
CM Aur	MSB 48	22.1	+43 21	134	+ 6	13	14.5	...	N	6	4	-28 e	...
+3°924	Lee 21	24.1	+ 3 23	168	-15	9.5	....	...	N	3	2	+14 c	...
RT Ori	36602	27.8	+ 7 4	165	-12	7.5	8.5	...	N	6	4	+ 5 c	...
S Cam	36972	30.2	+68 45	111	+20	7.8	10.8	324	R8e	.	.	-13 e	-17
.....	37212	31.7	-25 48	197	-26	7.9	....	...	N	4	3	+40 b	...
TU Tau	38218	39.1	+24 23	152	- 1	8.7	9.5	...	N	5	3	-24 c	...
Y Tau	38307	39.7	+20 39	155	- 3	6.9	8.9	241	N	5	3	+17 d	...
+15°921	MSB 13	39.7	+15 28	159	- 5	9.5	....	...	N	5	4	+22 e	...
AF Aur	38521	41.4	+44 50	134	+10	8.5	9.5	...	N	5	4	-11 e	...
.....	38572	41.7	+30 36	147	+ 2	9.0	9.3	...	N	8	3	+16 d	...
AZ Aur	MSB 15	54.2	+39 42	140	+10	10.5	15.5	416	Ne	8	2	+84 a	+65
XZ Aur	.....	56.9	+47 17	133	+13	12.0	13.2	...	N	4	4	+19 c	...
TU Gem	42272	6 4.7	+26 3	153	+ 5	7.4	8.3	...	N	6	3	+48 c	...
+8°1263	Lee 38	12.2	+ 8 34	169	- 2	9.5	....	...	N	6	4	+46 d	...
-0°1246	MSB 16	12.7	- 0 12	177	- 6	9.5	....	...	N	6	4	+34 e	...
MSB 17	.....	13.4	- 1 7	179	- 7	(9.2)	....	...	N	4	2	+80 e	...
V Aur	44388	16.5	+47 45	134	+17	8.3	[12.2	357	Ne	5	4	+ 6 e	+ 3
BN Mon	MSB 18	16.5	+ 7 21	171	- 2	13.0	15.3	...	N	6	4	+28 a	...
ZZ Gem	44653	17.8	+25 4	155	+ 7	8.9	9.9	...	Ne	3	1	+76 e	+64
-7°1402	MSB 20	18.5	- 7 25	184	- 8	9.5	....	...	N	5	4	+52 d	...
BL Ori	44984	19.8	+14 48	164	+ 2	6.6	....	...	N	6	3	+13 a	...
AB Gem	45087	20.3	+19 8	161	+ 5	8.2	9.8	...	N	6	4	+11 b	...
-26°2983	MSB 22	20.5	-27 1	202	-16	8.6	....	...	N	5	3	+23 e	...
+12°1177	MSB 23	25.3	+12 33	167	+ 3	9.4	....	...	N	3	4	- 8 d	...
Lee 50	.....	26.0	+16 11	164	+ 4	10.6	....	...	N	6	2	+17 e	...
RV Aur	46321	27.6	+42 34	141	+16	9.2	9.6	...	N	3	3	-52 e	...
+16°1194	MSB 49	28.5	+16 9	164	+ 5	9.2	....	...	N	8	3	+ 3 e	...
UU Aur	46687	29.7	+38 31	144	+15	6.2	6.7	235	N	6	4	+12 a	...
.....	47396	33.3	+22 42	159	+ 9	(9.2)	....	...	N	3	3	+45 e	...

TABLE 1--Continued

Star	HD or MSB	1900 R.A.	1900 Decl.	Galactic l	Galactic b	Magnitude Max.	Magnitude Min.	Period (Days)	Spect.	Intensity Na	Intensity C_2	Vel.(Km/sec) Abs.	Vel.(Km/sec) Em.
Lee 54	.....	$6^h34^m.7$	+18°50'	163°	+ 8°	10.5	....	...	N	4	4	+38 e	...
VW Gem	47883	35.7	+31 33	151	+14	8.6	8.8	110+	N	5	3	+14 c	...
MSB 50	.....	38.5	- 8 40	188	- 5	(9.0)	....	...	N	4	4	+32 e	...
.....	48664	39.4	+ 3 25	177	+ 1	9.3	....	...	N	6	2	+27 d	...
MSB 51	.....	41.7	-12 49	190	- 6	(9.0)	....	...	N	3	2	+67 e	...
Lee 60	.....	42.4	+ 0 47	179	+ 1	10	....	...	N	5	4	+77 e	...
W Mon	.....	47.5	- 7 2	187	- 2	9.7	12.2	...	N	4	1	0 d	...
.....	50436	48.2	- 4 27	185	0	9.2	10.4	...	N	7	3	+38 d	...
MSB 26	.....	50.2	+ 6 29	176	+ 5	(9.0)	....	...	Ne	3	2	+43 d	+19
UW Aur	50949	50.3	+41 14	143	+20	9.6	12.6	530	R6p	0	4	- 7 c	...
BG Mon	MSB 27	50.9	+ 7 13	175	+ 6	12	13.5	240	N	5	3	+71 c	...
.....	51208	51.3	-42 14	219	-17	6.0	....	...	N	8	2	+32 a	...
+6°1451	MSB 28	51.7	+ 6 29	176	+ 6	9.5	....	...	N	5	4	+57 e	...
RV Mon	51620	53.0	+ 6 18	176	+ 6	7.0	8.2	225	N	6	4	+16 b	...
.....	52432	56.1	- 3 6	185	+ 2	7.5	....	...	R6	.	.	+21 a	...
RY Mon	MSB 29	7 2.1	- 7 24	189	+ 1	7.7	9.1	466	N	4	3	+ 2 c	...
W CMa	54361	3.4	-11 46	193	- 1	6.9	7.5	...	N	6	4	+21 d	...
.....	.....	7.0	+ 0 58	182	+ 7	(11.6)	....	...	R2	.	.	+ 8 b	...
VX Gem	55284	7.2	+14 46	171	+12	10.8	14.9	377	Nep	8	2	+53 d	+42
MSB 52	.....	9.5	-19 32	201	- 3	(9.0)	....	...	N	6	2	+66 c	...
-17°1866	MSB 53	10.1	-17 13	198	- 2	(9.0)	....	...	N	6	3	+52 e	...
+5°1606	MSB 30	10.3	+ 5 14	179	+ 9	9.5	....	...	N	4	4	+52 d	...
RU Cam	56167	10.9	+69 52	118	+29	7.9	9.0	222	KO-RO	.	.	-24 a	...
MSB 54	.....	10.9	-17 20	198	+ 2	(10.5)	....	...	N	3	3	+87 e	...
BM Gem	57160	14.9	+25 10	161	+19	11.5	12.1	...	N	4	3	+98 e	...
.....	57884	18.1	- 4 2	188	+ 6	9.3	....	...	N	4	3	+55 c	...
.....	58195	19.4	-22 47	205	- 2	9.2	....	...	N	3	2	+44 c	...
.....	58337	20.1	+22 7	164	+18	10.0	....	...	R4	.	.	+ 4 e	...
.....	58364	20.2	+22 5	164	+18	9.8	....	...	R4	.	.	- 3 c	...
.....	58385	20.3	- 2 57	187	+ 7	9.1	....	...	N	3	1	+64 d	...
.....	59643	25.8	+24 44	161	+18	8.2	....	...	R6	.	.	+41 a	...
.....	60826	31.3	+ 2 18	184	+13	8.7	9.1	...	N	7	4	+44 b	...
.....	60952	31.8	-23 22	206	0	11.6	....	...	N	3	3	+10 c	...
MSB 55	.....	41.0	-11 43	198	+ 7	(9.5)	....	...	N	4	4	+32 c	...
W CMi	63353	43.4	+ 5 40	182	+17	9.8	11.3	...	R6	.	.	+21 e	...

MSB 31	.....	7h45.0m	- 0°38'	189°	+14°	(9.0)	....	...	R8	.	.	+ 4 d	...
MSB 32	.....	52.7	- 0 24	189	+16	(9.6)	....	...	Ne	4	2	+25 c	- 6
MSB 33	.....	57.7	- 1 51	191	+16	(9.5)	....	...	N	4	4	+26 e	...
RT Pup	67190	8 1.7	-38 29	222	- 3	9.3	10.2	...	N	.	.	+28 d	...
RU Pup	67507	3.2	-22 37	210	+ 6	9.4	11.6	...	N	6	4	+23 e	...
RY Hya	70072	14.9	+ 3 5	189	+22	8.3	9.6	535	Ne	5	3	+17 c	- 8
.....	70138	15.2	-17 57	208	+11	9.3	....	...	R7	.	.	+24 b	...
Lee 98	.....	15.4	+ 5 31	187	+24	10.0	....	...	R5	.	.	+29 b	...
T Lyn	.....	16.4	+33 50	156	+34	8.0	12.0	416	Ne	6	2	+ 6 b	-12
AC Pup	.....	18.2	-15 35	205	+13	8.9	10.1	...	N	5	3	+41 c	...
Lee 99	.....	36.4	+ 7 47	187	+29	10.6	....	...	R4	.	.	+31 c	...
.....	75021	42.4	-29 21	220	+ 9	7.6	....	...	R8	.	.	+11 a	...
X Can	76221	49.7	+17 37	178	+37	6.1	6.6	130	N	6	4	- 1 a	...
.....	76396	50.8	+51 49	134	+41	8.8	....	...	R4	.	.	-52 e	...
T Can	.....	51.0	+20 14	175	+37	8.0	10.2	500	R6	2	3	+ 7 a	...
.....	76846	53.6	+34 9	157	+42	9.2	....	...	R1	.	.	+25 a	...
.....	77234	56.2	+50 29	135	+43	9.5	....	...	R6	.	.	+ 5 a	...
.....	78278	9 2.2	+21 58	174	+41	(10.2)	....	...	R6	.	.	+19 b	...
.....	79319	8.3	+14 37	184	+39	8.9	....	...	R6	.	.	+ 4 a	...
MSB 57	.....	9.0	-22 59	219	+18	(9.0)	....	...	Ne	5	2	-10 b	-34
.....	85066	44.4	+53 7	130	+49	(9.7)	....	...	R3	.	.	-24 a	...
W Sex	85319	45.9	- 1 33	208	+39	10.3	12.3	...	N	4	2	+59 a	...
Y Hya	85405	46.4	-22 32	226	+24	6.5	8.0	95	N	5	4	+ 3 a	...
X Vel	86111	51.3	-41 7	239	+11	9.5	11.8	...	N	5	4	- 7 e	...
.....	88539	10 7.5	-34 50	238	+18	7.0	....	...	N	4	2	+ 4 b	...
.....	88627	7.9	+77 36	99	+37	(10.0)	....	...	R6	.	.	-92 b	...
U Ant	91793	30.8	-39 3	244	+16	8.3	9.3	168?	N	5	4	+37 b	...
U Hya	92055	32.6	-12 52	229	+39	4.5	6.3	...	N	6	4	-26 a	...
.....	92839	38.1	+67 56	106	+46	6.3	....	...	N	3	3	- 5 a	...
V Hya	.....	46.8	-20 43	237	+35	6.7	12.0	532	N	6	4	- 8 a	...
.....	95405	55.7	-25 19	242	+31	9.0	....	...	Kp	.	.	+12 e	...
+2°2446	Lee 106	11 28.6	+ 2 18	233	+59	9.5	....	...	R2	.	.	+20 b	...
.....	100764	30.7	-14 2	246	+45	8.7	....	...	R2	.	.	+ 5 b	...
Lee 107	.....	50.5	+13 8	229	+71	11.3	....	...	R5	.	.	-137 a	...
S Cen	107957	12 19.2	-48 53	266	+13	8.1	9.5	...	Np	.	.	-41 a	...
SS Vir	108105	20.1	+ 1 20	259	+63	7.2	9.0	354	Ne	5	4	+ 2 a	-22
.....	108683	24.0	-37 42	266	+24	9.3	....	...	N	5	4	-28 d	...
Y CVn	110914	40.4	+45 58	90	+72	4.8	6.0	316	N	5	4	+12 a	...
RU Vir	111166	42.2	+ 4 42	271	+66	8	12.6	439	R3e	.	.	+ 2 a	-21
RY Dra	112559	52.5	+66 32	88	+51	6.1	7.1	...	N	.	.	-20 d	...
.....	112869	54.7	+38 20	74	+79	9.2	9.6	...	R6p	0	4	-135 a	...
.....	113801	13 1.1	-19 31	276	+42	8.7	....	...	K5R	.	.	-16 c	...
Z Lup	128033	14 29.5	-42 56	290	+15	8.2	9.6	...	N	6	2	+ 8 c	...
.....	133332	58.8	- 2 28	323	+45	10.6	....	...	R6	.	.	-28 e	...
X TrA	134453	15 4.8	-69 42	282	-11	8.2	10.0	...	N	.	.	- 4 a	...

TABLE 1--Continued

Star	HD or MSB	1900 R.A.	1900 Decl.	Galactic l	Galactic b	Magnitude Max.	Magnitude Min.	Period (Days)	Spect.	Intensity Na	Intensity C_2	Vel.(Km/sec) Abs.	Vel.(Km/sec) Em.
.....	137613	$15^h21^m.9$	-24°49'	310°	+25°	7.4	....	...	RO	.	.	+55 a	...
Lee 114	.....	22.6	+ 1 3	332	+42	11.4	....	...	R4	.	.	-23 d	...
V CrB	141826	45.9	+39 52	30	+50	7.2	12.0	357	Ne	6	2	-115 a	-131
RR Her	144578	16 1.5	+50 46	46	+46	7.8	9.5	242	Nep	6	1	-37 a	-46
.....	145777	7.6	-14 57	326	+24	10.7	....	...	R4	.	.	+15 c	...
.....	148173	21.1	-43 27	306	+ 2	9.3	....	...	N	4	2	+ 7 c	...
V Oph	148182	21.2	-12 12	331	+23	7.0	10.5	301	Ne	.	.	-40 a	-58
SU Sco	.....	34.2	-32 11	317	+ 8	7.5	9.0	...	N	3	3	-19 c	...
MSB 58	.....	56.2	-32 31	320	+ 5	(9.0)	....	...	Ne	3	2	+ 1 d	-19
.....	156074	17 10.4	+42 15	37	+34	7.7	....	...	RO	.	.	-16 a	...
-40°11335	MSB 59	13.9	-40 16	316	- 3	9.3	....	...	N	6	3	- 9 d	...
-36°11460	.....	17.0	-36 24	319	- 1	9.5	....	...	R3	.	.	-67 b	...
-29°13477	MSB 60	17.7	-29 14	325	+ 3	9.0	....	...	N	5	3	-24 b	...
-39°11452	MSB 34	20.7	-39 55	316	- 4	10	....	...	N	6	4	-30 e	...
TW Oph	158377	23.8	-19 24	334	+ 7	7.8	....	...	N	5	4	+14 c	...
TT Sco	160205	33.5	-41 35	316	- 7	9.0	[11.2	...	N	6	4	+ 8 c	...
.....	160591	35.7	-35 12	322	- 4	10.7	11.6	...	R8	2	4	-57 e	...
SZ Sgr	161208	39.1	-18 37	336	+ 4	8.5	9.8	...	N	6	3	+19 b	...
SX Sco	161511	40.8	-35 39	322	- 6	9.6	11.1	128?	N	5	3	-36 c	...
.....	163838	53.2	+64 9	60	+30	(10.2)	....	...	R3	.	.	-38 b	...
Lee 115	.....	53.9	+13 10	6	+16	(10)	....	...	R4	.	.	-100 c	...
T Dra	.....	54.9	+58 14	53	+29	7.5	14.0	425	Ne	8	3	-23 a	-43
-19°4805	MSB 61	55.5	-19 10	338	0	9.7	....	...	N	5	3	+17 e	...
W CrA	.....	58.4	-39 20	321	-10	10.0	[11	109	R3	.	.	-103 d	...
-28°14163	MSB 62	18 1.2	-28 31	331	- 5	(9.8)	....	...	N	7	4	-11 e	...
.....	166097	4.0	+ 9 26	4	+12	10.0	....	...	R4	.	.	-19 b	...
MSB 63	.....	4.2	-26 55	332	- 5	(10.0)	....	...	N	7	2	- 5 c	...
.....	.....	8.1	+14 54	10	+14	(10.3)	....	...	R4	.	.	+ 8 b	...
.....	168227	13.6	-15 39	344	- 2	9.0	9.8	...	R6	.	.	-19 c	...
Lee 117	.....	19.4	+ 6 0	3	+ 7	11.2	....	...	RO	.	.	+34 b	...
.....	170282	23.4	-38 29	323	-14	10.3	....	...	R5	.	.	-75 c	...
SS Sgr	170495	24.6	-16 59	343	- 4	11.0	12.0	...	R3	1	2	0 c	...
TY Oph	170831	26.4	+ 4 19	2	+ 5	9	10	...	N	5	3	-19 b	...
T Lyr	.....	28.9	+36 54	33	+18	7.8	9.6	...	R6	1	2	-12 b	...
RX Set	171804	31.7	- 7 41	352	- 2	9.7	12.0	...	N	6	4	- 7 b	...

RV Sct	173138	$18^h38^m.7$	-13°20'	348°	- 6°	8.6	10.1	...	R3	2	3	- 4 c	...
.....	173291	39.4	+36 51	33	+17	8.1	....	...	N	6	4	- 5 a	...
.....	173409	40.0	-31 28	331	-14	9.2	....	...	RO	.	.	-65 e	...
+5°3950	MSB 64	42.6	+ 5 20	5	+ 1	9.5	....	...	N	6	4	-17 c	...
S Sct	174325	44.9	- 8 1	354	- 5	6.4	7.3	144?	N	4	4	0 a	...
T Sct	175377	50.0	- 8 19	354	- 6	8.8	9.3	...	N	6	2	+15 c	...
.....	175893	52.4	-29 38	335	-16	9.3	....	...	RO	.	.	+42 c	...
UV Aql	176200	54.0	+14 14	14	+ 4	9.6	11.6	355	N	5	4	+21 b	...
V Aql	177336	59.1	- 5 50	357	- 7	6.5	8.0	...	N	6	4	+37 a	...
.....	178316	19 3.0	-17 26	347	-13	10.6	....	...	R2	.	.	-42 c	...
SV Sge	.....	3.8	+17 29	18	+ 3	10.8	14.5	...	R2	.	.	+ 4 b	...
.....	179153	6.3	- 1 33	2	- 6	10.8	11.7	...	R8	2	3	+22 d	...
.....	179355	7.1	-31 7	335	-20	11.3	....	...	R3	.	.	+63 d	...
MSB 65	.....	9.8	+27 8	27	+ 6	(9.0)	....	...	R3	2	2	+13 e	...
MSB 66	.....	12.8	+21 45	22	+ 4	(9.0)	....	...	N	5	4	-20 e	...
.....	180953	13.4	-16 5	349	-15	7.2	....	...	N	6	4	-45 a	...
U Lyr	MSB 35	16.7	+37 37	37	+10	8.3	12.0	449	Ne	6	3	- 3 b	-36
.....	182040	17.7	-10 53	354	-13	7.0	....	...	R2	.	.	-47 a	...
UX Dra	183556	25.1	+76 23	75	+24	6.1	7.0	...	N	4	3	+ 6 a	...
V374 Aql	Lee 130	25.1	- 1 3	4	-11	12.5	15.1	...	Ne	7	2	+11 c	-11
AW Cyg	MSB 36	25.8	+45 50	46	+12	8.0	10.2	...	N	5	3	-12 c	...
AQ Sgr	184283	28.6	-16 35	351	-18	8.5	9.7	...	N	7	4	+14 a	...
V391 Aql	.....	33.0	+ 6 30	11	- 9	12.8	13.8	...	N	6	3	-28 b	...
.....	.....	35.4	+ 8 48	15	- 8	11.8	....	...	RO	.	.	+42 b	...
HV Cyg	MSB 68	36.6	+31 32	34	+ 4	13.2	[16.3	195+	N	6	4	+24 d	...
TT Cyg	186047	37.1	+32 23	35	+ 4	7.3	8.4	120	N	4	3	-49 a	...
UW Sgr	186665	40.6	-18 24	350	-22	8.4	10.2	...	N	7	1	-13 c	...
.....	187216	43.8	+85 9	85	+27	9.6	....	...	R3	.	.	-129 c	...
.....	188934	52.5	- 0 2	9	-16	9.8	....	...	R4	.	.	+57 c	...
AX Cyg	189256	54.0	+43 59	47	+ 7	7.4	7.9	...	N	5	4	- 6 a	...
.....	189605	55.7	- 7 39	2	-20	10.8	....	...	R4	2	4	+48 c	...
.....	189711	56.3	+ 9 14	17	-12	8.7	....	...	N	3	2	-168 a	...
.....	190048	58.0	+20 48	28	- 7	9.2	....	...	N	3	3	-14 b	...
MSB 69	.....	58.1	+39 42	43	+ 4	(9.5)	....	...	N	6	3	+ 8 e	...
MSB 37	.....	58.6	+30 23	36	- 1	(9.4)	....	...	N	4	4	+12 d	...
X Sge	190606	20 0.7	+20 22	27	- 7	8.7	9.7	196	N	5	4	+26 e	...
AY Cyg	.....	6.3	+41 12	45	+ 3	11.9	12.4	...	N	6	3	+21 e	...
SV Cyg	191738	6.4	+47 33	52	+ 8	8.5	9.4	...	R3	2	2	- 8 c	...
RY Cyg	191783	6.6	+35 39	40	0	9.2	11.0	...	N	6	4	+13 e	...
RS Cyg	192443	9.8	+38 26	43	+ 2	7.5	8.7	422	Ne	8	4	-50 a	-62
RT Cap	192737	11.3	-21 38	350	-29	8.6	10.4	211	N	5	4	-30 d	...
WX Cyg	193368	14.8	+37 9	43	0	9.0	12.2	410	Ne	8	2	+32 a	+ 9
U Cyg	193680	16.5	+47 35	52	+ 6	6.1	11.8	457	Ne	8	2	+13 a	- 4
Lee 143	.....	20.9	+17 34	28	-13	(9)	....	...	N	4	2	+51 c	...
MSB 70	.....	21.4	+55 55	58	+ 9	(9.5)	....	...	N	3	2	+25 c	...

TABLE 1--Continued

Star	HD or MSB	1900 R.A.	1900 Decl.	Galactic l	Galactic b	Magnitude Max.	Magnitude Min.	Period (Days)	Spect.	Intensity Na	Intensity C_2	Vel.(Km/sec) Abs.	Vel.(Km/sec) Em.
.....	195435	$20^h26^m.2$	-12°13'	1°	-29°	9.6	....	...	R6	.	.	-52 c	...
BD Vul	.....	33.0	+26 8	36	-10	12	15	448?	Ne	5	2	+31 c	+ 7
MSB 71	.....	33.8	+36 30	45	- 4	(9.7)	....	...	N	4	3	+18 d	...
MSB 38	.....	33.9	+59 44	63	+11	(9.5)	....	...	N	3	4	-34 c	...
V Cyg	MSB 39	38.1	+47 48	54	+ 3	6.8	13.8	429	Ne	8	2	+ 3 a	-24
+31°4201	MSB 40	39.4	+31 46	42	- 7	9.2	....	...	N	5	3	-26 c	...
.....	197604	39.7	+34 43	44	- 7	9.8	....	...	R4	.	.	+21 c	...
.....	198140	43.2	-19 24	355	-36	10.3	....	...	R1	.	.	+46 d	...
+32°3954	MSB 41	45.2	+32 51	44	- 7	9.2	....	...	N	5	4	-11 e	...
DS Cyg	198681	46.9	+45 2	53	0	12.9	15.1	...	N	5	3	- 6 c	...
RV Aqr	.....	21 0.7	- 0 36	17	-31	8.7	[15	453	Ne	7	2	- 1 b	-25
T Ind	202874	13.6	-45 27	323	-46	7.2	8.9	...	N	.	.	+ 2 a	...
+2°4338	Lee 150	14.1	+ 2 47	23	-31	9.5	....	...	R1	.	.	-50 b	...
YY Cyg	.....	18.6	+41 58	54	- 7	8.5	9.5	387	N	6	3	-10 c	...
.....	205777	32.5	+60 28	69	+ 6	10.3	....	...	N	5	4	-15 b	...
S Cep	206362	36.4	+78 10	81	+19	7.9	13.1	482	Ne	.	.	-34 b	-47
DS Peg	206570	37.8	+35 3	53	-14	6.0	7.0	...	N	4	4	+10 a	...
RV Cyg	206750	39.1	+37 34	56	-11	7.1	9.3	75	N	5	3	+ 2 a	...
LW Cyg	208512	51.6	+50 2	64	- 4	10.5	11.5	...	R3	2	4	-18 b	...
RX Peg	208526	51.7	+22 24	47	-25	7.7	8.6	175	N	3	2	-27 a	...
.....	209596	59.5	+45 5	63	- 8	(9.5)	....	...	N	6	2	-18 c	...
.....	209621	59.7	+20 34	47	-27	8.8	....	...	R3	.	.	-381 a	...
RZ Peg	209890	22 1.5	+33 2	56	-18	9.0	12.4	440	Ne	9	2	-27 d	-60
MSB 72	.....	28.5	+58 9	73	0	(9.5)	....	...	N	4	3	-18 c	...
Lee 153	.....	40.0	+17 36	54	-35	(9)	....	...	Ne	5	2	+17 b	-22
.....	215484	40.4	+61 12	76	+ 2	9.0	....	...	N	4	3	-30 c	...
+48°3827	MSB 73	40.7	+48 57	71	- 9	9.4	....	...	N	5	4	-13 b	...
MSB 74	.....	41.1	+56 5	74	- 2	(9.1)	....	...	N	4	4	-50 b	...
TX Lac	215673	41.8	+54 33	74	- 3	11.5	12.1	240	R6	.	.	-28 b	...
.....	216649	49.5	- 7 30	32	-57	(10.5)	....	...	R3	.	.	-42 b	...
TV Lac	216913	51.9	+53 41	74	- 5	11.7	12.7	...	N	.	.	-17 c	...
VY And	.....	57.3	+45 21	72	-13	9.5	11.0	149	R8	2	4	- 7 c	...
.....	218851	23 6.2	+45 46	73	-14	(9.5)	....	...	R2	.	.	-49 b	...
.....	218875	6.3	-21 32	11	-68	9.4	10.8	...	R0	.	.	+32 c	...
MSB 42	.....	19.1	+55 26	79	- 4	(9.5)	....	...	R8	.	.	-34 d	...

.....	220870	$23^h22^m.2$	+48°58'	77°	-11°	9.7	....	...	N	7	2	-18 c	...
ST And	222241	33.8	+35 13	75	-25	8.3	12.4	335	R3e	2	2	+32 c	+13
19 Psc	223075	41.3	+ 2 56	63	-56	5.3	....	...	N	7	3	+11 a	...
.....	223392	44.0	+ 5 50	66	-53	8.8	....	...	R3	.	.	-25 a	...
MSB 75	.....	54.0	+56 25	84	- 5	(10.2)	....	...	Ne	7	2	-46 b	-78
WZ Cas	224855	56.2	+59 48	85	- 2	6.9	8.5	193	N	9	1	-34 a	...
.....	224959	57.0	- 3 23	63	-64	9.9	....	...	RO	.	.	-132 c	...
SU And	225217	59.4	+43 0	82	-18	7.9	8.5	...	N	4	3	- 6 b	...

NOTES TO TABLE 1

HD 20234. Lick Obs. Pub., 18, 23, 1932.
HD 31996. R Lep. Velocity may vary slightly with phase.
HD 34842. UV Aur. Emission lines of [O III], Mg I, Fe I, and H have been observed near minimum. Absorption-line velocity may vary slightly with phase.
HD 38218. TU Tau. Spectrum is composite with A-type predominating in the violet, N-type in the visual region.
5^h 56.9^m. XZ Aur. See Allen and Edwards, M.N., 101, 295, 1941.
6^h 51.7^m. +6°1451. Harv. Announcement Card 616, 1942.
7^h 7.0^m. Harv. Bull. 837, 1926.
HD 56167. RU Cam. Velocity-curve. Mt. W. Contr., No. 372; Ap. J., 68, 408, 1928.
HD 95405. Class K5R.
HD 107957. S Cen. Lick Obs. Pub., 18, 100, 1932.
HD 108683. Velocity had wrong sign in Mt. W. Contr., No. 525; Ap. J., 82, 202, 1935.
HD 134453. X TrA. Lick Obs. Pub., 18, 119, 1932.
17^h 17.0^m. -36°11460. Harv. Circ. 224, 1921.
18^h 8.1^m. Harv. Circ. 231, 1922.
19^h 3.8^m. SV Sge. Harv. Bull. 837, 1926.
19^h 35.4^m. Harv. Bull. 837, 1926.
19^h 58.6^m. MSB 37. Lick Obs. Bull., 18, 48, 1937. See Area C4, star 28.
HD 193368. WX Cyg. λ6707 Li I nearly as strong as in WZ Cas.
HD 193680. U Cyg. Spectrum and radial velocity change with light-phase.
HD 202874. Lick Obs. Pub., 18, 176, 1932.
HD 209890. RZ Peg. Velocity may vary slightly.
HD 224855. WZ Cas. Has strongest known λ6707 Li I. Keenan and Morgan classify as the coolest carbon-band star. No star is known to have stronger D lines.

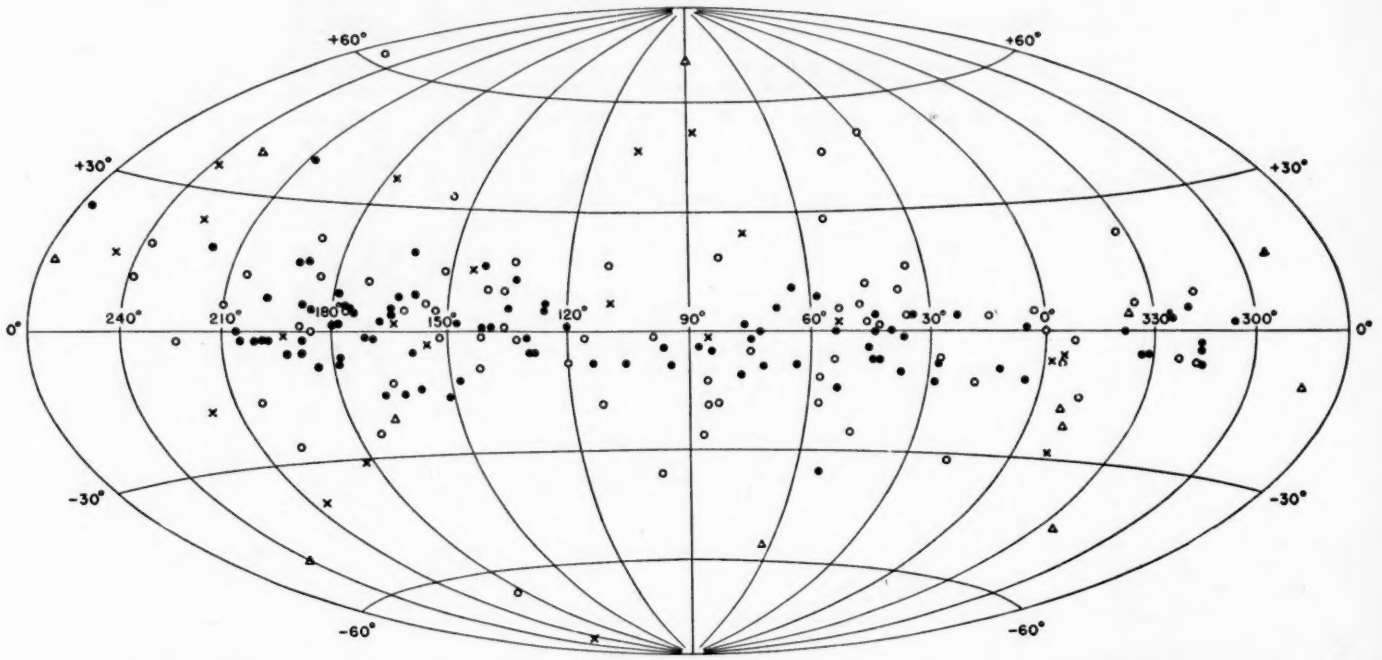

FIG. 1.—Class-N stars plotted in galactic co-ordinates. Triangles represent stars brighter than $6^m.0$, visual magnitude; crosses, $6^m.0$–$6^m.9$, inclusive; circles, $7^m.0$–$8^m.9$; and dots, $9^m.0$ or fainter. For variable stars, the magnitude at maximum is used. Photographic magnitudes have been converted to visual by applying a color index of $3^m.0$.

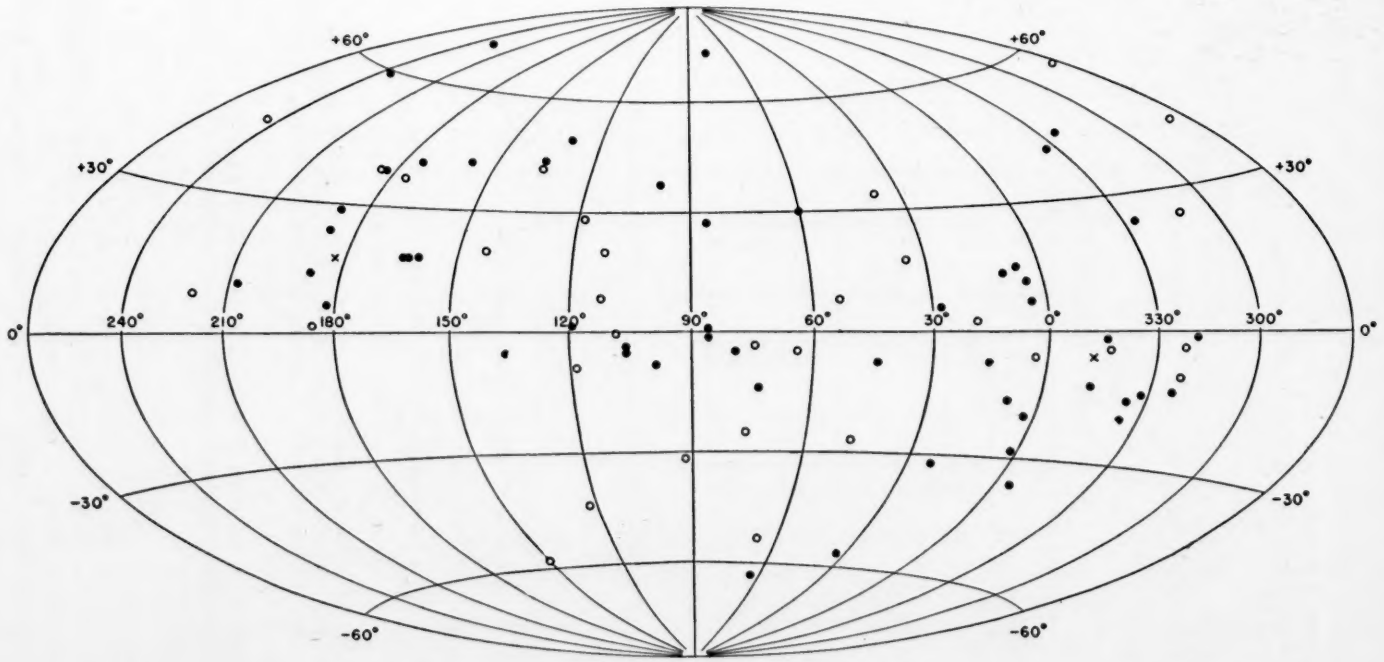

FIG. 2.—Class-R stars plotted in galactic co-ordinates, with circles for stars brighter than visual magnitude 9.0 and dots for those fainter

Within 30° of the galactic plane there are 171 stars of class N whose velocities can be studied for evidence of galactic rotation. Only HD 189711 was omitted on account of its outstandingly large velocity. These velocities, freed from solar motion (apex α 270°, δ +28°, and $V_0 = 20$ km/sec), have been gathered into thirteen velocity means (Table 2). The last column shows the mean radial velocity freed from solar motion and reduced to mean apparent visual magnitude 8.3. The effect of differential galactic rotation is evident from the plot of the data of Table 2 in Figure 3.

TABLE 2

NORMAL VELOCITIES—CLASS N

No. of Stars	$\bar{m}_v$	$\bar{l}$	$\bar{b}$	$\bar{\rho}$
13	7.5	358°	−9°	+17.4 km/sec
11	8.9	32	0	+17.8
20	8.3	49	−1	+12.0
10	9.0	72	+1	− 5.7
11	8.2	88	−7	−24.7
8	8.3	113	−2	−20.0
13	9.2	132	+4	+ 4.0
16	8.5	150	0	+ 5.4
24	8.9	170	0	+13.0
18	8.5	190	0	+19.1
13	7.9	218	+5	+ 8.4
8	7.8	295	+5	−11.3
10	7.8	328	+2	+ 3.8

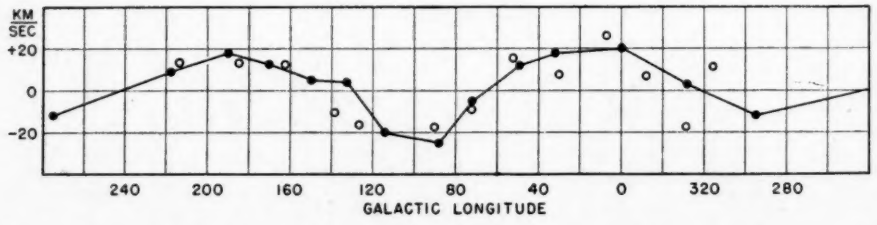

FIG. 3.—The mean velocities of class-N stars in Table 3 are plotted as dots and connected with straight lines. The mean velocities of class-R stars in Table 4 are plotted as circles; they have been corrected for K and dV (p. 159) and reduced to visual magnitude 9.8 (general absorption included).

The mean distance, $\bar{r}$, for class-N stars of magnitude 8.3 has been derived from the data of Table 2 by a least-squares solution of the conditional equation for differential galactic rotation:

$$\bar{r}A \sin 2(\bar{l} - l_0) \cos^2 \bar{b} = \bar{\rho} ,$$

wherein $A = 17.7$ km/sec/kiloparsec, $l_0 = 325°$, and $\bar{l}$ and $\bar{\rho}$ are from Table 2. The values of $\bar{b}$ in the fourth column differ so little from zero that $\cos^2 \bar{b}$ was assumed to be unity. The mean distance found for class-N stars of apparent visual magnitude 8.3 is 1.10 ± 0.08 kiloparsecs. The evaluation of the mean absolute magnitude depends to some extent upon what value is adopted for general absorption per kiloparsec. If 0.35 visual magnitude is assumed, the mean absolute visual magnitude becomes −2.3 ± 0.2. This may be

compared with −1.88 derived by R. E. Wilson[12] from proper motions and the radial velocities of the earlier catalogue.

Table 3 gives thirteen mean velocities derived from 62 stars of class R in the same way as the data for class N in Table 2. HD 187216 and HD 209621 were omitted because of their large velocities. $\bar{p}$ is for mean apparent visual magnitude 9.0. Inspection shows evidence of differential galactic rotation, but a lack of symmetry with respect to the axis of zero velocity suggested including the well-known K-term and a correction to V_0, the

TABLE 3

NORMAL VELOCITIES—CLASS R

No. of Stars	$\bar{m}$	$\bar{l}$	$\bar{b}$	$\bar{p}$
10	9.9	7°	− 3°	+14.1 km/sec
4	8.8	30	+ 6	+ 2.8
3	9.4	52	+10	+ 7.4
6	8.8	73	−10	− 7.7
3	9.5	90	− 3	−14.0
7	8.5	127	+ 6	−14.3
3	9.6	139	0	−11.0
3	9.3	163	+18	+ 2.6
6	9.2	185	+15	+ 4.3
2	8.4	214	+10	+ 2.6
2	8.4	315	+12	+ 3.9
7	9.4	329	− 8	−13.7
6	8.4	348	−12	+ 2.9

adopted solar motion, in making the solution for differential galactic rotation. A conditional equation of the form

$$K + dV \cos(\bar{l} - 20°) + \bar{r}A \sin 2(\bar{l} - l_0) = \bar{p}$$

was used ($\bar{b}$ assumed to be 0). Least-squares solution gave

$$K = -3.5 \pm 1.3 \text{ km/sec},$$
$$dV = +1.9 \pm 1.6 \text{ km/sec},$$
$$\bar{r} = 0.67 \pm 0.10 \text{ kiloparsecs}.$$

This mean distance is for a mean apparent visual magnitude 9.0. Absolute visual magnitude -0.4 ± 0.4 for class-R stars follows from the above mean distance and mean magnitude, if we use a general absorption of 0.35 mag. per kiloparsec. Wilson's[13] value is $\overline{M} = -0.50 \pm 0.20$.

The value of K might be interpreted as evidence of a systematic error in the velocities if it were not that intercomparison of velocities from spectrograms of high and low dispersion has shown no such error. No obvious explanation is at hand.

The value dV is only slightly larger than its probable error; hence, the use of a value differing significantly from the +20 km/sec actually applied for solar motion receives scant justification.

The values of $\bar{p}$ in Table 3 have been corrected for K and dV, derived above, and then made to correspond to a mean visual magnitude of 9.8 (corrected for general absorption).

[12] *Mt. W. Contr.*, No. 631; *Ap. J.*, **92**, 188, 1940.

[13] *Mt. W. Contr.*, No. 618; *Ap. J.*, **90**, 492, 1939.

The resultant values for $\bar{p}$, plotted as circles in Figure 3, are in fair accord with the values for class-N stars of mean visual magnitude 7.9 (8.3 uncorrected). This should be true, since class-R stars, which are fainter than class-N stars by the difference of their absolute magnitudes (1.9), should be at the same distance and therefore give similar curves for differential galactic rotation.

Table 4 contains those stars whose velocities after correction for solar motion are numerically larger than 100 km/sec.

TABLE 4

STARS OF HIGH VELOCITY

Star	m	Spect.	Vel. from Abs. Lines	l	b
HD 5223*.....	8.8	R3	−228 km/sec	91°	−32°
HD 13826*.....	8.3–9.0	R0	−163	122	−44
Lee 107.....	11.3	R5	−137	229	+71
HD 112869*.....	9.2–9.6	R6p	−135	74	+79
HD 187216.....	9.6	R3	−129	85	+27
HD 189711.....	8.7	N1	−167	17	−12
HD 209621*.....	8.8	R3	−379	47	−27
HD 224959.....	9.9	R0	−132	63	−64

TABLE 5*

INTERSTELLAR D LINES

Star	m	Spect.	Interstellar Velocity	Equiv. Width 0.5(D2+D1)	M
HD 5223.....	8.8	R3	0 km/sec	0.15 A	+2.2
13826†.....	Var.	R0	− 3	.49	−1.7
137613.....	7.4	R0	− 5	.28	−1.0
177336‡.....	Var.	N	−14	.28	−1.9
189711.....	8.7	N	−10	.56	−1.7
209621.....	8.8	R3	−10	0.27	+0.4

* Part of the data of this table appears in *Pub. A.S.P.*, **54**, 257, 1942.
† V Ari: mag 8.3–9.0.
‡ V Aql: mag 6.7–8.2.

Keenan and Morgan[14] have noted that the four stars marked with asterisks in Table 4 are characterized by very strong g-bands and weak atomic lines in the blue region. Lee 107, HD 187216, and HD 224959 are similarly characterized. All seven have large negative velocities. It may be worth noting that one of these stars (HD 5223) has the largest proper motion known for any star of class R or N. This suggests that this group of stars may be of lower absolute magnitude than the average class-R star.

Interstellar sodium lines.—Four class-R and two class-N stars have velocities large enough to permit the interstellar D lines to be separated from the stellar D lines. It has been possible to derive both the interstellar velocities and the total absorption of the interstellar D lines from the coudé spectrograms (Table 5). The values for 0.5 (D2 + D1)

[14] *Ap. J.*, **94**, 509, 1941.

have been used to read off distances for the stars of Table 5 by the curve of equivalent width versus distance given by P. W. Merrill for class-B stars.[15]

The absolute magnitude of HD 5223 from the interstellar D lines is +2.2, noteworthy as much fainter than the magnitudes obtained for the other stars of the table. This is

TABLE 6

ABSOLUTE MAGNITUDES

Method	Authority	Class R	Class N
Proper motions and radial velocities (*Contr.* 525)	R. E. Wilson	−0.5	−1.9
Radial velocities (Table 1)	R. F. Sanford	−0.4	−2.3
Total absorption of interstellar D lines	R. F. Sanford	−0.8 (0.0)	−1.8

quite consistent with this star's abnormally large proper motion, already alluded to. The mean of the absolute magnitudes of the four class-R stars is 0.0, or −0.8 if HD 5223 is omitted. The two class-N stars give a mean absolute magnitude of −1.8.

Absolute magnitudes for stars of classes R and N by three independent methods are brought together in Table 6. The class-N stars are unquestionably more than a magnitude brighter than class-R stars.

[15] *Mt. W. Contr.*, No. 569; *Ap. J.*, **86**, 35, 1937.

THE SPECTRUM OF COMET WHIPPLE-FEDTKÉ-TEVZADZE (1942g)

ANDREW MCKELLAR
Dominion Astrophysical Observatory
Victoria, B.C.
Received November 12, 1943

ABSTRACT

The results of wave-length measurements on eight spectrograms of Comet Whipple-Fedtké-Tevzadze (1942g) are presented. The spectrograms, obtained with relatively high spectral purity (projected monochromatic image of the slit at the plate ~ 0.5 angstroms for λ 3880), cover the ordinary photographic region. In addition to a general consideration of the spectrum of the comet, several points of particular interest are discussed. These include, first, the resolution of the *R* branch of the λ 3883 0, 0 *CN* band into its individual lines and, second, results of increased resolution in the cases of several features of the λ 4050 group of CH_2 bands, in particular the duplicity of the main maximum at λ 4051. Third, reasons are given for believing that the emission at λ 4752, which for other comets has been attributed to the $C^{13}C^{13}$ isotopic carbon molecule, is not in the present instance due to this molecule. Fourth, the interesting but possibly fortuitous wave-length coincidences between certain weak cometary emissions and bands, ascribed tentatively to the molecule SiO_2, are noted.

INTRODUCTION

Comet Whipple-Fedtké-Tevzadze (1942g) was a relatively bright object, being between the third and fourth magnitude for a few days.[1] At the time of its maximum brilliance it was unusually well situated for observation from northern latitudes. During late February and early March, 1943, some time after perihelion, which occurred on February 6, 1943, the comet unexpectedly increased in brightness; and during this period twelve spectrograms of its head were obtained at Victoria. In securing these observations two purposes were kept in mind. The first was to obtain spectrograms of the heretofore neglected visible spectral region to the red of λ 5000. The second was to photograph the spectrum of the comet in the ordinary photographic region, below λ 5000, under conditions of the highest practicable spectral purity. Some of the twelve plates were obtained with panchromatic emulsions and were useful in both these spectral regions.

The study of the visual region of the spectrum of Comet 1942g has been completed and was published[2] in a joint paper with P. Swings and R. Minkowski, who had secured data on the same region of cometary spectra at the McDonald and the Mount Wilson observatories. The main point of interest in that study was the tentative identification of the molecule NH_2 as the source of several of the strongest visible emission bands. The present article presents the results of measurements on eight spectrograms covering the ordinary photographic region. While most of the emission features of which wave-length measurements are given have been measured as such in the spectra of previous comets, our increased spectral purity has made possible the resolution of others among them into components not detected up to the present time.

THE OBSERVATIONAL MATERIAL

The plates were obtained with the single-prism form of the universal spectrograph. Two different cameras were employed, one having a focal ratio f/3 and the other f/5. All the data concerning the spectrograms thought to be of interest or value are assembled in Table 1, and they require little comment. In addition to the high spectral purity mentioned earlier, one further point may be noted, namely, that during the period over

[1] See, e.g., J. Ashbrook, *Pop. Astr.*, **51**, 362, 1943; N. T. Bobrovnikoff, *Pop. Astr.*, **51**, 481, 1943.

[2] P. Swings, A. McKellar, and R. Minkowski, *Ap. J.*, **98**, 142, 1943.

which the plates were taken the comet was at the relatively large heliocentric distance, $r = 1.4$ astronomical units. Most slit spectrograms of comets have been secured at values of r of 1 astronomical unit or less. Further reference will be made to this later. The distance of Comet 1942g from the earth in late February and early March, 1943, was ~ 0.5 astronomical unit.

THE MEASUREMENTS

The results of the measurements on the eight plates are given in detail in Table 2. After a brief description of the spectral feature measured, the wave length as found from

TABLE 1

DATA ON SPECTROGRAMS OF COMET WHIPPLE-FEDTKÉ-TEVZADZE (1942g)

Date (U.T.)	Comet's Heliocentric Distance, r	Radial Velocity of Comet with Respect to Earth	Spectrographic Dispersion		Spectral Purity, Projected Slit-Width*		Photographic Emulsion	Quality of Spectrogram
			At λ 3880	At λ 4740	At λ 3880	At λ 4740		
	Astronomical units	km/sec						
1943, Feb. 24.535....	1.38	+7.9	57 A/mm	130 A/mm	0.85 A	1.94 A	Eastman 103a0	Good
25.485....	1.38	8.0	32	72	0.57	1.30	Eastman 103a0	Good
27.486....	1.39	8.3	57	130	0.85	1.94	Eastman 103F	Fair
28.481....	1.39	8.5	32	72	1.14	2.60	Eastman 103F	Good
Mar. 1.468....	1.40	8.6	57	130	0.50	1.14	Cramer Hi-speed	Excellent
3.467....	1.40	8.9	57	130	0.41	0.94	Cramer Hi-speed	Fair
7.469....	1.42	9.5	57	130	0.57	1.30	Eastman 103a0	Weak
9.460....	1.43	+9.8	57	130	0.50	1.14	Eastman 103a0	Good

* In expressing "spectral purity" in terms of the width in angstrom units of a monochromatic image of the slit at the plate, as we have done, it is assumed that the spectral lines have rectangular profiles. Therefore we are not adhering to the strict definition of "spectral purity" as given originally by Schuster. The latter definition makes it a function, among other things, of the aperture of the collimator. However, our usage indicates the maximum resolution to be expected and would seem to provide important information on resolving-power not shown by presenting the dispersion alone.

each plate is listed and is succeeded by the mean value from all the plates. Then follows the identification of the emitting molecule where this is known, and, finally, the laboratory wave length of the feature is given. Directly below the date in the second to the ninth columns, the quality of the spectrogram is noted.

Results of the individual wave-length measurements, obtained from the micrometer settings by the Hartmann dispersion formula, were calculated to the hundredth of an angstrom unit. Many of the emissions were so diffuse that the last figure has little significance. Thus, in obtaining the mean cometary wave length, in cases where either the number of individual measurements was only one or two or the feature was diffuse, the wave length has generally been given only to the tenth of an angstrom. In deriving the mean value, the wave lengths found from the plate of March 1.468, in view of its excellent quality, were given double the weight of each of the others.

TABLE 2

DETAILED WAVE-LENGTH MEASUREMENTS ON THE SPECTRUM OF COMET WHIPPLE-FEDTKÉ-TEVZADZE (1942g)

Spectral Feature	Feb. 24.535 (Good)	Feb. 25.485 (Good)	Feb. 27.486 (Fair)	Feb. 28.481 (Good)	Mar. 1.468 (Excellent)	Mar. 3.467 (Fair)	Mar. 7.469 (Weak)	Mar. 9.460 (Good)	Mean Cometary Wave Length	Identification	Laboratory Wave Length
Emission feature	3806.85(½)								3806.8(0+)		
Emission line					3866.18(0+)				3866.18(0+)	0, 0 *CN* Band, *R*(12) line	3865.99*
Emission line					66.89(1s)				66.89(1s)	0, 0 *CN* Band, *R*(11) line	66.82*
Emission line						3867.20(1)					
Emission line				3867.49(2)	67.71(1+s)			3867.79(1s)	67.68(1+s)	0, 0 *CN* Band, *R*(10) line	67.62*
Emission line					68.44(1+s)				68.44(1+s)	0, 0 *CN* Band, *R*(9) line	68.41*
Emission line	68.91(5d)	3869.85(1d)	3868.80(2d)	69.88(3)	69.23(1+s)	69.85(1)	3868.87(1d)		69.23(1+s)	0, 0 *CN* Band, *R*(8) line	69.18*
Emission line					70.00(1½s)			70.11(1s)	70.04(1½s)	0, 0 *CN* Band, *R*(7) line	69.92*
Emission line					70.71(1½)				70.71(1½)	0, 0 *CN* Band, *R*(6) line	70.67*
Sharp minimum of intensity	71.53	72.07	71.49	71.06	71.43	71.79	71.80	71.24	(71.54)	Due to very strong *Fe* absorption lines λ 3878.0 and λ3878.7 in solar spectrum†	
Emission line								72.06(1s)	72.06(1s)	0, 0 *CN* Band, *R*(4) line	72.06*
Emission line	72.89(3)	73.32(1+)	73.00(½)	72.53(2d)	72.45(1½)	73.25(½)	73.56(½)	73.51(1s)	72.47(1½)	0, 0 *CN* Band, *R*(4)+ *R*(5) line	72.06* 72.72*
Emission line					73.45(1−)				73.47(1−s)	0, 0 *CN* Band, *R*(2) line	73.36*
Emission line					74.25(½−)				74.25(½−)	0, 0 *CN* Band, *R*(1) line	74.00*
Deep minimum (band origin)	74.93	74.75	74.70	75.09	75.08	74.87	75.09	74.93	(74.95)	0, 0 *CN* Band origin	75.20*
Emission feature	77.55(5)	77.04(2d)	77.27(2)	77.24(5)	77.33(2+d)	77.21(2)	77.43(2)	77.32(4)	77.30(4d)	0, 0 *CN* Band, *P*(3), (4), (5) lines	77.35*
Sharp minimum of intensity	78.43	78.56	78.49	78.44	78.67	78.52	78.42	78.52	(78.52)	Due to very strong *Fe* absorption lines λ 3878.0 and λ 3878.7 in solar spectrum†	
Center of intense remaining *P*-branch maximum of *CN* band	80.14(10)	79.67(3) 80.72(3)	80.08(4)	80.04(8)	80.24(5d)	80.15(5)	80.22(4)	80.15(6)	80.16(8d)	0, 0 *CN* Band, *P*-branch intensity maximum at about *P*(10) and *P*(11) lines	79.97* 80.33*
Possible minimum in this maximum		80.22			80.05				(80.11)	Possibly due to dip in solar spectrum from λ 3880.0 to λ 3880.4†	
Head (redward edge) of 0, 0 *CN* band	81.59	81.11	81.55	81.55	81.81	81.38	81.82	81.48	81.57	0, 0 *CN* band head, at about the *P*(15) line	3883.4‡*
Emission feature	3978.27(0+d)								3978.3(0d)	λ 4050 group of CH_2 bands§	Lab λ not yet pub.§
Emission feature	86.86(½d)								86.9(0+d)	λ 4050 group of CH_2 bands§	Lab λ not yet pub.§
Emission feature	92.17(1d)								92.2(½d)	λ 4050 group of CH_2 bands§	Lab λ not yet pub.§

* H. S. Uhler and R. A. Patterson, *Ap. J.*, **42**, 434, 1915; F. A. Jenkins and D. E. Woolridge, *Phys. Rev.*, **53**, 137, 1938.

†See P. Swings, *Lick Obs. Bull.*, **19**, 131, 1941; A. McKellar, *Rev. Mod. Phys.*, **14**, 179, 1942.

‡ Laboratory wave length dependent on excitation conditions, so exact coincidence with cometary wave length not to be expected.

§ G. Herzberg, *Ap. J.*, **96**, 314, 1942.

TABLE 2—*Continued*

‡ Laboratory wave length dependent on excitation conditions, so exact coincidence with cometary wave length not to be expected.
§ G. Herzberg, *Ap. J.*, **96**, 314, 1942.

TABLE 2—*Continued*

Spectral Feature	Feb. 24.535 (Good)	Feb. 25.485 (Good)	Feb. 27.486 (Fair)	Feb. 28.481 (Good)	Mar. 1.468 (Excellent)	Mar. 3.467 (Fair)	Mar. 7.469 (Weak)	Mar. 9.460 (Good)	Mean Cometary Wave Length	Identification	Laboratory Wave Length
Emission feature	.....	.....	.....	.....	4007.06(1−dd)	.....	.....	.....	4007.1(½d)	λ 4050 group of CH_2 bands§	Lab λ not yet pub.§
Emission feature					12.75(1)	.....	.....	.....	12.8(1)	λ 4050 group of CH_2 bands§	Lab λ not yet pub.§
Emission feature	4013.84(2dd)	4014.50(½)	.....	4014.00(0+)	14.45(1)	.....	.....	.....	14.37(1)	λ 4050 group of CH_2 bands§	Lab λ not yet pub.§
Emission feature					16.19(1)	.....	.....	.....	16.2(1)	λ 4050 group of CH_2 bands§	Lab λ not yet pub.§
Emission feature	19.48(3+)	19.26(½)	4019.92(0+)	19.57(½)	19.80(2+d)	4019.74(0+d)	.....	4019.76(1d)	19.67(2d)	λ 4050 group of CH_2 bands§	Lab λ not yet pub.§
Emission feature	39.14(4)	39.01(1−d)	39.45(0+)	39.74(1)	39.70(3+d)	39.75(½)	.....	39.53(2−d)	39.50(3)	λ 4050 group of CH_2 bands§	Lab λ not yet pub.§
Sharp minimum of intensity	40.96	41.05	.....	41.26	41.33	41.16	.....	41.25	(41.19)	Possibly due to strong sharp absorption lines in solar spectrum, *Fe*, λ 4041.28 and *Mn*, λ 4041.38	.....
Emission feature	43.01(4)	42.48(2)	42.88(0+)	42.57(1)	43.30(3+d)	43.72(½)	.....	43.27(2−d)	43.07(3)	λ 4050 group of CH_2 bands§	Lab λ not yet pub.§
Sharp minimum of intensity or absorption line	.....	.....	.....	.....	45.70	.....	.....	.....	(45.70)	Due to very strong *Fe* absorption line in solar spectrum at λ 4045.83	
Emission feature	.....	50.29(1+s)		50.39(2)	50.40(3s)		4050.65(½)		50.43(3s)	λ 4050 group of CH_2 bands§	Lab λ not yet pub.§
Emission feature	51.53(8)	51.68(4)	51.57(4)	51.61(5)	51.79(6s)	51.49(3)	51.86(1+)	51.76(4)	51.75(6s)	λ 4050 group of CH_2 bands§	Lab λ not yet pub.§
Emission feature	.....	.....	.....	64.88(0)	.....	.....	.....	.....	64.9(0)	λ 4050 group of CH_2 bands§	Lab λ not yet pub.§
Emission feature					66.04(½d)	.....	.....	66.43(0+)	66.17(½)	λ 4050 group of CH_2 bands§	Lab λ not yet pub.§
Emission feature	68.10(2dd)	.....	.....	67.80(½)	69.64(½+d)	.....	.....	70.17(½)	69.99(½+)	λ 4050 group of CH_2 bands§	Lab λ not yet pub.§
Sharp minimum of intensity or absorption line	71.68	.....	.....	.....	71.47	.....	.....	71.80	(71.61)	Due to very strong *Fe* absorption line in solar spectrum at λ 4071.75	
Emission feature	74.01(6)	4074.44(½d)	7376.(1½)	74.44(2d)	73.96(3)	73.79(½d)	73.89(0+)	73.74(3)	74.00(3)	λ 4050 group of CH_2 bands§	Lab λ not yet pub.§
Emission feature	89.14(1dd)	.....	.....	.....	.....	.....	.....	.....	89.1(0+d)	λ 4050 group of CH_2 bands§	Lab λ not yet pub.§
Emission feature	99.19(2−)	.....	.....	4100.39(½)	99.05(½s)	.....	.....	98.76(0+d)	99.29(½)	λ 4050 group of CH_2 bands§	Lab λ not yet pub.§
Emission feature	.....	.....	.....	.....	4136.15(½d)	.....	.....	.....	4136.2(0+)	λ 4050 group of CH_2 bands§	Lab λ not yet pub.§
Emission feature	4212.87(2)	4214.07(½+)	.....	.....	4212.68(1+)	4212.92(0+)	.....	4212.23(½d)	4212.91(1+)	0, 1 *CN* band, intensity maximum of *P* branch	‡
Head (redward edge) of 0, 1 *CN* band	15.16	.....	.....	.....	14.98	15.37	.....	15.50	15.20	0,1 *CN* band head	4216.0‡

TABLE 2—*Continued*

Spectral Feature	Feb. 24.535 (Good)	Feb. 25.485 (Good)	Feb. 27.486 (Fair)	Feb. 28.481 (Good)	Mar. 1.468 (Excellent)	Mar. 3.467 (Fair)	Mar. 9.460 (Weak)	Mar. 7.469 (Good)	Mean Cometary Wave Length	Identification	Laboratory Wave
Emission feature		28.37(0+)			28.86(0+s)			27.44(0)	28.38(0+s)	CH^+ or SiO_2?	See Table 3
Emission feature	31.88(½s)			4232.04(½−s)	31.77(0+s)			32.22(0+s)	31.94(0+s)	CH^+?	See Table 3
Emission feature					35.61(0+s)				35.6(0)	CH^+ or SiO_2?	See Table 3
Emission feature					39.42(0)				39.4(0)	CH^+ or SiO_2?	See Table 3
Emission feature								57.69(0+s)	57.7(0)	SiO_2?	See Table 3
Emission feature								63.73(0+s)	63.7(0)	SiO_2?	See Table 3
Emission feature					4300.17(½ss)				4300.17(0+s)	0, 0 *CH* band, $R_3(1)$ line	4300.31‖
Emission feature	4303.65(0s)			4304.26(½s)	03.95(1−)			4303.72(0+s)	03.91(½s)	0, 0 *CH* band, $R_1(1)$ line	4303.88‖
Emission feature	13.28(2−)		4313.28(½+)	13.48(½+)	13.18(1)			13.03(1−)	13.24(1+)	0, 0 *CH* band; intensity maximum of *Q* branches	4313‡‖
Emission feature					29.77(0s)				29.77(0s)	0, 0 *CH* band, *P*(3) line	4329.98‖
Emission feature	63.34(0+)								63.3(0)	4, 2 C_2 Swan band; intensity maximum of *P* branches	‡
Emission feature	4429.46(0+)				4432.72(½)				4431.6(½)		
Emission feature	38.18(0+)		4437.73(0+)		38.32(½)				38.14(½)		
Emission feature	46.57(0+)	4446.22(½s)	45.55(0+)		45.12(0+)				45.72(0+)		
Emission feature	77.13(0+)	77.10(½s)							77.12(0+)		
Emission feature	85.65(0+)								85.6(0)		
Emission feature	4522.28(½s)								4522.3(0+s)		
Emission feature	42.28(0)								42.3(0)		
Emission feature	87.81(½d)		4590.40(0)						89.1(0)		
Emission feature	4609.31(0+s)				4607.47(0+)				4608.1(0+)		
Emission feature	14.95(0+s)								15.0(0)		
Intensity maximum 5, 4 Swan band	78.25(1−)				76.81(1d)			4675.20(½+)	76.8(1−)	5, 4 C_2 Swan band; intensity maximum of *P* branches	‡
Intensity maximum 4, 3 Swan band	85.09(1−)				85.38(1d)				85.3(1d)	4, 3 C_2 Swan band; intensity maximum of *P* branches	‡
Intensity maximum 3, 2 Swan band	97.62(1−)		4696.30(1)	4696.77(1)	96.21(1+d)			96.59(1−)	96.6(1)	3, 2 C_2 Swan band; intensity maximum of *P* branches	‡
Head of 3, 2 Swan band	4700.00			97.95					98.6	Head of 3, 2 Swan band	4697.6¶
Intensity maximum 2, 1 Swan band	14.41(3)	4713.72(1)	4713.14(2)	4713.79(2)	4713.94(2)			4713.49(1d)	4713.8(2)	2, 1 C_2 Swan band; intensity maximum of *P* branches	‡
Head of 2, 1 Swan band	16.04	14.82		16.46	17.29				16.4	Head of 2, 1 Swan band	4715.2¶
Intensity maximum 1, 0 Swan band	36.16(4)		35.32(1)	36.55(3)	36.01(2)			35.74(1)	36.0(2)	1, 0 C_2 Swan band; intensity maximum of *P* branches	‡
Head of 1, 0 Swan band	39.02			38.17	37.91				38.2	Head of 1, 0 Swan band	4737.1¶
Emission feature	51.57(1−s)				53.45(½s)				52.8(½−)		
Emission feature					78.96(0+)				79.0(0)		
Emission feature					4821.58(0+d)				4821.6(0)		
Emission feature	4836.31(½)								36.3(0)	C_2? Unassigned band reported by Fox and Herzberg?	4836.1**

‖ A. McKellar, *Pub. A.S.P.*, **52**, 312, 1940; L. Gero, *Physik. Z.*, **155**, 1940

										ported by Fox and Herzberg?

‖ A. McKellar, *Pub. A.S.P.*, **52**, 312, 1940; L. Gero, *Physica*, **7**, 155, 1940

UNIV. OF MICH.

PLATE V

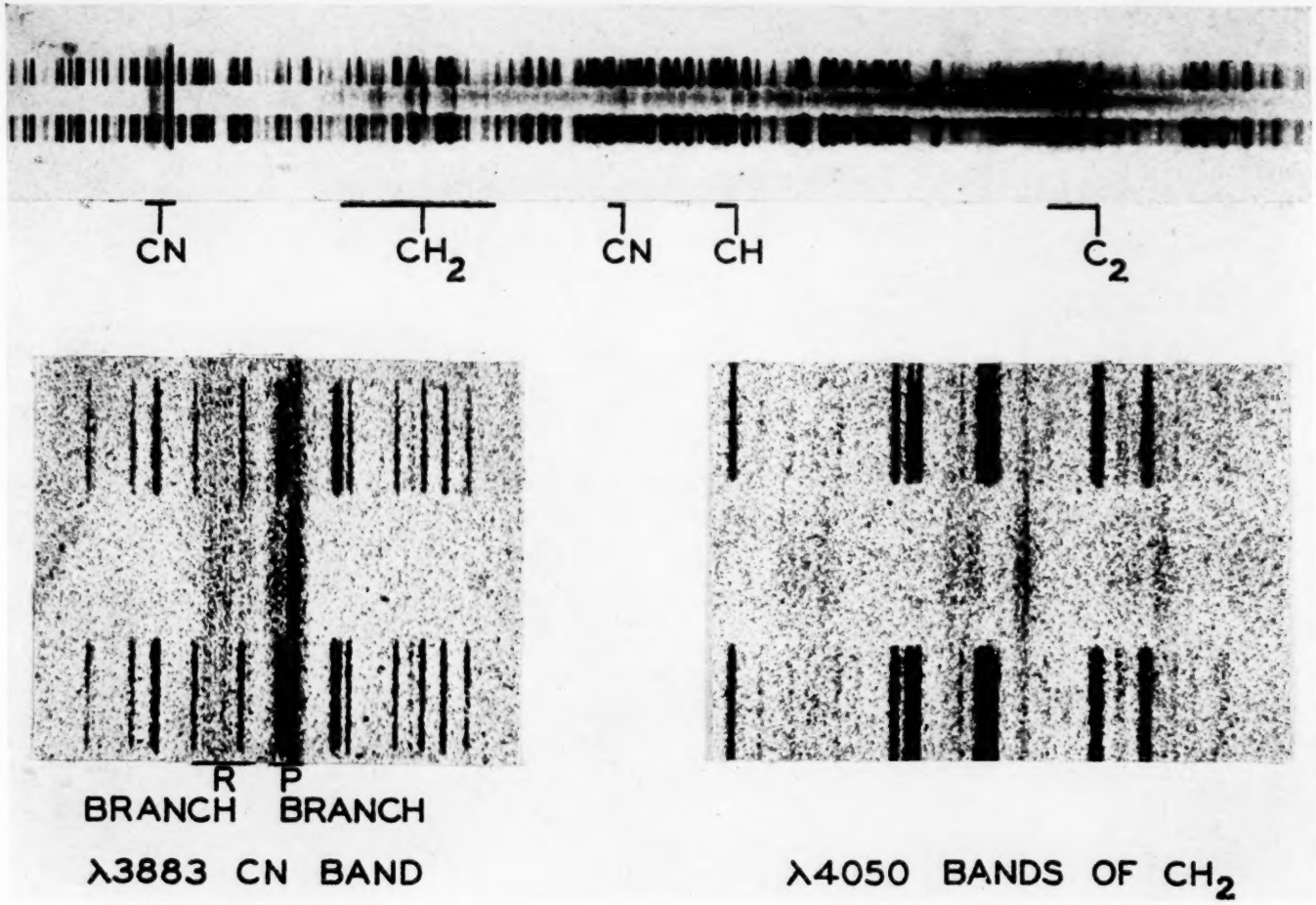

SPECTRA OF COMET WHIPPLE-FEDTKÉ-TEVZADZE (1942g)

Above, a reproduction of the spectrogram taken February 24, 1943. *Lower left*, λ 3883 *CN* band from the plate of March 1, 1943, greatly enlarged, showing resolution of rotational structure in the *R* branch. *Lower right*, λ 4050 group of CH_2 from the same plate. Note here the duplicity of the main maximum at λ 4051.

Three other points should be mentioned. First, the measured wave lengths were corrected to take account of the radial velocity of the comet with respect to the earth. Second, wave lengths of all band edges or band heads measured were further corrected for the effect of the lack of infinitely high spectral purity. That is, from the wave length of each red edge of an emission band measured, there was subtracted an amount equal to half the projected spectrographic slit width at that wave length, while this quantity was added to the wave lengths of the violet edges of the bands measured. Third, in the few cases in which an intensity minimum is identified as an actual Fraunhofer absorption line in the scattered solar spectrum (e.g., λ 4045) its wave length has been corrected also for the effect of the radial velocity of the comet with respect to the sun.

DISCUSSION

A reproduction of the spectrum of Comet 1942g is shown in Plate V. The most noteworthy feature of general interest regarding the spectrum of this comet, in the ordinary photographic region, is the relatively great strength of the λ 4050 group of bands due to CH_2. This group and the omnipresent and always strong λ 3883 0, 0 sequence of *CN* bands are the most outstanding of the emissions and are of approximately the same total intensity. The usually very strong λ 4737 1, 0 sequence of the Swan system of C_2 is less intense than either the *CN* or the CH_2 bands. The λ 4315 band of *CH* is faint but definitely measurable. These exceptional intensity ratios are doubtless a consequence of the considerable heliocentric distance of the comet, $r = 1.4$ astronomical units. At such a distance the breakdown of "parent" polyatomic molecules to form *CN*, *CH*, C_2, etc., by photodissociation under the influence of sunlight, has not proceeded to such an extent as at closer approach of the comet to the sun. Therefore, as pointed out previously,[3] the emission bands due to polyatomic molecules should be, and apparently are actually found to be, more intense with respect to those of diatomic molecules at the greater heliocentric distances. Much the same general observations as above and similar conclusions are contained in a brief note by Swings and Struve[4] on the spectrum of Comet 1942g.

THE BANDS OF *CN*

On every plate the λ 3883 0, 0 *CN* band exhibited the complex structure which has been the subject of study over the last few years.[5,6] This is evident from the measurements given in Table 2. One spectrogram, that of March 1, taken with projected slit width at λ 3880 of only 0.5 angstrom, showed unusually fine definition. The appearance of the band is shown in Plate V. On this plate the rotational structure of the *R* branch (nonhead-forming branch) of the λ 3883 band is just barely resolved. Reference to Table 2 will show that nearly all the individual lines from the short-wave-length extremity at the line *R*(12) up to the band origin have been measured. The intervals between successive lines are about 0.7–0.8 angstrom unit. In so far as the writer is aware, such resolution has not been obtained up to the present on the *CN* bands in the spectrum of any comet. Use will be made of this plate in a spectrophotometric study to determine the rotational distribution of the cometary *CN* molecules.

It will be noted in Table 2 that for the sharp lines in the *CN* band from *R*(12) to *R*(1), while the agreement between the accurate laboratory and the cometary wave lengths, determined mainly from one low-dispersion plate, is fairly good, there appears to be a small but definitely systematic difference between them. The mean difference for ten lines is λ (comet) − λ (lab.) = +0.09 angstrom unit. Unfortunately, there are no other spectral features with well-determined laboratory wave lengths and sharp enough in the

[3] See, e.g., P. Swings, *Rev. Mod. Phys.*, **14**, 190, 1942; G. Herzberg, *Rev. Mod. Phys.*, **14**, 195, 1942.

[4] P. Swings and O. Struve, *Pub. A.S.P.*, **55**, 150, 1943.

[5] P. Swings, *Lick Obs. Bull.*, **19**, 131, 1941.

[6] A. McKellar, *Rev. Mod. Phys.*, **14**, 179, 1942.

larged, showing resolution of rotational structure in the *R* branch. *Lower right*, λ 4050 group of CH_2 from the same plate. Note here the duplicity of the main maximum at λ 4051.

cometary spectrum to test the reality of this difference, except, perhaps, the λ 4300 and λ 4304 lines of *CH*. The measurements of these are not definitive enough to permit a decision on this point. Under the circumstances of observation the existence of a systematic error of this amount cannot be excluded. If, however, the shift of wave length can be attributed to a physical cause which may be referred to the comet, the only obvious explanation would appear to be an average motion of recession (toward the tail of the comet), the line-of-sight component amounting to some 7 km/sec. While no definite conclusion can be drawn from the present observations, the matter is of sufficient interest to warrant further attention in the future when greater spectrographic power is available for studies of this kind.

The matters of the over-all wave-length range of the *CN* band and its general intensity distribution are worthy of note. In the present case the short-wave-length limit of the band is at λ 3866.2, the $R(12)$ line, and the long-wave-length limit at λ 3881.5, the $P(15)$ line. Thus the band appears to be developed to such an extent that lines originating from the rotational levels up to $K' = 14$ appear. The maximum of intensity in the P (head-forming) branch occurs at λ 3880.16, between the lines $P(10)$ and $P(11)$. For comet Cunningham (1940c), it was found[6] that, for the heliocentric distances $r = 0.92$ and $r = 0.54$, lines from levels up to about $K' = 25$ were present and the P-branch maximum occurred at $P(13)$ for $r = 0.92$ and $P(20)$ for $r = 0.54$. Dufay[7] had earlier found from examination of spectra of several comets that the K'' corresponding to the *CN* band maximum advanced from $K'' = 6$ to $K'' = 14$ as r decreased from 1.8 to 0.5 astronomical units. The general intensity profile of the *CN* band in the spectrum of Comet 1942g is thus in conformity with these recent suggestions regarding the increase in "rotational temperature" (the term "temperature" being used only in the sense referring to the relative populations of the molecular rotational states) with decreasing heliocentric distance. Also, it yields another point in establishing the quantitative relationship between r and the K'' corresponding to maximum intensity. The role in the determination of this intensity maximum played by the radial velocity of the comet with respect to the sun and discussed in references 5 and 6, must not be ignored.

The 0,1 sequence of the violet *CN* system at λ 4216 appeared on the plates with moderate intensity. In view of the smaller spectrographic dispersion compared with λ 3880 and the lower intensity of this sequence, nothing worth while is gained by a detailed discussion of it.

THE λ 4050 GROUP OF CH_2 BANDS

On the spectrogram of March 1, 1943, the resolution in the region of the λ 4050 group of bands was also very good. Plate V includes a reproduction of the group from this spectrogram. The projected slit width at λ 4050 was 0.60 angstrom. These bands have recently been shown by Herzberg[8] to be due to the triatomic molecule CH_2. A comprehensive résumé, including previous summaries of the wave lengths of this group of bands in the spectra of many comets, is given by Swings, Elvey, and Babcock.[9]

Measurements on the present plates have revealed certain structure not previously noted. Of perhaps most interest is the duplicity of the strongest emission feature at λ 4051. On four of the eight plates it has been found to be double, with components at λ 4050.43 and λ 4051.75, the component of longer wave length being perhaps a little over twice as intense as the other. On the plate of March 1, the region from λ 4013 to λ 4020 appears to contain four intensity maxima. Also, the duplicity of the emission at λ 4068, heretofore suspected, is confirmed, components being measured at λ 4066.17 and λ 4069.99.

[7] J. Dufay, *C.R.*, **206**, 1948, 1938.

[8] *Loc. cit.*; and *Ap. J.*, **96**, 314, 1942.

[9] P. Swings, C. T. Elvey, and H. W. Babcock, *Ap. J.*, **94**, 342, 1941.

According to current ideas on the resonance or fluorescence origin of cometary emission bands, the observed intensity distributions over these bands would be expected to show certain definite differences from those encountered in laboratory studies. These differences would be a consequence of the intensity distribution over the region of the solar spectrum absorbed in the course of the production of the bands. In the case of the CH_2 bands, the three very strong *Fe* absorption lines at λλ 4045, 4063, and 4072 in the solar spectrum would doubtless have considerable effect in this way. They would cause intensity minima in the CH_2 bands at these three wave lengths and possibly other wave lengths, depending on the as yet unknown detailed band structure. The CH_2 bands shown in Plate V appear to exhibit this effect, particularly for λ 4072, where the emission centered at λ 4074 seems to be cut off sharply on its violet edge. The effect mentioned has, of course, to do only with the cometary *emissions*, not with that part of the cometary spectrum which is simply reflected or scattered solar radiation and which exhibits the normal Fraunhofer lines.

Unfortunately, the laboratory investigation and analysis of the λ 4050 group of CH_2 bands, from high-dispersion spectrograms, at present being conducted by Dr. Herzberg, is not yet completed. While it could be suggested that the main sharp maxima are probably *Q* branches, yet the detailed interpretation of the structural features of the band discussed above and of the intensity profile to be expected under cometary conditions of excitation cannot profitably be undertaken now. The band structure should be re-examined, however, when the complete laboratory data on the system become available.

THE SWAN BANDS OF C_2

As already noted, the Swan bands of C_2 appeared with somewhat lower intensity than usual. On the ordinary plates the 1, 0 sequence, λ 4737, was readily measured, and a trace of the 2, 0 sequence (the 4, 2 band) was found to be present. On the panchromatic plates the 0, 0 sequence, λ 5165, and the 0, 1 sequence, λ 5635, occurred.

One point of interest may be noted, namely, that on the two best plates a sharp emission feature was measured near λ 4752. This is the wave length of the head of the 1, 0 Swan band due to $C^{13}C^{13}$, the diatomic carbon molecule made up of two atoms of the carbon isotope of atomic weight 13. This band is the analogue of the λ 4737 Swan band due to ordinary $C^{12}C^{12}$.

The relative abundance of C^{12} to C^{13} has been reliably measured[10] in terrestrial samples of carbon as about 100 to 1. Also, a spectrographic analysis of some meteoritic samples[11] has indicated that the relative abundance of C^{13} in these is not sensibly greater than this value. If the abundance ratio C^{12} to C^{13} is a, the relative abundances of the isotopic molecular species $C^{12}C^{12}:C^{12}C^{13}:C^{13}C^{13}$ are as $a^2:2a:1$, that is, for terrestrial or meteoritic carbon, approximately 10,000:200:1.

Bobrovnikoff[12] and later Swings,[13] on the basis of their own measurements on the spectra of Comets Halley (1910) and Brooks (1911) and also Wright's measurements on the spectrum of Comet Brooks, concluded that the isotopic bands of $C^{12}C^{13}$ and $C^{13}C^{13}$ at λ 4745 and λ 4752 were present, hence that the carbon isotope, C^{13}, was a constituent of the heads of these comets. While this result is not specifically questioned, yet in the case of Comet 1942g the relatively low intensity of the main, $C^{12}C^{12}$, Swan system and also the absence of the $C^{12}C^{13}$ band head at λ 4745 lead us to conclude that the feature measured at λ 4752 is not due to the isotopic carbon molecule $C^{13}C^{13}$. Perhaps one would think that the fact that $C^{12}C^{13}$ is not a strictly homonuclear molecule and so probably has a different

[10] F. A. Jenkins and L. S. Ornstein, *Kon. Akad. v. Wetensch., Amsterdam*, **35**, 1212, 1932; A. O. Nier and E. A. Gulbransen, *J. Amer. Chem. Soc.*, **61**, 697, 1939.

[11] F. A. Jenkins and A. S. King, *Pub. A.S.P.*, **48**, 323, 1936.

[12] N. T. Bobrovnikoff, *Pub. A.S.P.*, **42**, 117, 1930; and *Pub. Lick Obs.*, **17**, 441, 1930.

[13] P. Swings, *Ap. J.*, **95**, 270, 1941; and *M.N.*, **103**, 86, 1943.

rotational distribution of molecules than $C^{12}C^{12}$ and $C^{13}C^{13}$ could be invoked to explain, partially at least, the absence of λ 4745. But the origin of this band is at about λ 4738, the band head occurs at about $K'' = 17$, and the rotational constant $B'' = 1.6$, so this argument is not strong. In any case, the matter of relative abundances inclines us to the view that in the present instance the emission at λ 4752 is due to some as yet unidentified emitter. Swings[13] has pointed out that for Comet Cunningham (1940c), on spectrograms on which the very intense Swan bands were strongly overexposed, there was no trace of the isotopic bands. He advances the suggestion that the relative abundance of C^{12} and C^{13} may be different in various comets. If our present view should be erroneous and the λ 4752 emission in the spectrum of Comet 1942g should actually be due to $C^{13}C^{13}$, this fact, together with the data on Comet Cunningham, would provide very strong evidence in favor of Swings's suggestion.

An additional point regarding the measured wave lengths of the heads of the 1,0, 2,1, and 3,2 bands of C_2 is evident from Table 2. These wave lengths are consistently about 1 angstrom unit greater than the laboratory values. Since, as was earlier stated, care was taken to correct the measured wave lengths by an amount equal to one-half the projected slit width, this cannot be the cause. No reason for this difference is apparent.

THE *CH* BANDS

While relatively weak, the λ 4315 0, 0 band of the $^2\Delta$, $^2\Pi$ transition was definitely present. The *Q*-branch maximum at λ 4313 and the sharp lines of the *R* branches at λ 4304 and λ 4300 were measured. No trace of the less intense band due to the $^2\Sigma$, $^2\Pi$ transition, with heads at λ 3872 and λ 3889, was detected.

OTHER EMISSIONS

Certain emission features occurring between the 0,1 *CN* band at λ 4216 and the *CH* band near λ 4300 may now be dealt with. Swings[13] has recently identified three of these at λλ 4231, 4238.5, and 4254.4 as the $R(0) + R(1)$, the $Q(1) + Q(2)$, and the $P(3)$ lines of the 0, 0 band of the violet CH^+ system. Incidentally, the first of these, suspected by Swings to be double on one of his plates, has been found to be so for Comet 1942g.

While examining wave-length material on the spectra of polyatomic molecules in connection with the spectrum of Comet 1942g, it was noted that the strongest bands of a system tentatively ascribed to SiO_2[14] occurred in this same region. Furthermore, it appeared that very good wave-length coincidences occurred between the most intense SiO_2(?) bands and certain of the cometary emissions. The state of affairs in this respect is presented in Table 3, which gives five columns containing data on the spectra of comets, followed by columns giving the laboratory wave lengths of CH^+ band lines and of SiO_2(?) band heads and intensity maxima. The letters "V," "R," and "M" following the wave length in the last column indicate the heads of bands degraded to the violet, those degraded to the red, and headless bands, respectively. All the numbers in parentheses give relative intensity estimates except in the CH^+ column, where, of course, they refer to the rotational quantum numbers used to designate the band line. When considering the wave-length region covered in Table 3, it should be called to mind that the two molecules responsible for all the emission bands known in the spectra of cometary tails have bands in this region. There are CO^+ band heads at λλ 4248.9, 4252.4, 4272.0, and 4274.3; and there are N_2^+ band heads at λ 4236.5 and λ 4278.1.

Strangely, the wave lengths of the CH^+ band lines and the SiO_2(?) bands are very similar, and the general agreement between cometary and laboratory values for the two molecular spectra is about the same. Favoring the conclusion that some of the cometary

[14] R. C. Pankhurst, *Proc. Phys. Soc.* (London), **52**, 707, 1940; R. W. B. Pearse and A. G. Gaydon, *The Identification of Molecular Spectra*, pp. 179–80, London: Chapman & Hall, Ltd., 1941; L. H. Woods, *Phys. Rev.*, **63**, 426, 1943.

emissions may be due to SiO_2(?) are (1) the close wave-length coincidences and (2) the fact that the bands occur in the comet spectrum at the heliocentric distance $r = 1.4$. Opposing this conclusion is the following greater number of points: (1) The lines at λ 4228 and λ 4232 are definitely sharp and so are more likely to be the single lines of the CH^+ band. (2) SiO_2 (quartz) in solid form is a most refractory compound and, if present in molecular form, must have been formed by dissociation of some parent polyatomic molecule. No obvious parent comes to mind. In this connection carbon is also very nonvolatile, and yet C_2 bands appear in the coolest hydrocarbon flames and in cometary spectra,

TABLE 3

COMETARY EMISSION BANDS IN THE λλ 4230–4280 REGION

Comet Whipple-Fedtké-Tevzadze (1942g) r=1.4 A.U.	Comet Cunningham (1940c)* $r\sim0.6$	Comet Brooks (1911c)† $r\sim0.5$	Comet Halley (1910)‡ $r\sim0.7$	Unidentified Nuclear Emissions, Summary by Baldet (1926)§	Wave Lengths of Lines of the 0,0 CH^+ Band‖	Wave Lengths of Bands Due to SiO_2(?)¶
.....	.....	.....	.....	.....	4225.26 } $R(4)$ line	.....
.....	.....	.....	.....	.....	4225.69 } $R(3)$	.....
.....	.....	.....	.....	.....	4225.80 } $R(5)$	.....
.....	.....	.....	.....	.....	4227.06 $R(2)$	.....
4228.4(0+s)	4229.1(1)	.....	.....	.....	4229.34 $R(1)$	4228.5V(9)
.....	.....	4230(0)(long line tail)	.....	4230(1)	.....	.....
4231.9(0+s)	4231.8(1)	.....	4231.2	.....	4232.54 $R(0)$	.....
4235.6(0)	.....	.....	.....	.....	4237.56 $Q(1)$	4235.5V(10)
4239.4(0)	4240.4(1−2n)	4238.5(0)(long line, tail)	.....	4238(1)	4239.37 $Q(2)$	4240 M(10)
.....	.....	.....	.....	.....	4242.11 $Q(3)$	.....
.....	.....	.....	.....	.....	4247.57 $P(2)$	.....
.....	.....	.....	.....	.....	.....	4252.4V(6)
.....	4254.3(1n)	4254.5(0+)(long line, tail)	.....	4255.8(2)	4254.38 $P(3)$	4254.4R(7)
4257.7(0)	.....	.....	.....	.....	.....	4256.6R(8)
4263.7(0)	.....	4265(0)	4264.5	4264.2(2)	4262.13 $P(4)$	4262.8R(6)
.....	.....	.....	.....	.....	.....	4269.6R(4)
.....	.....	4277.2(long line, CO^+?)	.....	.....	.....	4274.5R(4)
.....	.....	.....	4283.0	.....	.....	4283 M(9)

* P. Swings, *Ap. J.*, **95**, 270, 1942; *Contr. Lick Obs.*, Ser. II, No. 3.

† W. H. Wright, *Lick Obs. Bull.*, **7**, 8, 1912.

‡ N. T. Bobrovnikoff, *Lick Obs. Pub.*, **17**, 445, 1931.

§ F. Baldet, *Ann. obs. Astr. phys. Paris*, **7**, 58, 1926.

‖ A. E. Douglas and G. Herzberg, *Canad. J. Research*, **20**, 71, 1942.

¶ R. C. Pankhurst, *Proc. Phys. Soc.* (London), **52**, 707, 1940; R. W. B. Pearse and A. G. Gaydon, *The Identification of Molecular Spectra*, pp. 179–80, Chapman & Hall, Ltd., 1941; L. H. Woods, *Phys. Rev.*, **63**, 426, 1943.

where, of course, the molecular carbon results from dissociation. Also, Bobrovnikoff states[15] that for Comet 1882 I at $r = 0.87$ before perihelion and for Comet 1914 V at $r = 1.21$, the sodium D lines were observed in emission, despite the fact that the boiling-point of sodium is 877° C and, at $r = 1$, the temperature of a black body is only around 0° C. (3) If SiO_2 were present, one might expect to find bands due to SiH and SiN and perhaps CO_2 in the spectrum of the same comet. A careful search in the present case has not revealed these bands. (4) We do not know whether or not the bands produced in the laboratory and ascribed to SiO_2(?) arise from the ground state of the molecule, a condi-

[15] N. T. Bobrovnikoff, *Rev. Mod. Phys.*, **14**, 171, 1942.

tion necessary for their appearance by resonance and virtually necessary for appearance by fluorescence under cometary conditions.

It must be remembered that the emissions we have been considering in this section are among the weaker ones occurring in cometary spectra. In view of this and also the evidence against the significance of the possible $SiO_2(?)$ origin of the bands, as opposed to the less weighty favorable evidence, the writer is inclined to the belief that the $SiO_2(?)$ bands are probably not present. Nevertheless, it was thought worth while to discuss the matter as we have done, for it cannot be said to be settled with certainty. Two future developments—first, better observational data on bright comets and, second, further laboratory work on the $SiO_2(?)$ bands, clarifying their molecular origin and including their detailed vibrational and rotational analysis—should enable a definite conclusion to be reached on the matter.

There still remain in Table 2 about a dozen unidentified emission features. Study of all available laboratory data on molecular spectra has failed to reveal any reasonable identification for them. The recent studies resulting in evidence for the occurrence of CH_2 bands and probably NH_2 bands in cometary spectra would seem to enhance the possibility that an appreciable portion of these unidentified features may subsequently be found to arise from polyatomic rather than from diatomic molecules.

In conclusion, the need for and the value of good future spectrographic observations of comets should be emphasized. In the dicussion of the measurements which are the basis of the present paper there have arisen several problems, including possibly significant wave-length shifts of the sharp CN band lines, the identification of the weak λ 4752 emission with the $C^{13}C^{13}$ band, and the identification of emissions in the λλ 4230–4280 region, which cannot be settled with the data now at hand. Only by the study of better cometary spectrograms—and there is no substitute for these—can conclusive answers to the above questions be advanced. When the occurrence of a bright comet makes it possible, slit spectrograms secured with the highest practicable combination of dispersion and spectral purity should be obtained. Relatively few observatories have the telescopic and spectrographic equipment necessary for obtaining such spectra, and, when such factors as the transitory nature of comets and the diffuseness of even their nuclei are considered, it is understandable why so few high-purity cometary spectrograms have been secured. In urging that steps be taken to remedy this deficiency, by those who may be in a position to do so when a new bright comet should appear, we may state with certainty that such cometary spectrograms, when obtained, will be of great value. Not only will they help us to arrive at decisions on the above-mentioned matters, but also they will doubtless bring forward, and aid in the solution of, other and important problems in cometary physics.

ON THE SPECTRUM OF COMET 1940c

N. T. Bobrovnikoff
Perkins Observatory
Received November 19, 1943

ABSTRACT

The spectrum of the comet was measured on two spectrograms obtained at the Perkins Observatory on December 23 and 24, 1940. The structure of the main cyanogen and carbon bands is discussed. The fine structure of the cyanogen band (0, 0) can be identified with certain rotational lines in this band. The presence of sharp lines in the carbon band (1, 0) is established, but their connection with the band is doubtful. A list of other lines and bands measured on the plates is given.

OBSERVATIONAL MATERIAL

Owing to unfavorable weather, only two measurable spectrograms of Comet 1940c (Cunningham) could be obtained between December 1, 1940, and January 4, 1941. They were made with the two-prism spectrograph and the 350-mm camera, attached to the 69-inch reflector. The plates were Eastman 103-0. The width of the slit was 0.35 mm, and the length 10 mm. The projected slit width was 1.46 A for λ 3883 and 3.80 A for λ 4737. Because of the shortness of exposure, most cometary bands appear as sharp lines with a width much smaller than the above figures would indicate.

In view of a thorough investigation of the spectrum of this comet made elsewhere,[1] it might seem superfluous to give the results of my measurement. However, since our spectrograms have a much greater dispersion (16.1 A/mm at λ 3883 and 41.7 A/mm at λ 4737) than ordinarily used in comet spectroscopy, many details either only suspected by the former investigators or not noticed at all are quite clear. The difference in the intensity of the various bands in cometary spectra is so great that the faintest bands can be seen only when the strongest bands are overexposed and their structure concealed. While many of the fainter bands cannot be measured on our spectrograms, the structure of the stronger ones is striking.

The details for the spectrograms are as shown in the accompanying tabulation.

No.	Mid.-Exp. U.T.	Exp. Time
Pa 552	1940 Dec. 23.993	60^m
Pa 556	Dec. 24.999	76^m

The comet in the Cassegrain focus appeared as a strongly condensed globular body of 10″ in diameter, surrounded with a faint coma. Visual observers of that period state that the nucleus was stellar. Therefore, what appeared to be the nucleus on the slit of the spectrograph was in reality a dense spherical envelope around the stellar nucleus.

The slit was oriented along right ascension, and the nucleus of the comet held in the center of the slit. The guiding, in spite of the low altitude of the comet, was satisfactory. The measurement of the spectrograms shows that the nucleus was displaced from the geometrical center of the slit by only 0.11 mm or 2″.8 in angular measure. The nuclear line on the spectrograms is 11″.5 wide, corresponding to the spherical envelope around the nucleus mentioned above.

[1] Swings, Elvey, and Babcock, *Ap. J.*, **94**, 320, 1941; *Contr. McDonald Obs.*, No. 38. I adhere to the designation "1940c" used by these writers, although the correct designation may be 1940d, depending on whether Comet 1940a (Kulin) is a comet or an asteroid (*Pop. Astr.*, **48**, 490, 1940).

As the position angle of the radius vector on December 25.0 was 206.5°, the slit made an angle of 63.5° with the radius vector on the west side. The west side of the comet was therefore nearer to the sun than the east side. As a consequence of this fact, the structure of some bands shows a curious difference between the west and the east sides.

The plates were measured in both directions and reduced in four sections by the Hartmann formula. The main difficulty of measurement was the curvature of the lines introduced by the long slit. The wire of the micrometer was set on the tips of the iron comparison lines, and a correction of −0.0124 mm was applied to the measured abscissa of the comet lines. No evidence was found of any appreciable systematic error due to this difficulty in measurement. From the internal agreement of the measures of the cometary lines, as well as from the comparison lines not used in the derivation of the Hartmann formula, the reliability of measurement is estimated at 0.03 A for λ 3883 and 0.06 A for λ 4737.

All bands except the strongest parts of the *CN* (0, 0) and (1, 1) bands appear on the spectrograms as sharp lines, considerably sharper than comparison lines of comparable intensity. Therefore, the wire of the micrometer was set to bisect the cometary lines rather than on their red edge.

The measured wave lengths in the spectrum of the comet were corrected for the Doppler effect resulting from the relative motion of the comet and the earth. For December 23 this was −27.7 km/sec and for December 24, −28.7 km/sec. Although the hour angle of the comet was over five hours, the Doppler effect due to the rotation of the earth was only −0.3 km/sec.

WAVE LENGTHS

The finally adopted wave lengths are given in Table 1. Column *i* contains estimated intensities on an arbitrary scale, Column SEB the wave lengths reported by Swings, Elvey, and Babcock for the same comet, and Column H the wave lengths found by me in the spectrum of Halley's Comet.[2]

THE STRUCTURE OF *CN* BANDS

The fine structure of the (0, 0) band of *CN* at λ 3883 appears to be identical on both plates, the average difference being only +0.01 A. It is evident that no modification in the *CN* bands took place between these two dates.

The main portion of the (0, 0) band is overexposed, but the three lines in it can be seen without difficulty, especially farther away from the nucleus. The individual lines in the main portion of the (1, 1) band are not distinguishable, and we may speak only of the maxima of intensity.

As to the identification of the fine structure of the bands, I do not think the present observational material—or, in fact, any material so far published—is adequate to settle the question. Taking as an illustration the five lines in the (0, 0) band measured on both plates, we have the comparison between the cometary and laboratory wave lengths[3] for December 24 shown in Table 2.

Formally, such an identification must be regarded as highly satisfactory; yet the assignment of rotational lines is in every case different from that given by Swings[4] in his adopted cometary wave lengths for the (0, 0) sequence.

It would seem that the measured features are actually individual rotational lines and not groups of lines, but I think this conclusion would be erroneous. The lines in the band are rather symmetrically placed, and it is possible to select a combination of rotational lines resulting in the actually observed wave length of the line. For instance, taking six

[2] *Lick Obs. Pub.*, **17**, 433 ff., 1931.

[3] Laboratory wave lengths from Uhler and Patterson, *Ap.J.*, **42**, 434, 1915.

[4] *Lick Obs. Bull.*, **19**, 131, 1941.

TABLE 1

WAVE LENGTHS IN COMET 1940c

Dec. 24	Dec. 23	*i*	SEB	H	Identification	Description
3856.0	.....	1	57.7	55.2	*CN* *R*(1, 1)	Violet edge of a band
3862.5	.....	1	62.5	63.1	*CN* *P*(1, 1)	Red edge of a band
3866.31	.....	2	67.5		*CN* *P*(1, 1)	Max. int. in a band
3868.07	.....	3		69.0	*CN* *P*(1, 1)	Max. int. in a band
3870.41	.....	2	69.9	69.8	*CN* *R*(0, 0)	Max. int. in a band
3873.95	73.69	3	73.5	.....	*CN* *R*(0, 0)	Very sharp line
3876.87	76.92	4	76.8	76.3	*CN* *P*(0, 0)	Very sharp line
3879.57	79.89	7	80.2	79.5	*CN* *P*(0, 0)	Line in the main band
3880.97	80.96	10			*CN* *P*(0, 0)	Line in the main band
3882.37	82.32	10	82.0	81.8	*CN* *P*(0, 0)	Line in the main band
4038.96	.....	1	39.6	38.9	CH_2	Diffuse line
4043.27	.....	1	43.6	42.5	CH_2	Diffuse line
4047.29	.....	1	.....	49.6	?	Diffuse line
4051.77	.....	2	51.6	52.5	CH_2	Diffuse line
4054.62	.....	2	54.2	.....	CH_2	Diffuse line
4196.77	.....	1	97.0	97.4	*CN* *R*(0, 1)	Faint and diffuse line
4200.13	.....	1	.....	.....	*CN*	Faint and diffuse line
4203.12	.....	1	.....	.....	*CN*	Faint and diffuse line
4206.15	06.45	1	06	.....	*CN* *R*(0, 1)	Faint and diffuse line
4209.79	.....	1	10.2		*CN* *P*(0, 1)	Very sharp short line
4211.70	11.86	1		11.4	*CN* *P*(0, 1)	Very sharp short line
4213.72	.....	3	14.7	13.5	*CN* *P*(0, 1)	Long line
4215.49	14.92	3		15.0	*CN* *P*(0, 1)	Long line
4263.90	.....	1	.....	64.5	?	Very faint line
4265.52	.....	1	.....		?	Very faint line
4285.89	.....	1	85.7	.....	*CH* *R*(0, 0)	Very faint line
4288.40	.....	1	.....	.....	?	Very faint line
4292.56	91.67	2	91.7	.....	*CH* *R*(0, 0)	Diffuse line
4296.85	97.17	2	97.3	96.0	*CH* *R*(0, 0)	Diffuse line
4299.83	99.66	2	00.2	.....	*CH* *R*(0, 0)	Sharp line
4303.97	03.35	5	03.9	.....	*CH* *R*(0, 0)	Sharp line
4307.97	07.93	1	.....	.....	?	Sharp line
4309.08	.....	1	.....	.....	?	Sharp line
4313.21	13.13	8	13.2	.....	*CH* *Q*(0, 0)	Very sharp on violet edge
4321.40	21.39	1	.....	.....	?	Sharp line
4327.48	28.06	1	.....	.....	?	Sharp line
4330.98	.....	.....	29.3	29.5	*CH* *P*(0, 0)	Sharp line
4342.08	.....	1	44	42.8	*CH* *P*(0, 0)	Sharp line
4351.37	.....	1	48	50.8	*CH* *P*(0, 0)	Sharp line
4361.42	60.88	1	.....	59.2	?	Very hazy line
4363.92	63.91	4	.....	65.0	C_2 *P*(4, 2)	Sharp line
4371.32	70.42	3	.....	71.6	C_2 *P*(3, 1)	Sharp line
4375.62	75.01	1	.....	.....	?	Sharp line
4380.68	80.74	2	.....	80.4	C_2 *P*(2, 0)	Sharp line
4678.60	78.26	2	.....	77.9	C_2 *P*(5, 4)	Sharp line
4684.77	84.58	3	.....	84.7	C_2 *P*(4, 3)	Sharp line
4689.87	88.70	1	.....	.....	?	Diffuse line
4697.49	97.31	8	.....	97.4	C_2 *P*(3, 2)	Sharp line
4703.50	03.57	1	.....	05.9	?	Sharp line
4707.20	06.96	1	.....		?	Sharp line
4714.98	14.81	10	.....	15.2	C_2 *P*(2, 1)	Sharp line
4737.04	36.94	7	.....	37.2	C_2 *P*(1, 0)	Sharp line
4744.26	.....	1	.....	45.8	$C^{12}C^{13}$ (0, 0)	Diffuse line

rotational lines between λ 3882.58 and λ 3882.10, we would get the mean wave length 3882.35, which is within 0.02 A of the wave length measured in the comet. The width of this combination of lines would be only 0.48 A. A much higher dispersion and a narrower slit are evidently necessary to settle the question of identification.

One important consequence follows from Table 2, as well as from the data on other comets. There are no large radial velocities involved in the comet. Although *CN* has been shown to be an important constituent of halos and jets, constantly forming and expanding in many comets, the velocities of expansion are always small, seldom exceeding 1 km/sec. Such a velocity of approach would result in the displacement of the *CN* lines in the (0, 0) band of only 0.013 A to the violet. The sharp character of the *CN*, as well as of

TABLE 2

THE (0, 0) BAND OF *CN*

Comet	Laboratory	C−L	Identification	Comet	Laboratory	C−L	Identification
3882.37 A.....	3882.32 A	+0.05 A	*P*(18)	3876.87 A.....	3876.84 A	+0.03 A	*P*(3)
3880.97.....	3881.00	− .03	*P*(13)	3873.95.....	3874.00	−0.05	*R*(1)
3879.57.....	3879.58	−0.01	*P*(9)				

TABLE 3

WIDTH OF CORE OF THE +1 SEQUENCE OF C_2

Band	Width		Band	Width	
	Dec. 23	Dec. 24		Dec. 23	Dec. 24
1,0.....	2.29 A	2.52 A	4,3.....	2.33 A	1.91 A
2,1.....	2.34	2.38	5,4.....	3.54	2.10
3,2.....	2.14	2.02			

other lines, speaks against any great turbulence in the atmosphere of the comet. The absence of large velocities of ejection from the nucleus, up to 60 km/sec. required by the mechanical theory of cometary forms, is one of the most puzzling facts.

The distribution of intensity along the *CN* lines on either side of the continuous spectrum is uniform, the sunward side not being favored. The bands stretch across the whole spectrum more than 1′ in width, and undoubtedly extend much farther.

Plate VI shows the structure of the *CN* bands (the 0 sequence) on December 24. As fainter details are difficult to reproduce, the lower figure (*b*) shows the lines retouched on the original enlargement.

The (0, 1) *CN* band at λ 4216 has the structure analogous to that of the main band; but, because of the lower dispersion and faintness of the bands, the measures on the two dates are not in such good agreement as for the (0, 0) band.

THE STRUCTURE OF THE SWAN BANDS

Each plate has a set of five usual bands of the +1 sequence of C_2. The cores of these bands corresponding to the continuous spectrum are very sharply defined. Their width is given in Table 3.

The projected slit width was 3.80 A for the first band and 3.62 A for the last. There is

PLATE VI

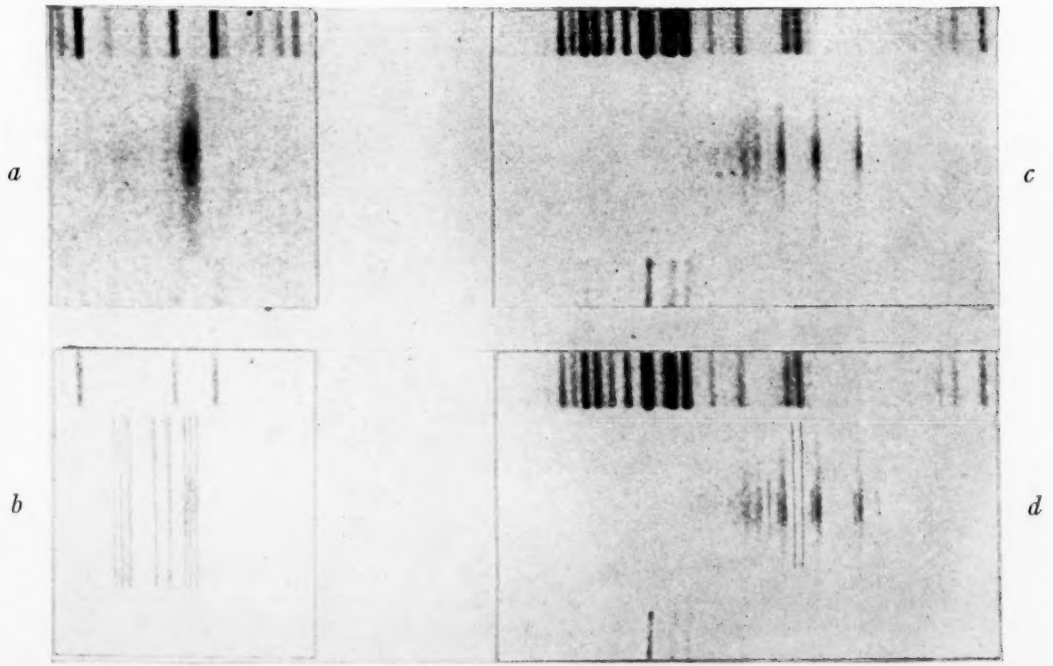

SPECTRUM OF COMET 1940c (CUNNINGHAM) ON DECEMBER 24.999, 1940

a, the *CN* band λ 3883; *b*, the same band retouched to show the structure; *c*, the carbon band λ 4737; *d*, the same band retouched. The upper side of the reproduction corresponds to the west, or sunward, side of the comet.

UNIV. OF MICH.

no significant difference in the width of these bands, except for the last one on December 23. It is strikingly wider and more diffuse on that date than on the following. It appears that some modification in the structure of the Swan bands took place within the one day which separated these two plates.

This conclusion is strengthened by the measurement of the wave lengths of the band. Table 4 gives the difference between the measured wave lengths of the *P*-heads in the comet and those in the laboratory.[5]

The measurement was repeated but with practically the same result. It appears that on December 23 the Swan bands were displaced to the violet by 0.22 A as compared with December 24. If interpreted as a Doppler effect, this corresponds to a velocity of ap-

TABLE 4

COMET–LABORATORY

Band	Dec. 23	Dec. 24	Band	Dec. 23	Dec. 24
1,0	−0.13 A	−0.03 A	4,3	−0.21 A	+0.05 A
2,1	− .39	− .22	5,4	−0.34	−0.01
3,2	−0.29	−0.11			
			Mean	−0.27 A	−0.05 A

TABLE 5

DISTANCE OF SATELLITES FROM MAIN BANDS

Bands	Dec. 23	Dec. 24
1,0	2.46 A	2.67 A
2,1	2.34	2.54
3,2	3.07	3.11

proach of 14 km/sec. Such an interpretation is in contradiction to the results obtained in the measurement of the *CN* bands; and in all probability we have to deal here with some modification in the structure of the *P*-heads of the Swan bands. The average difference between the wave lengths of the +2 sequence of the Swan bands on the above dates is −0.25 A, or 17 km/sec, an almost identical figure; but the measures are scattered, as these bands are much fainter than the +1 sequence.

The cores of the first three bands are accompanied on the violet side by satellites visible only in the nuclear line. The wave lengths of these satellites cannot be determined precisely, because they are somewhat diffuse; but the measures referred to the centers of the satellites are in good agreement for the two dates (Table 5).

Furthermore, between the bands (2, 1) and (3, 2) there are two very sharp emission lines extending across the whole width of the spectrum and especially well developed on the western, or sunward, side of the nucleus. Their weighted mean wave lengths are 4703.52 and 4707.12, corresponding to the "subhead" measured in Halley's and other comets as one band at λ 4705.7. There is no question that this is a double band; and, from the absence of a similar structure between other Swan bands, we must assume that it is independent of the Swan spectrum. The same remark applies to the sharp line measured at λ 4689.87.

On the other hand, there is no trace of a band at λ 4727, also measured in many comets as a "subhead" of λ 4737 (1, 0).

[5] W. Jevons, *Report on Band Spectra*, p. 11, Cambridge University Press, 1932.

Finally, on the plate of December 24 the isotopic band of the $C^{12} - C^{13}$ molecule is definitely present as a faint diffuse line. The spectrogram of December 23 has no trace of it, although, judging from the intensity of λ 4737, it should be present if it was of the same intensity as on December 24. The computed distance between the (1, 0) Swan band and the isotopic band is 7.55 A, the actually measured distance is 7.22 A. The discrepancy of 0.33 A is not significant in view of the faintness and diffuseness of the isotopic band.[6]

The McDonald observers could find no evidence of the carbon isotope band on their spectrograms; but my results are in agreement with the previously established fact[2] of the considerable variation in intensity of the isotope band with respect to the Swan bands. In Halley's Comet one plate would have the isotope band, while another with the Swan bands of the same intensity would have no trace of it.

The present results do not support Swings's hypothesis that the diffuse features at λ 4723 and λ 4706 are the (2, 1) and (3, 2) transitions of the isotope band. As has been

TABLE 6

RELATIVE INTENSITIES OF SWAN BANDS

	1, 0	2, 1	3, 2	4, 3	5, 4	T
West.....	9	10	8	5	5	2500°
Core.....	7	10	8	3	2	3000
East.....	9	10	10	1	2	2000

mentioned before, the band at λ 4706 is double, with a structure entirely different from the (1, 0) isotope band at λ 4745. The presumed (2,1) band is missing in Comet 1940c. On the other hand, in Comet 1941c, the feature at λ 4723 is very prominent, but neither the (1, 0) nor the (3, 2) band is present (unpublished results).

A few words can be said about the distribution of intensities along the bands in the direction perpendicular to the continuous spectrum. It has been shown[7] that the spectrum of various formations around the nucleus may differ considerably from the general spectrum of the head.

Such observations require, however, the co-operation of several observers unless the features are prominent enough to be seen on the slit of the spectrograph. The head of Comet 1940c in the 4-inch finder of the 69-inch telescope appeared structureless. A direct photograph obtained with a 6-inch Brashear lens attached to the tube of the 69-inch reflector is overexposed and shows the head as a round body of 4′ diameter surrounded by a spherical envelope 6′ in diameter. It is impossible to say exactly which features of the comet were on the slit during the exposure.

However, the Swan spectrum shows some interesting differences in the distribution of intensity along the bands, as can be seen in Plate VI (Figs. *c* and *d*). The last two bands (4, 3) and (5, 4) can be traced much farther on the west side than on the east side of the nucleus, but the first three bands are stronger on the east side. The estimated intensities of the bands on both plates in the continuous spectrum (core) and on the west and east side (about 16″ from the nucleus) are shown in Table 6.

The last column contains the temperature taken from Wurm's tables[8] for the distribu-

[6] The theoretical explanation of why $C^{12} - C^{12}$ bands are sharp and $C^{12} - C^{13}$ bands are diffuse is given by Swings, *M.N.*, **103**, 86, 1943.

[7] Observational evidence for this is discussed in my article in *Rev. Mod. Phys.*, **14**, 164, 1942.

[8] *Zs. f. Ap.*, **5**, 260, 1932. The tables were calculated for the case of absorption, but they will suffice to give a general idea of temperatures involved.

tion of intensities in the vibrational transitions of this molecule. In fact, we can find the distribution of intensity quite different from that given in Table 6 if we consider various distances from the continuous spectrum. At the very edge of the spectrum on the west side, for instance, all the bands appear to be of about the same intensity. This shows the artificiality of the temperature concept as applied to comets.

The position of the core of the bands with respect to the continuous spectrum is also not quite the same for different bands, as can be easily seen on the reproduction. Table 7 gives the results of measurement of the spectrogram of December 24.

At the geocentric distance of the comet, 0.801 astronomical unit, 1″ corresponds to 570 km. It is seen that the center of the core of the (1, 0) band was displaced by more than

TABLE 7

CORES OF SWAN BANDS

Band	Length	Displacement	Band	Length	Displacement
1,0	16″.1	2″.0 W	4,3	12″.1	0″.8 W
2,1	21.1	0.5 E	5,4	12.1	0.8 W
3,2	18.9	0			

1000 km west, or sunward, with reference to the nucleus, while the center of the (2,1) core was displaced by 300 km away from the sun. Of course, the line of the continuous spectrum is not very definite, but the positions of the cores were measured in reference to the sharp edge of the comparison spectrum. Therefore, the relative displacement of the two bands by 1300 km is real. What bearing this has on the physical processes in the head of the comet is hard to say, except that the vibrational transitions corresponding to these bands are localized in regions not symmetrical in respect to the nucleus. Even more striking differences in the distribution of intensity of *CH* bands with respect to the continuous spectrum seem to be present, but the bands are too faint for any precise measurement. The *CN* bands, on the other hand, do not show any difference in this respect.

The rest of the lines and bands given in Table 1 call for no especial comment except λ 4313, the strongest band in the *CH* system $A^2\Delta - x^2\pi$. It is impossible to identify it[1] with the whole complex of eight *Q* branches stretching from λ 4311.3 to λ 4314.2. The band was measured very consistently at λ 4313.21 and λ 4313.13 on the two plates as a sharp line of 1.32 A in width. It is especially sharply defined on the violet side, and there is no possibility of any emission to the violet of λ 4312.6.

ON THE RADIATIVE EQUILIBRIUM OF A STELLAR ATMOSPHERE

S. CHANDRASEKHAR
Yerkes Observatory
Received November 22, 1943

ABSTRACT

In this paper the equation of transfer

$$\mu \frac{dI}{d\tau} = I - I_0 ; \qquad I_0 = \int_{-1}^{+1} I d\mu$$

is solved by expanding I in terms of spherical harmonics in the form

$$I(\tau, \mu) = \sum_{l=0}^{\infty} I_l(\tau) P_l(\mu) .$$

It is shown how successively higher approximations to I can be obtained by retaining more and more terms in the foregoing expansion; thus, the first, second, and third approximations are obtained by retaining the first three, five, and seven terms, respectively, in the expansion. The first three approximations to $I_0(\tau)$ are explicitly obtained, and the corresponding laws of darkening derived.

The exact function describing the law of darkening and given by Hopf's theory is also numerically evaluated. A comparison of this exact law with those derived on our second and third approximations indicates that the method described in this paper is sufficiently rapidly convergent.

1. *Introduction.*—As is well known, the solution of the equation of transfer

$$\cos \vartheta \frac{dI}{d\tau} = I - J , \tag{1}$$

where

$$J = \frac{1}{2} \int_0^{\pi} I \sin \vartheta \, d\vartheta , \tag{2}$$

has occupied a central position in the theory of stellar atmospheres and has been the subject of investigations by Schwarzschild, Milne, Eddington, Jeans, Hopf, Bronstein, and others. An account of these investigations and the successive methods of approximation, as developed particularly by Milne and Eddington, will be found in the various treatises on the subject by Eddington, Milne, and Unsöld.[1] However, the methods described by these latter writers, while adequate for most purposes, are not sufficiently systematic, in the sense that no general procedure is outlined which would enable one to obtain solutions of increasing accuracy by retaining, for example, more and more terms in an expansion of some sort for I. More recently, however, an attempt in this direction has been made by L. Gratton[2] in a paper of considerable interest. Gratton's basic idea is to seek a solution of equation (1) of the form

$$I(\tau, \vartheta) = \sum_{l=1}^{\infty} I_l(\tau) P_l(\cos \vartheta) , \tag{3}$$

[1] A. S. Eddington, *The Internal Constitution of the Stars*, chap. xii, Cambridge, England, 1926; E. A. Milne, *Handb. d. Ap.*, **3**, No. 1, 114–126, Berlin: Springer, 1930; A. Unsöld, *Physik der Sternatmosphären*, pp. 89–104, Berlin: Springer, 1938.

[2] *Societa astronomica italiana*, **10**, 309–325, 1937.

in which the P_l's denote the various Legendre polynomials. In other words, we expand I in terms of spherical harmonics with the expectation that by retaining a sufficient number of terms in the expansion we shall be able to obtain solutions with any desired degree of accuracy. This is, of course, an entirely sound procedure; but, unfortunately, Gratton's specific treatment of the problem following this idea is vitiated by a number of errors and oversights which require corrections. Accordingly, it has been thought worth while to re-examine the whole problem *de novo* and obtain what might properly be described as the first, second, and third approximations to the solution of equation (1). We shall, moreover, compare the predictions of these approximate solutions with regard to those features (e.g., the law of darkening) for which the Hopf-Bronstein[3] theory provides exact information.

2. *The outline of the method.*—Denoting $\cos\vartheta$ by μ, we can re-write equation (1) in the form

$$\mu \frac{dI}{d\tau} = I - I_0 , \tag{4}$$

where I_0 is the first term in the expansion

$$I(\tau, \mu) = \sum_{l=0}^{\infty} I_l(\tau) P_l(\mu) . \tag{5}$$

Substituting the foregoing expansion for I in equation (4) and remembering that the P_l's satisfy the recursion formula

$$\mu P_l = \frac{1}{2l+1} [\,(l+1) P_{l+1} + l P_{l-1}] , \tag{6}$$

we find

$$\sum_{l=0}^{\infty} \frac{1}{2l+1} [\,(l+1) P_{l+1} + l P_{l-1}] \frac{dI_l}{d\tau} = \sum_{l=0}^{\infty} I_l P_l - I_0 . \tag{7}$$

Equating the coefficients of the various Legendre polynomials in equation (7), we obtain

$$\frac{l}{2l-1} \frac{dI_{l-1}}{d\tau} + \frac{l+1}{2l+3} \frac{dI_{l+1}}{d\tau} = I_l \qquad (l = 1, 2, \ldots .) \tag{8}$$

and

$$\frac{1}{3} \frac{dI_1}{d\tau} = 0 \qquad (l = 0) . \tag{9}$$

Equation (9) leads at once to the integral

$$I_1 = \text{constant} = \tfrac{3}{4}F \qquad \text{(say)} , \tag{10}$$

which clearly insures the constancy of the net integrated flux and determines the effective temperature of the star. Another integral of the equations is obtained by considering equation (8) for the case $l = 1$. For, according to this equation, for $l = 1$ we have

$$\frac{dI_0}{d\tau} + \frac{2}{5} \frac{dI_2}{d\tau} = I_1 , \tag{11}$$

[3] E. Hopf, *Mathematical Problems of Radiative Equilibrium* (Cambridge Mathematical Tract No. 31), Cambridge, England, 1934.

or, since I_1 is a constant (eq. [10]),

$$I_0 + \tfrac{3}{5} I_2 = \tfrac{3}{4} F\tau + a\,, \tag{12}$$

where a is an arbitrary constant at our disposal. This integral is readily verified to be the same as what is more generally known as the "K-integral."[4]

Before we proceed to outline our method of approximation we shall first formulate the boundary conditions of the problem.

For the problem of the radiative equilibrium of a stellar atmorphere the boundary condition at $\tau = 0$ is

$$I(0, \mu) = 0 \quad \text{for} \quad -1 < \mu < 0\,, \tag{13}$$

since no external radiation is assumed to be incident on the star. The implication of the boundary condition (13) for the I_l's as $\tau \to 0$ can be derived in the following manner. From equation (5) we conclude that for $\tau > 0$

$$\frac{2}{2l+1} I_l(\tau) = \int_{-1}^{+1} I(\tau, \mu) P_l(\mu)\, d\mu\,. \tag{14}$$

Passing now to the limit $\tau = 0$ and remembering that, according to equation (13), $I(0, \mu)$ vanishes for all negative values of μ, we obtain

$$\frac{2}{2l+1} I_l(0) = \int_0^1 I(0, \mu) P_l(\mu)\, d\mu\,. \tag{15}$$

On the other hand, for $\tau = 0$ (cf. eq. [5])

$$I(0, \mu) = \sum_{m=0}^{\infty} I_m(0) P_m(\mu)\,. \tag{16}$$

Hence, combining equations (15) and (16), we must have

$$\frac{2}{2l+1} I_l(0) = \sum_{m=0}^{\infty} I_m(0) \int_0^1 P_l(\mu) P_m(\mu)\, d\mu\,. \tag{17}$$

Thus the boundary condition (1) is equivalent to the infinite set of linear relations (17) among the I_l's as $\tau \to 0$.

It is now apparent that we cannot satisfy the entire set of relations (17) when a solution for I is sought by retaining only a finite number of terms in the expansion (5). But it is clear that the more the number of the relations (17) we are able to satisfy, the more, in general, we may expect the derived solution to be accurate. On the other hand, only as many of the relations (17) can be satisfied as there are disposal constants in the solution for the I_l's. It thus appears that the order of the approximation will be indicated by the number of constants of integration (other than F) which the solutions for the I_l's contain. Thus, as we shall presently show (§§ 3, 4, and 5, below), the solutions obtained by retaining only the first three, five, or seven terms in the expansion (5) involve respectively one, two, or three disposable constants of integrations. These, then, will provide the first, second, or third approximations to the solution of equation (1).[5]

[4] E.g., see Milne, *op. cit.*, p. 121, eq. (125), or Unsöld, *op. cit.*, p. 97, eq. (29.13).

[5] One of the oversights of Gratton (*loc. cit.*) consists precisely in his failure to recognize this point. Thus he obtains his "second" approximation by retaining terms up to and including I_3. However, as

For further reference we may note here that the relations (17) for the cases $l = 0$, 1, and 2 explicitly reduce to

$$2I_0(0) = I_0(0) + \tfrac{1}{2}I_1(0) - \tfrac{1}{8}I_3(0) + \tfrac{1}{16}I_5(0) + \ldots\ , \tag{18}$$

$$\tfrac{2}{3}I_1(0) = \tfrac{1}{2}I_0(0) + \tfrac{1}{3}I_1(0) + \tfrac{1}{8}I_2(0) - \tfrac{1}{48}I_4(0) + \tfrac{1}{128}I_6(0) + \ldots\ , \tag{19}$$

and

$$\tfrac{2}{5}I_2(0) = \tfrac{1}{8}I_1(0) + \tfrac{1}{5}I_2(0) + \tfrac{1}{8}I_3(0) - \tfrac{5}{128}I_5(0) + \ldots\ , \tag{20}$$

where on the right-hand sides we have retained all terms up to and including I_6. Remembering that $I_1 =$ constant $= 3F/4$, we can write more conveniently in the forms

$$\tfrac{1}{2}I_0(0) + \tfrac{1}{16}I_3(0) - \tfrac{1}{32}I_5(0) + \ldots\ = \tfrac{3}{16}F\,, \tag{21}$$

$$\tfrac{1}{2}I_0(0) + \tfrac{1}{8}I_2(0) - \tfrac{1}{48}I_4(0) + \tfrac{1}{128}I_6(0) + \ldots\ = \tfrac{1}{4}F\,, \tag{22}$$

and

$$\tfrac{2}{5}I_2(0) - \tfrac{1}{4}I_3(0) + \tfrac{5}{64}I_5(0) + \ldots\ = \tfrac{3}{16}F\,. \tag{23}$$

So far we have considered only the boundary conditions at $\tau = 0$. Turning next to the boundary conditions at $\tau = \infty$, it is evident that[6]

$$I_0 \sim \tfrac{3}{4}F\tau \quad \text{and} \quad I_l(\tau) \ \text{for} \ l > 0 \ \text{bounded as} \ \tau \to \infty\ . \tag{24}$$

3. *The first approximation.*—The first approximation is obtained by retaining the terms I_0, I_1, and I_2 in the expansion for I and considering only the first three equations (namely, for $l = 0$, 1, and 2) which result from equation (7). The equations for $l = 0$ and $l = 1$ lead, as we have already seen, to the integrals (10) and (12). The equation for $l = 2$ is

$$\frac{2}{3}\frac{dI_1}{d\tau} + \frac{3}{7}\frac{dI_3}{d\tau} = I_2\,. \tag{25}$$

Remembering that I_1 is a constant and that we have put $I_3 = 0$, it follows that

$$I_2 = 0\,. \tag{26}$$

Accordingly, our solution is

$$I_0 = \tfrac{3}{4}F\tau + a\,; \qquad I_1 = \tfrac{3}{4}F \tag{27}$$

and involves, as we see, the one disposable constant a. To determine this constant, we should use one or the other of the relations (17). Now the relation for $l = 1$ is given preference over all the others, since (as was first pointed out by Milne) this insures that the

---

we have indicated, the genuine second approximation is obtained only when the term I_4 is also included. A consequence of this is that Gratton's solution (after correcting some further arithmetical errors in his evaluation of the constants of integration) fails to satisfy certain other necessary conditions of the problem (see n. 7, below).

[6] Cf. Hopf, *op. cit.*

emergent flux is the same as the constant net flux in the interior. Accordingly, we use equation (22) to determine a. We readily find that

$$a = \tfrac{1}{2}F\,. \tag{28}$$

Thus,

$$I_0(\tau) = \tfrac{3}{4}F(\tau + \tfrac{2}{3})\,, \tag{29}$$

and the corresponding law of darkening is

$$I(0, \mu) = \tfrac{1}{2}F + \tfrac{3}{4}F\mu\,. \tag{30}$$

We therefore see that the first approximation on our present method reduces simply to the solution in the form first derived by Milne.

4. *The second approximation.*—As we shall now show, the second approximation for I is obtained by retaining the terms up to and including I_4 in the expansion (5). This requires the consideration of the first five equations which result from equation (7). Thus, in addition to the integrals (10) and (12), we have now to consider the following equations:

$$\left.\begin{aligned} \frac{3}{7}\frac{dI_3}{d\tau} &= I_2\,, \\ \frac{3}{5}\frac{dI_2}{d\tau} + \frac{4}{9}\frac{dI_4}{d\tau} &= I_3\,, \\ \frac{4}{7}\frac{dI_3}{d\tau} &= I_4\,. \end{aligned}\right\} \tag{31}$$

From the first and the last of the foregoing equations we obtain the integral

$$\tfrac{4}{3}I_2 = I_4\,. \tag{32}$$ [7]

Equations (31) also lead to the following differential equation for I_3:

$$\frac{16}{63}\frac{d^2I_3}{d\tau^2} = \frac{4}{9}\frac{dI_4}{d\tau} = I_3 - \frac{3}{5}\frac{dI_2}{d\tau} = I_3 - \frac{9}{35}\frac{d^2I_3}{d\tau^2}\,, \tag{33}$$

or

$$\frac{23}{45}\frac{d^2I_3}{d\tau^2} = I_3\,. \tag{34}$$

The solution of this equation appropriate for our present purposes is (cf. eq. [24])

$$I_3 = A\,e^{-a\tau}\,, \tag{35}$$

where A is an arbitrary constant and

$$a = \sqrt{\tfrac{45}{23}} = 1.399\,. \tag{36}$$

From equations (31) and (32) we now obtain

$$I_2 = -\tfrac{3}{7}A\,a\,e^{-a\tau}; \qquad I_4 = -\tfrac{4}{7}A\,a\,e^{-a\tau}\,. \tag{37}$$

[7] The existence of this integral reveals the inconsistency of an approximation in which I_3 is included but I_4 is not (see n. 5). A consequence of this inconsistency is that when the solution for I, including only terms up to I_3, is obtained, it is found that $I(0, 0) \neq I_0(0)$, contrary to what should be expected to be identically true (since at the limb we necessarily see only the surface layers).

The solutions for the I's are thus seen to involve only two disposable constants (namely, A and a) and therefore lead, as already stated, to the second approximation.

To determine the constants A and a, we use equations (21) and (22) as our boundary conditions. Under our present assumptions (namely, that I_5, I_6, etc., can all be ignored) these equations reduce to

$$\tfrac{1}{2}I_0(0) + \tfrac{1}{16}I_3(0) = \tfrac{3}{16}F \tag{38}$$

and

$$\tfrac{1}{2}I_0(0) + \tfrac{1}{8}I_2(0) - \tfrac{1}{48}I_4(0) = \tfrac{1}{4}F. \tag{39}$$

Eliminating $I_0(0)$ between the foregoing two equations, we obtain

$$\tfrac{1}{8}I_2(0) - \tfrac{1}{16}I_3(0) - \tfrac{1}{48}I_4(0) = \tfrac{1}{10}F. \tag{40}$$

This equation directly determines A. We find

$$A = -\frac{F}{1+\frac{2}{3}a} = -0.5175F. \tag{41}$$

Accordingly, our solutions for I_2, I_3, and I_4 are

$$I_2 = 0.3102Fe^{-a\tau}; \qquad I_3 = -0.5175Fe^{-a\tau}; \qquad I_4 = 0.4136Fe^{-a\tau}. \tag{42}$$

Equation (38) or (39) now determines $I_0(0)$. We find

$$I_0(0) = 0.4397F. \tag{43}$$

On the other hand, since (cf. eq. [12])

$$I_0(0) = a - \tfrac{2}{5}I_2(0), \tag{44}$$

we have

$$a = 0.5638F. \tag{45}$$

Thus, our solution for I_0 is

$$I_0(\tau) = \tfrac{3}{4}F\tau + 0.5638F - 0.1241Fe^{-a\tau}, \tag{46}$$

which for later comparisons (§ 6) we write in the form

$$I_0(\tau) = \tfrac{3}{4}F[\tau + q(\tau)], \tag{47}$$

where now

$$q(\tau) = 0.7517 - 0.1654e^{-1.399\tau}. \tag{48}$$

To obtain the corresponding law of darkening, we start from the exact relation

$$I(0, \mu) = \int_0^\infty I_0(\tau)\, e^{-\tau/\mu}\, \frac{d\tau}{\mu} \tag{49}$$

and substitute for $I_0(\tau)$ the solution (46). We thus find that

$$I(0, \mu) = F\left(0.5638 + 0.75\mu - \frac{0.1241}{1+1.399\mu}\right). \tag{50}$$

5. *The third approximation.*—To obtain the third approximation for I, we retain all the terms up to and including I_6 in the expansion for I and consider the first seven equations which result from equation (7). Accordingly, in addition to the two equations

which lead to the integrals (10) and (12), we have to consider the following five further equations:

$$\left.\begin{aligned} \frac{3}{7}\frac{dI_3}{d\tau} &= I_2\,, \\ \frac{3}{5}\frac{dI_2}{d\tau}+\frac{4}{9}\frac{dI_4}{d\tau} &= I_3\,, \\ \frac{4}{7}\frac{dI_3}{d\tau}+\frac{5}{11}\frac{dI_5}{d\tau} &= I_4\,, \\ \frac{5}{9}\frac{dI_4}{d\tau}+\frac{6}{13}\frac{dI_6}{d\tau} &= I_5\,, \\ \frac{6}{11}\frac{dI_5}{d\tau} &= I_6\,. \end{aligned}\right\} \tag{51}$$

From the first, third, and fifth of the foregoing equations we obtain the integral

$$\tfrac{4}{3}I_2+\tfrac{5}{6}I_6 = I_4\,, \tag{52}$$

which is our present analogue of the integral (32) we had in the second approximation.

Again, from equations (51) we obtain

$$\left.\begin{aligned} \frac{36}{143}\frac{d^2I_5}{d\tau^2} &= \frac{6}{13}\frac{dI_6}{d\tau} \\ &= I_5-\frac{5}{9}\frac{dI_4}{d\tau} \\ &= I_5-\frac{5}{9}\left(\frac{4}{7}\frac{d^2I_3}{d\tau^2}+\frac{5}{11}\frac{d^2I_5}{d\tau^2}\right). \end{aligned}\right\} \tag{53}$$

Similarly

$$\left.\begin{aligned} \frac{20}{99}\frac{d^2I_5}{d\tau^2} &= \frac{4}{9}\left(\frac{dI_4}{d\tau}-\frac{4}{7}\frac{d^2I_3}{d\tau^2}\right) \\ &= -\frac{16}{63}\frac{d^2I_3}{d\tau^2}+I_3-\frac{3}{5}\frac{dI_2}{d\tau} \\ &= -\frac{16}{63}\frac{d^2I_3}{d\tau^2}+I_3-\frac{9}{35}\frac{d^2I_3}{d\tau^2}. \end{aligned}\right\} \tag{54}$$

Equations (53) and (54) can be re-written alternatively in the forms

$$\left.\begin{aligned} \frac{59}{117}\frac{d^2I_5}{d\tau^2}-I_5 &= -\frac{20}{63}\frac{d^2I_3}{d\tau^2}\,, \\ \frac{23}{45}\frac{d^2I_3}{d\tau^2}-I_3 &= -\frac{20}{99}\frac{d^2I_5}{d\tau^2}. \end{aligned}\right\} \tag{55}$$

To solve the foregoing equations we make the substitutions

$$I_3 = A\,e^{-a\tau} \quad \text{and} \quad I_5 = Be^{-a\tau}\,, \tag{56}$$

where A, B, and a are constants, for the present unspecified. We obtain

$$\left.\begin{aligned}\left(\frac{59}{117}a^2-1\right)B&=-\frac{20}{63}a^2A\,,\\ \left(\frac{23}{45}a^2-1\right)A&=-\frac{20}{99}a^2B\,.\end{aligned}\right\}\tag{57}$$

Hence a^2 must satisfy the equation

$$\left(\frac{59}{117}a^2-1\right)\left(\frac{23}{45}a^2-1\right)=\frac{400}{63\times 99}a^4\,.\tag{58}$$

Solving this equation, we find that a can have either of the two values

$$a_1=1.9825 \quad \text{or} \quad a_2=1.1464\,.\tag{59}$$

Corresponding to these two roots for a, we must have

$$B_1=-1.2706A_1 \quad \text{and} \quad B_2=1.2368A_2\,.\tag{60}$$

Accordingly, the solutions for I_3 and I_5 appropriate for our present problem are

$$I_3=A_1e^{-a_1\tau}+A_2e^{-a_2\tau}\tag{61}$$

and

$$I_5=-1.2706A_1e^{-a_1\tau}+1.2368A_2e^{-a_2\tau}\,.\tag{62}$$

Using equations (51) and (52), we can now evaluate the remaining I's. We find

$$\left.\begin{aligned}I_2&=-0.8497A_1e^{-a_1\tau}-0.4913A_2e^{-a_2\tau}\,,\\ I_4&=+0.0121A_1e^{-a_1\tau}-1.2995A_2e^{-a_2\tau}\,,\\ I_6&=+1.3740A_1e^{-a_1\tau}-0.7733A_2e^{-a_2\tau}\,.\end{aligned}\right\}\tag{63}$$

We thus see that our solution for the I's involves three disposable constants (namely, A_1, A_2, and a) and leads, therefore, as we have already stated, to the third approximation for I.

To determine next the constants A_1, A_2, and a we use equations (21), (22), and (23) as our boundary conditions. Eliminating $I_0(0)$ between equations (21) and (22), we have

$$\tfrac{1}{8}I_2(0)-\tfrac{1}{16}I_3(0)-\tfrac{1}{48}I_4(0)+\tfrac{1}{32}I_5(0)+\tfrac{1}{128}I_6(0)=\tfrac{1}{16}F\,.\tag{64}$$

Equations (23) and (64) directly determine A_1 and A_2. We find

$$A_1=-0.3931F \quad \text{and} \quad A_2=0.2384F\,.\tag{65}$$

Substituting these values for A_1 and A_2 in equations (61), (62), and (63), we obtain

$$\left.\begin{aligned}I_2&=(+0.3340e^{-a_1\tau}-0.1171e^{-a_2\tau})F\,,\\ I_3&=(-0.3931e^{-a_1\tau}+0.2384e^{-a_2\tau})F\,,\\ I_4&=(-0.0048e^{-a_1\tau}-0.3098e^{-a_2\tau})F\,,\\ I_5&=(+0.4995e^{-a_1\tau}+0.2949e^{-a_2\tau})F\,,\\ I_6&=(-0.5402e^{-a_1\tau}-0.1844e^{-a_2\tau})F\,.\end{aligned}\right\}\tag{66}$$

The value of $I_0(0)$ can now be determined from equation (64). We find

$$I_0(0) = 0.4440F . \tag{67}$$

Equations (12), (66), and (67) now determine a. We find

$$a = 0.5307F . \tag{68}$$

Thus the solution for I_0 is given by

$$I_0(\tau) = \tfrac{3}{4}F\tau + 0.5307F - 0.1336Fe^{-a_1\tau} + 0.0469Fe^{-a_2\tau} ; \tag{69}$$

or, writing $I_0(\tau)$ in the form (47), we now have

$$q(\tau) = 0.7077 - 0.1781e^{-1.9825\tau} + 0.0625e^{-1.1464\tau} . \tag{70}$$

Finally, to determine the law of darkening we again start with the equation (49) but substitute for I_0 our present solution (69). In this manner we find

$$I(0, \mu) = F\left(0.5307 + 0.75\mu - \frac{0.1336}{1+1.19825\mu} + \frac{0.0469}{1+1.1464\mu}\right). \tag{71}$$

6. *A comparison of the second and the third approximations in their predictions regarding* q (τ) *and the law of darkening: the exact law of darkening.*—As is well known, Hopf and Bronstein have succeeded in deriving certain exact results concerning the solution of the equation of transfer (1) satisfying the boundary condition (13). Thus it has been shown (see Hopf, *op. cit.*) that, if the solution for I_0 be written in the form

$$I_0(\tau) = \tfrac{3}{4}F[\tau + q(\tau)], \tag{72}$$

then $q(\tau)$ is a monotonic increasing function of τ and that, moreover,

$$q(0) = \frac{1}{\sqrt{3}} = 0.57735 \tag{73}$$

and

$$q(\infty) = \frac{1}{\pi}\int_0^{\pi/2}\left(\frac{3}{\sin^2\phi} + \frac{\tan\phi}{\phi - \tan\phi}\right) d\phi . \tag{74}$$

The integral on the right-hand side of equation (74) was evaluated numerically, and it was found that

$$q(\infty) = 0.710447 . \tag{75}$$

These exact values for $q(0)$ and $q(\infty)$ should be compared with those given by equations (48) and (70) on our second and third approximations, respectively. We have

$$\left.\begin{aligned} q(0) &= 0.5862 ; \quad q(\infty) = 0.7517 \text{ (second approximation)} , \\ q(0) &= 0.5920 ; \quad q(\infty) = 0.7077 \text{ (third approximation)} . \end{aligned}\right\} \tag{76}$$

It is seen that, while the third approximation effects a marked improvement over the second in the agreement of $q(\infty)$ with the exact value (75), it worsens somewhat the agreement of $q(0)$ with its exact value (73). However, it appears that the third approximation actually represents a substantial improvement over the second over the entire range of τ except in the very immediate vicinity of the boundary $\tau = 0$. That this is so is indicated, for example, by the comparison made in Table 1 of the functions $q(\tau)$ given by

our second and third approximations with that given by Eddington's second approximation.[8] This conclusion is further strengthened when we compare the laws of darkening

TABLE 1

A COMPARISON OF THE FUNCTION $q(\tau)$ DERIVED ON THE BASIS OF THE SECOND AND THE THIRD APPROXIMATION (EQS. [48] AND [70]) WITH THAT DERIVED ON EDDINGTON'S SECOND APPROXIMATION

τ	$q(\tau)$			τ	$q(\tau)$		
	Second Approximation	Third Approximation	Eddington's Second Approximation		Second Approximation	Third Approximation	Eddington's Second Approximation
0.00	0.5862	0.5920	0.583	0.90	0.7047	0.7000	0.692
.05	.5974	.6053	.620	1.0	.7108	.7030	.694
.10	.6078	.6172	.635	1.2	.7208	.7070	.697
.15	.6175	.6280	.645	1.4	.7283	.7091	.699
.20	.6266	.6375	.653	1.6	.7340	.7102	.701
.25	.6351	.6460	.660	1.8	.7383	.7106	.702
.30	.6429	.6537	.665	2.0	.7416	.7106	.703
.35	.6503	.6605	.670	2.2	.7441	.7104	.704
.40	.6571	.6666	.673	2.4	.7459	.7101	.704
.50	.6695	.6768	.679	2.6	.7473	.7098	.705
.60	.6802	.6848	.683	2.8	.7484	.7095	.705
.70	.6895	.6912	.686	3.0	.7492	.7092	.706
0.80	0.6977	0.6962	0.689	∞	0.7517	0.7077	0.710

TABLE 2

A COMPARISON OF THE LAWS OF DARKENING GIVEN BY THE SECOND AND THE THIRD APPROXIMATION (EQS. [50] AND [71]) WITH THAT GIVEN BY THE EXACT FORMULA (EQ. [77])

μ	$I(0, \mu)/F$			$I(0, \mu)/I(0, 1)$		
	Second Approximation	Third Approximation	Exact	Second Approximation	Third Approximation	Exact
0	0.4397	0.4440	0.43301	0.3484	0.3530	0.34390
0.1	0.5299	0.5363	0.54011	0.4199	0.4264	0 42896
0.2	0.6168	0.6232	0.62802	0.4887	0.4955	0.49878
0.3	0.7014	0.7068	0.71123	0.5557	0.5620	0.56487
0.4	0.7842	0.7884	0.79210	0.6214	0.6268	0.62909
0.5	0.8657	0.8684	0.87156	0.6860	0.6904	0.69220
0.6	0.9463	0.9475	0.95009	0.7498	0.7533	0.75457
0.7	1.0261	1.0258	1.02796	0.8130	0.8156	0.81642
0.8	1.1052	1.1035	1.10536	0.8757	0.8774	0.87788
0.9	1.1838	1.1808	1.18238	0.9380	0.9388	0.93906
1.0	1.2620	1.2578	1.25912	1.0000	1.0000	1.00000

given by our two approximations with the exact law of darkening. This comparison is made in the following paragraph.

[8] Milne, *op. cit.*, pp. 122–124, and Unsöld, *op. cit.*, p. 102.

It has been shown by Hopf (*op. cit.*) that for the case under discussion the problem of darkening admits of an exact solution. Thus, expressing the emergent intensity $I(0, \mu)$ in the form

$$I(0, \mu) = \frac{\sqrt{3}}{4} F\Phi(\mu) , \tag{77}$$

Hopf has shown (*op. cit.*, p. 105) that

$$\Phi(\mu) = (1 + \mu) \exp\left\{ -\frac{\mu}{\pi} \int_0^{\pi/2} \frac{\log[(1 - \phi \cot \phi)/\sin^2 \phi]}{\cos^2 \phi + \mu^2 \sin^2 \phi} \, d\phi \right\} . \tag{78}$$

Although the foregoing solution has been known for over ten years, it does not appear that the integral defining $\Phi(\mu)$ has been evaluated. Accordingly, we have evaluated the function $\Phi(\mu)$ numerically for the values $\mu = 0, 0.1, 0.2, \ldots, 1.0$ and tabulated the resulting values of $I(0, \mu)$ in Table 2. In Table 2 we have also tabulated the functions $I(0, \mu)$ as given by the equations (50) and (71), i.e., by our second and third approximations, respectively. It is seen that, except for μ very close to zero, equation (71) for $I(0, \mu)$ provides an appreciably better approximation to the exact law of darkening than does equation (50). And, moreover, the agreement of either (50) or (71) with the exact law of darkening over the whole range of μ is entirely satisfactory.

In conclusion I wish to record my indebtedness to Miss Frances Herman, who carried out most of the numerical work connected with the preparation of Tables 1 and 2.

STELLAR ROTATION AND LARGE-SCALE CURRENTS

WASLEY KROGDAHL
Washington, D.C., and Yerkes Observatory
Received October 6, 1943

ABSTRACT

The general problem of stellar rotation is considered. It is shown that in viscous stars rotation will give rise to meridional currents, which, in turn, cause a differential rotation. A formal solution for the differential rotational velocity is given in terms of the meridional velocities. The equations to be satisfied by the meridional velocities are given, and an approximate method for their solution is suggested.

Ever since the presentations of what may be termed the "classical" investigations on stellar rotation—i.e., those in which the fundamental theorems of uniform rotation were first given—interest in the subject of rotating stars has been directed more and more to the particular topic of differential rotation. This course has been, to a large extent, a consequence of von Zeipel's enunciation of his well-known theorem, which would entail the impossibility of uniform stellar rotation under certain general conditions in stars in radiative equilibrium.[1] Moreover, a complete and satisfactory theoretical analysis of differential rotation in general, and of the sun's differential rotation in particular, was wanting. It is natural, then, that numerous investigators have sought to solve both the general problem of differential rotation and various special cases; however, their success has, in some respects, been of a restricted nature because of either great generality or great specificity.

The problem is that of finding a system of axially symmetric currents which either can or must exist in a star having a nonzero net angular momentum. The problem can be considered relative to any of four fundamental sets of circumstances: the stellar material may be either viscous or nonviscous (perfect), and at the same time there may or may not exist large-scale meridional currents in the star. However, Gunnar Randers has shown[2] that, if the fluid is perfect, stable meridional currents cannot exist; and S. Rosseland[3] has found that in nonviscous stars having no meridional currents the differential rotational velocity is indeterminate to the extent of an arbitrary function. Therefore, attention may be confined to viscous stars.

Motions in a viscous fluid will, of course, be subject to the decelerating forces due to viscosity; and the fluid velocity will, therefore, in general be a secularly varying vector-field. For the problem to be considered, however, it will be postulated that the velocities are stationary—i.e., independent of time—for it is only the equilibrium state of a rotating star which at present interests us. One therefore seeks only sustained motions.

To characterize a motion in a viscous fluid as "sustained" is to imply the existence of a sustaining force. In a rotating star such a sustaining force must be ultimately traceable to the star's over-all rotation; it must eventually be shown that any sustaining force is

[1] However, as Dr. S. Chandrasekhar has pointed out to the writer, von Zeipel's theorem does not appear in a theory in which only terms of the first order in ω_0^2 (where ω_0 denotes the angular velocity) are retained; it is only when terms of higher order in ω_0^2 are included that von Zeipel's theorem follows (cf. M. Schwarzschild, *Ap. J.*, **95**, 452, 1942). This should perhaps be emphasized, since in the case of the sun, for example, $\omega_0^2/4\pi G\rho_c \sim 10^{-5}$, and we cannot really be certain that the fundamental equations are valid in the higher order approximations, i.e., to at least one part in 10^{10}.

[2] *Ap. J.*, **94**, 123, 1941.

[3] *Astrophysica Norvegica*, **2**, 173, 1936; *ibid.*, p. 249, 1937.

generated by the rotation, for presumably sustained (steady-state) motion would not exist in a static star (in which no preferred directions could be defined).

With these assumptions and restrictions, consider now the problem of general large-scale motions in a rotating star.

I

The distribution and behavior of the matter in a star must satisfy six general equations; they are (in the convenient tensor notation): (*a*) the hydrodynamical equations[4]

$$\frac{1}{\rho}\frac{\partial p}{\partial x^m}=\frac{\partial \mathfrak{V}}{\partial x^m}-\left[\frac{\partial v_m}{\partial t}+v_{m,\,s}v^s\right]+\frac{\lambda}{\rho}\left[\frac{1}{3}\frac{\partial \psi}{\partial x^m}+g^{sj}v_{m,\,sj}\right] \qquad (m=1,\,2,\,3), \quad (1)$$

where ρ is the density, p the total pressure, $\mathfrak{V}$ the gravitational potential, v_m the (covariant) velocity vector,[5] λ the coefficient of viscosity, g^{sj} the fundamental tensor, and where

$$\psi=\frac{1}{\sqrt{g}}\frac{\partial}{\partial x^s}(\sqrt{g}\,g^{sj}v_j) \qquad (2)$$

is the divergence of the velocity (g being the determinant $|g_{sj}|$); (*b*) Poisson's equation

$$\frac{1}{\sqrt{g}}\frac{\partial}{\partial x^s}\left(\sqrt{g}\,g^{sj}\frac{\partial \mathfrak{V}}{\partial x^j}\right)=-4\pi G\rho\,; \qquad (3)$$

(*c*) the equation of continuity

$$\frac{1}{\sqrt{g}}\frac{\partial}{\partial x^s}(\rho\sqrt{g}\,g^{sj}v_j)+\frac{\partial \rho}{\partial t}=0\,; \qquad (4)$$

(*d*) an equation of state

$$p=p\,(\rho,\,T)\,, \qquad (5)$$

(where T is the temperature), usually taken to be

$$p=\frac{k}{\mu^* H}\,\rho T+\tfrac{1}{3}aT^4\,; \qquad (6)$$

(*e*) the radiant flux equation

$$\frac{1}{\rho}\frac{\partial p''}{\partial x^s}=-\frac{\kappa}{c}F_s\,, \qquad (7)$$

where p'' is the radiation pressure, κ the opacity, c the velocity of light, and F_s the radiative flux vector; and (*f*), the equation of conservation of energy

$$\frac{1}{\sqrt{g}}\left\{p\,\frac{\partial}{\partial x^s}(\sqrt{g}\,g^{sj}v_j)+\frac{\partial}{\partial x^s}(\sqrt{g}\,g^{sj}[F_j'+\gamma\rho v_j])\right\}=\epsilon\rho+q\,, \qquad (8)$$

where γ is the total subatomic and thermal energy per unit mass of stellar material, F_j' the total (radiative plus conductive) flux, ϵ the rate of generation of energy per unit mass, and q the heat generated per unit time and volume by viscosity. Equations (1), (3), (4), (5), (7), and (8) are the fundamental equations of the problem.

[4] See A. J. McConnell, *Applications of the Absolute Differential Calculus*, p. 282, London: Blackie & Son, 1936.

[5] Those indices preceded by a comma denote covariant differentiation with respect to the corresponding variable.

For future convenience and consistency it will be found of service to express these equations in dimensionless variables according to the transformations.

$$\left.\begin{aligned} x^1 &= r = r^*\xi\,, \\ P = P_c\eta &= (4\pi G\rho_c^2 r^{*2})\,\eta\,, \\ \rho &= \rho_c\zeta\,, \\ \mathfrak{V} &= (4\pi G\rho_c r^{*2})\,\chi\,, \\ T &= T_c\sigma\,, \\ \frac{\lambda}{\rho} &= (4\pi G\rho_c r^{*2})^{1/2} v\,. \end{aligned}\right\} \tag{9}$$

Using these variables and taking the co-ordinate system $x^1 = r$ (the radius vector), $x^2 = \mu = \cos\varphi$ (where φ is the polar angle), $x^3 = \theta$ (the azimuthal angle), with the corresponding (contravariant) velocities $v^1 = (4\pi G\rho_c r^*)^{1/2} r^*\,\alpha^*$, $v^2 = (4\pi G\rho_c r^*)^{1/2}\,\beta^*$, and $v^3 = (4\pi G\rho_c r^*)^{1/2}\,\omega^*$, the hydrodynamical equations (1) for a stationary (i.e., $\partial v_m/\partial t \equiv 0$), rotating, axially symmetric star are, in full,

$$\left.\begin{aligned} \frac{1}{\zeta}\frac{\partial\eta}{\partial\xi} = \frac{\partial\chi}{\partial\xi} &- \left[\alpha^*\frac{\partial\alpha^*}{\partial\xi} + \beta^*\left(\frac{\partial\alpha^*}{\partial\mu} - \frac{\xi\beta^*}{1-\mu^2}\right) - \xi\,(1-\mu^2)\,\omega^{*2}\right] + v\left\{\frac{1}{3}\frac{\partial}{\partial\xi}\right. \\ &\times\left[\frac{1}{\xi^2}\frac{\partial}{\partial\xi}(\xi^2\alpha^*) + \frac{\partial\beta^*}{\partial\mu}\right] + \frac{1}{\xi^2}\left[\xi^2\frac{\partial^2\alpha^*}{\partial\xi^2} + 2\xi\frac{\partial\alpha^*}{\partial\xi} - 2\alpha^*\right. \\ &\left.\left. + \frac{\partial}{\partial\mu}\left([1-\mu^2]\frac{\partial\alpha^*}{\partial\mu}\right)\right] - \frac{2}{\xi}\frac{\partial\beta^*}{\partial\mu}\right\}, \end{aligned}\right\} \tag{10}$$

$$\left.\begin{aligned} \frac{1}{\zeta}\frac{\partial\eta}{\partial\mu} = \frac{\partial\chi}{\partial\mu} &- \left[\frac{\xi^2}{1-\mu^2}\left\{\alpha^*\left(\frac{\partial\beta^*}{\partial\xi} + \frac{\beta^*}{\xi}\right) + \beta^*\left(\frac{\partial\beta^*}{\partial\mu} + \frac{\alpha^*}{\xi} + \frac{\mu\beta^*}{1-\mu^2}\right)\right\}\right. \\ &\left. + \xi^2\mu\omega^{*2}\right] + v\left\{\frac{1}{3}\frac{\partial}{\partial\mu}\left[\frac{1}{\xi^2}\frac{\partial}{\partial\xi}(\xi^2\alpha^*) + \frac{\partial\beta^*}{\partial\mu}\right] + \frac{1}{1-\mu^2}\left[\frac{\partial^2}{\partial\xi^2}(\xi^2\beta^*)\right.\right. \\ &\left.\left. + (1-\mu^2)\frac{\partial^2\beta^*}{\partial\mu^2}\right] + \frac{2}{\xi}\frac{\partial\alpha^*}{\partial\mu}\right\}, \end{aligned}\right\} \tag{11}$$

and

$$\left.\begin{aligned} \xi^2\left\{\alpha^*\left[\frac{\partial\omega^*}{\partial\xi} + 2\frac{\omega^*}{\xi}\right] + \beta^*\left[\frac{\partial\omega^*}{\partial\mu} - 2\frac{\mu\omega^*}{1-\mu^2}\right]\right\} - v\left\{\xi^2\frac{\partial^2\omega^*}{\partial\xi^2} + 4\xi\frac{\partial\omega^*}{\partial\xi}\right. \\ \left. + (1-\mu^2)\frac{\partial^2\omega^*}{\partial\mu^2} - 4\mu\frac{\partial\omega^*}{\partial\mu}\right\} = 0\,. \end{aligned}\right\} \tag{12}$$

The condition that all velocities vanish with the rotational velocity plus the obvious properties that α^* and β^* must be even functions of ω_0 (the over-all angular velocity), whereas ω^* is to be odd in ω_0, make it possible to choose velocities of the form

$$\left.\begin{aligned} \omega^* &= \omega_0\,(1 + \omega_0^2\omega + \omega_0^4\omega' + \ldots.)\,, \\ \alpha^* &= \omega_0^2\,(\alpha + \omega_0^2\alpha' + \ldots.)\,, \\ \beta^* &= \omega_0^2\,(\beta + \omega_0^2\beta' + \ldots.)\,, \end{aligned}\right\} \tag{13}$$

where $\omega, \omega', \ldots, \alpha, \alpha', \ldots, \beta, \beta', \ldots,$ are functions of ξ and μ. Similarly, one may for convenience represent the dimensionless quantities $\eta, \zeta, \chi, \ldots,$ corresponding to the pressure, density, potential, etc., by expansions in ω_0^2, namely,

$$\left.\begin{aligned} \eta(\xi, \mu; \omega_0^2) &= \eta_0(\xi) + \omega_0^2 \eta^{(1)}(\xi, \mu) + \ldots, \\ \zeta(\xi, \mu; \omega_0^2) &= \zeta_0(\xi) + \omega_0^2 \zeta^{(1)}(\xi, \mu) + \ldots, \\ \chi(\xi, \mu; \omega_0^2) &= \chi_0(\xi) + \omega_0^2 \chi^{(1)}(\xi, \mu) + \ldots, \\ &\cdots\cdots\cdots\cdots\cdots \end{aligned}\right\} \tag{14}$$

etc. By introducing expressions (13) and (14) into equations (10)–(12) and equating terms of like order in ω_0, one obtains the equations to be satisfied by the rotational perturbations of the various orders. This procedure is simply an expedient by which ω_0 may be eliminated from the equations to be dealt with. Specifically, the equations of the first-order perturbation effects are

$$\left.\begin{aligned} &\frac{1}{\zeta_0}\left[\frac{\partial \eta^{(1)}}{\partial \xi} - \frac{\zeta^{(1)}}{\zeta_0}\frac{d\eta_0}{d\xi}\right] - v_0\left\{\frac{1}{3}\frac{\partial}{\partial \xi}\left[\frac{1}{\xi^2}\frac{\partial}{\partial \xi}(\xi^2 \alpha) + \frac{\partial \beta}{\partial \mu}\right] + \frac{1}{\xi^2}\left[\xi^2 \frac{\partial^2 \alpha}{\partial \xi^2} + 2\xi \frac{\partial \alpha}{\partial \xi}\right.\right. \\ &\qquad \left.\left. - 2\alpha + \frac{\partial}{\partial \mu}\left([1-\mu^2]\frac{\partial \alpha}{\partial \mu}\right)\right] - \frac{2}{\xi}\frac{\partial \beta}{\partial \mu}\right\} = \frac{\partial}{\partial \xi}(\chi^{(1)} + \tfrac{1}{2}\xi^2[1-\mu^2]), \end{aligned}\right\} \tag{15}$$

$$\left.\begin{aligned} &\frac{1}{\zeta_0}\frac{\partial \eta^{(1)}}{\partial \mu} - v_0\left\{\frac{1}{3}\frac{\partial}{\partial \mu}\left[\frac{1}{\xi^2}\frac{\partial}{\partial \xi}(\xi^2 \alpha) + \frac{\partial \beta}{\partial \mu}\right] + \frac{1}{1-\mu^2}\left[\frac{\partial^2}{\partial \xi^2}(\xi^2 \beta) + (1-\mu^2)\right.\right. \\ &\qquad \left.\left. \times \frac{\partial^2 \beta}{\partial \mu^2}\right] + \frac{2}{\xi}\frac{\partial \alpha}{\partial \mu}\right\} = \frac{\partial}{\partial \mu}(\chi^{(1)} + \tfrac{1}{2}\xi^2[1-\mu^2]), \end{aligned}\right\} \tag{16}$$

and

$$\frac{2\xi^2}{v_0}\left[\frac{\alpha}{\xi} - \frac{\mu \beta}{1-\mu^2}\right] = \xi^2 \frac{\partial^2 \omega}{\partial \xi^2} + 4\xi \frac{\partial \omega}{\partial \xi} + (1-\mu^2)\frac{\partial^2 \omega}{\partial \mu^2} - 4\mu \frac{\partial \omega}{\partial \mu}. \tag{17}$$

From the form in which equations (15) and (16) have been written it is clear that they are gradient equations. They must therefore satisfy the condition (applied to the right-hand sides)

$$\frac{\partial}{\partial \mu}\left\{\frac{\partial}{\partial \xi}(\chi^{(1)} + \tfrac{1}{2}\xi^2[1-\mu^2])\right\} = \frac{\partial}{\partial \xi}\left\{\frac{\partial}{\partial \mu}(\chi^{(1)} + \tfrac{1}{2}\xi^2[1-\mu^2])\right\}, \tag{18}$$

which, when applied to the left-hand sides, becomes, after collecting and rearranging terms,

$$\left.\begin{aligned} &\frac{v_0}{\xi^2}\left\{\frac{\partial}{\partial \mu}\left[\xi^2 \frac{\partial^2 \alpha}{\partial \xi^2} + \frac{\partial}{\partial \mu}\left([1-\mu^2]\frac{\partial \alpha}{\partial \mu}\right)\right] - \frac{1}{1-\mu^2}\left[\xi^2 \frac{\partial^2}{\partial \xi^2}\left(\frac{\partial}{\partial \xi}[\xi^2 \beta]\right)\right.\right. \\ &\quad + (1-\mu^2)\frac{\partial^2}{\partial \mu^2}\left(\frac{\partial}{\partial \xi}[\xi^2 \beta]\right)\Big]\Big\} - \frac{1}{\xi^2}\frac{dv_0}{d\xi}\left\{\frac{1}{1-\mu^2}\left[\xi^2 \frac{\partial^2}{\partial \xi^2}(\xi^2 \beta) + (1-\mu^2)\right.\right. \\ &\qquad \left.\left. \times \frac{\partial^2}{\partial \mu^2}(\xi^2 \beta)\right] + \frac{1}{3}\left[\frac{\partial}{\partial \xi}\left(\xi^2 \frac{\partial \alpha}{\partial \mu}\right) + \xi^2 \frac{\partial^2 \beta}{\partial \mu^2}\right] + 2\xi \frac{\partial \alpha}{\partial \mu}\right\} = v_0 \frac{\partial f}{\partial \mu}, \end{aligned}\right\} \tag{19}$$

where

$$v_0 \frac{\partial f}{\partial \mu} = \frac{\partial}{\partial \mu}\left\{\frac{1}{\zeta_0}\left(\frac{\partial \eta^{(1)}}{\partial \xi} - \frac{\zeta^{(1)}}{\zeta_0}\frac{\partial \eta_0}{\partial \xi}\right)\right\} - \frac{\partial}{\partial \xi}\left\{\frac{\partial}{\partial \mu}\left(\frac{\eta^{(1)}}{\zeta_0}\right)\right\}. \tag{20}$$

At this point the equations may be made somewhat more manageable by a suitable choice for the forms of the solutions. Thus, without loss of generality,[6] one can take

$$\left.\begin{aligned}
\eta^{(1)}(\xi,\mu) &= \sum_k \eta_{1,k}(\xi) P_k(\mu) ,\\
\zeta^{(1)}(\xi,\mu) &= \sum_k \zeta_{1,k}(\xi) P_k(\mu) ,\\
\chi^{(1)}(\xi,\mu) &= \sum_k \chi_{1,k}(\xi) P_k(\mu) ,\\
\alpha(\xi,\mu) &= \sum_k \alpha_k(\xi) P_k(\mu) ,\\
\beta(\xi,\mu) &= \sum_k \beta_k(\xi) S_k(\mu) ,
\end{aligned}\right\} \tag{21}$$

where $P_k(\mu)$ is the Legendre polynomial of kth order and where

$$\left.\begin{aligned}
S_k(\mu) &= (1-\mu^2)\frac{dP_k}{d\mu} = -\frac{k(k+1)}{2k+1}(P_{k+1}-P_{k-1}) ,\\
\frac{dS_k}{d\mu} &= -k(k+1)P_k , \qquad (1-\mu^2)\frac{d^2S_k}{d\mu^2}+k(k+1)S_k = 0 .
\end{aligned}\right\} \tag{22}$$

The substitution of (21) into (19) reduces the latter to a set of equations in ξ alone, namely,

$$\left.\begin{aligned}
\xi^2\frac{d^2}{d\xi^2}\left[\alpha_k-\frac{d}{d\xi}(\xi^2\beta_k)\right]-k(k+1)\left[\alpha_k-\frac{d}{d\xi}(\xi^2\beta_k)\right]-\frac{1}{v_0}\frac{dv_0}{d\xi}\left\{\xi^2\frac{d^2}{d\xi^2}\right.\\
\times(\xi^2\beta_k)-k(k+1)(\xi^2\beta_k)+2\xi\alpha_k+\frac{1}{3}\left[\frac{d}{d\xi}(\xi^2\alpha_k)\right.\\
\left.\left.\left.-k(k+1)(\xi^2\beta_k)\right]\right\}=\xi^2 f_k ,
\end{aligned}\right\} \tag{23}$$

where

$$f_k(\xi) = \frac{1}{\zeta_0 v_0}\left[\frac{\eta_{1,k}}{\zeta_0}\frac{d\zeta_0}{d\xi}-\frac{\zeta_{1,k}}{\zeta_0}\frac{d\eta_0}{d\xi}\right]. \tag{24}$$

It is to be noted that equation (23) is an equation of condition. It merely imposes restrictions on α_k and β_k (or on $\eta_{1,k}$ and $\zeta_{1,k}$) which, when satisfied, make it possible to write the first two hydrodynamical equations, (15) and (16), as gradient equations. With solu-

[6] It is well known that any suitably behaved function of μ may be expressed uniquely in the Legendre polynomials; hence it is obvious that there are no unnecessary restrictions placed on $\eta^{(1)}$, $\zeta^{(1)}$, $\chi^{(1)}$, or α by assuming solutions of the form (21). In addition, β could likewise be expressed in terms of the P_k, but it is a simple matter to show that the only solution in this form which satisfies the equation of continuity would allow of a grouping of terms which would bring it to the form given in (21).

tions of the form assumed and satisfying (23), equations (15) and (16) reduce simply to the set of equations

$$\left.\begin{aligned}\frac{d}{d\xi}\left\{\frac{\eta_{1,k}}{\zeta_0}-v_0\left[\frac{1}{3}\left(\frac{1}{\xi^2}\frac{d}{d\xi}(\xi^2 a_k)-k(k+1)\beta_k\right)+\frac{d^2}{d\xi^2}(\xi^2\beta_k)-k(k+1)\right.\right.\right.\\ \left.\left.\left.\times\beta_k+\frac{2}{\xi}a_k\right]-R_k\right\}=\frac{d\chi_{1,k}}{d\xi}\qquad(k=0,1,2,\ldots.),\end{aligned}\right\}\tag{25}$$

where

$$R_k=0\quad(k\neq 0,2),\qquad R_0=\tfrac{1}{3}\xi^2,\qquad R_2=-\tfrac{1}{3}\xi^2.\tag{26}$$

Thus far, the only equations of the problem to be considered have been the hydrodynamical equations, which have been brought to the form given in equations (17), (23), and (25). In addition, the various functions must satisfy the perturbation equations derived from (3), (4), (5), (7), and (8). From Poisson's equation ([3]) one readily obtains the first-order equation

$$\frac{1}{\xi^2}\left\{\frac{d}{d\xi}\left(\xi^2\frac{d\chi_{1,k}}{d\xi}\right)-k(k+1)\chi_{1,k}\right\}=-\zeta_{1,k},\tag{27}$$

while from the equation of continuity ([4]) one finds (for stationary motion)

$$\left(\frac{1}{a_k}\frac{da_k}{d\xi}+\frac{2}{\xi}+\frac{1}{\zeta_0}\frac{d\zeta_0}{d\xi}\right)a_k-k(k+1)\beta_k=0.\tag{28}$$

Combining equations (25) and (27) and setting

$$v_0\left[\frac{1}{3}\left(\frac{1}{\xi^2}\frac{d}{d\xi}(\xi^2 a_k)-k(k+1)\beta_k\right)+\frac{d^2}{d\xi^2}(\xi^2\beta_k)-k(k+1)\beta_k+\frac{2}{\xi}a_k\right]=\Phi_k,\tag{29}$$

one has (from eqs. [24], [25], [27], and [29])

$$\frac{1}{\xi^2}\left\{\frac{d}{d\xi}\left(\xi^2\frac{d\Phi_k}{d\xi}\right)-k(k+1)\Phi_k\right\}+\frac{v_0\zeta_0^2}{\dfrac{d\eta_0}{d\xi}}f_k=\mathfrak{L}\left(\frac{\eta_{1,k}}{\zeta_0}\right),\tag{30}$$

where

$$\left.\begin{aligned}\mathfrak{L}\left(\frac{\eta_{1,k}}{\zeta_0}\right)=\frac{1}{\xi^2}\left\{\frac{d}{d\xi}\left(\xi^2\frac{d}{d\xi}\left[\frac{\eta_{1,k}}{\zeta_0}-R_k\right]\right)-k(k+1)\left[\frac{\eta_{1,k}}{\zeta_0}-R_k\right]\right\}\\ +\left[\frac{\eta_{1,k}}{\zeta_0}\right]\frac{\zeta_0\dfrac{d\zeta_0}{d\xi}}{\dfrac{d\eta_0}{d\xi}}.\end{aligned}\right\}\tag{31}$$

Equations (23), (24), (28), and (30) are the principal equations pertaining to the velocities in the meridional plane. A discussion of their solution will be considered later. First consider the third hydrodynamical equation.

II

Consider equation (17), to be satisfied by the differential rotational velocity. It can be written in the form

$$\frac{1}{\xi^2}\left\{\xi^2\frac{\partial^2}{\partial\xi^2}(\xi^2\omega)+\frac{\partial^2}{\partial\mu^2}[(1-\mu^2)(\xi^2\omega)]\right\}=\frac{2\xi^2}{v_0}\left[\frac{\alpha}{\xi}-\frac{\mu\beta}{1-\mu^2}\right].\tag{32}$$

Let ω have the form[7]

$$\omega = \sum_k \omega_k(\xi) M_k(\mu) , \tag{33}$$

where

$$M_k(\mu) = \frac{dP_k}{d\mu} . \tag{34}$$

Then, since (from [34])

$$\frac{d^2}{d\mu^2}[(1-\mu^2) M_k] + k(k+1) M_k = 0 , \tag{35}$$

equation (32) reduces to

$$\left.\begin{aligned} \frac{1}{\xi^2}\sum_k M_k \left\{ \xi^2 \frac{d^2}{d\xi^2}(\xi^2\omega_k) - k(k+1)(\xi^2\omega_k) \right\} \cdot \\ = \frac{2\xi^2}{v_0}\sum_k \left\{ \frac{a_k}{\xi} P_k - \beta_k \left(\frac{\mu S_k}{1-\mu^2} \right) \right\} . \end{aligned}\right\} \tag{36}$$

But

$$P_j = \frac{1}{2j+1}[M_{j+1} - M_{j-1}]$$

and

$$\left.\begin{aligned} \frac{\mu S_j}{1-\mu^2} = \mu \frac{dP_j}{d\mu} = \frac{d}{d\mu}(\mu P_j) - P_j \\ = \frac{1}{2j+1}[jM_{j+1} + (j+1) M_{j-1}] , \end{aligned}\right\}$$

so that, for each k, one has from (36)

$$\left.\begin{aligned} \xi^2 \frac{d^2}{d\xi^2}(\xi^2\omega_k) - k(k+1)(\xi^2\omega_k) = \frac{2\xi^4}{v_0} \left\{ \frac{1}{\xi} \left[\frac{a_{k-1}}{2k-1} - \frac{a_{k+1}}{2k+3} \right] \right. \\ \left. - \left[\frac{(k-1)\beta_{k-1}}{2k-1} - \frac{(k+2)\beta_{k+1}}{2k+3} \right] \right\} \\ = \xi^2 g_k(\xi) . \end{aligned}\right\} \tag{37}$$

A formal solution of (37) can easily be obtained by the method of variation of parameters; it is

$$\left.\begin{aligned} \xi^2\omega_k = \xi^{k+1} \left(w_k - \frac{1}{2k+1} \int_\xi^{\xi_0} x^{-k} g_k(x)\, dx \right) + \xi^{-k} \left(w_k' + \frac{1}{2k+1} \right. \\ \left. \times \int_\xi^{\xi_0} x^{k+1} g_k(x)\, dx \right) , \end{aligned}\right\} \tag{38}$$

[7] The function M_k is found as a solution of equation (35), which must necessarily be satisfied if ω is to have a solution separable in ξ and μ. The set of functions M_k is complete, and all M_k are bounded for $-1 \leqslant \mu \leqslant 1$, the only other properties which they are required to possess.

where w_k and w_k' are constants of integration. However, if this solution is to remain finite at $\xi = 0$, one must have

$$w_k' = -\frac{1}{2k+1}\int_0^{\xi_0} x^{k+1} g_k(x)\, dx\,,$$

so that, in final form,

$$\xi^2\omega_k = \xi^{k+1}\left(w_k - \frac{1}{2k+1}\int_\xi^{\xi_0} x^{-k} g_k(x)\, dx\right) - \frac{\xi^{-k}}{2k+1}\int_0^{\xi} x^{k+1} g_k(x)\, dx\,. \quad (39)$$

The constant w_k is fixed by the boundary condition that the stress due to ω vanish at the surface. This requires that[8]

$$\frac{d\omega_k}{d\xi} = 0\,, \qquad (\xi = \xi_0)\,. \quad (40)$$

Here two points are worthy of note. The first is that, quite generally, if there are no meridional currents (i.e., if $g_k \equiv 0$), there can be no differential rotation, for then

$$\omega_k = w_k \xi^{k-1}\,,$$

which will satisfy the condition (40) only with $w_k = 0$. This makes it clear that a differential rotation is a *consequence* of the existence of meridional velocities and does not call the latter into being to preserve stability. Second, consider the behavior of ω_k as $v_0 \to 0$. The function g_k will become infinite if α_k and β_k remain finite, in which case conditions of stability will be violated, as Randers has shown. On the other hand, if α_k and β_k are made to vanish, the function g_k may be made to approach any function whatever. This is precisely Rosseland's result.

It should also be pointed out that, as was stated before, the differential rotation must be motivated and sustained by some generating force. This force is represented by the function g, and, as is to be expected, the vanishing of g entails the vanishing of ω.

It has been shown that the vanishing of α and β implies the vanishing of ω. It is a simple matter to prove the converse theorem. Thus, from (32) it follows that for $\omega \equiv 0$ the condition

$$\alpha = \frac{\xi\mu\beta}{1-\mu^2}$$

must be satisfied. In general, such a condition is incompatible with the equation of continuity and the hydrodynamical equations, except for $\alpha \equiv 0 \equiv \beta$, for it imposes a special condition on an already determinate function α. Hence, in general, the condition $\omega \equiv 0$ (i.e., no differential rotation) implies the result $\alpha \equiv 0 \equiv \beta$, proving the theorem.

Now it follows further from (23) and (24) that with no meridional velocities the functions f_k all vanish identically, thereby satisfying the necessary and sufficient condition that η be a function of ζ[9]—that there exist a pressure-density relation. Hence it has been shown that the existence of a pressure-density relation is both a necessary and a sufficient condition for the existence of uniform rotation, and conversely.

It is an interesting corollary of this theorem that the structure of a uniformly rotating star depends only on the pressure-density relation of the corresponding unperturbed configuration. For, as has been shown, if the star rotates uniformly, there must exist a pressure-density relation. This relation must be the same as that which governs the unperturbed configuration, for the pressure and density at every point are the sums of their respective unperturbed values and first-order perturbations. But, since a pressure-

[8] See eq. (47).

[9] W. S. Krogdahl, *Ap. J.*, **96**, 128, 1942.

density relation does exist, the first-order perturbations can be found from a knowledge of the pressure- and density-gradients of the unperturbed configuration.[10] The perturbed pressure and density thus found satisfy the original pressure-density relation.

As a special case, one may consider two static configurations—one a polytrope of index $n = 3.25$ with K an absolute constant, the other a model in radiative equilibrium in which the energy generation is uniform and the opacity is given by Kramers' law; the latter model is also known to be built on a polytropic model with $n = 3.25$. The pressure-density relations, expressed parametrically as $\rho = \rho(r)$, $p = p(r)$, are identical in the two cases. The corollary states that the corresponding uniformly rotating configurations will likewise have identical pressure-density relations.

III

The problem is now reduced, in principle, to that of finding solutions to equations (23), (24), (28), and (30) and imposing on them the appropriate initial and boundary conditions.

Consider the boundary conditions which are to be satisfied by the velocities. First is the obvious condition that the velocity normal to the surface must vanish. Now the surface is defined by the condition

$$\zeta = \zeta_0 + \omega_0^2 \zeta^{(1)} + \ldots = \text{constant} = 0 . \tag{41}$$

Hence the normal to the surface will have the components

$$\left.\begin{aligned} \nu_1 &\propto 1 + \omega_0^2 \sum_k \left(\frac{\frac{d\zeta_{1,k}}{d\xi}}{\frac{d\zeta_0}{d\xi}} \right)_{\xi_0} P_k(\mu) + \ldots , \\ \nu_1 &\propto \omega_0^2 \sum_k \left(\frac{\zeta_{1,k}}{\zeta_0} \right)_{\xi_0} \frac{dP_k}{d\mu} + \ldots , \\ \nu_3 &\propto 0 . \end{aligned}\right\} \tag{42}$$

Therefore, the condition on the normal velocity, namely,

$$v^m \nu_m = 0 \qquad (r = r_0) ,$$

gives the first-order condition $v^1 = 0$ $(r = r_0)$ or

$$a_k = 0 \qquad (\xi = \xi_0) . \tag{43}$$

Three additional conditions on the velocities are that they be such that the viscous stresses shall vanish at the surface. This means that

$$T_{mn} \nu^n = 0 , \tag{44}$$

where $T_{mn} = \frac{1}{2}(v_{m,n} + v_{n,m})$ is the velocity stress tensor. Using (42), the three first-order conditions are seen to be

$$T_{11} = 0 , \quad T_{21} = 0 , \quad T_{31} = 0 \qquad (r = r_0) ; \tag{45}$$

and, since

$$T_{11} = \frac{\partial v^1}{\partial r} , \quad T_{21} = \frac{1}{2} \left[\frac{\partial v^1}{\partial \mu} + \frac{r^2}{1-\mu^2} \frac{\partial v^2}{\partial r} \right] , \quad T_{31} = \frac{1}{2} \frac{\partial v^3}{\partial r} , \tag{46}$$

[10] *Ibid.*

together with (43) they reduce to

$$\frac{da_k}{d\xi}=0\,,\qquad \frac{d\beta_k}{d\xi}=0\,,\qquad \frac{d\omega_k}{d\xi}=0 \qquad (\xi=\xi_0)\,. \quad (47)$$

At $\xi = 0$, on the other hand, the radial velocity and its first derivative must vanish; i.e.,

$$a_k=0\,,\qquad \frac{da_k}{d\xi}=0 \qquad (\xi=0)\,. \quad (48)$$

The second of conditions (47) is seen to be a condition on β_k, but this may be translated into a condition on a_k by use of the equation of continuity. For, from the equation of continuity, one has

$$\frac{da_k}{d\xi}+\left(\frac{2}{\xi}+\frac{1}{\zeta_0}\frac{d\zeta_0}{d\xi}\right)a_k-k\,(k+1)\,\beta_k=0\,,$$

and from the boundary conditions it is possible to express a_k and β_k near the boundary as

$$a_k=a_k^{(2)}\,(\xi-\xi_0)^{\,2}+a_k^{(3)}\,(\xi-\xi_0)^{\,3}+\ldots\,,$$

$$\beta_k=\beta_k^{(0)}+\beta_k^{(2)}\,(\xi-\xi_0)^{\,2}+\ldots\,.$$

Also, the function $(2\xi^{-1}+\zeta_0^{-1}d\zeta_0/d\xi)$ can be put in the form

$$\frac{2}{\xi}+\frac{1}{\zeta_0}\frac{d\zeta_0}{d\xi}=\frac{l^{(-1)}}{\xi-\xi_0}+l^{(0)}+l^{(1)}\,(\xi-\xi_0)+\ldots\,.$$

Introducing these series forms into the equation of continuity,

$$[-k\,(k+1)\,\beta_k^{(0)}]+[a_k^{(2)}\,(2+l^{(-1)})]\,(\xi-\xi_0)+[\,(3+l^{(-1)})\,a_k^{(3)}+l^{(0)}a_k^{(2)}$$
$$-k\,(k+1)\,\beta_k^{(2)}]\,(\xi-\xi_0)^{\,2}+\ldots=0\,,$$

or

$$\beta_k^{(0)}=0\,;$$

and, since in general $2+l^{(-1)}\neq 0$,

$$a_k^{(2)}=0\,,\qquad a_k^{(3)}=\frac{k\,(k+1)\,\beta_k^{(2)}}{3+l^{(-1)}}\,.$$

Therefore, the second of conditions (47) may be replaced by the condition

$$\frac{d^2a_k}{d\xi^2}=0 \qquad (\xi=\xi_0)\,; \quad (49)$$

and from equations (47), (48), and (49) it is clear that any acceptable solution a_k must be expressible as

$$a_k=\xi^2\,(\xi_0-\xi)^{\,3}A_k\,(\xi)\,, \quad (50)$$

where $A_k(\xi)$ is a bounded continuous function of ξ in the interval $0\leq\xi\leq\xi_0$.

Several further properties of the velocities may be known without actually obtaining their solutions. First, it is clear that for all nonzero a_k and β_k, k must be even to obtain solutions for a and β respectively even and odd in μ, while for all nonzero ω_j, j must be odd to obtain a solution ω which is an even function of μ. This property is consistent with equation (37). Further, a_0 and β_0 must vanish, since they correspond simply to a radial expansion, which cannot exist in a star in equilibrium.

Second, consider the boundary condition $d\omega_k/d\xi = 0$ ($\xi = \xi_0$) on ω_k. From (39) one has

$$\omega_k = \xi^{k-1}\left[w_k - \frac{1}{2k+1}\int_\xi^{\xi_0} x^{-k} g_k dx\right] - \frac{\xi^{-k-2}}{2k+1}\int_0^\xi x^{k+1} g_k dx\,, \tag{51}$$

whence

$$\frac{d\omega_k}{d\xi} = (k-1)\,\xi^{k-2}\left[w_k - \frac{1}{2k+1}\int_\xi^{\xi_0} x^{-k} g_k dx\right] + \frac{(k+2)\,\xi^{-k-3}}{2k+1}\int_0^\xi x^{k+1} g_k dx\,. \tag{52}$$

At $\xi = \xi_0$,

$$\left(\frac{d\omega_k}{d\xi}\right)_{\xi_0} = (k-1)\,\xi_0^{k-2} w_k + \frac{(k+2)\,\xi_0^{-k-3}}{2k+1}\int_0^{\xi_0} x^{k+1} g_k dx = 0\,,$$

or

$$\left.\begin{aligned} w_k &= \frac{(k+2)}{(k-1)}\,\frac{\xi_0^{-2k-1}}{2k+1}\int_0^{\xi_0} x^{k+1} g_k dx \qquad (k \neq 1)\,, \\ &\int_0^{\xi_0} x^2 g_1 dx = 0\,. \end{aligned}\right\} \tag{53}$$

But, by (37),

$$g_1 = \tfrac{1}{5}\,\xi\,(3\,\xi\beta_2 - \alpha_2)\,; \tag{54}$$

and, since in general the second of equations (53) holds only if $g_1 \equiv 0$, one must in general have $\alpha_2 \equiv 0 \equiv \beta_2$.[11]

The only other initial conditions to be specified are those which must be satisfied by the temperature and density perturbations. If one chooses to consider configurations for which[12]

$$\zeta_{1,\,k} = 0\,, \qquad \sigma_{1,\,k} = 0 \qquad (\xi = 0)\,, \tag{55}$$

then, after requiring also that

$$\frac{d\zeta_{1,\,k}}{d\xi} = 0\,, \qquad \frac{d\sigma_{1,\,k}}{d\xi} = 0 \qquad (\xi = 0)\,, \tag{56}$$

the problem is completely determinate.

One now has to solve the equations (23), (24), and (30), subject to (29), (28), (7), (8), and the initial and boundary conditions. Clearly, any attempt to find explicit and rigorous solutions of these equations would soon involve one in an impossible maze of equations and conditions. At best, therefore, any direct procedure must, for practical reasons, be at some point short-circuited. But, first, it may be asked whether any nontrivial solutions (i.e., not identically zero) for α_k, β_k, $\eta_{1,k}$, etc., exist. To answer this question, note

[11] The possibility

$$\alpha_2 = 3\xi\beta_2$$

is excluded, since, by combining it with the equation of continuity, one finds that

$$\frac{d}{d\xi}\log\,(\alpha_2\xi^2\zeta_0) - \frac{2}{\xi} = 0\,,$$

$$\alpha_2 = \frac{\text{constant}}{\zeta_0}\,.$$

[12] The particular initial values of $\zeta_{1,\,k}$ and $\sigma_{1,\,k}$ are immaterial and are taken as in (55) only for convenience. Therefore, a specification of these initial values does not amount to fixing two disposable constants, but rather to the adoption of a particular convention. Equations (56) do, however, correspond to the fixing of two constants of integration, namely, those which arise from the radiant flux equation and the equation of conservation of energy—equations (7) and (8), respectively.

that by combining equations (23), (28), (29), and (30) one can obtain an equation in a_k of the form

$$\left[\sum_{j=0}^{5} X_{kj}(\xi)\left(\frac{d}{d\xi}\right)^j\right] a_k = \mathfrak{L}\left(\frac{\eta_{1,k}}{\zeta_0}\right). \tag{57}$$

Since this is an ordinary linear differential equation, a nontrivial solution can, in general, be expected to exist, provided the number of conditions imposed upon it does not exceed the number of available adjustable parameters; such a solution will be unique if the number of conditions equals the number of adjustable parameters. From this result there follows another, of considerable importance for general purposes. Thus, it is clear that to require that

$$\left.\begin{aligned} \xi^2 f_k = \xi^2 \frac{d^2}{d\xi^2}\left[a_k - \frac{d}{d\xi}(\xi^2\beta_k)\right] - k(k+1)\left[a_k - \frac{d}{d\xi}(\xi^2\beta_k)\right] - \frac{1}{v_0}\frac{dv_0}{d\xi} \\ \times\left\{\xi^2\frac{d^2}{d\xi^2}(\xi^2\beta_k) - k(k+1)(\xi^2\beta_k) + 2\xi a_k + \frac{1}{3}\left[\frac{d}{d\xi}(\xi^2 a_k)\right.\right. \\ \left.\left. - k(k+1)(\xi^2\beta_k)\right]\right\} \equiv 0 \end{aligned}\right\} \tag{58}$$

is equivalent to imposing on a_k an infinite number of conditions in addition to the two initial conditions and three boundary conditions. Hence, this relation can be expected to be true only if $a_k \equiv 0$ ($\equiv \beta_k$, by the equation of continuity). That is, $f_k \equiv 0$ in general implies $a_k \equiv 0$, and conversely.

The significance and interpretation of this result can be seen in the following argument. Ideally, a star in static gravitational equilibrium will be a radially symmetric configuration. Mathematically this means that any function describing some property of the star will be a function of a single variable, such as the distance from the center. Thus, if two or more stellar functions are specified as functions of the radius vector, this specification may be regarded as a statement in parametric form of the dependence of these functions on each other. This fact may be looked upon as a sort of mathematical degeneracy implied by the radial symmetry. If the star is made to rotate, however, one degree of the degeneracy is removed, for now the specification of any function throughout the star must be made in terms of two independent variables (such as ξ and μ, for example) and any two stellar functions will, in general, be independent of each other. In particular, the pressure and density will *in general* be independent functions. (As will be seen, an important exception to this general rule is that where the star rotates with a constant angular velocity [see next paragraph]). Thus, if the pressure and density are independent stellar functions, then in any region within a rotating star any other function is expressible as a function of both p and ρ. Specifically, if the gravitational potential is $\mathfrak{V} = \mathfrak{V}(p, \rho)$, the isobaric and equipotential surfaces will not coincide. Therefore, the pressure- and gravitational-gradients cannot be parallel; their difference is an acceleration (vector) which must be compensated in some way if the star's structure is to be stationary. In a viscous star the compensation will be afforded by the viscous and inertial forces acting in opposition to the accelerating forces. This is merely a verbal statement of the hydrodynamical equations and, when put thus, seems obvious.

This argument does not apply if, contrary to assumption, the potential is either independent of ρ or if p is a function of ρ. But, if $\mathfrak{V}$ is to satisfy Poisson's equation, it cannot be independent of ρ. On the other hand, the necessary and sufficient condition that p be a function of ρ is that[13]

$$v_0\zeta_0 f_k = \frac{\eta_{1,k}}{\zeta_0}\frac{d\zeta_0}{d\xi} - \frac{\zeta_{1,k}}{\zeta_0}\frac{d\eta_0}{d\xi} \equiv 0\,,$$

[13] See above, n. 9.

which has already been seen to imply, in general, the vanishing of α and β. Clearly, then, the function f is the generating function which gives rise to the meridional currents. It is a result of the over-all rotation in the sense that rotation removes the degeneracy which implies the vanishing of f.

It is clear, now, how the differential rotation is brought about. The over-all rotation creates a force, in the manner just described, which generates large-scale currents in the meridional plane. These, in turn, provide a rotational acceleration which gives rise to a differential rotation; the meridional currents are second-order effects, the differential rotation a third-order effect. The cause-and-effect relation of the two phenomena is sometimes reversed, and for this reason it is well to specifically point it out.

IV

It is clear that to obtain rigorous solutions for all the fundamental equations simultaneously is an almost impossible task. A convenient method of approximation would be desirable. One method is suggested by equation (50). This method makes use of a well-known theorem that any bounded continuous function may be approximated in a particular interval to any arbitrary degree of exactness by a suitable polynomial. Therefore, let A_k in (50) be given as a polynomial in ξ with undetermined coefficients. To determine the coefficients, first determine the solutions $\eta_{1,k}^{(m)}, \zeta_{1,k}^{(m)}, \ldots$, etc., corresponding to the particular polynomial $A_k^{(m)} = \xi^m$. In so doing, use will be made of equations (23), (24), (28), (29), (30), (31), and (5), but not of (7) and (8). Then the coefficients may be so chosen as to satisfy equations (7) and (8) as nearly as possible.[14] Even this procedure, while representing a considerable simplification, is at best laborious, and it will not be undertaken here. However, it is quite simple and may prove instructive to derive the meridional streamlines for the various "harmonic components" of the meridional velocities.

The streamlines for the kth harmonic component of the meridional velocities are defined as curves along which

$$\frac{d\xi}{\alpha_k P_k} = \frac{d\mu}{\beta_k S_k}, \tag{59}$$

or

$$k(k+1)\frac{\beta_k}{\alpha_k}\,d\xi = \frac{k(k+1)P_k}{(1-\mu^2)\dfrac{dP_k}{d\mu}}\,d\mu = -\frac{\dfrac{d}{d\mu}\left[(1-\mu^2)\dfrac{dP_k}{d\mu}\right]}{(1-\mu^2)\dfrac{dP_k}{d\mu}}\,d\mu. \tag{60}$$

But, by the equation of continuity,

$$k(k+1)\frac{\beta_k}{\alpha_k} = \frac{1}{\xi^2\zeta_0\alpha_k}\frac{d}{d\xi}(\xi^2\zeta_0\alpha_k) = \frac{d}{d\xi}\log(\xi^2\zeta_0\alpha_k),$$

so that, from (60)

$$d\log\left\{\xi^2\zeta_0\alpha_k(1-\mu^2)\frac{dP_k}{d\mu}\right\} = 0$$

and the streamlines are the curves

$$(\xi^2\zeta_0\alpha_k)\left[(1-\mu^2)\frac{dP_k}{d\mu}\right] = c_k = \text{constant} \quad (k = 4, 6, 8, \ldots). \tag{61}$$

Figure 1 shows the shape of the streamlines for the case $A_4 = \xi$, $\zeta_0 = (\theta_{3.25})^{3.25}$, where $\theta_{3.25}$ is the Emden function of index 3.25. Note that the streamline $c_k = 0$ is formed by

[14] That is, either a best fit, in the sense of least squares, or exactly at a prescribed number of points equal in number to the number of adjustable coefficients in the polynomial A_k.

the outer boundary ($\zeta_0 = 0$), the axis ($\mu = 1$), the equatorial plane ($\mu = 0$), the cones over which $dP_k/d\mu = 0$, and the spheres over which $a_k = 0$.

Finally, it may be found of interest to *fit* a solution of the form (33) for ω to the rotation observed in the sun. No pretense is made of having thus obtained a rigorous solution; and the results are in no sense intended as data against, or in support of, the theory

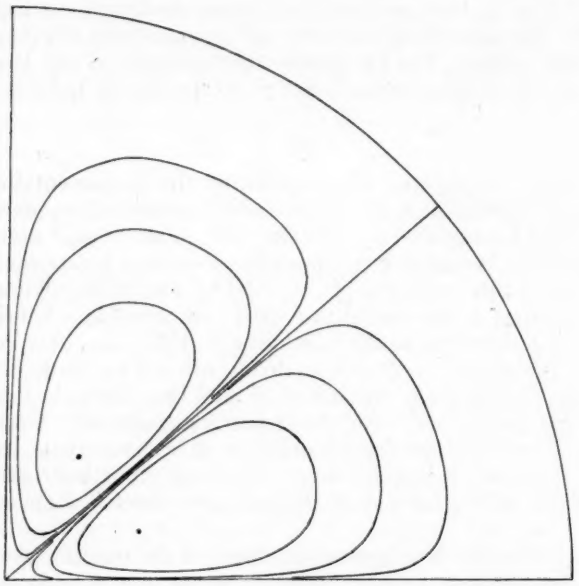

FIG. 1.—Meridional streamlines of the first non-vanishing harmonic component for the special case $A_4 = \xi$, $\zeta_0 = (\theta_{3.25})^{3.25}$.

TABLE 1

Latitude	v^3, "pred."	v^3, obs.
15°	14°.305/day	14°.31/day
45	12.79	12.79
75	11.28	11.27
90	11.05	11.04

given in Section II, for any smooth function of μ could be well fitted by a polynomial in the $dP_k/d\mu$. By using the observed solar rotational velocity at latitudes 60°, 30°, and 0°, the angular velocities at other latitudes may be calculated from a three-term series. Table 1 shows the observed[15] and "predicted" values for four latitudes.

It is a pleasure to acknowledge my indebtedness to Dr. S. Chandrasekhar for his unfailing encouragement and helpful advice and to Mr. Robert M. Snow for numerous fruitful discussions.

[15] Observed data are taken from the *Handb. d. Ap.*, **4**, 167, Table VII.

NOTES ON STELLAR SPECTRA*

OTTO STRUVE
McDonald and Yerkes Observatories
Received September 15, 1943

ABSTRACT

The P Cygni star HD 169226 = MWC 293 shows radial velocities ranging from − 143 km/sec for *H* to − 50 km/sec for *Mg* II. The emission lines of *H* give + 89 km/sec, and the emission lines of *He* I give + 141 km/sec.

The star HD 217050 = MWC 394 has a peculiarly poor spectrum on the violet side of λ 3647, with only *Ni* II very strong. The other lines, *Fe* II, *Ti* II, *Cr* II, etc., must be suppressed by continuous *H* absorption within the shell.

The color of HD 160529 = MWC 266 has been found to be similar to that of a late F or early K star. The spectral type is A4se*a*.

Pleione has shown, in July, 1943, an increase in intensity of *Sc* II and *Fe* I, which now definitely establishes the evolution of its shell toward lower ionization.

AG Pegasi showed, in the summer of 1943, P Cygni absorption lines of increased strength, while Z Andromedae had stronger emission lines of *Fe* I than in the preceding fall and winter.

HD 169226

This star is MWC 293[1] and is described by Merrill as showing an *Hβ* line of the P Cygni type on a spectrogram taken at Mount Wilson on July 20, 1924. Two spectrograms were taken at the McDonald Observatory, on July 7 and July 8, 1943, with the

TABLE 1

RADIAL VELOCITIES OF HD 169226

Atom	No. of Lines	Velocity	Atom	No. of Lines	Velocity
H absorption.....	7	−142.8 km/sec	*Ca* II absorption...	1	− 10.8 km/sec
H emission.....	3	+ 88.6	*N* II absorption....	1	− 78.9
He I absorption....	7	− 84.0	*O* II absorption....	7	− 61.0
He I emission.....	1	+141.4	*Si* III absorption...	3	− 95.9
Mg II absorption...	1	− 49.8	*C* II absorption....	1	− 80.6

Cassegrain quartz spectrograph, giving a dispersion of 40 A/mm at λ 3933. The star is very red and therefore represents a difficult object, even for a powerful instrument. The P Cygni character is very pronounced. In fact, among the P Cygni type stars which I have observed, it resembles P Cygni more than any of the other members of the group. But the emission lines are conspicuous only for *H* and weak for *He* I. The other atoms have only absorption lines. *Ca* II is probably interstellar and is very strong. There is a conspicuous broad absorption feature at λ 4430, agreeing with Beal's unidentified interstellar band in this position. The mean radial velocities from the two plates, in Table 1, show a large range, but there is no obvious relation with ionization potential, as in the case of P Cygni. The large positive velocities obtained from the emission lines are of interest in connection with the analogous result recently obtained by Beals[2] for MWC 374.

**Contributions from the McDonald Observatory, University of Texas*, No. 81.

[1] $\alpha = 18^h18^m.6$; $\delta = -12°15'$ (1900), mag. 9.1.

[2] *J.R.A.S., Canada*, **37**, 245, 1943.

HD 217050

The spectrum of this shell in the ordinary photographic region has been recently described by R. B. Baldwin.[3] The star is MWC 394 or HR 8731.[4] Several early Yerkes spectrograms are valuable in establishing the variations of this spectrum. These plates have already been used by E. B. Frost in establishing the fact that the emission lines of *H* are variable in this star.[5] The shell features were, however, not recognized as such at that time and remained unnoticed. On July 28, August 4, and October 9, 1913, the *H* lines showed strong sharp cores, which are typical of shell absorption. On August 5 and 30, 1918, these shell absorptions were completely missing: they had disappeared, together with the emission lines. The next Yerkes plate is one taken June 4, 1929. It shows the sharp cores of *H*, together with double emission lines and probably a few faint, fairly narrow lines of *Fe* II. A longer series of plates was started on September 15, 1941, and shows the shell spectrum very much as described by Baldwin. I have the impression that there are fairly rapid changes in the intensities of the *a* Cygni lines, but they never disappear as in AX Monocerotis or HD 218393 and only seem to be weaker at certain times. I have not been able to find a period, but the suspected changes take place within a few days. The radial velocities of the Yerkes plates are given in Table 2.[6] They are based upon the lines *Hε*, *Hδ*, Hγ, *Hβ*, *Ca* II K and half a dozen of the stronger *Fe* II lines.

The ultraviolet spectrum of HD 217050 is of considerable interest. I obtained a strongly exposed spectrogram with the McDonald Cassegrain quartz spectrograph on Eastman Process emulsion and have measured on it the lines listed in Table 3. The date of the plate is June 22, 1943, 10^h28^m U.T. Considering the fact that the ordinary photographic region is rich in lines which, though fainter than in Pleione or 48 Librae, crowd our plate on the red side of the region which I have measured, the poverty of lines on the violet side of the Balmer limit is an interesting example of continuous *H* absorption within the shell—a phenomenon to which I have already called attention in the case of 48 Librae.[7] There is another interesting similarity between HD 217050 and 48 Librae: both stars show the ultraviolet lines of *Ni* II with great strength and apparently with little effect from the continuous *H* absorption. At least, there seems to be no noticeable weakening of these lines as compared to *Ni* II 4067. It is probable, though perhaps not certain, that *Ni* II occupies a relatively high level within the shell.

HD 160529

This star is MWC 266[8] and was last discussed by Swings and Struve[9] and by Merrill and Burwell.[10] The spectrum shows very strong *a* Cygni lines, whose radial velocities suggest expansion in varying degrees. Merrill remarks that the interstellar line λ 6284 is very strong. Swings and I pointed out earlier that the *H* lines are weak but that the star is so red that it was difficult to observe it in the ultraviolet region. Repeated efforts to get the ultraviolet region with our normal dispersion of 40 A/mm at λ 3933 having failed, I obtained in the summer of 1943 several plates with the dispersion of 100 A/mm at λ 3933. These plates were obtained in part to get the ultraviolet spectrum and in part to determine the reddening. For the latter purpose the slit was opened quite wide and

[3] *Ap. J.*, **97**, 388, 1943.

[4] Also BD+47°3985; $\alpha = 22^h52^m7$; $\delta = +48°9'$ (1900), mag. 5.2.

[5] *Ap. J.*, **49**, 61, 1919.

[6] The radial velocities after August 24, 1943, were added in the proof.

[7] *Ap. J.*, **98**, 98, 1943.

[8] $\alpha = 17^h35^m3$, $\delta = -33°27'$, mag. 6.7, Sp. A4sea.

[9] *Ap. J.*, **91**, 592, 1940.

[10] *Ap. J.*, **98**, 356, 1943.

TABLE 2

RADIAL VELOCITIES OF HD 217050

Date	U.T.	Radial Velocity	Quality	Date	U.T.	Radial Velocity	Quality
1929 June 4...	8:48	−12.1 km/sec.	p	1943 July 22...	7:08	−25.9 km/sec.	g
1941 Sept. 15...	7:19	20.1	g	July 28...	4:10	18.0	p
Sept. 26...	7:04	13.0	g	July 28...	5:20	10.8	p
Sept. 27...	1:45	15.4	g	Aug. 10...	3:48	21.1	g
Oct. 6...	2:25	12.6	g	Aug. 10...	5:03	29.9	g
Oct. 16...	1:16	21.5	g	Aug. 17...	5:50	20.8	g
Nov. 18...	2:12	18.6	g	Aug. 18...	4:42	23.4	g
Nov. 19...	2:02	27.2	g	Aug. 24...	3:22	29.9	g
Dec. 20...	0:07	22.4	g	Aug. 24...	4:52	20.8	g
1492 July 3...	6:18	24.6	g	Sept. 21...	1:25	23.8	g
Sept. 1...	5:06	19.5	p	Sept. 23...	1:57	28.8	p
Sept. 16...	2:57	13.1	g	Sept. 24...	1:34	15.1	g
Sept. 17...	3:15	22.5	g	Sept. 28...	2:34	23.4	g
Sept. 25...	6:02	19.0	g	Sept. 29...	1:30	27.2	p
Sept. 27...	5:09	21.3	g	Oct. 6...	1:22	19.7	g
Sept. 28...	2:48	19.9	g	Oct. 7...	1:29	27.3	g
Oct. 6...	2:07	30.2	g	Oct. 8...	1:06	27.4	g
Oct. 7...	1:25	23.0	g	Oct. 15...	1:39	19.2	g
Oct. 8...	1:57	23.9	g	Oct. 20...	0:50	11.1	g
Oct. 19...	1:48	20.7	g	Oct. 21...	1:50	19.0	p
Oct. 28...	0:24	24.9	g	Oct. 27...	0:41	25.3	g
Nov. 13...	1:00	19.7	g	Oct. 29...	0:12	29.7	g
Nov. 27...	0:00	20.0	g	Nov. 28...	1:12	19.1	g
Dec. 4...	0:42	19.4	g	Dec. 5...	3:05	24.1	g
Dec. 5...	1:03	17.6	g	Dec. 24...	2:49	16.0	g
Dec. 12...	0:52	23.9	g	Dec. 25...	23:47	23.1	g
1943 Apr. 8...	10:10	17.8	g	1944 Jan. 3...	2:10	27.4	p
May 28...	8:08	26.7	g	Jan. 10...	1:00	26.3	g
June 11...	7:26	21.2	g	Jan. 17...	23:56	−28.0	p
July 22...	6:07	−25.9	g				

TABLE 3

ULTRAVIOLET ABSORPTION LINES OF HD 217050

λ	Int.	Identification	λ	Int.	Identification
3337.83.....	1	.....	3598.95.....	0	*He* I 99.32(1)
3340.08.....	0	*Cr* II 39.80(50)	3620.88.....	1	*Fe* II 21.27(6)
3372.14.....	0n	*Ti* II 72.80(400)	3632.42.....	1nn	*He* I 34.24(2);
3374.07.....	1	*Ni* II 73.98(4)			(*Cr* II 31.72(40))
3387.02.....	1n	(*Fe* II 87.84(2))	3659.63.....	1	*Ti* II 59.76(150)
3404.34.....	1	(*Cr* II 03.32(100))	3661.27.....	1	*H*31 61.22
3407.35.....	1	*Ni* II 07.32(8)	3662.31.....	1	*H*30 62.26
3432.88.....	1n	*Cr* II 33.30(75)	3663.44.....	2	*H*29 63.40
3454.30.....	2	*Ni* II 54.16(5)	3664.79.....	3	*H*28 64.68
3465.61.....	3	*Ni* II 65.62(1)	3666.12.....	3	*H*27 66.10
3468.59.....	1	*Fe* II 68.68(8)	3667.70.....	4	*H*26 67.68
3471.26.....	2	*Ni* II 71.35(2)	3669.50.....	4	*H*25 69.47
3514.01.....	5	*Ni* II 13.94(8)	3671.37.....	6	*H*24 71.48
3520.23.....	0nn	*Ti* II 20.26(18)	3673.78.....	6	*H*23 73.76
3576.66.....	3	*Ni* II 76.76(3)	3676.30.....	7	*H*22 76.36
3579.95.....	1	*Fe* I 81.19(1000)	3679.27.....	7	*H*21 79.36

was oriented north and south, so that all the light of HD 160529 and the neighboring comparison stars was admitted, in spite of the large amount of atmospheric dispersion at $\delta = -33°$. The comparison stars were taken near the meridian and immediately after HD 160529; and, since they are located within a fraction of 1° from this star, differential extinction can be neglected. The exposures were 5 minutes each; the night was very clear and the seeing steady. The results are summarized in Table 4. We estimate that the energy distribution of HD 160529 resembles that of a late F or early K star. A long exposure with narrow slit, taken on July 7, 1943, shows that the *H* lines are very narrow and weak, though they can be seen to about *H*24. They are thus much weaker than in normal supergiants, like α Cygni, or in shells, like 48 Librae, but they are stronger than in *v* Sagittarii, where Greenstein could measure *H*24 on plates of more than

TABLE 4

COMPARISON OF ENERGY DISTRIBUTION IN HD 160529 AND NEIGHBORING STARS ON JULY 7, 1943

Star	Time (U.T.)	HD Spectrum	Mag.		Remarks
			Ptm.	Ptg.	
HD 160529....	5:47	(Oe5)	6.7	7.6	
160748....	5:58	Ma	6.5	8.0	Redder than HD 160529
160461....	6:50	A0	7.8	7.5	Bluer than HD 160529
160410....	6:59	F0	8.4	8.2	Bluer than HD 160529

twice the dispersion and much more contrasty emulsion.[11] The spectrogram of HD 160529 shows no noticeable Balmer discontinuity—which is in accord with the intensities of the *H* lines. The metallic lines in the ultraviolet region appear to be normal in intensity.

PLEIONE

Spectrograms taken by Messrs. C. A. Bauer and G. Münch on Eastman Process emulsion show that the evolution of this remarkable shell spectrum since the winter of 1942–43 has proceeded in the direction of increased intensity for *Sc* II, *Fe* II, and probably *Ti* II. This change shows almost conclusively that the general evolution[12] since 1940 has been in the direction of lowered ionization. There have been strange departures from normal ionization conditions, but the general trend has been from *Ni* II, I.P. 18.2 volts, in 1940, to *Sc* II, I.P. 12.8 volts, in 1943. This result will help in establishing the ionization sequence of other shells. The recent plates were taken on July 19 and July 29, 1943.

HD 193182[13]

In 1923 Merrill announced that HD 193182, or MWC 632, has a bright *Hα* line and that *Hβ* is an absorption line with bright borders. The star was classified by him as F, although the Henry Draper classification was given as A0. In 1939 Morgan[14] pointed out that this star has all the characteristics of high luminosity usually associated with the designation c, and hence he assigned it to class cA0, with an absolute magnitude of − 5.0. The star is located in the vicinity of γ Cygni, where several other supergiants of early type were noted. But, while several of these supergiants are very greatly reddened

[11] *Ap. J.*, **91**, 438, 1940.

[12] *Ap. J.*, **97**, 428, 1943.

[13] $\alpha = 20^h13^m8$, $\delta = +39°16'$, mag. 7.0.

[14] *Ap. J.*, **90**, 632, 1939.

PLATE VII

PLATE VII

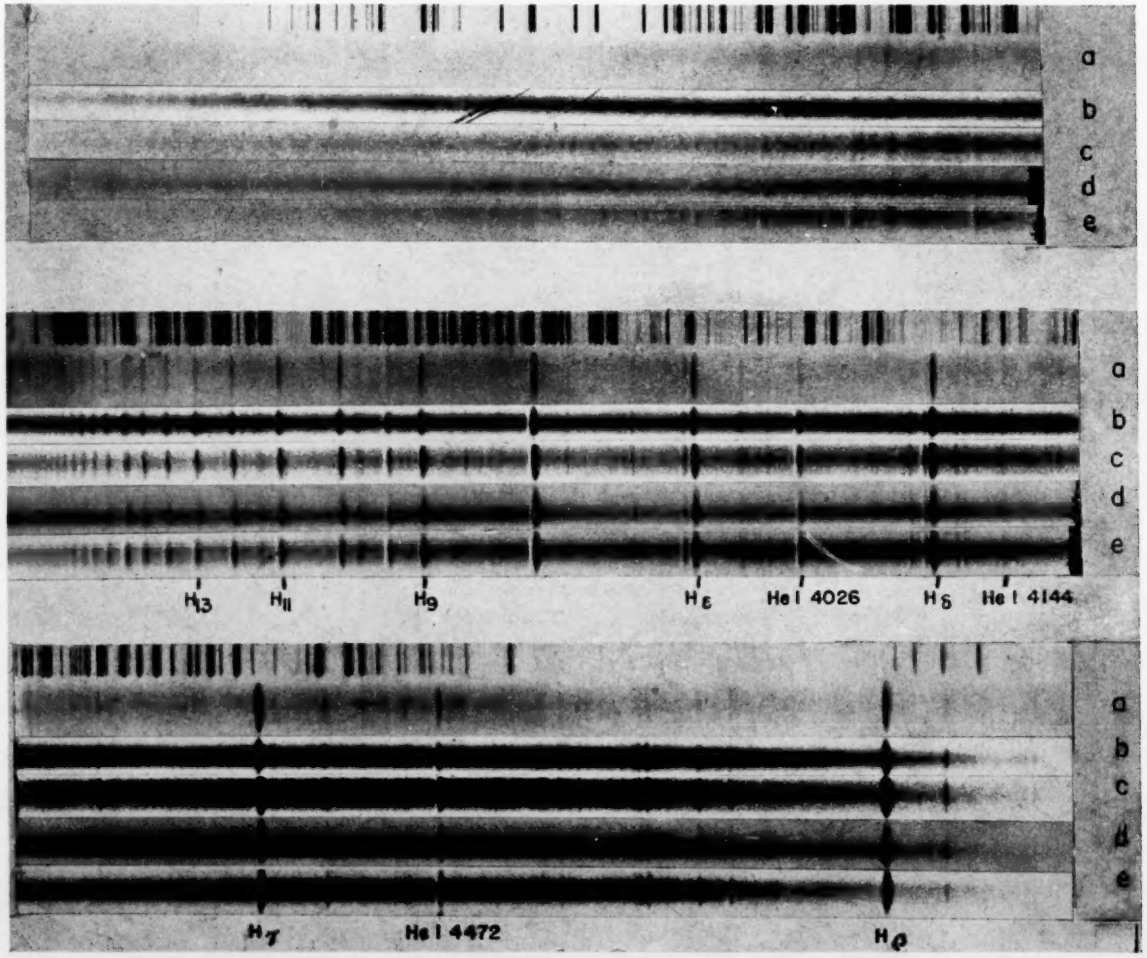

UNIV. OF MICH.

SPECTRUM OF AG PEGASI

(*a*) Dec. 1, 1939; (*b*) Nov. 9, 1941; (*c*) July 13, 1942; (*d*) Nov. 23, 1942; (*e*) July 5, 1943

PLATE VIII

Z ANDROMEDAE
June 28, 1943, 8^h29^m U.T.

UNIV. OF MICH.

by space-absorption, Morgan stated that "HD 193182 is probably not reddened more than one- or two-tenths of a magnitude." Quite recently Merrill[15] suggested that this spectrum may be a "false c-star," like 48 Librae or Pleione.

In order to test whether the spectrum is that of a shell, several plates were obtained in June and July, 1943, at the McDonald Observatory with the Cassegrain quartz spectrograph giving a dispersion of 40 A/mm at λ 3933. The spectrum is exceedingly rich in lines and leaves no question as to its origin: the hydrogen lines consist of very narrow and deep cores, which can be seen to *H*32. These cores are symmetrically superposed over wide wings suggestive of Stark effect; the lines of *Mg* II 4481 and of *Si* II are very weak and show that dilution of radiation is conspicuous. There are probably present broad and shallow lines of *He* I 4026 and 4472, so that the underlying stellar spectrum may be that of a fairly rapidly rotating B star. The shell spectrum is of particular interest, because it is rich in lines of relatively low ionization potential; for example, *Fe* I is strong. This spectrum is, therefore, the latest shell spectrum thus far observed, except that of 14 Comae Berenices.[16] In this latter star there are large differences in rotational broadening observed in lines of different atoms. No such effect is seen in HD 193182 with the dispersion used in this work. On the McDonald spectrograms *Hβ* is a sharp narrow absorption line, probably without bright edges. *Hα* is not shown.

AG PEGASI

A spectrogram of this star[17] taken on July 5, 1943, is interesting because of the great strength with which the P Cygni absorption lines are now visible in the higher members of the *H* and *He* I ($2^3P - n^3D$) series. Plate VII shows the progressive change in this spectrum since 1939.

Z ANDROMEDAE

The principal change shown by a spectrogram taken on June 28, 1943, from plates taken in January, 1943, is a strengthening of the bright lines of *Fe* I. The decline in excitation recorded some months ago[18] has thus continued. The spectrogram is reproduced in Plate VIII. The line *Fe* I 4045 is now quite easily visible, although it had not been measured in 1940, 1941, and 1942.[19]

I am indebted to Miss J. Ringstad and Miss G. Peterson for assistance in the measurements of spectrograms of HD 217050.

[15] *Ap. J.*, **98**, 364, 1943.

[16] *Ap. J.*, **94**, 305, 1941.

[17] BD + 11°4673 = HD 207757; see also Merrill's detailed investigation, *Ap. J.*, **95**, 386, 1942.

[18] Swings and Struve, *Ap. J.*, **98**, 93, 1943.

[19] Swings and Struve, *Ap. J.*, **98**, 200, 1943. *Note added in proof:* On a spectrogram of November 14, 1943, the excitation is again much greater. The lines of *Fe* I are much weaker, and those of [*Fe* VII] and [*Ne* V] much stronger than in June, 1943. The line [*Fe* VII] 3586 is very diffuse.

NEW ORBITS FOR THE SPECTROSCOPIC BINARIES HD 163181 AND HD 78316 (76 κ CANCRI)*

OTTO STRUVE
McDonald and Yerkes Observatories
Received November 10, 1943

ABSTRACT

HD 163181.—A new orbit has been derived for this eclipsing variable from 55 McDonald Observatory plates. The elements agree with those determined in 1928 at Mount Wilson, except that e is 0.10 instead of 0.065. The velocity-curve shows a conspicuous rotation effect at phases on both sides of 6 days—which is Gaposchkin's secondary minimum. The system consists of a very luminous B star with strong absorption lines and an equally luminous star which is associated with an emitting nebulosity of *H* and *He* I.

HD 78316 (κ Cancri).—A new orbit has been derived from 84 Yerkes single-prism spectrograms and 3 McDonald Cassegrain plates. The elements agree well with those recently determined at Victoria except for an unexplained difference in γ and a small difference in ω. The spectrum contains unusually strong lines of *Mn* II.

HD 163181[1]

This star is of special interest because it has bright lines of variable intensity, which have sometimes been likened to the bright lines in the spectrum of β Lyrae. A comparison of the two stars is, however, at first quite disappointing. On the first few spectrograms taken at the McDonald Observatory the bright lines were very weak; and, although on later dates they became somewhat stronger, they never even remotely resembled the conspicuous emission lines of β Lyrae. However, a more critical examination of the 55 spectrograms obtained between July 9 and September 15, 1943, shows a number of very interesting features which may help in elucidating some of the puzzles which abound in our discussions of Be stars.

The binary nature of HD 163181 was discovered at the Mount Wilson Observatory, and an orbit was published in 1928 by Humason and Nicholson.[2] The period is almost exactly 12 days, and the range in velocity is 385 km/sec. The eccentricity is 0.065, and the longitude of periastron is 23.2°. Humason and Nicholson discovered the variability of the emission lines and also of the absorption lines and established the principal characteristics of these variations. Through their kindness I was able to examine several of their spectrograms. There seems to have been no appreciable change in the intensity or appearance of the bright and dark lines.

The star took an added importance when S. Gaposchkin,[3] in 1938, announced that it is an eclipsing variable with two almost equal minima, whose depths are 0.43 and 0.42 mag., respectively. Since then the variable has also been observed by Hertzsprung[4] and his associates, who find a β Lyrae-type light-curve and closely confirm the results of Gaposchkin. I have adopted Gaposchkin's epoch of principal minimum, JD 2428429.79, and his period of 12.004211 days and have computed my phases with the help of these data. The radial velocities are listed in Table 1. Separate columns give the mean results from all lines except those of interstellar calcium, from the calcium lines, and from the *H* lines.

* *Contributions from the McDonald Observatory, University of Texas*, No. 86.

[1] V453 Sco; $\alpha = 17^h49^m.7$; $\delta = -32°27'$ (1900), mag. 6.6, Sp. B0.

[2] *Ap. J.*, **67**, 341, 1928.

[3] *Harvard Bull.*, No. 909, p. 20, 1938; *Ap. J.*, **89**, 125 and 322, 1939.

[4] Quoted by Mrs. C. P. Gaposchkin from a letter by Professor Hertzsprung to Dr. Harlow Shapley dated December 9, 1940.

TABLE 1

RADIAL VELOCITIES OF HD 163181

DATE 1943	U.T.	JD 2430000+	PHASE	QUAL.	VELOCITIES IN KM/SEC						O−C
					No. of Lines	All Lines	No. of Lines	*Ca* II	No. of Lines	*H*	
July 9...	5:48	914.74	0.08	g	14	− 72.6	.....	.....	2	− 81.0	− 2.2
9...	6:07	914.76	0.16	g	15	− 60.1	1	+16.2	3	− 73.9	+ 3.5
11...	6:22	916.77	2.11	g	15	+111.8	2	+ 2.1	6	+108.6	− 3.1
11...	7:26	916.81	2.15	g	18	+107.4	2	− 7.3	6	+102.0	−10.8
12...	5:33	917.73	3.07	g	17	+156.2	2	− 4.5	4	+150.8	−10.3
12...	6:16	917.76	3.10	g	15	+162.4	2	− 4.9	3	+165.1	− 4.7
13...	5:26	918.73	4.07	g	15	+158.0	2	− 0.9	4	+162.0	+ 5.3
13...	5:56	918.75	4.09	g	16	+135.5	2	−15.0	6	+140.5	−16.2
14...	5:51	919.74	5.08	v.p.	5	+ 61.9	.....	.....	1	+ 44.7	− 7.8
14...	6:09	919.76	5.10	g	13	+ 78.0	1	+ 3.1	3	+ 56.7	+10.4
18...	5:28	923.73	8.07	g	16	−217.0	1	− 5.3	3	−202.0	−22.0
22...	6:55	927.79	1.12	p	8	+ 48.9	.....	.....	1	+ 10.8	+22.0
22...	7:15	927.80	1.13	g	6	+ 30.9	.....	.....	1	+ 7.2	+ 3.2
23...	6:14	928.76	2.09	g	15	+113.3	1	− 6.1	3	+102.7	− 0.3
28...	4:32	933.69	7.02	p	2	−128.3	.....	.....	1	−170.0	+ 2.9
28...	4:50	933.70	7.03	g	13	−146.1	.....	.....	2	−146.2	−13.9
29...	4:15	934.68	8.01	g	18	−196.0	1	−60.3	3	−178.2	− 3.3
Aug. 6...	2:37	942.61	3.94	g	15	+149.8	2	−12.0	3	+166.7	− 9.0
7...	2:34	943.61	4.94	p	8	+112.3	.....	.....	2	+ 87.5	+28.2
8...	2:46	944.62	5.95	g	13	+ 6.7	2	+10.5	2	− 11.4	+33.3
8...	3:06	944.63	5.96	g	15	− 8.7	2	+ 4.2	2	− 5.2	+18.9
9...	2:24	945.60	6.93	v.p.	6	−137.4	.....	.....	1	−119.2	−13.7
9...	2:39	945.61	6.94	g	8	−121.6	.....	.....	1	−112.0	+ 2.9
13...	2:49	949.62	10.95	g	9	−157.7	.....	.....	1	−190.7	− 2.2
14...	3:43	950.66	11.99	g	21	− 77.9	.....	.....	3	− 85.8	+ 0.5
15...	2:50	951.62	0.95	g	15	+ 8.2	.....	.....	2	− 20.1	− 2.0
20...	2:53	956.62	5.95	g	10	+ 1.1	2	+11.7	2	− 0.1	+27.7
25...	2:12	961.59	10.92	g	8	−163.4	.....	.....	1	−152.5	− 6.0
25...	2:30	961.60	10.93	g	12	−177.0	.....	.....	2	−154.5	−20.4
27...	2:30	963.60	0.92	g	10	+ 10.1	.....	.....	2	− 20.5	+ 2.8
27...	2:54	963.62	0.94	g	14	+ 3.5	.....	.....	2	− 23.2	− 5.7
28...	2:27	964.60	1.92	g	8	+ 91.4	.....	.....	2	+ 78.5	− 8.3
29...	2:24	965.60	2.92	g	12	+159.5	1	−10.7	2	+155.8	− 2.4
30...	2:14	966.59	3.91	g	15	+164.6	2	−38.0	3	+164.8	+ 4.6
Sept. 4...	1:54	971.58	8.90	g	16	−208.6	1	+ 6.4	5	−202.0	+ 5.6
5...	4:14	972.68	10.00	g	14	−200.2	1	0.0	3	−194.2	+ 0.2
5...	4:36	972.69	10.01	g	8	−187.5	.....	.....	2	−222.9	+12.1
6...	2:00	973.58	10.90	g	16	−169.2	1	+ 3.1	3	−160.2	−10.6
6...	2:20	973.60	10.92	g	16	−169.5	1	−15.1	3	−156.8	−12.1
7...	2:03	974.59	11.91	g	17	− 87.7	2	+ 4.0	2	− 89.5	− 2.5
7...	2:47	974.62	11.94	g	18	− 90.8	2	+ 2.4	2	−100.8	− 8.1
8...	1:54	975.58	0.90	g	17	+ 10.7	1	+12.0	2	− 29.2	+ 5.4
8...	2:15	975.59	0.91	g	16	− 0.6	1	+18.1	2	− 21.3	− 6.9
8...	2:51	975.62	0.94	g	20	+ 16.7	1	− 1.8	3	− 3.9	+ 7.5
8...	3:26	975.64	0.96	g	17	+ 9.1	1	− 0.3	2	− 9.1	− 2.2
12...	1:54	979.58	4.90	g	14	+102.8	1	−15.8	2	+116.5	+14.8
12...	2:16	979.59	4.91	g	15	+ 95.8	1	− 6.8	3	+ 98.2	+ 9.0
13...	1:47	980.57	5.89	g	13	− 15.9	1	− 6.8	3	− 12.3	+ 4.0
13...	2:19	980.60	5.92	g	16	+ 0.2	1	+ 2.2	3	− 15.7	+23.4
13...	2:49	980.62	5.94	g	15	− 6.6	1	−13.0	3	− 12.8	+18.9
14...	1:44	981.57	6.89	g	17	−128.7	1	− 6.9	3	−142.1	− 8.1
14...	2:17	981.60	6.92	g	16	−152.6	1	−16.1	3	−142.4	−29.5
14...	2:59	981.62	6.94	g	17	−143.3	1	+ 2.2	3	−140.5	−18.8
15...	2:06	982.59	7.91	g	20	−188.9	1	+ 2.1	3	−187.3	− 0.7
15...	2:30	982.60	7.92	g	13	−189.9	.....	.....	2	−198.3	− 1.3

The plates were grouped in 13 normal places as is shown in Table 2. The values of O−C are those which result from a least-squares solution. Table 3 shows a comparison of the velocities from the *H* lines with those from all stellar lines. The velocity curve is given in Figure 1, where the observations refer to the normal points. Because the period is so nearly 12 days, the observations are grouped at intervals of about 1 day, and there are no intermediate observations. The orbital elements were derived by means of Schlesinger's least-squares method and are shown in Table 4. The probable error listed in the line

TABLE 2

NORMAL PLACES

No.	Limits of Phase	Mean Phase	No. of Plates	O−C	
1.....	0.08– 0.16	0.120	2	+ 0.65	
2.....	0.90– 0.96	0.931	7	− 0.16	
3.....	1.12– 2.15	1.753	6	+ 0.48	
4.....	2.92– 3.10	3.030	3	− 5.80	
5.....	3.91– 4.09	4.002	4	− 3.82	
6.....	4.90– 5.10	4.986	5	+10.92	Rotation effect
7.....	5.89– 5.96	5.935	6	+21.03	
8.....	6.89– 7.03	6.953	7	−11.17	
9.....	7.91– 8.07	7.978	4	− 6.82	
10.....	8.90–.....	8.900	1	+ 5.60	
11.....	10.00–10.01	10.005	2	+ 6.05	
12.....	10.90–10.95	10.924	5	−10.26	
13.....	11.91–11.99	11.947	3	− 3.37	

TABLE 3

COMPARISON OF *H* AND OTHER LINES

Normal Place	Mean Phase	No. of Plates	*H*−(All Lines)	$\frac{H\delta+H\gamma}{2}$ −(All Lines)	Normal Place	Mean Phase	No. of Plates	*H*−(All Lines)	$\frac{H\delta+H\gamma}{2}$ −(All Lines)
1.....	0.120	2	−11.0	+ 2.2	8.....	6.953	7	+ 2.9	+25.9
2.....	0.931	7	−26.4	−26.4	9.....	7.978	4	+ 7.0	− 0.6
3.....	1.753	6	−15.7	−18.6	10.....	8.900	1	+ 6.6	+22.2
4.....	3.030	3	− 2.1	− 8.3	11.....	10.005	2	−14.7	+ 9.6
5.....	4.002	4	+ 6.5	+13.3	12.....	10.924	5	+ 4.4	+32.3
6.....	4.986	5	− 9.5	−15.4	13.....	11.947	3	− 6.6	− 0.8
7.....	5.935	6	− 5.6	+ 3.4					

for γ is that for Schlesinger's unknown Γ. The value of T is given in days counted from zero phase at JD2428429.79. The normal points were all given equal weight, in order to reduce the influence of physical factors, such as rotation, which tend to distort the velocity-curve. The value of $\Sigma\Delta v^2$ was reduced from 1793 to 966. The probable error of a single normal point is ±7 km/sec; that of a single plate is ±8.7 km/sec. These values are large; Humason's and Nicholson's observations give an even larger value, namely, ±9.2 km/sec for one plate.

The agreement of my elements with those of Humason and Nicholson is very satisfactory. There has been no change in ω, and the only significant difference is in e. The Mount Wilson value was 0.065. The observations show at once that there is a pro-

nounced rotation effect. The residuals are positive at phases near 5 and 6 days and negative at phases near 7 days. The range in these residuals is of the order of ± 25 km/sec, so that the rotational velocity must be considerable. It would be premature to compute it without an accurate velocity-curve over the entire range of phases concerned. The effect is also unmistakably present in the Mount Wilson velocity-curve, though it was

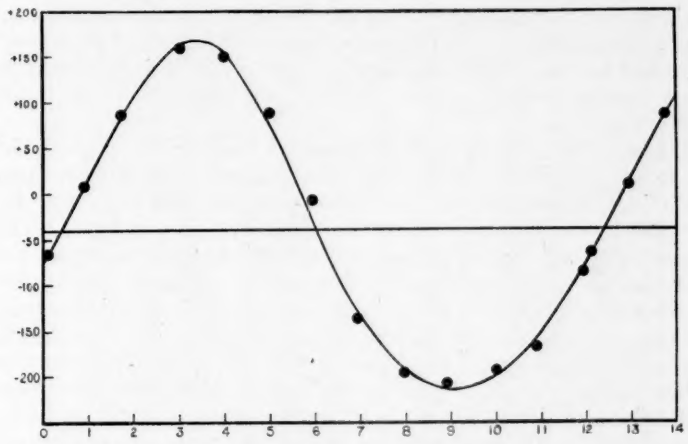

FIG. 1.—Velocity-curve of HD 163181

TABLE 4

ORBITAL ELEMENTS OF HD 163181

Preliminary	Final	Probable Errors
$P=12.004211$ days	$P=12.004211$ days	.....
$\gamma=-42.8$ km/sec	$\gamma=-39.8$ km/sec	± 3.5 km/sec
$K=189.5$ km/sec	$K=192.6$ km/sec	± 2.9 km/sec
$\omega=+46.2°$	$\omega=+23.7°$	$\pm 22.2°$
$e=0.04$	$e=0.10$	± 0.014
$T=4.78$ days	$T=4.04$ days	± 0.76 day

not originally interpreted in this way. With my elements the time of mid-eclipse should occur when $v + \omega = 90°$, or when the radial velocity is

$$\gamma + Ke \cos \omega = -22.2 \text{ km/sec}.$$

The Mount Wilson elements give

$$\gamma + Ke \cos \omega = -30.3 \text{ km/sec}.$$

Whichever value we use, there is a strong indication that the spectroscopic rotation effect is slightly unsymmetrical with respect to this point. Both velocity-curves give positive residuals of considerable size at that phase at which the velocity is approximately -26 km/sec. The observations also suggest that the rotation effect begins at least 1 full day before mid-eclipse and lasts at least 1 full day after it. The limits may well be as great as ± 1.5 days. This does not accord well with Gaposchkin's photometric result, $D = 0.09$. $P = 1.33$ days, for the entire duration of eclipse. If the observations affected by the

rotation effect are excluded, the probable error of one plate is reduced to a value which is consistent with the internal precision of the measurements.

Probably the most remarkable result of Gaposchkin's work is the fact that his principal eclipse falls $0.5P$ earlier than the eclipse of the B star which we have just discussed. Yet there is no indication in the spectrum of a second set of absorption lines which would correspond to that body which is eclipsed at phase 0, if we depend upon an extrapolation of Gaposchkin's period, or at phase 0.6 day, if we again use the spectrographic criterion $v + \omega = 270°$. My observations in this respect agree with those of Humason and Nicholson, who searched for the other component but could not find its absorption spectrum. This apparent paradox is of the utmost interest, and its solution will undoubtedly lead to important results.

I believe that a satisfactory solution of the paradox is obtained from the following considerations. In the vicinity of my phase 0 or Humason and Nicholson's phase 9.5 days, the absorption lines are very strong. This is precisely the phase of Gaposchkin's principal mid-eclipse. The B star stands in front, the unknown star is eclipsed. The absorption lines, which are weak at all other phases, are greatly enhanced, and the amount of this enhancement appears to be very closely the same for all lines. The critical test comes from the absence of any dilution effect in the lines of *He* I or in the intensity of *Mg* II 4481. These lines are normal. The *H* lines are strong and narrow, but they lack the typical sharpness of *H* lines produced in a tenuous shell. We conclude that we are observing the absorption spectrum of a star, not that of a shell. It is clear that this star must be the normal B-type component of the binary system whose absorption lines, at all other phases, are weakened by the superposition of the strong continuous spectrum of the unknown component. This latter, then, does display a continuous spectrum, even though it does not show absorption lines at the times of elongation. At our phase 0, when the absorption lines of the B star are strong, the emission lines are very weak or absent. We conclude that the unknown star has emission lines in its spectrum and that the gases giving rise to them are eclipsed at phase 0.

At phase 6 days, when Gaposchkin observes his secondary eclipse, the unknown star is in front, and the emission lines are little affected. The absorption lines of the B star are weak and show the rotation effect, but they never quite disappear. Since no absorption lines belonging to the unknown star are observed at the elongations—in spite of the fact that Gaposchkin finds for its total light $L_2 = 0.46$ as against $L_1 = 0.54$ for the B star—we must conclude that the unknown star is not responsible for the absorption lines at phase 6 days. The eclipse is probably not total, though we cannot be quite certain of this because of the gaps in our observations. It may be annular, because at phases near 0 days the emission lines do seem to disappear completely.

The general run of the values O−C in Table 2 shows that there is no rotation effect on the two sides of phase 0. The B star is in front, and its lines should, of course, not show such an effect. But the bright *H* lines disappear at phase 0. Hence we might expect a rotation effect in the measures of the *H* absorption lines, if the latter are to any extent produced by absorption of the continuous light of the unknown star in the emitting shell. Table 3 might suggest that such an effect does exist: for $H\delta$ and $H\gamma$ we have positive residuals at phases 8.9, 10.0, and 10.9 days, and negative residuals at phases 0.9, 1.8, and 3.0 days. During the larger part of this interval the emission lines are very weak or absent, so that there can be no serious trouble from blending. But the *H* lines which we measure are those of the B star, not of the unknown star. Hence the phenomenon, if it is real, is not a simple rotation effect. It is more probable that the *H* lines of the B star are blended with those of the unknown star and that the residuals of the *H* velocities reflect, very slightly, the motion of the unknown star. The question is whether or not we can be certain of any absorption lines of the unknown star. At phase 8.0 days the emission lines are strong and are greatly displaced toward the red. They are single, without central reversal, so that, if there is any absorption line due to the unknown star's shell, it must

PLATE IX

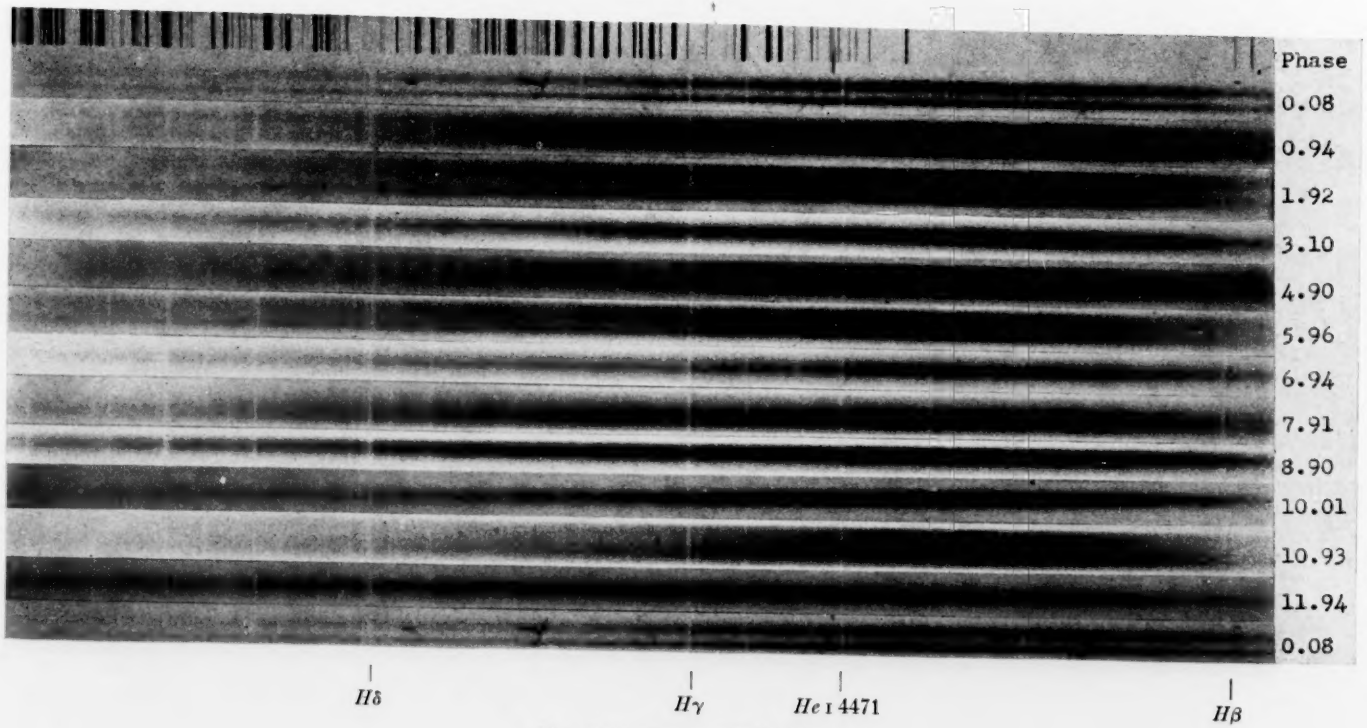

THE SPECTRUM OF HD 163181

UNIV. OF MICH.

blend with the *H* lines of the B star and shift it toward the red. But at phase 8.0 days the residual is nearly zero: there is no absorption from the shell. At phases near 6 days the emission lines are double. But the eclipse of the B star is presumably annular, or partial, so that the *H* absorption lines may belong to it. The emission lines are too weak to show whether the absorptions are rendered shallow by the superposition of emission or are cut below the continuous spectrum by high-level gases. We must, therefore, leave undecided the origin of the *H* residuals in Table 3.

Our picture is complicated by the fact that the emission lines are quite dissimilar at the two elongations. At phases around 3 and 4 days they are very weak and shifted toward the violet of the absorption lines. At phases around 9 days they are strong and shifted conspicuously toward the red. There can be no question that the velocity of the emission line taken as a whole shifts, relative to the absorption line, with a phase difference of 0.5*P*. Whether the emission line also shifts with respect to the center of mass of the system is not quite certain because it is exceedingly difficult to measure the bright lines without being influenced by the disturbing presence of the absorption lines. It is my impression that the emission lines do shift but that their range is considerably smaller than that of the absorption lines. This does not mean, however, that the unknown star is the more massive one, because it is possible that the velocity of the emission lines does not represent the velocity of the unknown star.

Why, then, is the appearance of the emission lines so different at the two maxima? I suggest that the unknown star has a continuous spectrum of approximately the same intensity as the B star and that it has very weak absorption lines which are never seen at the elongations or at secondary minimum. It does, however, have associated with it a set of emission lines whose velocities are systematically shifted toward the red by perhaps 1.5 A, as are the emission lines of 29 Canis Majoris or of the Wolf-Rayet component of HD 193576.[5] In 29 Canis Majoris the red shift occurs in the brighter component of the binary, and the displaced emission lines oscillate in phase with the absorption lines. In HD193576 and HD 163181 the displaced emission lines belong to one of two approximately equally luminous stars, and they oscillate with a phase difference of 0.5*P* from the absorption lines. It is quite probable that the red shift of the emission lines is a fairly general phenomenon among spectroscopic binaries of very early type. We cannot explain it, but we are fully aware that it constitutes an important problem in astrophysics. It is almost certainly related to the red shift observed by C. S. Beals[6] in the emission lines of the P Cygni-type star, MWC 374. In this remarkable spectrum the shift is probably caused by self-absorption in a decelerated expanding shell. There is, at present, no evidence of expansion in the gaseous shell of the unknown component of HD 163181. Even if such expansion does exist, it would be difficult to avoid the complication of a violet shift, which should probably be present in an expanding shell that is small enough to fit within the rather small amount of space allowed by Gaposchkin's revised photometric elements. These considerations, together with O. C. Wilson's results for HD 193576, leave the problem of the red shift unsolved, though I should not want to go so far as to question, with Wilson, the expanding-shell hypothesis in the case of a normal Wolf-Rayet star. Self-absorption in the manner considered by Beals for MWC 374 undoubtedly is important in some stars. Unfortunately, neither HD 163181 nor HD 193576 has forbidden lines. If such lines were present, their velocities should not be affected by self-absorption, and the test would be easy.

The *H* emission lines of HD 163181 are strong at phases 7, 8, and probably 9 days. But at phase 10 days they are much weakened. They remain about constant in intensity until phase 11 days, being then clearly double, with the stronger component on the red side. At phase 0 they are double and very weak. But their presence—enhanced, perhaps, by the longer exposures necessary at minimum light—suggests that the *H* shell is never

[5] O. C. Wilson, *Ap. J.*, **95**, 402, 1942.

[6] *J.R.A.S. Canada*, **37**, 241, 1943.

totally eclipsed but remains as a luminous fringe around the totally eclipsed unknown star. At phases 1, 2, 3, and 4 days the emission lines are very weak, presumably because of the general red shift, which would bring their strongest portion roughly in coincidence with the absorption lines of the B star. It is difficult to decide whether the intensities of the latter are consistent with this interpretation, because of the weakness of the emission lines. But the weakening of the emission lines at phase 10 days, only 1 day after elongation, would then indicate that the eclipse of the emitting shell of the unknown star is already well under way 2 full days before mid-eclipse. It is entirely possible that the emitting gases are not symmetrically distributed around the unknown star, but it is not possible to separate such an effect from the proposed red shift.

HD 78316 (76 κ CANCRI)[7]

The binary nature of κ Cancri was discovered in 1904 by Frost and Adams from 5 spectrograms taken at the Yerkes Observatory. An orbit, based upon 25 Yerkes plates,

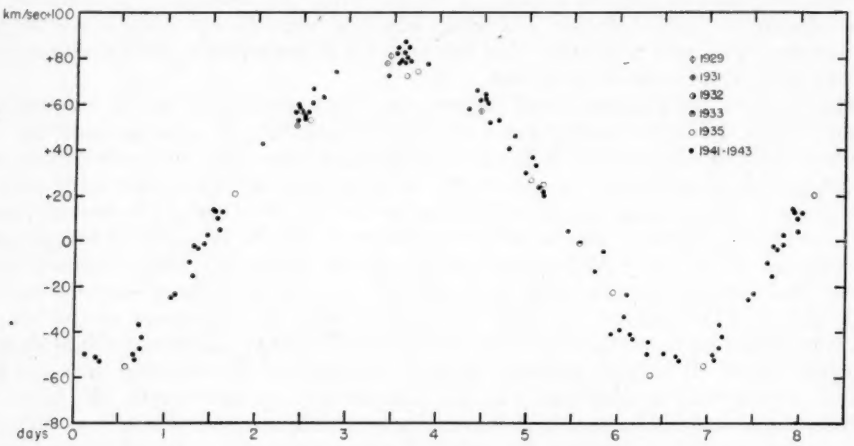

FIG. 2.—Velocity-curve of 76 κ Cancri

was obtained by N. Ichinohe[8] in 1907. The eccentricity of this orbit was 0.15, and the velocity-curve was sufficiently unsymmetrical to place the star among those objects for which a new determination is desirable in order to test whether there has been a change in the line of apsides during the last 36 years. A new series of single-prism spectrograms was started at the Yerkes Observatory in 1929 and was continued, with interruptions, until May, 1943. In the meantime J. A. Pearce and Phoebe Riddle[9] have published the results of their measurements of 32 high-dispersion spectrograms of κ Cancri taken between March and May, 1938, with the Victoria 72-inch reflector. The dispersion used for this work at Victoria was much greater than that used at Yerkes, and the precision of the Victoria orbit is greater than that obtained by me. Nevertheless, there are certain features in my velocity-curve which appear to justify its publication. In the first place, the Yerkes observations have a gap between 1935 and 1941 and therefore do not duplicate in time the observations made at Victoria. In the second place, my velocity-curve differs appreciably in shape from that computed with the Victoria elements, and a small difference in ω is indicated. Since this difference is not consistent with the fact that the value

[7] $\alpha = 9^h2^m3$; $\delta = +11°4'$ (1900), mag. 5.1, Sp. B8.

[8] *Ap. J.*, **25**, 315, 1907.

[9] *Pub. A.A.S.*, **10**, 65, 1940.

obtained by Pearce and Riddle is almost identical with the value obtained by Ichinohe, there is no evidence of a rotation of the line of apsides. But Ichinohe's orbit is based upon a relatively small number of plates, and, while his mean error per plate is only ±4.2 km/sec, the minimum of the velocity-curve was not observed sufficiently to allow a very critical determination of ω.

The 84 new Yerkes observations and 3 McDonald observations are listed in Table 5. The phases were computed with the period obtained at Victoria, and zero phase is the Victoria value of the time of periastron passage. The observations were arranged in 15

TABLE 5

RADIAL VELOCITIES OF 76 κ CANCRI

Plate	Date	U.T.	Phase	Vel. (Km/Sec)	Plate	Date	U.T.	Phase	Vel. (Km/Sec)
1R9180	1929 Apr. 14	3h50m	2d450	+51.1	1R13040	1942 Dec. 12	11h36m	6d108	−23.6
9188	Apr. 15	2 44	3.404	+78.2	13049	Dec. 16	10 03	3.651	+80.4
9197	Apr 16	4 46	4.488	+57.6	13050	Dec. 16	11 05	3.694	+79.2
9995	Dec. 19	8 20	3.483	+80.9	13056	1943 Jan. 15	7 06	1.562	+13.9
10005	1932 Jan. 19	6 35	2.444	+57.1	13057	Jan. 15	8 10	1.606	+ 4.4
10884	1933 Dec. 6	11 35	5.585	− 0.3	13078	Feb. 16	7 10	1.598	+10.1
11663	1935 Mar. 11	5 36	5.028	+27.0	13079	Feb. 16	8 14	1.643	+13.2
11668	Mar. 13	4 11	0.575	−55.7	13089	Feb. 18	5 25	3.526	+82.1
11672	Mar. 15	4 43	2.597	+52.6	13090	Feb. 18	6 85	3.574	+78.3
11678	Mar. 16	5 49	3.643	+72.4	13091	Feb. 18	7 52	3.628	+87.8
11687	Mar. 24	3 50	5.168	+25.6	13092	Feb. 18	8 51	3.669	+85.3
11694	Mar. 27	3 59	1.781	+21.4	13097	Feb. 19	5 38	4.535	+61.7
11702	Mar. 29	3 47	3.773	+74.5	13098	Feb. 19	6 51	4.586	+52.1
11705	Apr. 7	3 50	6.382	−59.9	CQ1945	Mar. 2	7 59	2.847	+74.3
11707	Apr. 13	3 35	5.978	−22.7	CQ1959	Mar 4	8 05	4.851	+46.5
12648	1941 Nov 18	11 34	0.696	−52.3	CG2053	Mar. 13	8 11	1.068	−25.4
12654	Nov. 20	11 46	2.704	+63.2	1R13108	Mar. 21	3 16	2.470	+59.9
12659	Dec. 6	9 56	5.842	− 4.8	13109	Mar. 21	4 25	2.518	+53.8
12669	Dec. 11	10 10	4.459	+62.3	13110	Mar. 21	5 40	2.570	+56.7
12676	Dec. 14	11 18	1.113	−23.2	13111	Mar. 21	6 43	2.614	+67.7
12700	1942 Jan. 6	7 55	4.792	+41.0	13117	Mar 22	4 48	3.534	+84.6
12707	Jan. 13	9 13	5.453	+ 4.7	13118	Mar. 22	5 54	3.580	+78.3
12717	Jan. 23	8 00	2.617	+60.1	13119	Mar. 22	6 57	3.624	+82.1
12724	Jan. 24	7 45	3.606	+79.0	13126	Mar. 30	4 08	5.113	+24.1
12732	Feb. 12	8 20	3.450	+72.7	13127	Mar. 30	5 45	5.181	+20.8
12736	Feb. 13	6 04	4.356	+58.1	13130	Mar. 31	3 34	6.089	−33.2
12741	Feb. 20	6 35	4.984	+30.6	13131	Mar. 31	4 45	6.139	−41.5
12747	Feb. 21	5 58	5.958	−41.1	13132	Mar. 31	5 49	6.183	−43.2
12749	Mar. 5	5 52	5.168	+21.7	13134	Apr. 1	4 13	0.724	−36.9
12752	Mar. 19	4 05	6.307	−49.8	13135	Apr. 1	5 15	0.767	−42.2
12753	Mar. 19	4 58	6.344	−44.2	13142	Apr. 8	2 37	1.264	− 8.9
12757	Mar. 30	4 02	4.519	+64.1	13143	Apr. 8	3 39	1.307	−15.3
12759	Apr. 1	3 55	0.121	−49.7	13144	Apr. 8	4 53	1.358	− 3.4
12766	Apr. 12	2 55	4.686	+52.4	13154	Apr. 21	1 43	1.439	− 1.4
12772	Apr. 13	4 05	5.735	−13.6	13155	Apr. 21	2 52	1.488	+ 3.2
12784	Apr. 15	3 25	1.314	− 2.5	13156	Apr. 21	3 56	1.532	+14.0
12794	Apr. 29	2 00	2.468	+53.5	13162	Apr. 22	1 40	2.438	+47.1
12976	Nov. 6	11 47	2.082	+43.1	13163	Apr. 22	2 43	2.481	+57.2
12991	Nov. 17	10 46	0.252	−51.3	13164	Apr. 22	3 46	2.525	+54.9
12992	Nov. 17	11 48	0.295	−52.8	13170	May 1	1 45	5.048	+37.1
13009	Nov. 27	11 34	3.893	+77.3	13171	May 1	2 48	5.092	+32.9
13019	Dec. 4	10 43	4.464	+66.3	13179	May 3	2 18	0.678	−50.1
13020	Dec. 4	11 50	4.511	+62.2	13180	May 3	3 45	0.738	−47.6
13039	Dec. 12	10 31	6.063	−39.1					

normal places (Table 6), and the values of O−C were computed separately for each plate with the help of the preliminary elements and were then averaged for each normal place. A least-squares solution was made following the method of Schlesinger and adopting equal weights for all normal points. This was done in order to minimize the possible effect of physical causes which are sometimes known to distort a velocity-curve. The value of $\Sigma\Delta v^2$ was reduced from 123.8 to 63.6, and the probable error of one normal velocity is ±1.6 km/sec; that of one plate is of the order of ±3.5 km/sec. The elements are shown in Table 7. The time of periastron passage is expressed in days counted from phase 0, or from JD 2429012.081. The probable error listed in the second line is that obtained for Schlesinger's variable Γ. The principal difference from the elements of Pearce and Riddle

is in the value of γ, for which they find +25.3 km/sec. It is possible that this difference of 4.2 km/sec is due to a systematic difference between the two instruments, though the amount is alarmingly large. The published systematic differences for stars of classes B8–A3 are:

$$\text{Yerkes} - \text{Lick} = +0.95 \text{ km/sec},$$

$$\text{Victoria} - \text{Lick} = -0.95 \text{ km/sec}.^{10}$$

However, these determinations (which incidentally are in the wrong sense) probably do not apply in the present case. In September, 1941, a change was made in the Bruce spec-

TABLE 6

NORMAL PLACES

No	Limits of Phase	Mean Phase	No. of Plates	Computed Velocity	O−C	No.	Limits of Phase	Mean Phase	No. of Plates	Computed Velocity	O−C
1.....	0.12–0.30	0.22	3	−53.8	+2.3	9.....	3.65–3.89	3.73	5	+77.5	+2.1
2.....	0.58–0.77	0.70	6	−44.7	−2.3	10.....	4.36–4.59	4.49	8	+60.4	+0.3
3.....	1.07–1.36	1.24	6	−13.6	+0.5	11.....	4.69–4.85	4.78	3	+47.8	−1.3
4.....	1.44–1.64	1.55	7	+ 7.3	+0.7	12.....	4.98–5.18	5.10	8	+30.0	−2.6
5.....	1.78–2.08	1.93	2	+31.0	+1.5	13.....	5.45–5.84	5.65	4	− 7.1	+3.6
6.....	2.44–2.52	2.47	8	+57.2	−3.1	14.....	5.96–6.18	6.07	7	−35.0	+0.1
7.....	2.57–2.85	2.66	6	+64.1	−1.4	15.....	6.31–6.38	6.34	3	−47.8	−3.4
8.....	3.40–3.64	3.55	11	+78.2	+1.0						

TABLE 7

ORBITAL ELEMENTS OF 76 κ CANCRI

Preliminary	Final	Probable Errors
P=6.39316 days	P=6.39316 days	.....
γ=+21.1 km/sec	γ=+21.1 km/sec	±0.8 km/sec
K= 66.9 km/sec	K= 66.1 km/sec	±0.6 km/sec
ω=161.0	ω=174.6°	±2.4°
e= 0.14	e= 0.137	±0.086
T= 0.00	T=+0.21 day	±0.065 day

trograph which resulted, according to Hynek's measures of ζ Tauri, in the following difference:

$$\text{Yerkes new} - \text{Yerkes old} = -2.0 \text{ km/sec}.$$

Measures of several plates of standard-velocity stars have given a similar result. Since formerly the systematic error of the Yerkes plates was +1.0 km/sec, it should now be about −1.0 km/sec. It is difficult to account for the rest of the discrepancy. The plot of the velocities in Figure 1 certainly does not warrant the idea that there has existed since 1941 a systematic difference of −4 km/sec, which did not exist in 1929–1935. If there is a difference, it is in the opposite sense. It is not impossible that the velocity of the center of mass of κ Cancri is slightly variable. This question must be postponed until more material on the systematic errors is available.

In spite of this uncertainty, the other elements are known with considerable precision. There is no spectrum of the secondary component, and it is probable that what Ichinohe

[10] J. H. Moore, *Pub. Lick Obs.*, **18**, xi, 1932.

TABLE 8

LIST OF LINES IN THE SPECTRUM OF κ CANCRI

Wave Length	Int.	Identification	Wave Length	Int.	Identification
3289.40	0	*Fe* II 9.35	3497.60	3	*Mn* II 7.53
3295.86	1n	*Cr* II 5.42, *Fe* II 5.81	3499.71	1	*Fe* II 9.88
3298.21	2	*Fe* II 7.89	3507.93	0	*Fe* II 7.39
3303.19	1	*Fe* II 2.86, *Fe* II 3.47	3510.38	1	*Ti* II 0.85
3313.71	1	*Fe* II 14.00	3516.29	1	*Fe* II 5.82
3322.68	1	*Ti* II 2.93, *Fe* II 3.07	3535.83	1	*Ti* II 5.41
3327.78	1	*Ti* II 6.76, *Cr* II 8.35	3563.39	1	.....
3329.38	0	*Ti* II 9.5	3576.87	1	*Ni* II 6.76
3335.12	0	*Ti* II {5.17 / 5.22}, *Cr* II 5.28, *Cr* II 5.46	3585.90	0	*Cr* II 5.31
			3627.55	1	*Fe* II 7.17
			3631.59	1	*Cr* II 1.49, *Cr* II 1.72
3336.28	2	*Cr* II 6.32	3682.55	0nn	*H* 20 2.81
3337.51	1	*Ti* II 7.85	3685.48	2	*Ti* II 5.20
3339.79	0	*Cr* II 9.80, *Ti* II 0.34	3687.09	1	*H* 19 6.83
3341.71	0	*Ti* II 1.84	3691.71	1nn	*H* 18 1.56
3349.02	1	*Ti* II 9.00, *Ti* II 9.41	3697.11	2nn	*H* 17 7.15
3355.78	0	*Fe* II 6.26	3704.03	3nn	*H* 16 3.86
3358.39	2	*Cr* II 8.50	3706.06	1n	*Ca* II 6.04, *Ti* II 6.23
3360.05	1	*Cr* II 0.30	3708.40	1	*Mn* II 8.06
3363.02	1	.....	3710.37	1	*Mn* II 9.88
3365.98	1	*Ti* II 6.18	3712.18	4nn	*H* 15 1.97
3368.03	1n	*Cr* II 8.05	3715.66	1	*Cr* II 5.19, *Cr* II 5.45
3372.52	1	*Ti* II 2.80	3717.58	1	.....
3374.62	0	*Ti* II 4.35	3722.15	5nn	*H* 14 1.94
3376.55	0	*Cr* II 6.27	3730.21	2	.....
3379.62	1	*Cr* II 9.82	3734.61	7nn	*H* 13 4.37
3383.52	1	*Ti* II 3.76	3735.33	2	.....
3387.67	2	*Ti* II 7.84	3736.77	3	*Ca* II 6.92
3389.74	1	.....	3741.67	1	*Ti* II 1.65
3394.51	1n	*Ti* II 4.55, *Cr* II 4.32	3743.44	2	*Fe* I 3.37
3399.89	1	*Cr* II 9.54	3750.28	10nn	*H* 12 0.15
3403.39	1	*Cr* II 3.32	3759.50	2n	*Ti* II 9.30
3408.70	1	*Cr* II 8.77	3761.48	1n	*Ti* II 1.32
3419.47	1	(*Fe* I 8.51)	3763.93	4	*Fe* I 3.80, *Fe* II 4.11
3421.11	1	*Cr* II 1.20	3765.84	0	*Cr* II 5.62
3422.83	1	*Cr* II 2.74	3767.61	0	*Fe* I 7.21
3428.13	1n	*Cr* II 8.94	3770.70	10nn	*H* 11 0.63
3433.52	0	*Cr* II 3.30	3774.73	0	*V* II 4.34, *Ti* II 4.65
3436.28	0	*Fe* II 6.11	3778.44	2	*V* II 8.36
3439.05	5	*Mn* II 8.96	3781.27	0	*Fe* II 1.51
3442.04	7	*Mn* II 1.98	3798.16	10nn	*H* 10 7.90
3446.07	1	*Co* II 6.40	3812.49	2	*Fe* I 2.96
3451.69	1	*Fe* II 1.23, *Fe* II 1.32	3814.50	1	*Fe* II 4.12
3457.78	1n	*Cr* II 7.62	3821.84	1n	*Fe* II 1.97
3460.21	7	*Mn* II 0.33	3825.22	1	*Fe* II 4.91
3464.45	0nn	*Fe* II 4.50	3827.69	1	*Fe* II 7.08, *Fe* II 7.69, *Fe* I 7.83
3468.72	1	*Fe* II 8.68			
3471.76	0	*Ni* II 1.35	3832.49	0	*Mg* I 2.31
3474.13	7	*Mn* II 4.06, *Mn* II 4.15	3835.52	10nn	*H* 9 5.39
3475.55	0	*Cr* II 5.13, *Fe* II 5.25, *Fe* II 5.74	3844.35	4	*Mn* II 3.98
			3847.30	0	*V* II 7.32, *Mg* II 8.24
3482.03	1	.....	3854.00	4	*Si* II 3.67
3483.11	3	*Mn* II 2.91	3856.27	5	*Si* II 6.03, *Mn* 6.53
3488.79	4	*Mn* II 8.68	3862.84	5	*Si* II 2.60
3490.42	0	*Fe* I 0.60, *Ti* II 1.06	3878.08	1	*Fe* I 8.02
3492.48	1	.....	3879.25	3	(*Fe* I 8.58)
3494.41	0	*Fe* II 4.67	3889.34	10nn	*H* 8 9.05
3495.80	3	*Mn* II 5.84	3896.00	0nn	*V* II 6.16

TABLE 8—*Continued*

Wave Length	Int.	Identification	Wave Length	Int.	Identification
3898.06	2n	*Fe* I 7.89, *Fe* I 8.01	4192.51	0	*Ni* II 2.02
3900.68	2n	*Ti* II 0.54, *Al* II 0.68	4198.12	0	*Si* II 8.25, *Fe* I 8.31
3902.56	1n	*Fe* I 2.95	4200.40	1n	*Ti* II 0.40, *Mn* II 0.25
3905.56	1n	*Cr* II 5.64, *Si* I 5.53	4202.65	1n	*Fe* I 2.03, *V* II 2.34
3906.27	0	*Fe* II 6.04	4205.49	2	*V* II 5.09, *Fe* II 5.48
3913.63	0	*Ti* II 3.46	4206.63	3	*Mn* II 6.43
3918.99	0	*Fe* II 8.51	4215.53	1n	*Sr* II 5.52
3920.85	2	*Fe* I 0.26	4219.93	0	*Fe* I 9.36
3926.33	1	*Mn* II 6.47	4222.59	1	*Fe* I 2.22
3930.99	1	*Fe* I 0.31	4229.62	1n	.....
3933.72	7	*Ca* II 3.67	4233.29	3	*Fe* II 3.17
3935.96	1	*Fe* II 5.94	4235.22	0	*Fe* I 5.94
3939.04	0	*Fe* II 8.97	4237.72	1	.....
3941.25	1	*Fe* I 0.82	4239.33	2	*Mn* 9.72
3942.52	0	*Fe* I 2.44	4240.53	1	*Al* II 0.75
3943.84	3	*Mn* II 3.82	4242.48	3	*Cr* II 2.38, *Mn* II 2.38
3958.58	0	*Cr* II 8.07	4244.36	1	*Mn* II 4.25
3968.38	3	*Ca* II 8.47	4246.91	1	*Sc* II 6.83
3969.98	10nn	*H* ϵ 0.08	4248.17	1	*Mn* II 7.95, *Fe* I 8.23
3981.35	0	*Fe* I 1.77, *Fe* II 1.61	4251.65	2n	*Mn* II 1.77
3983.86	5	*Fe* I 3.96, *Cr* I 3.91	4253.18	3	*Cr* II 2.62, *Mn* II 3.02
3999.79	1	*Mn* II 00.06	4256.02	3	.....
4002.30	0	*Fe* II 2.55	4259.38	3	*Mn* II 9.26
4006.48	1	.....	4262.11	2	*Cr* II 1.92
4013.82	0	*Fe* I 3.82, *Fe* I 3.79	4264.07	0	*Fe* II 3.89
4024.26	2n	*Fe* II 4.55	4267.26	3n	*C* II 7.02, *C* II 7.27, *Fe* I 6.97
4026.11	3nn	*He* I 6.19			
4028.15	0	*Ti* II 8.34	4269.26	0	*Cr* II 9.28
4030.27	1	*Fe* I 0.49, *Mn* I 0.75, *Cr* II 0.28	4273.39	1	*Fe* II 3.32
			4275.75	0	*Cr* II 5.57
4032.59	2	*Fe* II 2.95	4278.55	1	*Fe* II 8.13, *Cr* II 8.10
4034.38	0	(*Mn* I 4.49)	4282.45	3	*Mn* II 2.50, *Fe* I 2.41
4038.98	1	*Mn* II 8.73	4284.26	1	*Cr* II 4.21
4044.32	1	*Fe* II 4.01	4288.07	0	*Ti* II 7.88
4045.80	0	*Fe* I 5.81	4292.25	3	*Mn* II 2.25
4050.29	1	.....	4296.43	1n	*Fe* II 6.58
4063.51	0	*Fe* I 3.60	4300.23	3	*Ti* II 0.05, *Mn* II 0.22
4066.93	0	*Ni* II 7.05	4303.43	2	*Fe* II 3.17
4070.82	0	*Cr* II 0.90	4305.89	0	*Fe* I 5.45, *Sc* II 5.71
4075.17	0	*Si* II 5.45, *Cr* II 5.63	4308.27	2n	*Ti* II 7.90, *Fe* I 7.91
4076.47	1	.....	4314.61	1	*Fe* II 4.29
4081.13	1	.....	4318.47	0	*Fe* II 8.22
4085.10	1	(*Fe* I 5.32)	4322.73	1	.....
4101.51	10nn	*H* δ 1.74	4325.49	2	*Fe* I 5.76
4104.75	0	*Mn* II 5.01	4326.78	3	*Mn* II 6.76
4110.50	2	*Cr* II 1.01	4340.58	10nn	*H* γ 0.46
4120.74	1n	*He* I 0.81	4344.17	4	*Ti* II 4.29, *Mn* II 4.03
4122.78	0n	*Fe* II 2.64	4345.80	1	.....
4127.97	6	*Si* II 8.05	4348.35	1	*Mn* II 8.49
4130.89	6	*Si* II 0.88	4350.62	0	*Ti* II 0.83
4136.94	4	*Mn* II 6.91	4351.94	1	*Fe* II 1.76
4140.29	0	*Mn* II 0.19	4357.32	1n	*Fe* II 7.57
4144.05	0	*He* I 3.76, *Fe* I 3.87	4363.39	0	*Cr* II 2.93
4163.89	0n	*Ti* II 3.65	4377.42	1n	(*Mo* II 7.76)
4171.82	1n	*Ti* II 1.90	4379.85	1	*Mn* II 9.74
4173.79	2n	*Fe* II 3.45	4385.30	1	*Fe* II 5.38
4177.69	1	*Fe* I 7.60, *Y* II 7.55, *Fe* II 7.70	4388.11	0	*He* I 7.93, *Fe* I 7.90
			4409.46	1	*Ti* II 9.22, *Ti* II 9.52
4178.78	3	*Fe* II 8.85	4414.66	0	*Fe* I 5.12
4183.85	0n	*V* II 3.43	4416.94	1	*Fe* II 6.82

TABLE 8—*Continued*

Wave Length	Int.	Identification	Wave Length	Int.	Identification
4420.89	1	.....	4508.32	1	*Fe* II 8.28
4431.22	0	*Fe* II 1.63	4511.81	0	(*Cr* II 1.82)
4434.10	0	*Mg* II 3.99	4515.59	1	*Fe* II 5.34
4451.66	0	*Fe* II 1.54	4519.28	1	(*Fe* II 0.22)
4462.88	1n	.....	4522.93	1	*Fe* II 2.63
4466.11	0n	*Fe* I 6.55	4525.76	1	.....
4468.20	1n	*Ti* II 8.50	4528.33	0	*Fe* I 8.62, *V* II 8.51
4471.68	3n	*He* I 1.48, *He* I 1.68	4549.45	3	*Fe* II 9.47, *Ti* II 9.63, *Fe* II 9.21
4475.41	1	.....			
4478.65	2	*Mn* II 8.74	4555.68	1	*Fe* II 5.89
4481.48	6	*Mg* II 1.33	4558.32	1	*Cr* II 8.66
4483.78	1	.....	4583.50	0	*Fe* II 3.83
4491.47	1	*Fe* II 1.40	4588.41	1	*Cr* II 8.22
4499.32	0	*Fe* II 9.71	4590.24	1	*Ti* II 9.95, *Cr* II 9.89

thought was the spectrum of the secondary was really due to faint lines of *Mn* II, belonging to the primary, which were not identified in 1907. There is, in particular, a line of *Mn* II at λ 4478.74, which looks deceptively like a component of *Mg* II 4481.33. I have measured a considerable number of lines on two McDonald Observatory spectrograms on Eastman Process emulsion. The list of these lines is given in Table 8. The appearance of the spectrum is that of a typical *Mn* II star with sharp lines.

THE SPECTROGRAPHIC PROBLEM OF U CEPHEI*

OTTO STRUVE
McDonald and Yerkes Observatories
Received December 31, 1943

ABSTRACT

The velocity-curve of this eclipsing binary was redetermined from measures of 115 McDonald Observatory spectrograms. If this curve is interpreted in the usual way, the elements are: $P = 2.493$ days, $\gamma = -5$ km/sec, $K = 120$ km/sec, $e = 0.20$, $\omega = 40°$, and $T =$ phase 2.16 days after minimum light. Although the eccentricity is much smaller than that obtained by Carpenter from plates taken nearly 20 years ago, the asymmetry of my velocity-curve does resemble his and confirms the discrepancy between spectrographic and photometric observations. In the partial phases of the eclipse the lines of the B8 star show a large rotation effect which suggests that the equatorial velocity of rotation of the brighter B8 star is 200 km/sec. That of the fainter, G2, star is less than 50 km/sec, in spite of the greater size of this star. The rapid angular velocity of the B8 star, which is far in excess of the angular velocity in the orbit, constitutes a particularly interesting cosmogonical problem. During the partial phases there appear sharp lines of *H* and *Ca* II which are displaced from those of the limbs of the B8 star and which give velocities of about +100 km/sec before totality and −150 km/sec after totality. These lines are not produced by the G2 star but must originate in a tenuous stream of gas which may circle around the G2 star in a manner similar to that of the streams in β Lyrae and SX Cassiopeiae. The spectrum of the B8 star shows systematically weaker lines in the first partial phase than in the second. Similarly, the lines of the receding stream (before totality) are weaker than the lines of the approaching stream (after totality). The lines of *He* I confirm Redman's conclusion that lines broadened by Stark effect must be weaker at the limb of the B8 star than in the center. On the other hand, *Ca* II does not appreciably change in equivalent width and therefore becomes more conspicuous (narrower and deeper) as totality is approached. This constitutes an argument against the hypothesis that "pure absorption" is predominantly responsible for the formation of lines in the B8 star. It is suggested that the asymmetry of the velocity-curve may be caused by the same stream which gives rise to sharp *H* lines in the partial phases.

1. *The problem.*—The eclipsing binary U Cephei[1] presents one of the most intriguing puzzles in stellar spectroscopy. Its light-curve unmistakably points toward an orbit in which the value of $e \cos \omega$ is close to zero, because its shallow secondary minimum is almost exactly halfway between its deep primary minima. On the other hand, Carpenter[2] found from 34 Lick Observatory spectrograms that the velocity curve is very unsymmetrical, giving $e = 0.474$ and $\omega = 25.0°$, so that

$$e \cos \omega = 0.43 .$$

If this conclusion from the spectrographic results were correct, the secondary eclipse would occur 0.51 day or 12.2 hours later than has actually been observed with the photometer. The uncertainty with which the secondary eclipse has been placed at phase $0.5P$ probably does not greatly exceed 0.1 day. We are, therefore, confronted with a serious contradiction between the photometric and the spectrographic results. Most photometric observers have, perhaps somewhat arbitrarily, assumed that $e = 0$. The depth of the secondary eclipse in visual light is only of the order of 0.1 mag., and in violet light it is even less. Hence, the shape of this shallow minimum cannot be accurately determined; and there is, at present, no reliable photometric method to determine for this star $e \sin \omega$, from which e and ω could be separately obtained. Nevertheless, the period is so short (2.493 days) that the assumption $e = 0$ must certainly be regarded as a close approximation to the truth. Among the photometric investigators, only two have at-

* *Contributions from the McDonald Observatory, University of Texas*, No. 87.

[1] HD 5679; $\alpha - 0^h53^m4$, $\delta = +81°20'$ (1900), mag. 6.85–9.19, Sp. HD A0.

[2] *Ap. J.*, **72**, 205, 1930.

tempted to determine e and ω, although others[3] had recognized a displacement of the secondary minimum by about 0.1 day. Completely at variance from all other light-curves is the result of J. Ellsworth,[4] who obtained a displacement of secondary minimum by $+0.3$ day from phase $0.5P$ and, with the help of Carpenter's radial velocities, computed $e = 0.221$, $\omega = 15°$. It is doubtful whether this result is correct, because Walter[5] and Carrasco,[6] who observed U Cephei at nearly the same time as Ellsworth, failed to get any noticeable displacement of secondary minimum. More recently the entire problem has been rediscussed by N. Tchudowitchev.[7] Using his own photographic observations and those of all preceding workers, he represented the observed epochs of primary minimum by means of an expression of the form

$$O-C=\Delta T_0+\Delta P\cdot E-\frac{P\cdot e}{\pi}\cos(\Delta\omega\cdot E+\omega)\,, \qquad (1)$$

where ΔT_0 is the error of the initial epoch (determined by Wendell), ΔP is the error of the period (also determined by Wendell), e is the eccentricity of the orbit, ω is the longitude of the periastron, and $\Delta\omega$ is the change in ω during one revolution. The last, periodic, term results from an assumed slow rotation of the line of apsides in a slightly eccentric orbit.[8] The observations gave

$$O-C=-0.0050+0.0000165E-0.063\cos(0.028°E+235°)\,. \qquad (2)$$

This led to the following values:

$$e=0.080\,; \qquad \omega=99°\ (\text{for } E=8000)\,; \qquad \Delta\omega=0.028°\,.$$

The determination rests upon several unreliable old observations and may be seriously in error. The most recent observations, upon which the present investigation is based, give an appreciable departure in O − C from formula (2). Nevertheless, the general idea is probably correct. Tchudowitchev shows that qualitatively, at least, the advance of the line of apsides by $0.028°E$ per revolution, or by 2π in 99 years, is consistent with the fact that the earlier light-curves by Wendell (1895–1912), Dugan[9] (1914–1917), and Baker (1914–1916) show a positive shift of secondary minimum of the order of $+0.1$ day, while the most recent curves by Walter (1931–1933) and Tchudowitchev (1934–1935) show a small negative shift of the order of -0.03 day. This could be interpreted as an advance in ω from about 0° to 90° in an interval of a quarter of a century. The photometric data require an eccentricity of $e < 0.1$, which is entirely inconsistent with Carpenter's velocity-curve.

The question arises whether Carpenter's velocity-curve is in error or whether it is distorted by other effects. My discussion of the radial velocities of SX Cassiopeiae[10] has shown that such distortion can result from currents in the outer atmosphere of a binary system which resemble the currents first found in the system of β Lyrae. The only other investigation of the radial velocity of U Cephei known to me is a study by Z. Kopal[11] of a series of 34 slit spectrograms obtained at Victoria by R. O. Redman for an investiga-

[3] R. H. Baker, *Bull. Laws Obs.*, **2**, 257, 1921.

[4] *Pub. Lyon*, **2**, fasc. 1, 82, 1936.

[5] *A.N.*, **250**, 333, 1933.

[6] *Boll. Obs. Madrid*, **1**, Nos. 12–13, 1933.

[7] *Bull. Engelhardt Obs., Kasan U.*, No. 17, 1939.

[8] This term was first used by Tisserand to explain a periodic term in the distribution of minima of Algol, *C.R.*, **120**, 125, 1895.

[9] *Contr. Princeton U. Obs.*, No. 5, 1920.

[10] *Ap. J.*, **99**, 89, 1944.

[11] *Harvard Bull.*, No. 914, 1940.

tion of the center-to-limb variation of the absorption lines during the partial eclipse. Kopal measured 5 spectrograms taken in full light between phases 0.921 and 1.057 days (counted from minimum light), 15 spectrograms taken during the partial phases, −0.234 to +0.137 day, and 10 spectrograms taken during the time of totality when the spectrum was that of the faint secondary. From these latter 10 observations, with the help of an additional velocity obtained by Joy, Kopal derived the values

$$\gamma = +7.3 \pm 1.0 \text{ km/sec} \quad \text{and} \quad K_2 = 200 \pm 11 \text{ km/sec},$$

under the assumption that $e = 0$. Using the value of γ thus obtained, and again taking $e = 0$, he next derived from the 5 plates taken at almost the same phase

$$K_1 = 62 \pm 6 \text{ km/sec}.$$

This value is completely different from Carpenter's result,

$$K_1 = 109.9 \pm 3.1 \text{ km/sec}.$$

Kopal's value was determined by means of the formula

$$V_1 = K_1 \sin (M + \pi) + \gamma,$$

where γ is taken from the observations of the secondary and where M (the mean anomaly) has practically the same value for all 5 observations. The mean phase of these observations was 1.0 day, which is only 0.225 day removed from inferior conjunction. Hence, a small systematic error in the mean velocity measured on the 5 plates will be magnified by a factor of 2 in the determination of K_1. Similarly, an error in γ, which incidentally is very sensitive to the precision with which the phases are known in Kopal's work, will have a large effect upon K_1. Carpenter found $\gamma = -6.0 \pm 3.7$ km/sec. The difference of 13 km/sec between the two results is somewhat too large to be ignored. The probable error found by Kopal for γ is probably too small—perhaps partly because of an uncertainty in establishing the exact time of central primary eclipse. This latter epoch was computed by Kopal with an average period of 2.492934 days, which he had found to represent satisfactorily 48 observations of minimum light covering an interval of 20 years. The period of U Cephei is believed to show appreciable fluctuations in a rather complicated manner, so that, according to Carrasco,[12] two sine terms are needed, in addition to a term containing E and another containing E^2. Experience has shown that errors amounting to 1 hour, or 0.042 day, may occur when a constant period is used over an interval of 20 years. A shift in the epoch of minimum by 0.04 day would change γ by almost 20 km/sec. However, Dr. Kopal has advised me that for the Victoria observations there could have been no appreciable error in the time of minimum light. Hence, it would seem that the discrepancy between his and Carpenter's results cannot be explained in this manner. Whatever the cause may be, it would seem advisable, in view of the unfavorable distribution of Kopal's observations in full light, not to make use of his determination of K_1. His actual measurements, however, are in very good accord with my new velocity-curve. His mean velocity of −31 km/sec at phase 1.004 days falls well within the permissible range of my observations, even if allowance is made for the uncertainty of his and my phases.

The problem of this investigation is to derive a new velocity-curve in order to ascertain whether Carpenter's results were correct or whether Kopal's procedure has given a more reliable value of K_1, and consequently of the absolute dimensions of the system.

2. *The observations.*—During the long nights of November it is possible to observe U Cephei, with its high northern declination, for 12½ hours each night. Since the period is almost exactly 2.5 days, it is possible to cover the entire cycle in five consecutive nights.

[12] *Bol. Obs. Madrid*, 1, No. 16, 1933.

Whenever it is desired to make certain that secular effects do not influence the results, such a quick coverage is especially desirable. The observations described in this paper were made at the McDonald Observatory, using the quartz Cassegrain spectrograph attached to the 82-inch reflector. The linear dispersion of all plates was 40 A/mm at λ 3933. The observations were made on nine consecutive nights—November 5–13—and cover parts of four consecutive cycles. The best exposure time outside of eclipse was found to be 10 minutes, for fair seeing. In poor seeing the exposure times were increased to 15 minutes or even longer. During the principal eclipse the star becomes so faint and so red that exposures of 1 hour are required to obtain satisfactory densities. The total number of spectrograms measured is 115. Table 1 gives a list of the stellar wave lengths used for the determination of the radial velocities.

TABLE 1

LIST OF STAR LINES USED FOR RADIAL-VELOCITY DETERMINATION

B8 STAR					
H 10	3797.90	*Ca* II	3933.68	*Hγ*	4340.46
H 9	3835.39	*Hε*	3970.08	*He* I	4387.93
He I	3862.59	*He* I	4026.19	*He* I	4471.48
H 8	3889.05	*Hδ*	4101.74	*Mg* II	4481.26
G2 STAR					
Fe I	3952.73	*Fe* I	4143.87	*Sc* II	4374.51
Fe I	4005.25	*Sr* II	4215.54	*Fe* I	4383.55
Mn I	4033.00	*Ca* I	4226.73	*Fe* I	4404.77
Fe I	4045.82	*Fe* I	4260.48	*Fe* I	4415.16
Fe I	4063.29	*Ti* II	4290.22	*Fe* I	4422.60
Fe I	4066.98	*Fe* I	4325.77	*Fe* I	4435.01
Fe I	4070.78	*Hγ*	4340.46	*Ti* II	4443.80
Fe I	4071.75	*Fe* I	4346.56	*Mg* II	4481.26
Hδ	4101.74	*Fe* I	4352.74		

The phases of all exposures were computed by means of the formula given in the 1940 edition of Schneller's catalogue of variable stars:[13]

$$\text{Principal minimum} = 2424253.660 + 2.492934E\,. \qquad (3)$$

The value of the period is identical with the one used by Kopal. The epoch is almost exactly 1049 cycles earlier than the value adopted by Kopal. Hence, the phases computed by me are on precisely the same system as those used by him.

Because of the great uncertainty that is attached to extrapolations of linear formulae for the epoch of central primary eclipse, I have determined, as accurately as possible, the time of mid-eclipse, using the finder of the 82-inch telescope for making visual comparisons of U Cephei with two neighboring stars. The mean result from estimates on November 8 and 13 gives

$$\text{Mid-eclipse} = 1943,\ \text{Nov. } 8,\ 9^h20^m\ \text{U.T.} = \text{JD } 2431036.889\,.$$

This value may be in error by ±10 minutes or ±0.007 day. I have neglected the small correction from the earth to the sun. The observed minimum occurs too early, if compared to formula (3), by

$$(O-C) = -0.044\ \text{day}\,,$$

so that on the system of phases here used mid-eclipse actually took place between phases 2.442 and 2.456 days. This departure of a little more than 1 hour is unquestionably real.

[13] *Kl. Veröff. Berlin-Babelsberg*, No. 21, p. 195, 1939.

The same departure is found when we use Kopal's formula. It is customary to determine the departure (O − C) from Wendell's elements:

$$\text{Mid-eclipse} = 2407890.301 + 2.4928840E\,. \qquad (4)$$

The result is

$$(\text{O} - \text{C})_{\text{Wendell}} = +0.160 \qquad (E = 9285)\,.$$

Miss Edith Jones[14] found in 1937: O − C (Wendell) = +0.1515 for $E = 8262$, and Tecza[15] obtained almost the same result.[16] My determination of (O − C) suggests that after a prolonged interval, during which the period of U Cephei increased, it has now started to decrease very slightly. If the observations by Miss Jones, Tecza, and myself are plotted on Tchudowitchev's curve relating $(\text{O} - \text{C})_{\text{Wendell}}$ and E, we find that the last observation falls considerably below the extrapolated curve and suggests a bending which may be due either to an error in Tchudowitchev's period for the apsidal motion or to the remaining inequalities which were considered by Carrasco but which have not, as yet, been accounted for physically.

Table 2 contains the radial velocities as measured on my plates. The lines are exceptionally poor, except during totality; and the settings are very uncertain. Hence, a large amount of scatter is to be expected.

3. *Description of the system of U Cephei.*—The photometric and spectrographic investigations are in full accord regarding the general characteristics of the system. The brighter star is of type B8 or B9 (not A0, as was heretofore believed, because the *He* I lines are visible and *He* I 4472 = *Mg* II 4481) and has a slightly elliptical shape, with $r_{\max} = 0.18a$ and $r_{\min} = 0.17a$. The light of this star is 0.84 of the total luminosity. The larger star is of type gG2 (not G8 or K0, as was heretofore believed).[17] Its larger semiaxis is $r_{\max} = 0.42a$, and its smaller semiaxis is $r_{\min} = 0.32a$. According to Tchudowitchev, this star is much more elliptical than the B8 star. It contributes only 0.16 to the luminosity of the system (in visual light) and can be observed only during the principal eclipse. This eclipse is total, and the lines of the B8 star disappear completely during the total phase. The system has an appreciable amount of darkening at the limb (the coefficient of darkening $u = \frac{2}{3}$ for visual light, according to Dugan) and varies with the wave length, according to Rosenberg.[18] It has, however, been shown by Krat[19] that, although Rosenberg's discussion furnishes a qualitative indication of the change of darkening with λ, his numerical values are dependent upon the elements of the light-curve which he used. Dugan found an asymmetry in the light-curve, in the sense that the total light prior to eclipse is smaller than after eclipse and that the descent toward total phase is less steep than the ascent after totality. This asymmetry has been confirmed by most other observers, except by Rosenberg, who, instead, found a considerable decline in brightness during totality. Dugan suggested that the asymmetry of the light-curve can be explained by assuming that the B8 star rotates in a period shorter than 2.5 days and that this rapid rotation carries the tidal bulge forward by 24°. Tchudowitchev finds a tidal lag of 26° and a libration at principal minimum of 8°. He attributes this libration to the G2 component, which presumably rotates with a period of 2.5 days—equal to that of orbital revolution.

[14] *Bull. Harvard*, No. 905, 1937. [15] *Acta Astr.*, C, **3**, 131, 1937.

[16] I am indebted to Professor R. Prager, of the Harvard Observatory, for a list of recent references of photometric observations of U Cephei.

[17] I am indebted to Professor W. W. Morgan for helping me with the classification of this spectrum and for furnishing a series of standard spectra having approximately the same dispersion as my spectrograms of U Cephei.

[18] *Ap. J.*, **83**, 67, 1936.

[19] *Veränder. Sterne, Nishni Novgorod-Gorki, U.S.S.R.*, **5**, No. 7, 214, 1938.

PLATE X

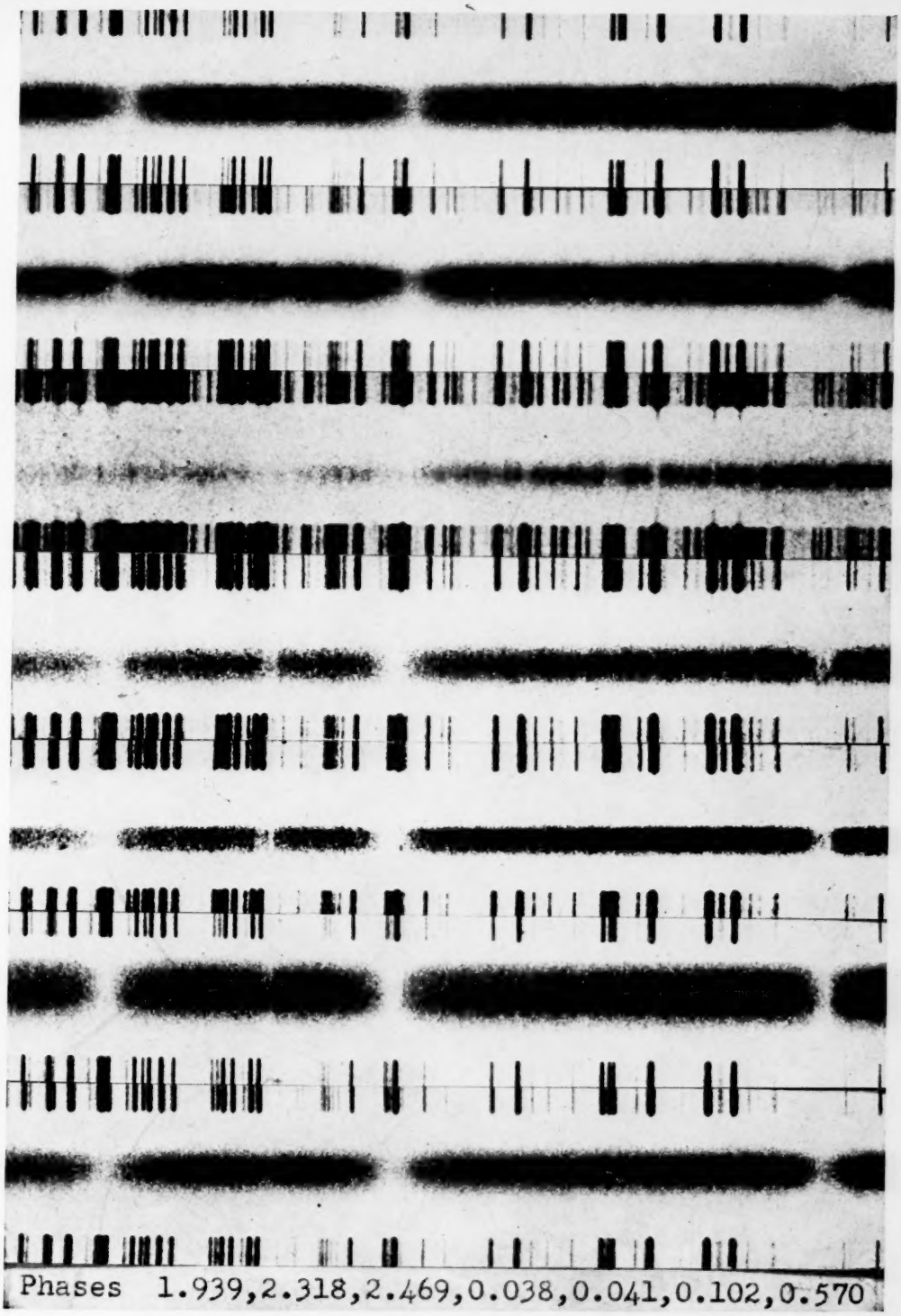

SPECTRA OF U CEPHEI BETWEEN $H\zeta$ AND $H\delta$

The first spectrogram was taken near maximum radial velocity; the last, near minimum radial velocity. The second plate, phase 2.378 days, shows narrow lines of $H\zeta$ and $H\delta$ unsymmetrically superposed over the broad lines from the limb of the B8 star. The third plate shows the spectrum of the G2 star during totality. The plates at phases 0.038 and 0.041 show the doubling of *Ca* II and *H* after totality. The plate at phase 0.102 shows unsymmetrical lines of *H* and *Ca* II after totality.

UNIV. OF MICH.

TABLE 2

RADIAL VELOCITIES OF U CEPHEI

No.	Date 1943	U.T.	Phase	Velocity (Km/Sec)	Remarks*	No.	Date 1943	U.T.	Phase	Velocity (Km/Sec)	Remarks*
	Nov.						Nov.				
2525	5	4h48m	1.752	+ 80.2		2595	9	8h48m	0.934	− 62.1	
2526		5 18	1.773	+ 81.6		2596		9 00	0.942	− 43.6	
2528		7 11	1.851	+ 93.3		2597		9 12	0.950	− 68.7	
2529		7 23	1.860	+107.8		2599		10 45	1.015	− 57.6	
2530		10 48	2.002	+148.0		2600		10 59	1.025	− 63.2	
2531		11 01	2.011	+154.3		2602		12 27	1.086	− 45.2	
2535	6	8 02	0.395	− 92.8		2603		12 43	1.097	− 53.2	
2536		8 15	0.404	− 85.5		2604	10	0 42	1.596	+ 71.0	
2538		9 52	0.471	−115.0		2605		0 55	1.605	+ 69.3	
2539		10 07	0.482	− 97.7		2606		1 09	1.615	+ 68.9	
2540		10 26	0.495	−106.2		2607		1 22	1.624	+ 49.3	
2541		10 47	0.509	−104.9		2609		3 25	1.709	+ 79.8	
2542		11 08	0.524	−104.0		2610		3 38	1.718	+ 59.4	
2543		11 33	0.541	−116.3		2612		5 03	1.777	+ 58.8	
2544		11 56	0.557	− 98.0		2613		5 16	1.786	+ 67.5	
2545		12 15	0.570	−105.8		2615		6 57	1.857	+108.4	
2546		12 33	0.583	−111.8		2616		7 08	1.864	+ 90.2	
2547		12 46	0.592	− 95.0		2618		8 44	1.931	+117.5	
2548	7	0 40	1.088	− 77.3		2619		8 55	1.939	+140.2	
2549		0 52	1.096	− 53.8		2620		10 45	2.015	+151.4	
2550		1 04	1.104	− 51.1		2621		11 18	2.038	+136.7	
2551		1 18	1.114	− 43.6		2622		11 59	2.067	+127.8	
2553		3 14	1.195	− 53.6		2623	11	0 40	0.102	− 63.8	(1)
2554		3 32	1.207	+ 2.4		2624		1 01	0.116	− 69.2	(1)
2555		3 58	1.225	− 37.8		2625		1 20	0 130	− 49.0	(1)
2557	8	0 40	2.088	+130.9		2626		1 36	0.141	− 31.8	(1)
2558		0 53	2.097	+135.0		2627		2 01	0.158	− 56.3	(1)
2559		1 22	2.117	+117.0		2628		2 17	0.169	− 55.1	(1)
2560		1 42	2.131	+113.4		2630		4 18	0.253	− 81.5	
2561		2 09	2.150	+127.6		2631		4 32	0.263	− 80.7	
2563		3 44	2.216	+ 86.1		2632		4 47	0.273	− 83.1	
2564		3 59	2.226	+ 69.9		2634		6 26	0.342	− 84.6	
2565		4 13	2.236	+ 82.0		2635		6 42	0.353	− 86.2	
2566		4 30	2.248	+ 54.6		2636		7 00	0.366	− 95.2	
2567		4 51	2.262	+ 50.8		2649	12	5 02	1.284	+ 28.0	
2568		5 14	2.278	+ 33.6		2650		5 14	1.292	+ 40.8	
2569		5 41	2.297	+ 26.3		2651		5 24	1.299	+ 9.6	
2570		6 12	2.318	+117.4		2654		6 47	1.357	+ 21.9	
2571		6 49	2.344	+150.6		2655		6 58	1.364	+ 30.4	
2572		7 32	2.374	+192.6	(1)	2656		7 09	1.372	+ 22.7	
2573		8 15	2.404	− 39.0	(2)	2660		9 22	1.464	+ 38.2	
2574		9 18	2.448	− 26.0	(2)	2661		9 33	1.472	+ 36.4	
2575		10 22	2.492	+ 5.8	(2)	2662		10 02	1.492	+ 46.5	
2576		11 18	0.038	+ 21.6	(2)	2663		10 13	1.500	+ 27.9	
2577		12 04	0.070	−159.2	(1)	2664		10 25	1.508	+ 32.2	
2578		12 34	0.091	−101.5	(1)	2665		10 36	1.516	+ 61.9	
2579	9	0 54	0.605	−114.3		2672	13	3 43	2.229	+ 71.6	
2580		1 06	0.613	−104.3		2673		3 54	2.236	+ 66.2	(1)
2581		1 18	0.621	−111.4		2677		6 57	2.364	+163.6	(1)
2582		1 32	0.631	−107.9		2678		7 18	2.378	+195.2	(1)
2585		4 03	0.736	− 95.1		2679		7 45	2.397	− 18.1	(2)
2586		4 31	0.755	− 83.5		2680		8 19	2.421	− 21.2	(2)
2587		4 43	0.764	− 94.1		2681		9 29	2.469	− 2.4	(2)
2588		4 54	0.771	− 59.1		2682		10 29	0.018	+ 8.0	(2)
2590		6 21	0.832	− 47.2		2683		11 02	0.041	−244.4	(1)
2591		6 38	0.843	− 70.2		2684		11 35	0.064	−156.9	(1)
2592		6 56	0.856	− 78.5		2685		12 00	0.081	−135.2	(1)
2594		8 33	0.923	− 57.1							

* (1) Velocity of B8 star from *Ca* II, *He* I, *Mg* II, and *Si* II lines; (2) velocity of G2 star.

The spectrum outside of total eclipse consists of a strong, normal set of *H* lines and of very weak and shallow lines of *Ca* II 3933, *He* I, *Mg* II 4481, and *Si* II. These lines are all exceedingly broad; and even the *H* lines have broad centers, suggestive of rapid axial rotation. The lines other than those of *H* are exceedingly weak and are difficult to measure.[20] Carpenter did not mention them at all; and Kopal did not measure them, although Redman had mentioned them in his paper.[21] The lines are very weak on my plates, but I have found them very useful for radial-velocity measurements. An estimate from the width of *Ca* II 3933 gives for the equatorial velocity of rotation

$$V\ (\text{rot}\ B) = 180\ \text{km/sec}\ .$$

This may be in error by as much as ± 50 km/sec. It is not possible to improve the determination appreciably by measuring actual contours, because the total intensities of these lines are very low. The strong *H* lines are, of course, not suitable, because they are influenced by Stark effect. It is, however, certain that the rotational velocity is very much larger than the value of 50 km/sec obtained by Kopal from his measurements of the Victoria plates. He had used this value in support of the hypothesis that there exists synchronism of rotation and revolution in the early-type star, whose radius he had found to be 1,800,000 km. A rotational velocity of 50 km/sec is ruled out by two additional considerations: (1) so small a velocity produces a hardly noticeable broadening of the lines in full light, with a dispersion of 40 A/mm (as used in my observations, at λ 3933); and (2) the lines of the secondary are actually sharp on my plates, yet, if synchronism existed for both stars, they should be at least 50 per cent broader than the lines of the B8 star. I estimate from my plates that the rotational velocity of the G2 star is

$$V\ (\text{rot}\ G) < 50\ \text{km/sec}\ .$$

We have here a result of exceptional interest, which in a most unexpected manner confirms Dugan's hypothesis for the explanation of the tidal lag of the early-type component. The B8 star rotates three or four times faster than the G2 star, despite the fact that its radius is 50 per cent smaller.

4. *The velocity-curve.*—The results of my measures are plotted in Figure 1. The minimum is at phase 0.56 day and gives $V = -105$ km/sec. The maximum is at phase 2.00 days and gives $V = +135$ km/sec. The range in velocity is therefore 240 km/sec and

$$K_1 = 120\ \text{km/sec}\ .$$

This is close to the value obtained by Carpenter ($K_1 = 110$ km/sec) and is almost twice the value derived by Kopal. Although the scatter is quite large, K_1 cannot be greatly in error. The curve is unsymmetrical, the interval from minimum velocity to maximum being 1.44 days and the interval from maximum to minimum being 1.05 days. This asymmetry is very pronounced and is, without question, real. The maximum is narrow, while the minimum is fairly broad. If we wish to interpret these results in terms of orbital elements, we should find

$$e = 0.20\ , \qquad \omega = +40^\circ\ .$$

Unfortunately, it is futile to try to improve these elements. The velocity-curve is so seriously distorted on its important descending branch by the rotation effect, and it also shows such a peculiar deformation at maximum, that no amount of refinement can give

[20] On many plates outside of eclipse the lines of *Ca* II *K* and *He* I look double or unsymmetrical. Sometimes they are single but fairly narrow, while at other times they are very broad and diffuse. There appears to be no regularity in these observations, and I believe they are not physically real. Spectral lines which are always near the limit of visibility are greatly influenced by accidental grain patterns in the emulsion. A somewhat similar conclusion has been reached by Redman.

[21] *M.N.*, **96**, 488, 1936.

elements of greater precision. The curve departs very markedly from Carpenter's velocity-curve. In terms of orbital elements this difference is principally illustrated by the two sets of values for ω and e:

$$\text{Carpenter: } \omega = +25^\circ ; \quad e = 0.47 ,$$

$$\text{Struve: } \omega = +40^\circ ; \quad e = 0.20 .$$

Carpenter's curve shows a much broader minimum than my curve, and I am unable to account for this difference. Moreover, my curve descends to $V = -105$ km/sec, while Carpenter's minimum falls near $V = -80$ km/sec. The two maxima are also somewhat different. It is impossible to say whether there has been a real change in the velocity-

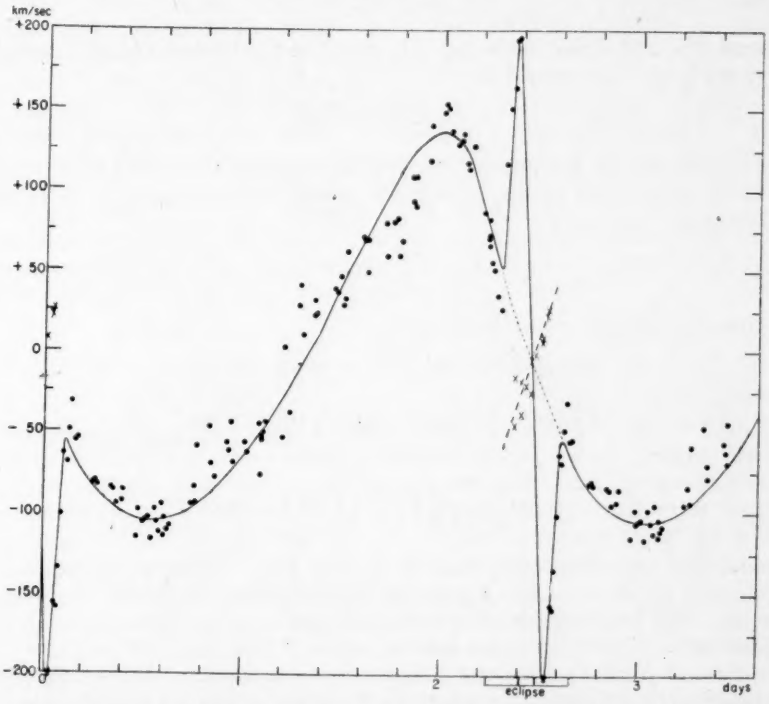

FIG. 1.—Velocity-curve of U Cephei. Solid circles represent the velocities of the B8 star. Crosses designate the velocities of the G2 star. The rotational disturbance during the partial phases of the eclipse is particularly striking. The rest of the curve is noticeably unsymmetrical, suggesting an eccentricity which is incompatible with the photometric investigations.

curve since Carpenter's observations were made, in 1923–1925. It is entirely possible that the great uncertainty of his and of my measures may account for the difference. Although the difference in e is large, it is significant that the asymmetry of my velocity-curve does resemble that found by Carpenter; it should be noted that the inequality of the "crest-intervals,"[22] which is the most conspicuous feature of my curve, depends upon ω as well as upon e. The same inequality could be obtained with $e = 0.3$, $\omega = 60^\circ$ and with $e = 0.40$, $\omega = 70^\circ$. The reason for preferring $e = 0.20$, $\omega = 40^\circ$ is the almost straight ascending branch of my velocity-curve. I believe we can be certain that the shape of the

[22] See E. S. King, *Harvard Ann.*, **81**, 231, 1920.

velocity-curve is not in harmony with the photometric results. The value of γ which best fits my observations is

$$\gamma = -5 \text{ km/sec},$$

in excellent agreement with Carpenter. The measures of the G2 star at totality give the slope of the secondary's velocity-curve between phases 2.37 and 0.05 days. Although the scatter of my points is quite large—partly because of underexposure of several plates and partly because of the greater slit width used for these exposures—the slope is determined with a fair degree of precision and is almost identical with the slope of the primary curve undisturbed by rotation. The mass ratio is thus close to

$$\frac{m_G}{m_B} = 1.0.$$

If we assume that the shape of the velocity-curve of the G star is similar to that of the B star, its semiamplitude would be

$$K_2 = 120 \text{ km/sec}.$$

If, on the other hand, we assume that the velocity-curve of the B star is distorted by unknown causes, while that of the G star is genuine, we can compute K_2 by means of Kopal's formula:

$$V_2 = \frac{2\pi}{P} K_2 t + \gamma.$$

We find from my velocity-curve that for

$$\text{Phase 2.60 days: } V_2 = +50 \text{ km/sec},$$

$$\text{Phase 2.30 days: } V_2 = -60 \text{ km/sec}.$$

Hence,

$$K_2 = \frac{P}{\Delta t \cdot 2\pi} \Delta V_2 = 146 \text{ km/sec}.$$

This is much less than the value found by Kopal. I am unable to account for the fact that the slope of my observations is different from his. Possibly the best that can be done at the present time is to use the mean slope of Kopal's measures and mine, which would be consistent with $K_2 = 173$ km/sec and $m_G/m_B = 0.7$ or 0.8.

At the time of partial eclipse the velocity-curve is distorted by the rotation effect. This phenomenon is discussed in the following section. The best possible elements from my velocity-curve are

$$P = 2.493 \text{ days}, \qquad \omega = 40°,$$

$$\gamma = -5 \text{ km/sec}, \qquad T = \text{phase } 2.16 \text{ days},$$

$$e = 0.20, \qquad a_1 \sin i = 4 \times 10^6 \text{ km},$$

$$K_1 = 120 \text{ km/sec}, \qquad \frac{m_2^3 \sin^3 i}{(m_1 + m_2)^2} = 0.42 \odot.$$

The dotted line which in Figure 1 represents the radial velocities of the G2 component intersects the interpolated velocity-curve of the B8 star at $\gamma = -5$ km/sec. This is a confirmation of our elements. Although my value of γ agrees closely with that determined by Carpenter, the minima of the two curves differ appreciably, and the agreement

in γ may be accidental. Kopal[23] has remarked that in U Cephei "the presence of a third body seems to be ruled out by the constancy of the radial velocity of the center of mass," but it is not clear upon what evidence this statement is based. Kopal's own value of γ differs considerably from Carpenter's and from mine. There is probably not enough information available at the present time to ascertain whether γ remains constant.

If the spectrographic elements were consistent with the photometric observations, mid-eclipse should take place when $v + \omega = 90°$ or 270°, or when the radial velocity is

$$V_c = \gamma + Ke \cos \omega = +13.5 \text{ km/sec}.$$

This predicted mid-eclipse would fall at phase 2.400. The observed value was 2.449. The difference of O − C = +0.049 is too large to be caused by errors in the photometric observations.

5. *Spectroscopic phenomena during partial eclipse.*—The durations of the entire eclipse and of its total phase are $10^h5^m.6 = 0.421$ day and $1^h54^m.8 = 0.080$ day, respectively.[24] Since on the system of phases used in this paper[25] mid-eclipse occurs at phase 2.449 = −0.044 day, the phases of the four contacts should be 2.239, 2.409, 2.489, and 0.166 days. The uncertainty of each of these phases is estimated to be ±0.007 day. If we follow the velocity-curve forward from the maximum, we find good agreement until phase 2.300. Thereafter the velocity-curve rises very suddenly to a maximum of +195 km/sec at phase 2.38 and then drops to a minimum at −244 km/sec at phase 2.53 = 0.04 day. This is the rotation effect of the B8 star. At the two critical phases we observe the velocities of the receding and of the approaching limbs of the B8 star, and we may therefore take for the rotational velocity at the equator (since $i \approx 90°$)

$$V \text{ (rot)} = \frac{195 + 244}{2} = 220 \text{ km/sec}.$$

Our direct estimate from the widths of the undisturbed lines was 180 km/sec. The agreement is satisfactory and confirms the unusual absence of synchronization of the periods of rotation and revolution. The rotational velocity of the B8 star is twice its orbital velocity, and the rotational effect observed during partial eclipse is the largest found for any eclipsing star. The lines used for the determination of the radial velocities in the partial phases include all lines of *He* I, *Mg* II, *Ca* II, and *Si* II but do not include the lines of *H*. The reason for omitting *H* will be explained at once.

Table 3 lists the details of my measures during the primary eclipse. The material is arranged in such a way as to show at one glance the division into three groups: first partial phase, totality, and second partial phase. The velocities of the *H* lines have been segregated from those of the faint lines of the B8 star: *He* I, *Mg* II, *Ca* II, and *Si* II. It will be seen that the *H* lines show a smaller rise than do the lines of *He* I, *Mg* II, and *Ca* II at phase 2.38 days. There may also be a somewhat smaller drop of the *H* lines at phase 2.53 = 0.04 day, although the departure is not as striking as it was before totality. The question arises whether the *H* lines or the group of *He* I, *Mg* II, *Ca* II, and *Si* II show the true rotational effect of the B8 star.

In order to answer this question, we turn to a description of the B8 spectrum during the partial phases. Nothing abnormal can be seen until phase 2.278 days. At phase 2.297 the *H* lines are distinctly unsymmetrical, with a strong core on the violet side of the diffuse, Stark-broadened line. At phase 2.318 these cores have become somewhat stronger, and they are very sharp. These fine lines are superposed over the fairly broad and unsymmetrical feature produced by the partly occulted rotating disk of the B8 star. They

[23] *Ann. New York Acad. Sci.*, **41**, 46, 1941.

[24] Dugan, *Contr. Princeton U. Obs.*, No. 5, p. 34, 1920.

[25] Formula (3).

do not look like the unsymmetrical minima of the rotational contours. The sharp cores are still more conspicuous at phases 2.344, 2.364, 2.374, and 2.378 days, although they always remain narrow and sharp. It is clear that I have measured these cores, and not the underlying broad lines, which at all these phases are displaced toward the red with respect to the cores. The lines of *He* I, *Mg* II, and *Ca* II are too weak to show the narrow cores, even if they existed. Hence, these lines show the undisturbed rotational shift.

TABLE 3

RADIAL VELOCITIES OF U CEPHEI DURING ECLIPSE

No.	Date 1943	U.T.	Phase	Exp. (Min.)	Radial Velocity			Remarks
					He I, *Ca* II, *Mg* II, *Si* II	*H*	G Star	
2565	Nov. 8	4h 13m	2.236	12	+ 66.2	+ 74.2	.....	
2566	8	4 30	2.248	20	+ 54.6	+ 84.8	.....	
2567	8	4 51	2.262	22	+ 50.8	+ 62.6	.....	
2568	8	5 14	2.278	22	+ 33.6	+ 66.9	.....	
2569	8	5 41	2.297	30	+ 26.3	+ 92.0	.....	
2570	8	6 12	2.318	30	+117.4	+ 80.4	.....	
2571	8	6 49	2.344	43	+150.6	+107.5	.....	
2677	13	6 57	2.364	20	+163.6	+108.5	.....	
2572	8	7 32	2.374	35	+192.6	+ 90.4	−46.0	
2678	13	7 18	2.378	20	+195.2	+ 37.2	−16.2	(1)
2679	13	7 45	2.397	32	.....	.....	−18.1	
2573	8	8 15	2.404	50	.....	.....	−39.0	
2680	13	8 19	2.421	32	.....	.....	−21.2	
2574	8	9 18	2.448	74	.....	.....	−26.0	
2681	13	9 29	2.469	93	.....	.....	− 2.4	
2575	8	10 22	2.492	50	.....	.....	+ 5.8	
2682	13	10 29	0.018	32	.....	.....	+ 8.0	
2576	8	11 18	0.038	60	.....	.....	+21.6	
2683	13	11 02	0.041	30	−244.4	−194.4	+25.4	(2)
2684	13	11 35	0.064	30	−156.9	−160.2	.....	(3)
2577	8	12 04	0.070	30	−159.2	−122.0	.....	(4)
2685	13	12 00	0.081	18	−135.2	−103.4	.....	
2578	8	12 34	0.091	28	−101.5	−100.9	.....	
2623	11	0 40	0.102	21	− 63.8	− 83.6	.....	
2624	11	1 01	0.116	20	− 69.2	− 74.4	.....	
2625	11	1 20	0.130	15	− 49.0	− 59.4	.....	
2626	11	1 36	0.141	15	− 31.8	− 59.4	.....	
2627	11	2 01	0.158	15	− 56.3	− 48.3	.....	
2628	11	2 17	0.169	15	− 55.1	− 52.1	.....	

(1) A second component of *Ca* II K gives +49.0; (2) of *Ca* II, *Hδ* and *Hγ*, gives −53.3; (3) of *Hδ* gives −42.8; (4) of *Ca* II K gives −43.8.

In order to be quite certain that the sharp *H* cores represent superposed lines and are not to be identified with the unsymmetrical minima of the rotational contours from the partly eclipsed disk of the B8 star, it is necessary to investigate these contours. Thus far, the only investigation of such contour (as distinct from studies of the shift of the center of gravity of unsymmetrical lines) was made by Struve and Elvey[26] in the case of Algol. The eclipse of this star is partial; and the resulting contours become very unsymmetrical, with the steeper edge on that side toward which the line, as a whole, is shifted. The ob-

[26] *M.N.*, 91, 667, 1931.

servations very clearly demonstrated that the lines were really unsymmetrical in the sense predicted. But it should be realized that, while in a binary system in which the direction of axial rotation of each component coincides with the direction of orbital motion the shift of the line is always in the positive sense before totality and in the negative sense after totality, there is no such uniformity with regard to the asymmetry of the line. Under certain conditions the red wing may be the steeper, while under other conditions the violet wing may be the steeper.

We shall assume that the B8 star has a circular disk during the eclipse and that its equatorial velocity is v_0. Then

$$\Delta\lambda_0 = \frac{\lambda v_0}{c}.$$

If we consider the center of the star's disk as coinciding with the center of co-ordinates, the x-axis falling along the equator, and the y-axis along the axis of rotation, then, if the radius of the B8 star is 1,

$$v = v_0 x$$

and

$$x = \frac{\Delta\lambda}{\Delta\lambda_0}.$$

The contour of an infinitely narrow line will be converted by rotation, in the absence of an eclipse and without limb darkening, to

$$I(x) = \frac{2}{\pi}\sqrt{1 - x^2}. \tag{5}$$

If the intrinsic line contour is given by an expression $J(x)$, then the actual broadened contour is

$$I'(x) = \int_{-\infty}^{+\infty} I(y)\, J(x - y)\, dy. \tag{6}$$

Equation (5) suggests a very simple graphical procedure for drawing the contours of lines distorted by the eclipse. If the radius of the B8 star is taken equal to 1, then $\sqrt{1 - x^2}$ represents the equation of a half-circle whose diameter is given by $x = \pm 1$. For any value of x, the square root is the half-length of the chord drawn on the disk of the B8 star at right angles to the abscissa. If there is an eclipse, some of the chords are cut short by the disk of the eclipsing star. If we draw to scale the relative positions of the disks of the eclipsing and eclipsed stars and measure the uneclipsed sections of vertical chords on the B8 disk, we obtain at once a representation of the corresponding "pure" rotational contour. The actual contour can then be easily obtained by carrying out integration (6). In Figures 2 and 3 I have shown several typical cases. Figure 2, *a*, corresponds to the system of U Cephei. The inclination is 90°, and the radius of the eclipsing star is 1.8 times that of the bright star. At first contact the contour $I(x)$ is undisturbed. At second contact, $I(x) = 0$, since totality sets in at that moment. The intermediate contours are for $\frac{1}{4}$, $\frac{1}{2}$, and $\frac{3}{4}$ of the partial phase, in time. The five contours correspond to phases 2.239, 2.281, 2.324, 2.367, and 2.409. The theoretical contour for "edge $\frac{3}{4}$," or phase 2.367, corresponds to the time when we observe the narrow H core, giving a velocity of the order of +100 km/sec, as compared to a velocity of nearly +200 km/sec for the lines of *He* I, *Mg* II, and *Ca* II. It is quite certain that the theoretical contour does not give rise to a sharp minimum at one-half of the displacement of the center of gravity of the line. There can be no doubt that broadening by Stark effect will produce for the case "edge $\frac{3}{4}$" an almost symmetrical, although greatly shifted, contour. Incidentally, the contours at "edge $\frac{1}{4}$" and "edge $\frac{1}{2}$" are interesting because of the sharp cutoff on the violet side which

they predict. We do not observe this cutoff, which is another argument in favor of the suggestion that Stark effect obliterates the details in the *H* lines, while the other lines are too weak to show the contours clearly. Figure 2, *b* and *c*, and Figure 3, *a*, *b*, and *c*, correspond to other conditions and show the variety of contours that may be observed in eclipsing variables. The contours, as drawn, have not been normalized to retain their areas constant. To do this, we should have to take

$$I''(x) = \frac{I(x)}{\int_{-\infty}^{+\infty} I(x)\,dx}.$$

But it is not necessary to carry out this normalization if it is only desired to compare the shapes of the resulting curves. In Figure 2, *b*, the diameters of the two stars are the same.

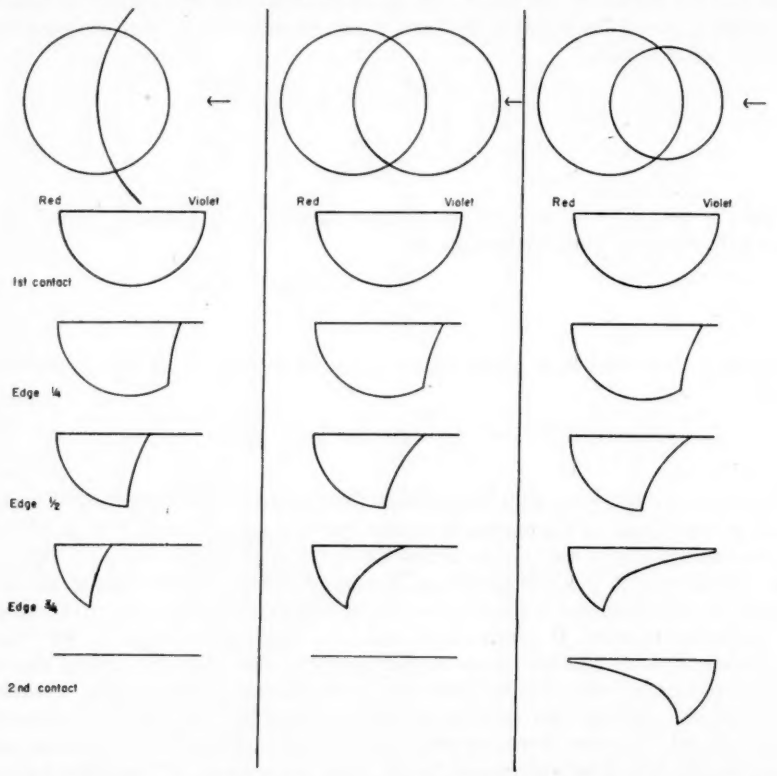

FIG. 2.—Typical contours of intrinsically narrow spectral lines of rapidly rotating stars in different stages of eclipse. The first case corresponds to U Cephei, where the eclipsing star is 1.8 times larger than the bright eclipsed star. In the second case the diameters of the two stars are the same, and in the third case the eclipsing star is the smaller. In all three cases the inclination is 90°. The contours have not been normalized to preserve constancy of the equivalent widths.

In Figure 2, *c*, the eclipsing star is the smaller. In Figure 3, *a*, *b*, and *c*, the inclination differs from 90°.

I believe it is safe to conclude that, while the asymmetry of the contours in U Cephei is such as to make the violet edge of the line slightly steeper than the red, the observed sharp core cannot be due to this asymmetry and must be produced in a stream of gas whose motion is in the same direction as the direction of rotation of the B8 star but whose velocity is only about one-half of the equatorial velocity of this star. The sharpness of the

superposed absorption lines shows that the gas is at very low pressure, because there are no wings produced by Stark effect. We may tentatively attribute these lines to a stream which starts from the B8 star and passes along the following side of the G2 star, to return toward the B8 star along the preceding side of the G2 star. This interpretation would be consistent with that advanced in the case of SX Cassiopeiae.[27]

The lines of the G2 star are not at all visible at phases 2.318 and 2.344. They are very weakly, but unmistakably, present at phase 2.364 and later. But the radial velocity of the G star at these phases is of the order of -40 km/sec. The *H* cores give $+100$ km/sec. Hence, they are not to be identified with the *H* lines of the fainter component. Further-

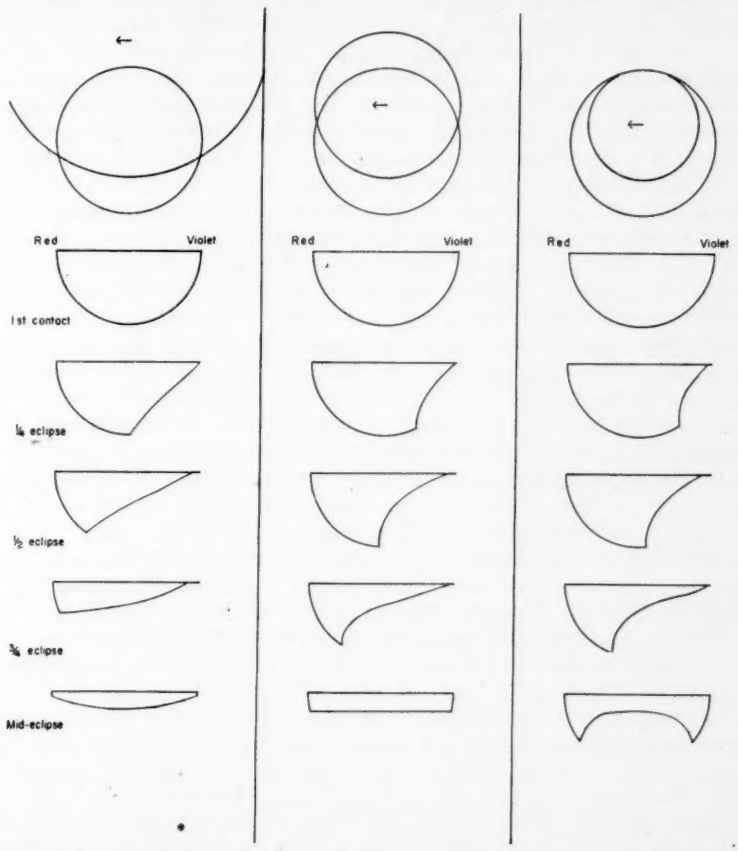

FIG. 3.—Contours of intrinsically narrow spectral lines of rapidly rotating stars in different stages of eclipse. The ratios of the diameters of the two stars are the same as in Fig. 2, but the inclination is not 90°.

more, the sharp *H* cores are present at $H\zeta$ and at other extreme violet members of the Balmer series, which are not strongly enough exposed to show the G star at all. At phase 2.378 there is a clear indication that *Ca* II K is double. But it is impossible to separate the effect of the G star completely. The exposure lasted 20 minutes—from 2.371 until 2.385. The continuous spectrum of the B8 star is quite strong, as is shown by the broad ultraviolet Balmer lines. The lines of the G star are quite weak, and it is almost certain that a 20-minute exposure would fail to register its continuous spectrum at λ 3933. The first G-type line on the violet side is *Fe* I 4005, which appears very weakly. I am almost cer-

[27] Struve, *op. cit.*, p. 94.

tain that the duplicity of *Ca* II K has nothing to do with the G-type spectrum. Either it may be due to an effective separation of a *Ca* II line in the stream from one produced in the rapidly rotating limb of the B8 star, or it may be due to an emission line in a "flash-spectrum" just preceding total eclipse. This feature is not brought out in the notes to the radial velocities of Table 3.

In connection with my observation of the ultraviolet lines of the B8 star at phase 2.378, it is of interest to recall Redman's[28] measures of the equivalent widths of $H\beta$, $H\gamma$, and $H\delta$ in the partial phases of U Cephei. He found that these lines become gradually weaker as totality is approached and that they may disappear completely at the extreme limb of the B8 star. Redman[29] has remarked that this behavior is to be expected, not only in the case of lines produced by "pure absorption," but also in the case of lines broadened by Stark effect. The evidence from my plates seems to confirm the weakening of the *H* lines toward the limb, accompanied by an appreciable reduction in width. But at all phases at which the B8 star was not totally eclipsed, its Balmer lines are clearly visible. Even at phase 2.397 (from 2.386 until 2.408) the higher Balmer lines of the B8 star are present. If it is recalled that second contact came at 2.409, the curve given by Redman for the equivalent widths predicts an intensity of the *H* lines which is roughly one-quarter of that observed outside of eclipse. Although my plates are not suitable for accurate spectrophotometry, I should have estimated the ultraviolet *H* lines to be considerably more intense—perhaps of the order of 0.5 their normal equivalent widths. These ultraviolet lines are completely free of the disturbing effect of the G star, for which Redman made suitable corrections in the case of $H\beta$, $H\gamma$, and $H\delta$.

During the totality, only the G-type spectrum is seen. On one plate, phase 2.448, I suspect the presence of central emission lines at *Ca* II K and *H*. There is no change in the spectrum during the total phase. At phase 0.018 the spectrum is still entirely that of the G star, in spite of the fact that third contact came at $2.489 = -0.004$ day. Perhaps my principal minimum is slightly in error. But, it is also possible that the asymmetry in the light-curve observed by Rosenberg near third contact reduces the brightness of the B8 star to such an extent that it does not show until phase 0.038. At this phase the lines of the G star are still weakly present. In fact, they are seen as late as phase 0.041. The ultraviolet Balmer lines of the B8 star are strong at phase 0.038; but they look much narrower, and deeper, than outside of eclipse. At phases 0.038, 0.041, 0.064, and perhaps 0.070 the lines *Ca* II K, $H\delta$, and $H\gamma$ are conspicuously double; probably $H\beta$, $H\epsilon$, and $H\zeta$ are also double on one or two plates. This doubling is much more conspicuous than that observed on one plate before totality. The violet components are in all lines fainter and more diffuse than the red components. This is especially well shown in the case of *Ca* II 3933. The violet components of *Ca* II and *H* agree with *He* I and *Mg* II and undoubtedly represent the narrowed unsymmetrical contour of the approaching limb of the B8 star. Their velocity is of the order of -150 to -200 km/sec. The red absorption components of *H* and *Ca* II K give about -45 km/sec and must be caused by the approaching side of the stream of gas whose presence we already detected in the pretotality observations. Again these lines cannot be identified with the *H* lines of the G star because the velocity of the latter is now of the order of $+20$ km/sec. They are much stronger than before totality and more diffuse, but the *H* lines have the appearance of lines broadened by turbulence and not by Stark effect. It is interesting that the stream on this side shows a fairly strong line of *Ca* II K, while on the other side we only suspected a trace on one plate.

I am not yet entirely certain whether the narrow space between the two absorption components of *Ca* II K, $H\delta$ and $H\gamma$, is continuous spectrum or true atomic emission. The rotational contour becomes quite narrow for phases which are close to totality, but I am a little surprised to find it sufficiently narrow to give such a clear separation of the absorption lines. On the other hand, *Ca* II K shows the doubling more distinctly than $H\delta$

[28] *Op. cit.*, p. 504.

[29] *Observatory*, **59**, 287, 1936.

or $H\gamma$, and this is what should be expected from the absence of Stark effect in *Ca* II. At phase 0.081 the two absorption components are blended, producing a single unsymmetrical line, with a strong and rather broad core on the red side. This core corresponds to the narrow sharp core observed on the violet side of the unsymmetrical line before totality. This appearance of the *H* lines continues, with gradually diminishing asymmetry, until phase 0.141, which is well past the $\frac{1}{4}$ stage of the partial eclipse. It is about at this same phase that the measured radial velocities, which are now indistinguishable for the B8 star and the stream, again agree with the velocity-curve computed without regard for the rotation effect.

The question arises whether the stream of gas which produces the extra "satellite" lines in U Cephei (to use an expression coined by Baxandall to describe a similar phenomenon in β Lyrae) may not, in reality, be the rotating atmosphere of the G2 star. There is a distinct possibility that we observe the light of the B8 star shining through the outer atmosphere of the G2 star. The velocity, +108 km/sec before totality and −194 km/sec after totality, is, however, much too large to be consistent with this hypothesis. We had found that the equatorial velocity of rotation of the G2 star, V_e, is less than 50 km/sec. Yet, the light of the B8 star would give us an integrated line for regions of the G2 star from latitude 0 to some higher latitude, where the rotational velocity is less than V_e. Although the size of the G2 star is such that this effect is small, it is difficult to accept a value for V_e greater than 50 km/sec. Another difficulty is the fact that only *H* and *Ca* II show the satellite components. In the normal spectrum of the G2 star *Ca* II is enormously stronger than *H*, and *Fe* I and *Ca* I are quite similar to *H*. The stream would therefore have a different stage of ionization and excitation than the normal atmosphere of the G2 star. Finally, geometrical conditions are such that a hypothetical ζ Aurigae effect would be greatest at or before the halfway point of each partial eclipse. In reality the satellite lines are conspicuous between the three-quarter point and totality. I am inclined, therefore, to favor the stream hypothesis, although the three arguments advanced do not entirely rule out the ζ Aurigae effect for the extra components observed at phases 2.378, 0.041, 0.064, and 0.070 days.

Redman has pointed out that it would be of great interest to follow lines other than those of *H* during the partial eclipse of the B8 star. This is especially true because we have shown that the *H* lines themselves are not simple lines, originating in the atmosphere of the B8 star, but are complicated by absorption lines produced in a detached stream of gas. The lines of *He* I are probably least affected by disturbing factors. If we consider first the second half of the eclipse and follow their appearance from phase 0.169 backward, we observe that they, together with *Ca* II K, *Mg* II 4481, and probably the lines of *Si* II, become narrower and deeper—precisely as we should expect from the rotational effect. At phases 0.116, 0.102, and 0.091 all these lines are fairly conspicuous, although they are still less intense than we would expect to find them in a nonrotating B8 star. These phases are close to the halfway mark of the partial eclipse (phase 0.081 day). From there on, and especially at phases 0.070, 0.064, 0.041, and 0.038, the *He* I and *Mg* II lines not only cease to increase in depth but become appreciably weaker. At phase 0.038 they are present and can be measured, but they are much less conspicuous than at phase 0.116. The *Mg* II line behaves like *He* I, but I am not entirely certain that this effect is free of influence from the continuous spectrum of the G star. There is no such difficulty in the case of *He* I. With the short exposure times during partial eclipse the line λ 4026 is quite free of any continuous spectrum of the G star. The *Ca* II K line continues to increase in intensity as we approach totality: the violet component at phases 0.038 and 0.041 is much more conspicuous than the undisturbed line outside of eclipse: it is narrower and very much deeper, approaching the kind of line we should expect to observe in a slowly rotating star. The same is certainly true of *Si* II 3862, which is quite conspicuous at these two phases, while it is exceedingly difficult to see outside of eclipse. I believe that the equivalent widths of *Si* II and *Ca* II remain essentially constant throughout the par-

tial eclipse, while *He* I remains constant until about phase 0.116 and then decreases toward totality.

The difference in the behavior of *He* I (and perhaps *Mg* II), on one side, and of *Ca* II and *Si* II, on the other, is interesting. Those *He* I lines which could be used in these comparisons belong to the series $2^3P - n^3D$ and $2^1P - n^1D$. Both are strongly influenced by Stark effect. Hence, it is probable that we must regard the weakening of *He* I toward the limb (and, by analogy, the phenomenon observed by Redman for *H*) as in the nature of an absolute-magnitude effect. The lines appear weaker at the limb because the pressures are lower, and not because the mechanism of line formation is predominantly one of "pure absorption."

In the first half of the eclipse the lines of *He* I are systematically weaker than in the second half. There is a marked increase in the conspicuousness of *He* 4471 from phase 2.236 to phase 2.364, the line becoming narrower and deeper. The same may be true of *He* I 4026 and one or two other *He* I lines. But at this phase all *He* I lines are weaker than at the corresponding phase after totality. Certainly, the *He* I lines do not continue to become more noticeable after phase 2.364. The line *Ca* II K does, however, become more noticeable as totality is approached. At phase 2.374 it is fairly conspicuous, though the *He* I lines are barely visible. But this line, too, is systematically weaker at phases 2.374 and 2.378 than at phases 0.038 and 0.041. There appears to be a real difference in the intensities of lines produced by the receding and approaching limbs of the B8 star, the former having the weaker lines. We have already seen that the *H* and *Ca* II components which we have attributed to the stream are also stronger after totality than before. Both phenomena are related, but it is impossible to determine their causes. The well-known asymmetry of the light-curve in the partial phases may be related to this spectroscopic difference in spectral line intensities. According to Dugan, the tidal bulge is carried forward by the rapid rotation of the B8 star. This bulge makes the star slightly fainter just before eclipse than after its end. We must, then, conclude that the lines originating from the tidal bulge are fainter than those which come from other parts of the B8 star's surface.

6. *Discussion.*—The velocity-curve contradicts the photometric observations. The former gives $e = 0.20$ and $\omega = 40°$. The latter, according to Tchudowitchev, are consistent with $e = 0.08$ and $\omega = 99°$. No amount of refinement in the solution can remove this fundamental difficulty: in both Carpenter's and my velocity-curves the rise from minimum to maximum takes approximately 1.4 days, while the descent from maximum to minimum requires only 1.0 day. The observations do not reveal a definite clue to the solution of this problem, as they do in the case of SX Cassiopeiae. There is no dilution effect in the absorption lines, outside of eclipse, and hence no direct proof of the existence of an extended shell. But the existence at partial phases of superposed lines, originating in a stream of gas, links the problem with that of SX Cassiopeiae and suggests that the asymmetry of the velocity-curve may be produced by the same stream. Kopal remarked in his paper "that the profile of $H\gamma$ (as well as of other members of the Balmer series) is distinctly asymmetrical during full light and in the early partial stages, when the rotational effect is still insignificant." My plates show no asymmetry at phases near 1.0 day, where Kopal's plates, in full light, were taken. I have suspected some asymmetry in the contours of the hydrogen lines near maximum radial velocity (phase 2.0 days) in the sense that the deepest part of the line is displaced toward the red from the geometrical center of the line. But I am not certain that this effect is real.

The absence of strong emission lines may not affect the stream hypothesis. But, in the case of SX Cassiopeiae, the eclipse of the violet and red emission components clinched the argument. We conclude that, while there is a possibility that the velocity-curve of U Cephei is distorted by absorption in gaseous streams, there is no such compelling evidence as in the case of SX Cassiopeiae.

NOTE ON THE PROBLEM OF U CEPHEI

ZDENĚK KOPAL
Harvard College Observatory
Received February 29, 1944

ABSTRACT

Attention is called to the fact that several stars are now known to exhibit appreciable spectroscopic eccentricities while their photometric orbits are practically circular. It is pointed out that previous attempts to explain spurious spectroscopic eccentricities have not been successful; and an attempt is made to attribute the spectroscopic eccentricities to distortion of the velocity-curve in a mass of gas in the outer parts of the stars whose density is so low that the distribution of mass in the system remains sensibly unaffected. The asymmetry of the light-curve of U Cephei may possibly be explained in terms of a theory proposed by Cowling.

Recent researches by O. Struve[1] have brought to the focus of attention striking discrepancies between spectroscopic and photometric eccentricities (as well as spectroscopically and photometrically determined times of conjunctions) of certain eclipsing

STAR	ELEMENTS	
	Spectroscopic	Photometric
U Cephei.....	$e=0.47\pm0.02$ (p.e.) $\omega=25°\pm3°$ (p.e.) Carpenter, *Ap.J.*, **72**, 205, 1930	$e=0.0$ Many investigators
	$e=0.20$ $\omega=40°$ Struve, *Ap.J.*, **99**, 228, 1944	.....
MR Cygni.....	$e=0.12$ $\omega=103°$ Pearce, *J.R.A.S. Canada*, **29**, 413, 1935	$e\leq0.01$ Swope, *Harvard Bull.*, No. 914, 1940
u Herculis.....	$e=0.05\pm0.01$ (p.e.) $\omega=93°\pm10°$ (p.e.) Sterne, *Proc. Nat. Acad.*, **27**, 175, 1941	$e\leq0.01$ Martin, *B.A.N.*, **8**, 265, 1938

variables. In systems like SX Cassiopeiae this may perhaps be explained by a special mechanism suggested by Struve on page 96 of the first paper cited; but Struve himself pointed out that such a mechanism seems of little avail in a more "normal" system like U Cephei, showing few if any spectral peculiarities characteristic of SX Cassiopeiae. The aim of this note is to point out that such discrepancies between photometric and spectroscopic elements may quite possibly be a common, rather than an exceptional, feature of close binary systems and call for an explanation on a more general basis.

The fact that the orbital eccentricities, as determined spectroscopically, usually come out too large in comparison with the photometric eccentricities has from time to time been commented upon by several writers;[2] and the accompanying tabulation of a few such

[1] *Ap. J.*, **99**, 89 and 222, 1944. The writer is greatly indebted to Professor Struve for having enabled him to see the latter paper in advance of publication.

[2] Cf., e.g., Luyten, *Minnesota Pub.*, Vol. **2**, No. 2, 1935.

representative systems shows that these discrepancies may be of varying order of magnitude.

The photometric evidence that the orbits of all these systems are practically circular is so sound and definite that there is but little room for doubt that, in the measured Doppler displacements of lines of these stars, shifts of undisclosed origin must be superposed upon purely orbital velocities to yield a resultant which may sometimes bear only a distant relation to the actual orbit. Hopes were entertained for some time that discrepancies as small as that found for u Herculis could perhaps be explained by effects, upon radial velocity, of limb- and gravity-darkening of distorted rotating components,[3] or by the reflection effect[4]—both of which were found, indeed, to simulate an orbital eccentricity with the apsidal line parallel to the line of sight. Upon closer scrutiny these effects proved, however, to be too small to account for the discrepancy between spectroscopic and photometric eccentricity for u Herculis[5] and still less so for the other stars listed above, not to mention the fact that the apsidal line of the spectroscopic orbit of U Cephei is manifestly not parallel to the line of sight. The discrepancy, therefore, remains unexplained, and we may ask with Struve, ". . . . if we cannot trust the velocity-curve . . . . for which the photometric observations provide the crucial test, how can we trust the velocity-curve of any other spectroscopic binary to give us an orbit which has a dynamical meaning?" This is a far-reaching question which deserves close attention. Since the theory has thus far been unable to provide much guidance to its approach, we shall attempt to survey the problem in the light of available statistical data.

It is to be stressed at the outset that eccentric eclipsing binaries, for which photometric observations may provide the crucial test, are, unfortunately, rare. The displacement of minima specifies, as a rule, only one component of the eccentricity, namely, $e \cos \omega$;[6] while $e \sin \omega$ can be obtained only from the unequal durations of both minima with usually much less accuracy. In systems with stationary or slow-moving apsides a separation of e and ω is therefore an inherently difficult task; in consequence of which for only very few variables are genuine photometric determinations of e and ω available. From these we may conclude that, in all systems for which spectroscopic observations have indicated a circular orbit, photometric observations are consistent with it. This seems to be true for very close binaries (β Lyrae) as well as fairly well separated ones (Algol); no exception from this rule is known thus far. On the other hand, spectroscopically eccentric orbits may or may not be also photometrically eccentric. For Y Cygni, for instance, the spectroscopic and photometric values of e and ω are in almost perfect agreement.[7] For the majority of systems a consistency of spectroscopic and photometric elements cannot be readily tested because the photometric observations yield only $e \cos \omega$;[8] while for certain others (such as those listed above) the spectroscopic eccentricities are definitely at variance with the photometric evidence; and the significant fact is that such eccentricities seem to be wholly, not partly, spurious.

Of the three systems listed above, U Cephei appears to be not only the most striking representative of its group but is also observationally best known. It is, therefore, tempting to try to relate the occurrence of anomalous spectroscopic eccentricity with certain other peculiarities shown by U Cephei, namely, the asymmetry of its light-curve and

[3] Sterne, *Proc. Nat. Acad.*, **27**, 168, 1941.

[4] Kopal, *Proc. Amer. Phil. Soc.*, **86**, 351, 1943.

[5] *Ibid.*, pp. 361–362.

[6] In more precise terms, the observed displacement of minima due to central eclipses specifies $e \cos \omega(1 - e^2)^{-\frac{1}{2}}$.

[7] Dugan, *Princeton Contr.*, No. 12, 1931.

[8] A combination of spectroscopic e and photometric $e \cos \omega$ need, therefore, not necessarily lead to a true longitude of periastron—a point to be borne in mind in any future discussion of apsidal motions in close binary systems.

suspected fluctuations of orbital period. It has been known now for more than thirty years that the light-curve of U Cephei exhibits asymmetry throughout the whole cycle. The principal asymmetry-generating term varies between minima as sin 2θ (θ being the phase-angle), and its coefficient increases with effective wave length of observation exactly as the fractional luminosity of the secondary component.[9] This proves that the asymmetry of the light-curve between minima is due to some peculiar action of the *secondary*, not the primary, star. After the light-curve has been rectified for the variation of light between eclipses, the primary minimum still remains asymmetric; nearly all observers have found that the brightness of U Cephei within minima diminishes less rapidly than it increases [10] in visual, as well as photographic, light.

Various suggestions have been offered to account for this asymmetry. Dugan[11] thought it to be a consequence of "tidal lag" invoked by fast rotation of the primary component, while Walter[9] attributed it to bodily librations of the secondary star. Taylor[12] invoked certain resonance phenomena for its explanation, while Cowling[13] suggested that it may be due to a lag between variation in light and radius of a distorted configuration exhibiting forced nonradial oscillations. Of these the hypotheses by Dugan and Walter, although interesting innovations at the time of their publication, can no longer be maintained. It has been recognized for some time that tides *cannot* lag by any appreciable amount in systems consisting of *fluid* components—and there is very little room for doubt that the stars behave almost like perfect fluids; neither can there be any libration. The secondary component of U Cephei could librate in the way envisaged by Walter only if it were *solid* from the core to the surface; not otherwise. If synchronism exists between rotation and revolution in systems consisting of fluid components, the tidal bulge will form a standing wave (or a system of waves of the same phase) on the surface of the distorted star. If the latter rotates faster (or slower) than its mate revolves, the tidal wave will merely sweep along its equator so as to remain always pointed to the center of mass of the disturbing body. The viscosity of stellar matter is too small to allow the tides to lag by any observable amount.[14]

On the other hand, the theoretical basis of Taylor's explanation of asymmetries of eclipsing binary systems was largely invalidated by Cowling, whose own hypothesis may be summarized as follows: It is known from observations of Cepheid variables that the variation in light emitted by a radially oscillating star lags behind the variation in radius. Now, if the rotational and orbital velocities differ, the tidal distortion of the components in eccentric binary systems becomes a forced nonradial oscillation. We may then expect that the variation in light, which may accompany such nonradial oscillations, will also lag behind the vertical displacement; and this may produce the observed asymmetry. To this one might remark that it is not yet certain whether nonradial oscillations of components in close eccentric systems are accompanied by any light-variation. Such variations in radially oscillating stars originate presumably in the deep interiors of the stars, while nonradial oscillations of tidal origin are a relatively superficial phenomenon. At

[9] Walter, *A.N.*, **250**, 342, 1933.

[10] A suggestion by Tchudowitchev (*Engelhardt Obs. Bull.*, No. 17, 1939) that the asymmetry of minima oscillates in sign remains still to be confirmed. His geometrical explanation of this phenomenon as a consequence of the revolution of apsides is, however, certain to fail. Apart from the fact that any evidence for apsidal motion in U Cephei is still slight, an orbital eccentricity considered by Tchudowitchev is entirely insufficient to produce any observable difference in duration of the ascending and descending branches of the primary minimum.

[11] *Princeton Contr.*, No. 5, 1920.

[12] *Ap. J.*, **94**, 46, 1941.

[13] *M.N.*, **101**, 367, 1942.

[14] Struve's conclusion that the observed fast rotation of the B8 component . . . . "in a most unexpected manner confirms Dugan's hypothesis of the tidal lag of the early-type component" seems, therefore, to have been premature. The observed phenomena admit also of alternative explanations.

any rate, Cowling's suggestion still remains to be tested by detailed comparison with the observations, and the origin of asymmetry of the light-curve of U Cephei and other eclipsing variables appears still uncertain.

We may pursue the problem one step further and inquire as to whether or not the spurious spectroscopic eccentricity or the asymmetry of light-changes of U Cephei are more likely to be due to a mere peculiar distribution of *light* on the surfaces of its components or to a peculiar distribution of *mass* in the system itself; for, unlike the former alternative, the latter should give rise to dynamical perturbations of simple orbital motion, some of which—namely, those of orbital period—could possibly be detected. It has, indeed, been suspected for a long time that the orbital period of U Cephei is not entirely constant; at least in recent decades it has been appreciably longer than at the time of its discovery seventy years ago. On the other hand, the existence of complicated periodic variations, postulated from time to time by several writers,[15] should still be considered as doubtful. The evidence for such variations was based almost exclusively on old series of observations from 1880 to 1910; and several considerations indicate that, with a few exceptions,[16] these should be given much less weight than has been done hitherto. The light-curve of U Cephei is now known to be asymmetric; the light within minima diminishes less rapidly than it increases; and even during totality it fails to remain constant. The bearing of these facts upon the determination of the times of minima is obvious; yet they were only gradually realized after decades of observations. Whenever old observations of the minima were published *in extenso*, we may reconstruct their form and often find the moments of central eclipse to differ appreciably from those given by the observer; but minima based on unpublished data (especially if the observations were few or on one branch only) should not be included in any precise analysis. With the advent of modern photometric methods the accuracy of known minima has increased considerably. The writer rediscussed in detail 48 minima observed between 1923 and 1940[17] but found the period to be constant within a second[18] and no indication of any oscillation with an amplitude in excess of 5 minutes or a period of less than a century.[19] Thus it appears that, except for a possibly abrupt lengthening of the orbital period in the years 1900–1905, there is no sufficient evidence of any period variation in U Cephei which could be traced back to dynamical perturbations. In consequence we may conclude, with some hesitation, that the effects generating the asymmetry of light and (or) velocity-curve have their origin in peculiar distribution and motions of matter in the outer parts of the stars, whose density is so low that the distribution of mass in the system remains sensibly unaffected. The detailed mechanism generating these effects is still a mystery. So long as it remains so, the conventional parameters defining the amplitudes, phase, or skewness of the anomalous velocity-curves should be regarded as mere constants which do not readily admit of conventional dynamical interpretation. The really disturbing fact is that so far we have no idea as to how many ordinary (i.e., noneclipsing) spectroscopic binaries may have their elements vitiated in the same manner as U Cephei or MR Cygni or u Herculis —a fact which necessarily detracts from the significance of certain correlations obtained by statistical analyses of elements of spectroscopic binaries.

There exists, possibly, one hopeful avenue of approach to the solution of our problem, and that is a detailed study of line profiles in the spectrum of U Cephei and other similar

[15] Chandler, *A.J.*, **9**, 49, 1889; Yendell, *A.J.*, **23**, 213, 1903; Carrasco, *Madrid Bol.*, **1**, No. 16, 1933.

[16] A long series of photometric measurements by Wendell, rediscussed by M. B. Shapley (*Ap.J.*, **44**, 51, 1916), being a notable exception.

[17] Unpublished.

[18] *Harvard Bull.*, No. 914, 1940.

[19] U Cephei is, incidentally, by no means the only variable for which most of the anomalous period oscillations seem to have just about ceased with the advent of photographic and photoelectric photometry; Algol is another conspicuous example.

systems. The contours of the hydrogen lines of the B8 spectrum of U Cephei appeared distinctly unsymmetrical on the Victoria spectrograms taken one day after mid-primary minimum.[17] This was questioned by Struve; but both he and Joy[20] confirmed the unsymmetrical appearance of the lines at phases near 2 days. The settings, for any measurements of radial velocity, on extremely broad and asymmetric hydrogen lines of the principal spectrum of U Cephei then represent a special problem; and the writer is inclined to believe that conspicuous discrepancies between spectrographic orbits derived by Carpenter,[21] Struve, and the writer[22] are largely due to this cause.

Two final remarks remain to be added. First, it is very unlikely that, in U Cephei at least, any of its peculiarities could be ascribed to the presence of a third body. Struve is quite right in pointing out that the spectroscopic evidence on this point is still unsatisfactory. A stronger argument against the presence of any third body in U Cephei follows, however, from the photometric evidence. If any third star were present, the orbital period of the eclipsing pair would have to exhibit regular oscillations due to the light-equation in the third orbit. From the writer's analysis of minima in 1923–40[16] it appears reasonably certain that any such oscillation, if it exists, must have an amplitude of less than 5 minutes, or a period in excess of 100 years, or both. Either alternative would, however, imply that the mass of the hypothetical third body should be less than $0.1\odot$ and its luminosity probably too small to exhibit any noticeable effect.

The second remark concerns the speed of axial rotation of the B8 component of U Cephei. This star, according to Struve, rotates much faster than it revolves, and he considers this to be the spectroscopically most firmly established fact of his study.[23] To this one might add that the existing observational evidence seems consistent in showing that the components of spectroscopic binaries revolving in eccentric orbits rotate as a rule *faster* than they revolve[24]—usually the faster, the greater the spectroscopic eccentricity. U Cephei thus seems to present no exception. The fact that its velocity-curve between eclipses is thoroughly deformed by effects of unknown origin may, however, cast some doubt also on the interpretation of the rotational effect within minima. A development of the suggestion that abnormally large rotational effects observed in eccentric spectroscopic binaries may also be partly spurious, as a result of the same causes which deform the velocity-curves between minima, must, however, be left to a more courageous individual.

[20] In a letter to Dr. Shapley, which the present writer had the privilege of seeing.

[21] *Ap.J.*, **72**, 205, 1930.

[22] *Harvard Bull.*, No. 914, 1940. The orbital elements in this paper were derived *under the assumption* of a circular orbit, since no material was on hand to check it.

[23] Personal communication.

[24] A table of such systems was compiled by the writer in *Harvard Circ.*, No. 443, 1940 (Part I, sec. 3).

NOTES

COLOR INDICES OF PROPER-MOTION STARS

In the course of the determination of the color indices of proper-motion stars in the Northern Hemisphere, six stars were found whose color indices appear to be so much less than expected that it seems highly probable that they are either white dwarfs or

TABLE 1

Name	α (1900)	δ (1900)	Pg. Mag	μ	p	I.C.
L 1011–71.....	0^h30^m5	+ 1° 21′	16.0	0″.41	205°	0.3
L 1455–23.....	4 41.6	32 59	13.7	.36	103	.5
L 1863–4.....	6 20.4	66 29	12.0	.40	188	.3
L 1261–24.....	11 51.6	18 56	15.8	.32	274	.2
L 1139–56.....	19 07.8	6 34	12.8	.34	220	.3
L 1140–73.....	19 35.5	+ 8 40	14.1	0.21	209	0.1

"intermediates." If they were stars of an absolute magnitude normal for their color, their linear tangential velocities would be in excess of 500 km/sec. Data for these stars are given in Table 1.

W. J. Luyten
P. D. Jose
J. F. Foster

Steward Observatory
University of Arizona
December 22, 1943

ERRATA

In the list of dwarf M stars in Volume **97**, page 383, Table 1, the right ascension of star No. 42 should be 13^h28^m0 and not 12^h28^m0.

A. N. Vyssotsky

On page 71, Volume **99**, line 35 from the top, read "VV Cephei" instead of "VV Cygni."

On page 115 of Volume **99**, in line 17 of the article "Astrophysical Research in France in 1940–1942," read "120-cm reflector" instead of "120-inch reflector."

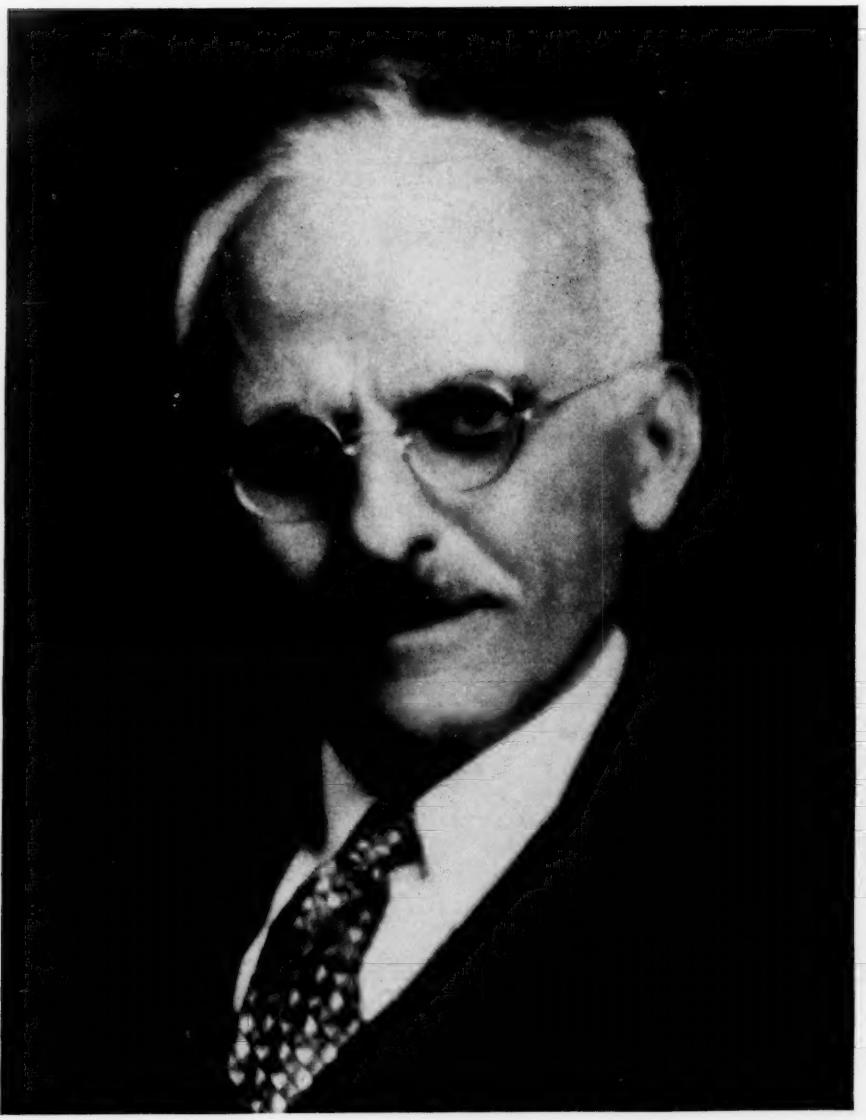

HEBER DOUST CURTIS
1872–1942

UNIV. OF MICH.